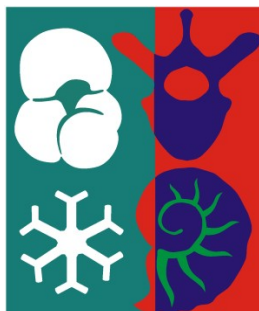




ARISTOTLE UNIVERSITY OF THESSALONIKI
Interinstitutional Program of Postgraduate Studies in
PALAEOLOGY – GEOBIOLOGY

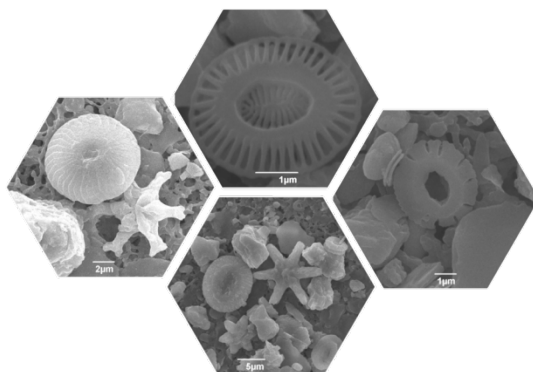


FATOUROU EUGENIA
Geologist

NANNOFOSSIL BIOSTRATIGRAPHY OF ARGOSTOLI GULF
QUATERNARY MARINE SEQUENCE (KEFALLONIA ISLAND, IONIAN
SEA)

MASTER THESIS

DIRECTION: Micropalaeontology-Biostratigraphy
Directed by: National & Kapodistrian University of Athens





ATHENS
2020





Interinstitutional
Program of
Postgraduate
Studies in
PALAEONTOLOGY – GEOBIOLOGY

supported by: Fatourou Eugenia

	<p>Τμήμα Γεωλογίας ΑΠΘ School of Geology AUTH</p>
	<p>Τμήμα Βιολογίας ΑΠΘ School of Biology AUTH</p>
 National and Kapodistrian University of Athens Faculty of Geology and Geoenvironment	<p>Τμήμα Γεωλογίας & Γεωπεριβάλλοντος ΕΚΠΑ Faculty of Geology & Geoenvironment NKUA</p>
 Department of GEOLOGY	<p>Τμήμα Γεωλογίας Παν/μίου Πατρών Department of Geology, Patras Univ.</p>
 UNIVERSITY OF THE AEGEAN	<p>Τμήμα Γεωγραφίας Παν/μίου Αιγαίου Department of Geography, Aegean Univ.</p>





FATOUROU EUGENIA
ΦΑΤΟΥΡΟΥ ΕΥΓΕΝΙΑ
Πτυχιούχος Γεωλογίας -Γεωπεριβάλλοντος

NANNOFOSSIL BIOSTRATIGRAPHY OF ARGOSTOLI GULF QUATERNARY MARINE SEQUENCE (KEFALLONIA ISLAND, IONIAN SEA)

ΒΙΟΣΤΡΩΜΑΤΟΓΡΑΦΙΑ NANNOΑΠΟΛΙΘΩΜΑΤΩΝ ΤΗΣ ΤΕΤΑΡΤΟΓΕΝΟΥΣ
ΘΑΛΑΣΣΙΑΣ ΑΚΟΛΟΥΘΙΑΣ ΤΟΥ ΚΟΛΠΟΥ ΤΟΥ ΑΡΓΟΣΤΟΛΙΟΥ (ΚΕΦΑΛΟΝΙΑ,
ΙΟΝΙΟ ΠΕΛΑΓΟΣ)

Υποβλήθηκε στο ΔΠΜΣ Παλαιοντολογία-Γεωβιολογία

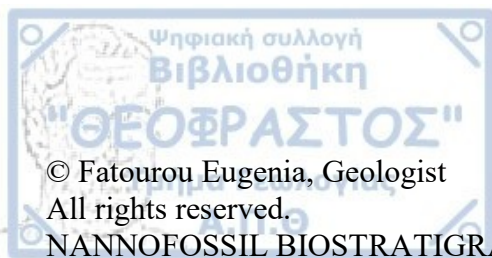
Ημερομηνία Προφορικής Εξέτασης: 21/02/2020
Oral Examination Date: 21/02/2020

Three-member Examining Board

Triantaphyllou Maria (Supervisor – Professor, NKUA)
Apostolopoulos Georgios (Professor, NTUA)
Underhill John (Professor, Heriot-Watt University)

Τριμελής Εξεταστική Επιτροπή

Καθηγήτρια Τριανταφύλλου Μαρία, Επιβλέπουσα, ΕΚΠΑ
Καθηγητής Αποστολόπουλος Γεώργιος, Μέλος Τριμελούς Εξεταστικής Επιτροπής, ΕΜΠ
Καθηγητής Underhill John, Μέλος Τριμελούς Εξεταστικής Επιτροπής, Heriot-Watt University



NANNOFOSSIL BIOSTRATIGRAPHY OF ARGOSTOLI GULF QUATERNARY MARINE SEQUENCE (KEFALLONIA ISLAND, IONIAN SEA) – *Master Thesis*

© Φατούρου Ευγενία, Γεωλόγος - Γεωπεριβαλλοντολόγος, 2020

Με επιφύλαξη παντός δικαιώματος.

ΒΙΟΣΤΡΩΜΑΤΟΓΡΑΦΙΑ ΝΑΝΝΟΑΠΟΛΙΘΩΜΑΤΩΝ ΤΗΣ ΤΕΤΑΡΤΟΓΕΝΟΥΣ ΘΑΛΑΣΣΙΑΣ ΑΚΟΛΟΥΘΙΑΣ ΤΟΥ ΚΟΛΠΟΥ ΤΟΥ ΑΡΓΟΣΤΟΛΙΟΥ (ΚΕΦΑΛΟΝΙΑ, ΙΟΝΙΟ ΠΕΛΑΓΟΣ) – *Μεταπτυχιακή Διπλωματική Εργασία*

Citation:

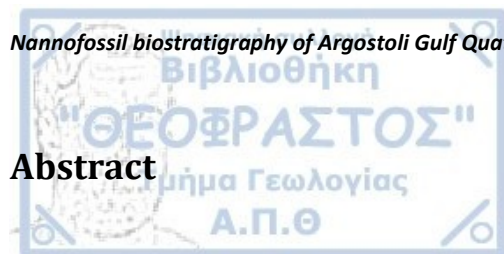
Fatourou E., 2020. – Nannofossil biostratigraphy of Argostoli Gulf Quaternary marine sequence (Kefallonia Island, Ionian Sea). Master Thesis, Interinstitutional Program of Postgraduate Studies in Palaeontology-Geobiology. School of Geology, Aristotle University of Thessaloniki, 85 pp.

It is forbidden to copy, store and distribute this work, in whole or in part, for commercial purposes. Reproduction, storage and distribution are permitted for non-profit, educational or research purposes, provided the source of origin is indicated. Questions concerning the use of work for profit-making purposes should be addressed to the author.

The views and conclusions contained in this document express the author and should not be interpreted as expressing the official positions of the Aristotle University of Thessaloniki.







Abstract

The purpose of this thesis was to study the Quaternary sediments of the Argostoli Gulf of Kefallonia, located on the Ionian Sea in NW Greece. This study was carried out with the help of calcareous nannofossils, which provide information on biostratigraphy, paleogeography and paleoenvironment of the study area.

This research was carried out in the framework of the Odysseus Unbound project, in collaboration with the Odysseus Unbound Foundation (OUF), the National Technical University of Athens (NTUA), and the National and Kapodistrian University of Athens (NKUA). This program had as its main goal the proof of the theory that NW Kefalonia and more specifically the Paliki peninsula is the Homeric Ithaca.

Samples from three different boreholes from Livadi 1, Livadi 2 and Livadi 4 were used to carry out this work. Originally the sampling was conducted at the School of Mining Engineering, of National Technical University of Athens. The samples were taken from three boreholes, which were mentioned above, and more specifically from the cores 7, 8, 9 and 10 of each borehole. Sampling was conducted steadily every 10 centimeters in each core. Afterwards, the specimens were processed in the laboratory of the Department of Historical Geology and Paleontology of the National and Kapodistrian University of Athens, following the standard micropaleontological methods and techniques. Then, the micropaleontological analysis and taxonomy of the calcareous nannoplankton was carried out under the light microscope (LM) and the scanning electron microscope (SEM).

The samples analyzed under the SEM were 83 in total, originated from all three boreholes. Where it was considered necessary we took more samples and the cores were analyzed in high resolution. After the identification and the statistical analysis of the samples, the biozonal indicators were used in order to verify the biostratigraphic age assignment. These biozones give us the relative geological age of the sediments and thus the reconstitution of the past, the absence or presence of biozonal indicators and coccolithophores, in general, is another index that provides us with useful information on paleoenvironment.



Περίληψη

Η παρούσα διπλωματική εργασία είχε ως στόχο τη μελέτη των Τεταρτογενών ιζημάτων του κόλπου του Αργοστολίου της Κεφαλονιάς, η οποία βρίσκεται στο Ιόνιο πέλαγος στην ΒΔ Ελλάδα. Η μελέτη αυτή πραγματοποιήθηκε με την βοήθεια των ασβεστολιθικών ναννοαπολιθωμάτων, τα οποία δίνουν πληροφορίες για την βιοστρωματογραφία, την παλαιογεωγραφία και το παλαιοπεριβάλλον της περιοχής μελέτης.

Η προκείμενη έρευνα έγινε στα πλαίσια του προγράμματος Οδυσσέας Λυόμενος, σε συνεργασία με το Odysseus Unbound Foundation (OUF), το Εθνικό Μετσόβιο Πολυτεχνείο (ΕΜΠ) και το Εθνικό και Καποδιστριακό Πανεπιστήμιο Αθηνών (ΕΚΠΑ). Το συγκεκριμένο πρόγραμμα είχε θέσει ως βασικό και κεντρικό στόχο την απόδειξη της θεωρίας πως η ΒΔ Κεφαλονιά και πιο συγκεκριμένα η χερσόνησος της Παλικής είναι η Ομηρική Ιθάκη.

Για την εκπόνηση της εργασίας αυτής, χρησιμοποιήθηκαν δείγματα από τρεις διαφορετικές γεωτρήσεις, από την περιοχή του κόλπου του Λιβαδίου, με ονόματα Livadi 1, Livadi 2 και Livadi 4. Αρχικά το σύνολο των δειγμάτων, συλλέχθηκε από την Σχολή Μεταλλειολόγων Μηχανικών, του Εθνικού Μετσόβιου Πολυτεχνείου, από τις προαναφερθείσες γεωτρήσεις και πιο συγκεκριμένα από τους πυρήνες 7, 8, 9 και 10 (με κωδικούς Livadi-1.7, Livadi-1.8, Livadi-1.9, Livadi-1.10, Livadi-2.7, Livadi-2.8, Livadi-2.9, Livadi-2.10 και Livadi-4.7, Livadi-4.8, Livadi-4.9, Livadi-4.10). Στην συνέχεια, τα δείγματα δέχθηκαν ειδική επεξεργασία στο εργαστήριο του τομέα Ιστορικής Γεωλογίας και Παλαιοντολογίας του Εθνικού και Καποδιστριακού Πανεπιστημίου Αθηνών, όπου ακολουθήθηκαν οι γνωστές μικροπαλαιοντολογικές μέθοδοι. Έπειτα, έγινε η συλλογή, η μικροπαλαιοντολογική ανάλυση και η αναγνώριση του ασβεστολιθικού ναννοπλαγκτού με την βοήθεια του πολωτικού (LM) και του ηλεκτρονικού μικροσκοπίου (SEM – scanning electron microscope).

Το σύνολο των δειγμάτων που αναλύθηκαν ήταν 83 δείγματα και από τις τρεις γεωτρήσεις. Η λογική που πάρθηκαν ήταν ανά δέκα εκατοστά σε κάθε πυρήνα και στην συνέχεια η μικροπαλαιοντολογική ανάλυση έγινε ανά πέντε συλλεχθέντα δείγματα, όπου κρίθηκε απαραίτητο η μελέτη έγινε πιο λεπτομερής και αναλύθηκαν παραπάνω δείγματα έτσι ώστε να εξαχθούν καλύτερα και πιο εμπειριστατωμένα αποτελέσματα.

Τέλος, μετά την αναγνώριση και την στατιστική ανάλυση των δειγμάτων, χρησιμοποιήθηκαν τα ποσοστά των απολιθωμάτων – δεικτών, σύμφωνα με τα οποία πραγματοποιήθηκε η βιοστρωματογραφική ταξινόμηση των δειγμάτων και προσδιορίστηκε η σχετική τους ηλικία, επιτρέποντας την παλαιοπεριβαλλοντική ανασύσταση των μελετηθείσων ακολουθιών.

Acknowledgments

The present thesis was written in the frame of the Graduate program 'Micropaleontology – Biostratigraphy'. The experimental procedures and the micropaleontological analysis were carried out in the Department of Historical Geology and Paleontology, in the Paleontological Analysis Laboratory and in Scanning Electron Microscope Laboratory of the Faculty of Geology and Geoenvironment, in the National and Kapodistrian University of Athens. It was the last stage to the completion of my postgraduate program.

I would first like to express my deep gratitude to my thesis advisor and supervisor Triantaphyllou Maria, professor in Micropaleontology – Paleoenvironment – Stratigraphy, for her guidance through every stage of the process. Not only had she given me the opportunity to work on a Geoarchaeological – Biostratigraphic – Micropaleontological subject, but she also trusted me to work in the Scanning Electron Microscope Laboratory. The door of her office was always open, whenever a problem or a question came up, during my research or writing. The assistance and the advices given by her during the development of this research work were greatly appreciated.

I would also like to acknowledge the Professor of the School of Mining and Metallurgical Engineering of National Technical University of Athens (NTUA), George Apostolopoulos as the second member of the examination committee, for providing us the 4 boreholes from Kefallonia, Ionian Sea, NW Greece, so we could sample and analyze them in standard micropaleontological methods and I am grate-fully indebted to him for his hospitality and help at the department of NTUA, where the sampling of the cores was conducted.

I would like to express my appreciation to Professor of Stratigraphy in the Grant Institute of Geology in the School of Geosciences at The University of Edinburgh, Scotland and Associate Professor in the Institute of Petroleum Engineering, Heriot-Watt University, John R. Undehill, for providing us the 4 boreholes from Kefallonia, Ionian Sea, NW Greece in collaboration with Professor G. Apostolopoulos of NTUA, his helpful advises on the geology and tectonics in Kefallonia and especially in Paliki area and in Argostoli Gulf and also, I am grateful for his trust to our hard work on the sample analysis.

At this point I would like to offer my special thanks to the Odysseus Unbound Foundation, for entrusting us with this wonderful work and made us part of the romantic research of Homer's Ithaca. Without their help with the drilling project in Argostoli Gulf and especially without their trust to us, this thesis could not have been conducted.

I also like to acknowledge Professor Kosmas Pavlopoulos (SUAD), Assistant Professor Konstantinos Athanassas (NTUA) and Dr. Dimitrios Vandarakis (HCMR) who were responsible for the correct procedure in the drilling and borehole sampling, Mr. Konstantinos Markantonis responsible for the drilling equipment, Mr. Dimitrios Manias responsible for the marine platform, and finally, Mr. John Crawshaw (OUF) for the logistics related with the marine drilling project.

My friends and my boyfriend could not be excluded of course. I am thankful for their unceasing encouragement and patience as well as the times of happy distraction. Finally, I must express my profound gratitude to my family for providing me with unfailing support and continuous encouragement throughout my years of study and through the process of researching and writing this thesis. This accomplishment would not have been possible without them.



Table of Contents

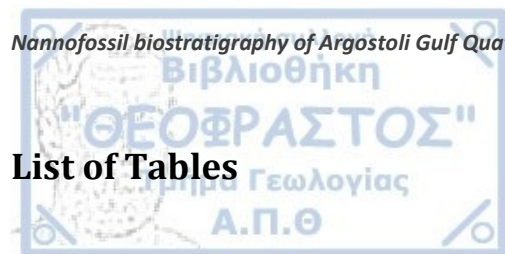
Abstract	1
Περίληψη.....	2
Acknowledgments	3
Symbols and Acronyms	6
List of Tables	7
List of Pictures	8
List of Figures.....	9
1. Introduction.....	10
1.1 Study Area	10
1.2 Research Scope.....	10
2. Geological Overview	11
2.1 The Geographical Position.....	11
2.2 Outer Platform of Hellenides.....	11
2.3 Pre-Apulian or Paxos unit	13
2.4 Tectonics and Stratigraphy of the Paxos unit.....	13
2.5 Geological setting of Kefallonia Island	16
3. Calcareous Nannoplankton	20
3.1 What are Coccolithophores?	20
3.2 The Biological Pump	20
3.3 Coccolithophores Cytology and Life Cycle.....	21
3.4 Biostratigraphy and Calcareous Nannoplankton.....	23
3.5 Calcareous nannofossil studies on Kefallonia Island	26
4. Odysseus Unbound Foundation	27
4.1 The Enigma and the Historical Background.....	27
4.2 Previous Research – Geoscience 2011-2014.....	29
5. Material and Methods.....	30
5.1 Sampling	30
5.2 Sample preparation	32
5.3 Laboratory Procedure.....	32
5.4 Micropalaeontological Analysis Procedure	35

6. Results	39
6.1 Livadi 1	39
6.2 Livadi 2	57
6.3 Livadi 4	83
7. Discussion	111
7.1 Reworked Coccoliths within Holocene	111
7.2 Biostratigraphy	112
7.2.1 Biostratigraphic Analysis of Livadi 1	112
7.2.2 Biostratigraphic Analysis of Livadi 2	113
7.2.3 Biostratigraphic Analysis of Livadi 4	114
7.3 Paleoenvironment	115
7.3.1 Paleoenvironmental Analysis of Livadi 1	115
7.3.2 Paleoenvironmental Analysis of Livadi 2	119
7.3.3 Paleoenvironmental Analysis of Livadi 4	121
7.4 Paleoenvironmental Correlation between the studied boreholes	123
8. Conclusions	125
Bibliography	126



Symbols and Acronyms

BC	Before Christ
AD	anno Domini
OUF	Odysseus Unbound Foundation
NTUA	National Technical University of Athens
NKUA	National and Kapodistrian University of Athens
Au	Aurum / Gold
Pt	Platinum
e.g.	For Example (exemplī grātiā)
i.e.	in other words (id est)
etc.	et cetera (and other similar things)
CaCO ₃	calcium carbonate
CO ₂	carbon dioxide
Na ₂ CO ₃	sodium carbonate
LM	Light Microscope
SEM	Scanning Electron Microscope
NW	Northwest
SE	Southeast
NE	Northeast
SW	Southwest
N	North
S	South
ENE	East-northeast
WSW	West-southwest
N	Haploid reproduction
2N	Diploid reproduction
V/R	vertical / radial structure
DSDP	Deep Sea Drilling Project
ODP	Ocean Drilling Project



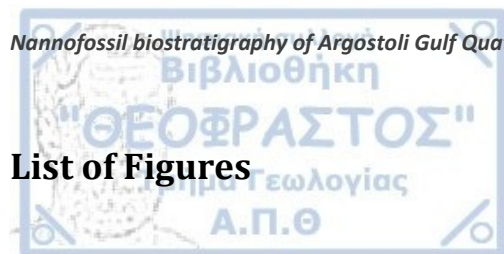
List of Tables

Table 1: SEM pictures from borehole Livadi-1:	48
Table 2: Table of borehole Livadi 1. Samples, depth, sample interval in every core. Calcareous nannoplankton that collected and identified in every sample, the biozonal indicators in each one and the biostratigraphic age. 56	
Table 3: SEM pictures from borehole Livadi 2:.....	74
Table 4: Table of borehole Livadi 2. Samples, depth, sample interval in every core. Calcareous nannoplankton that collected and identified in every sample, the biozonal indicators in each one and the biostratigraphic age. 82	
Table 5: SEM pictures from borehole Livadi 4:.....	98
Table 6: Borehole Livadi 4. Samples, depth, sample interval in every core. Calcareous nannoplankton that collected and identified in every sample, the biozonal indicators in each one and the biostratigraphic age.....	110



List of Pictures

Picture 1: Upper left picture – Livadi harbor site, beside Kastelli Hill. Bottom left picture – Aerial photograph of Livadi Gulf (from Underhill, 2008). Two right pictures – The drilling rig on a platform, for the drilling project in Livadi Gulf (2017, drilling project of OUF).....	30
Picture 2: Left picture – Drilling project in Livadi Gulf, right picture – Boreholes retrieved.....	32
Picture 3: Laboratory of Historical Geology and Paleontology Department of NKUA.	32
Picture 4: McLane wet Rotated Divider.	33
Picture 5: Whatman 111206 Polycarbonate Nuclepore Track – Etched Membrane Filter, 50mm Diameter, 0.2 Micron and on the right a petri dish.	34
Picture 6: On the left: C carbon based, electrically conductive, double sided adhesive disc, also known as Leit tab and on the right: a SEM Cylinder Specimen Mount (Stub).	34
Picture 7: SEM laboratory and on bottom picture, SEM in use for micropaleontological analysis.	36



List of Figures

Figure 1: Satellite map of Livadi Gulf, Kefallonia Island, Western Greece.	10
Figure 2: The stages of paleogeographic and geodynamic evolution of the continental terranes in the Hellenides (Papanikolaou, 2013).	12
Figure 3: Stratigraphic column of Paxos unit (Karakitsios & Rigakis, 2007.)	14
Figure 4: Geological map of Kefallonia and Western Greece (Bornovas and Rontogianni-Tsiabaou, 1983 and Underhill, 1989 modified by van Hinsbergen, 2006).....	16
Figure 5: a. Instrumental seismicity in the broader study area. b. Spatial distribution of the 2014 sequence with the use of an optimum local velocity model. (Kassaras et al., 2017)	18
Figure 6: Geological map of Kefallonia, NW Greece (Lekkas et al., 2016).	19
Figure 7: Geological structures of the Thinia valley and the Gulf of Livadi (Underhill, 2009).....	19
Figure 8: The biological pump.	21
Figure 9: Schematic representation of the cell structures of coccolithophores (on the left). On the right picture: Schematic illustration of coccolithophorid life cycles.	22
Figure 10: a. Summary of Neogene nannofossil biostratigraphic zonation schemes and bioevents. b. Pliocene and Pleistocene biozones and biohorizons (Backman et al. 2012).	25
Figure 11: Neogene calcareous nannofossil biozonation (modified from Backman et al. 2012 by Agnini et al. 2017).....	26
Figure 12: a. Livadi Gulf currently formed in a sub-Holocene valley and the presumed onshore line of a channel that links it to the offshore. b., c. Maps describing the depth to the Base Holocene unconformity in the Gulf of Livadi. The pictures show the previous regional surveys conducted in the area (from Underhill, 2008)	29
Figure 13: Geomorphological map of Kefallonia Island with the boreholes Livadi 1,2,3 and 4 (Karymbalis et al. modified)	31
Figure 14: Pliocene and Pleistocene biounits and biohorizons (Backman et al. 2012).....	37
Figure 15: Neogene calcareous nannofossil biozonation (modified from Backman et al. 2012 by Agnini et al. 2017).....	38
Figure 16: Diagrams of calcareous nannoplankton assemblages vs. core depth in borehole Livadi -1. First diagram shows the coccoliths in situ and the second the reworked coccoliths.	50
Figure 17: Diagrams of calcareous nannoplankton assemblages vs. core depth in borehole Livadi 2 (> 3%). First diagram: coccoliths in situ and second diagram: reworked coccoliths.....	77
Figure 18: Diagrams of calcareous nannoplankton assemblages vs. core depth in borehole Livadi 4. First diagram: coccoliths in situ and second diagram: reworked coccoliths.	102
Figure 19: Reworked coccoliths in boreholes Livadi 1, 2 and 4.....	111
Figure 20: Biostratigraphic age assignment for Livadi-1 borehole (cores 7 – 10).....	112
Figure 21: Biostratigraphic age assignment for Livadi 2 borehole (cores 7 – 10).	113
Figure 22: Biostratigraphic age assignment for Livadi 4 borehole (cores 7 – 10).	114
Figure 23: Paleoenvironmental Interpretation of Livadi-1 borehole.	118
Figure 24: Paleoenvironmental Interpretation of Livadi-2 borehole.	121
Figure 25: Paleoenvironmental Interpretation of Livadi-4 borehole.	122
Figure 26: Correlation graph of the four boreholes Livadi 1, 2, 3 and 4.	124

1. Introduction

1.1 Study Area

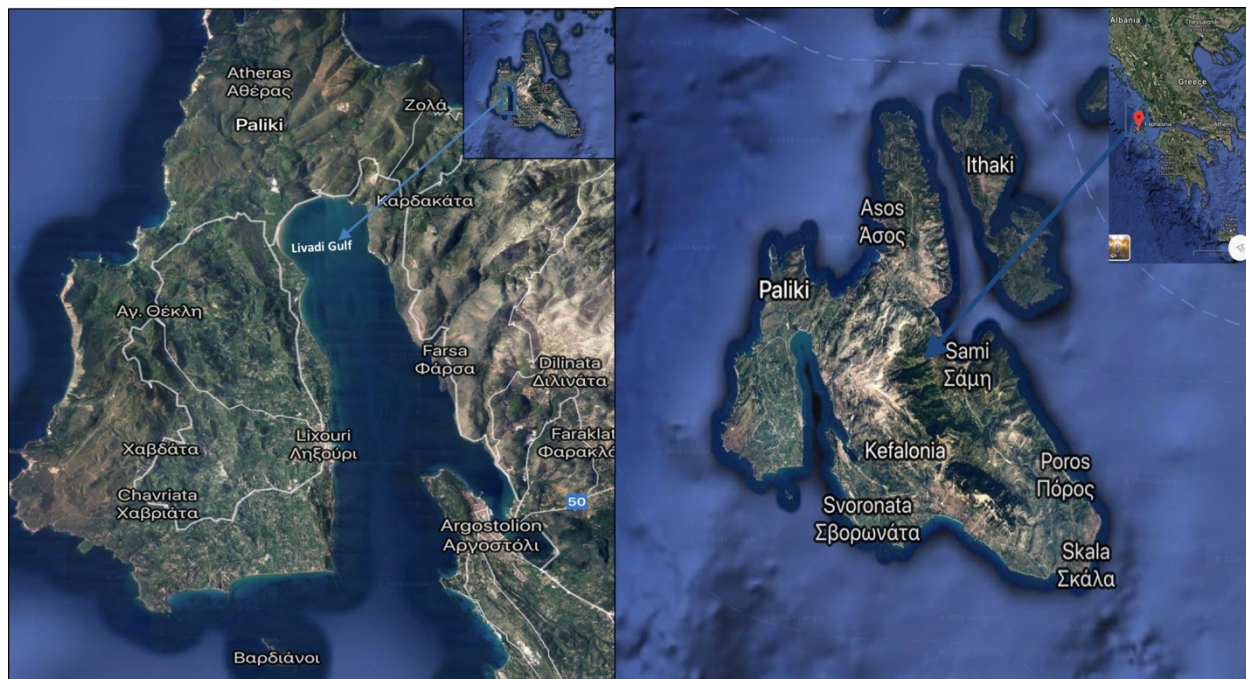


Figure 1: Satellite map of Livadi Gulf, Kefallonia Island, Western Greece.

The study area is Kefallonia, it belongs to the Ionian Islands complex of Western Greece. It is the largest of the Ionian Islands, with a total area of 808Km². Located south of Lefkas and Ithaki, north of Zakynthos and opposite the opening of the Corinthian / Patraikos Gulf. More specific, the area of study of this master thesis is defined in the Argostoli Gulf (in between Thinia, Paliki and Livadi areas) and our samples were retrieved from three boreholes. Kefallonia Island is located on the tectonic front of the Hellenic thrust and the geological structure of the upper crust includes the relative autochthon unit of Paxos, occurring on Paliki peninsula in the west and on the major part of the central Kefallonia, and the allochthon tectonic nappe of the Ionian unit, occurring along the eastern part (Papanikolaou et. al., 2013).

1.2 Research Scope

The present thesis is about the Quaternary marine sequence of Argostoli Gulf, in Kefallonia, Western Greece. The scope of our work is to contribute the hypothesis of Paliki, the peninsula on the western coast of Kefallonia, to be Odysseus' homeland of Ithaca, as described by Homer. The theory at the time being is based on the geographical position of Paliki, which is facing west, while the surrounding islands face east; it's the furthest out to sea of the group of Ionian Islands and it's lying lower. After years of study, it was realized that a marine channel could have separated Paliki from the main part of the island in the late Mycenaean age (around the 12th century BC) and it could have been filled in as a result of landslips from earthquakes and other major

tectonic events, turning the island into the peninsula we see today (Poulter et al., 2012, Gaki-Papanastasiou et al., 2011, Pirazzoli et al., 1994, Stiros et.al., 1994).

The main objectives of the present study are to date the Quaternary marine sequence from Livadi Gulf, to determine their relative age through detailed biostratigraphic assignment. Our investigations will provide us with a stratigraphic framework of the Quaternary formations and the careful micropalaeontological core analysis will give us all the important dates for when sea levels rose to fill the channel between Paliki and the rest of Kefallonia. Biostratigraphy is based on calcareous nannofossil analysis and biozonal scheme and subsequent ages. Calcareous nannofossil analysis will be conducted with light microscopy (LM) and under the scanning electron microscope (SEM), in order to justify the biostratigraphic age assignment of the study area.

Dating the sequence it is fundamental, because if our results can show what happened within the 3.200 years BC and that the marine channel still existed at the time, then Paliki was an island at the time of Odysseus and the theory about the landslip which made the peninsula today might be validated.

2. Geological Overview

2.1 The Geographical Position

The study area is located on the island of Kefallonia, which belongs to the external Hellenides and it consists of two different geotectonic units, with general direction NW – SE, the Pre – Apulian (Aubouin, 1959) or Paxos zone which extends to the west and the Ionian zone to the east. The Ionian zone is an overthrust nappe above the Paxos zone, (Aubouin 1962; Aubouin & Decourt, 1962, 1970; Bernoulli & Laubscher, 1972; Papanikolaou 1997, Underhill, 1989). Kefallonia Island is located on the tectonic front of the Hellenic thrust and represents the active plate boundary between the European and African plates, which is characterized of an oceanic and continental subduction (Papanikolaou, 2011). Paxos unit of the External Hellenides occupies most of the island of Kefallonia, unlike Ionian unit which only occupies a small area on the southeastern part of the island. Our study area is located on the western part of the island of Kefallonia and more specifically in Argostoli Gulf which subsequently means that the surroundings of the area belongs to the Pre – Apulian zone.

2.2 Outer Platform of Hellenides

According to Papanikolaou, (2013), there are two tectonostratigraphic models for the two distinctive types of terranes in the Hellenides, continental and oceanic, as they result from the general rifting, drifting, ocean opening and accretion of paleogeographic and geodynamic stages. These geodynamic phenomena have occurred inside or outside the Tethyan belt and apply the two tectono-stratigraphic models in the five continental (H1, H3, H5, H7 and H9) and four oceanic terranes (H2, H4, H6 and H8) of the Hellenides. Here, we are going to quote and describe the subduction, tectonics and stratigraphic history of Outer Hellenides.

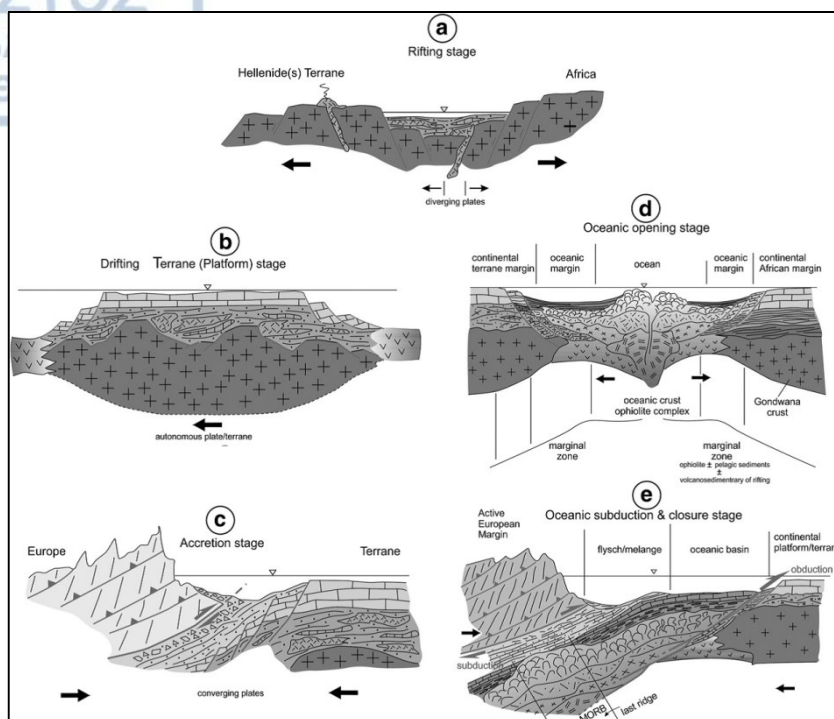


Figure 2: The stages of paleogeographic and geodynamic evolution of the continental terranes in the Hellenides (Papanikolaou, 2013).

The start of the major orogenetic phenomena of the alpine cycle began in the Hellenides, as well as in the rest of Tethys during the upper Jurassic – Lower Cretaceous. These events took place in the internal part of the Hellenic arc, are characterized as paleo-alpine and were fossilized under the Cenomanian transgression. Afterwards, the alpine cycle continued with the shallow – marine carbonate sedimentation on the site throughout the Upper Cretaceous, and during the Eocene closed permanently with flysch, and then the secondary orogenetic phenomena began during upper Eocene – Oligocene, where the alpine cycle was ended.

The geotectonic units of the Hellenic area were divided into Outer and Inner, mainly on the basis of the orogenetic tectonism that the formations of these units have undergone. More precisely, the External Units have undergone a single orogenetic tectonism during the Tertiary and occupy the western and southern parts of Greece, while the Internal Units, in addition to Tertiary tectonics, have also undergone an early orogenetic deformation, which took place during the Upper Jurassic – Lower Cretaceous, and occupy the eastern (inner) part of Greek territory.

In Outer Hellenides belong the following units with orientation from west to east: Paxos or Pre-Apulian units, Ionian unit, unit of Plattenkalk (tiled limestones), Phyllitic – Quartz unit, Gavrovos-Tripolis unit, the unit of Pindos or Olonos-Pindos unit, the submarine ridge units of Koziakas – Trilofos – Penterion – Geranion – Trapezonas, the units of the submarine trough Vardousia – Epidauros, Parnassos or Parnassos – Giona unit, Viotia unit and the new - Hellenic tectonic cover unit. Outer Hellenides are placed in Apulian microplate, which was detached from Gondwana and represent areas of continuous continental neritic sedimentation during the Alpine ages (Karakitsios & Rigakis, 2007).

Pre-Apulian unit (Aubouin, 1959) or Paxos unit (Renz, 1940) is characterized by a continuous carbonaceous sedimentation and the absence of typical flysch deposits, which is observed in the other units.

Ionian unit on the other hand, it is believed to be a submarine trough (Philippon, 1898) and according to Aubouin (1959) it's a geo-syncline. Gavrovos unit (Aubouin, 1959) or Gavrovos-Tripolitza unit (Dercourt, 1964) it is a ridge which separates the Ionian trough and the Pindos trough. As it was said before, Pindos unit, like Ionian unit it's a trench (Pindos is deeper than the Ionian) and those two units were characterized as geo-synclines.

2.3 Pre-Apulian or Paxos unit

Paxos unit is the most external unit of Hellenides, it was named after Paxos islands by Renz (1940) and it is characterized from the lack of typical flysch. Aubouin (1959), named the unit pre-Apulian, because it is the inner (eastern) margin of the Apulian unit, which responds in the form of an underwater platform in the southern Italian region. It is considered to be extended western in the Ocean of eastern Mediterranean, in the Ionian Sea (H0), before the recent subduction beneath Paxos Island and the rest of the platform H1. It is a ridge in Greece but it is considered also as a slope, and becomes a clear platform in the Apulian peninsula (South Italy) (Papanikolaou, 1989, 2009).

Pre-Apulian's thickness, as it has been documented by the terrestrial impressions and the drillings, it increases very significantly from north to south. In Paxos Island it is less thick and in Zakynthos island much thicker, while in Kefallonia it has an intermediate thickness. This explains the position of the Ionian Islands in relation to the continental slope. Zakynthos is near the Apulian unit, Kefallonia is in the middle of the slope and Paxos is near the Ionian basin.

Paxos unit is displayed, in Paxos island, Antipaxos, in the western section of Lefkada island, in Kefallonia and Zakynthos islands. The largest section of the Paxos unit it is certain that, it appears underwater in the Ionian Sea.

2.4 Tectonics and Stratigraphy of the Paxos unit

West of the Ionian islands, which are formed by both the Paxos and Ionian unit formations, is the Hellenic trench, along which we have the great movement of the Hellenic arc, which reflects the sinking of the northern margin of the African plate below the Eurasian plate. This movement, which for the Paxos unit stopped at the Miocene – Pliocene boundary, continues today by activating another surface, located several kilometers to the west (Papanikolaou, 1997, 2010).

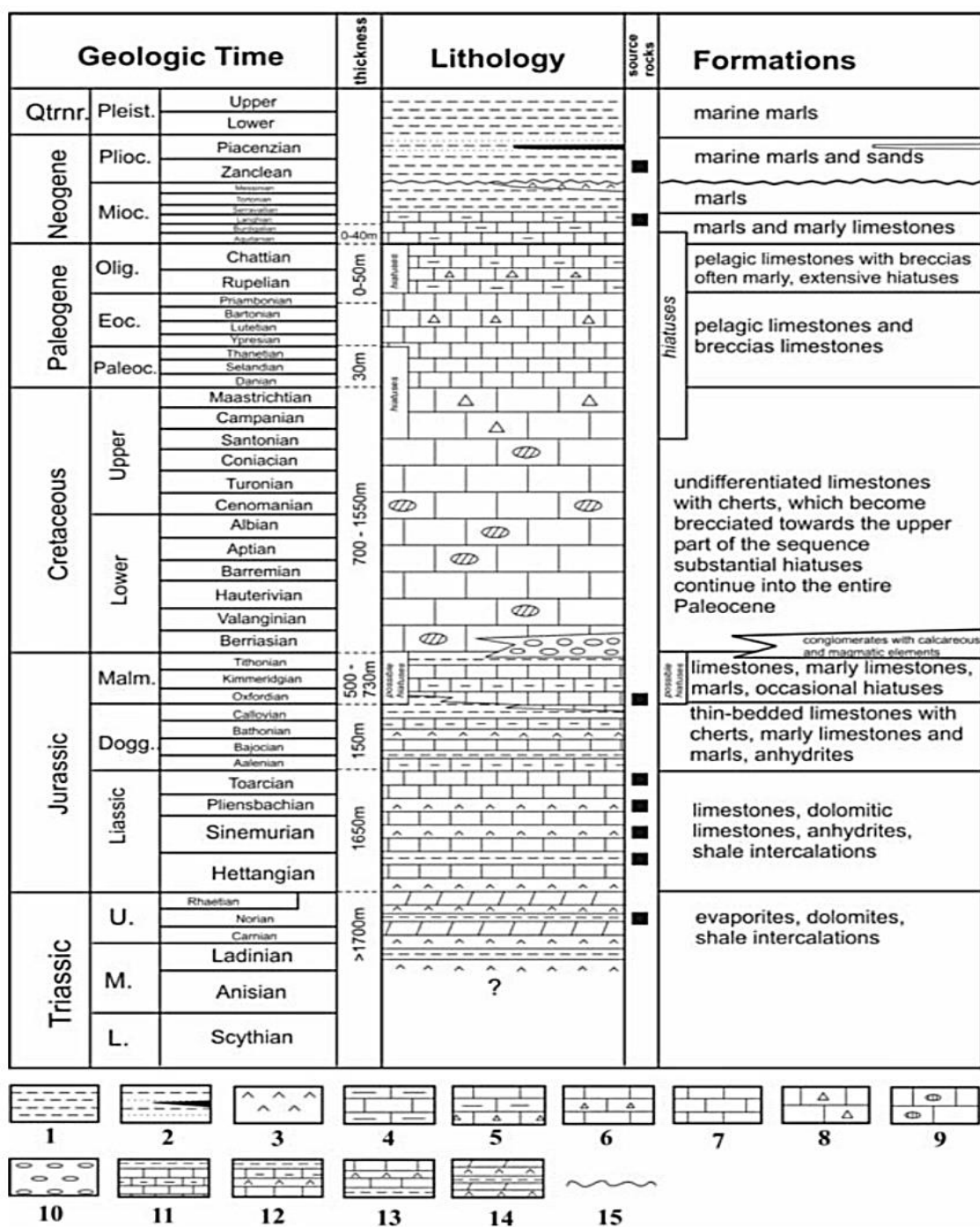
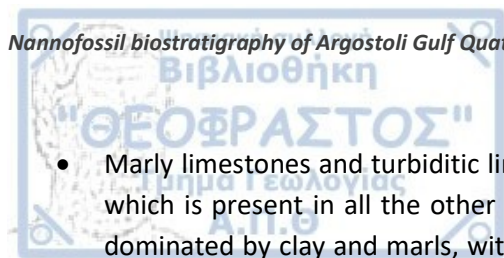


Figure 3: Stratigraphic column of Paxos unit (Karakitsios & Rigakis, 2007.)

Stratigraphically speaking, Paxos unit is a neritic carbonate sequence (Jurassic up to Miocene), with some disconformities in Paleogene (i.e. Zakynthos). The stratigraphic structure of the Paxos unit, from the newest to oldest stratigraphic horizons, is (Papanikolaou, 1997 and Underhill, 1988, 1989):



- Marly limestones and turbiditic limestones appear in the Aquitanian period, replacing the typical flysch, which is present in all the other geotectonic units. Paxos unit in Burdigalian and in Middle Miocene is dominated by clay and marls, without characteristic sandstone horizons and that is the reason why it is considered as the only unit of Hellenides that lacks a typical flysch.
- Oligocene and Eocene are represented by neritic limestones, which are similar to the limestones, of the Apulian unit, and they are characterized by alterations with micro-breccia limestones. All these limestones are rich in micro-fossils (*Globigerina*, *Nummulites*, *Orbitoides*, *Dscocyclus*, *Alveolina*).
- The carbonated sequence continues to the Paleogene (Oligocene, Eocene, Paleocene) and throughout the Cretaceous with deposition of neritic limestones and small breccias, with total thickness 1.500 meters, approximately.
- In more detail, the Upper Cretaceous is represented by neritic and reefal limestones with *Hippurites* and horizons with *Orbitoides*, *Globotruncana* (Maastrichtian).
- Continuing downwards, there are Upper Jurassic limestones and dolomites (*Clypeina* sp.) with insertions of slates and marls laminations. Their thickness is about 500 meters.
- Finally, evaporites, dolomites and neritic limestones, from Upper to Middle Jurassic age, are the oldest sediments of this unit and show a clear analogy with those of the Ionian unit. Their thickness is approximately 1.500 meters.

Pre-apulian or Paxos unit it is considered as the foreland of Hellenides. In the geotectonic map of Greece, the last overthrust is the one that brings Ionian unit on top of the Paxos unit, and it can be spotted in the perimeter of the Hellenic arc on the west. Paxos unit tectonism is taking place during Miocene and more specifically in Zakynthos and Kefallonia it is detected on the boundary of Pliocene – Miocene (Underhill, 1989). In Zakynthos the stratigraphic column ends with the Messinian gypsum and on top of that, is placed with tectonic contact, the Triassic gypsum of the Ionian unit in Scopos peninsula. In Zakynthos, a complete stratigraphic profile can be found of several hundred meters thick (Dermitzakis, 1978). In between the tectonism of the Messinian – Lower Pliocene strata and the Upper Pliocene – Middle Pleistocene strata (disconformity), there is a stratigraphic gap which is translated in 1 – 2 Ma (Papanikolaou et al., 2010).

This unit is characterized by high curvature folds and is considered autochthonous, while all other units of Hellenides are allochthonous. On the island of Kefallonia the faults and tectonic folds that have been observed, have direction NW – SE, NE – SW, N – S and ENE – WSW (Underhill, 1989). The main tectonic forms created during the phase of alpine deformation on the island are genetically linked to the placement of the Ionian nappe on the Paxos unit during the Lower Pliocene. These tectonic forms are (Underhill, 1989, Lekkas et al., 2001):

- inverted faults with direction NW – SE or SW – NE and folds with axes of the same orientation as in Paxos unit, which are considered to be older tectonic structures, which during the sedimentation period defined the various paleogeographic regions of Pre-Apulian platform. In some of these faults a horizontal movement component is observed besides the thrust (e.g. Agia Efimia SW of Oros Kalo, Ainos ridge),
- thrusts, anticlines are observed with direction NW – SE,
- gravity faults with NE – SW and E – W directions within the Ionian unit. Folds' axes and thrusts are parallel to the main tectonic surface of the Ionian overthrust on the Paxos unit. In the older tectonic forms of Lower Pliocene are added newer structures which are associated with the deformation episodes of the Pliocene – Pleistocene. These structures are called neotectonic forms and are mainly represented by the faults, which intersect all the geological formations of the island. There is a wide

variety of faults, with their upthrow ranging from a few meters to a few tens of meters and fault slump with vertical component and horizontal sliding.

The structure of Kefallonia is the result of series of successive tectonic depressions that are mainly compressive, but these structures have been interrupted by periods of solid rock decompression and gravitational phenomena corresponding to a tensile regime.

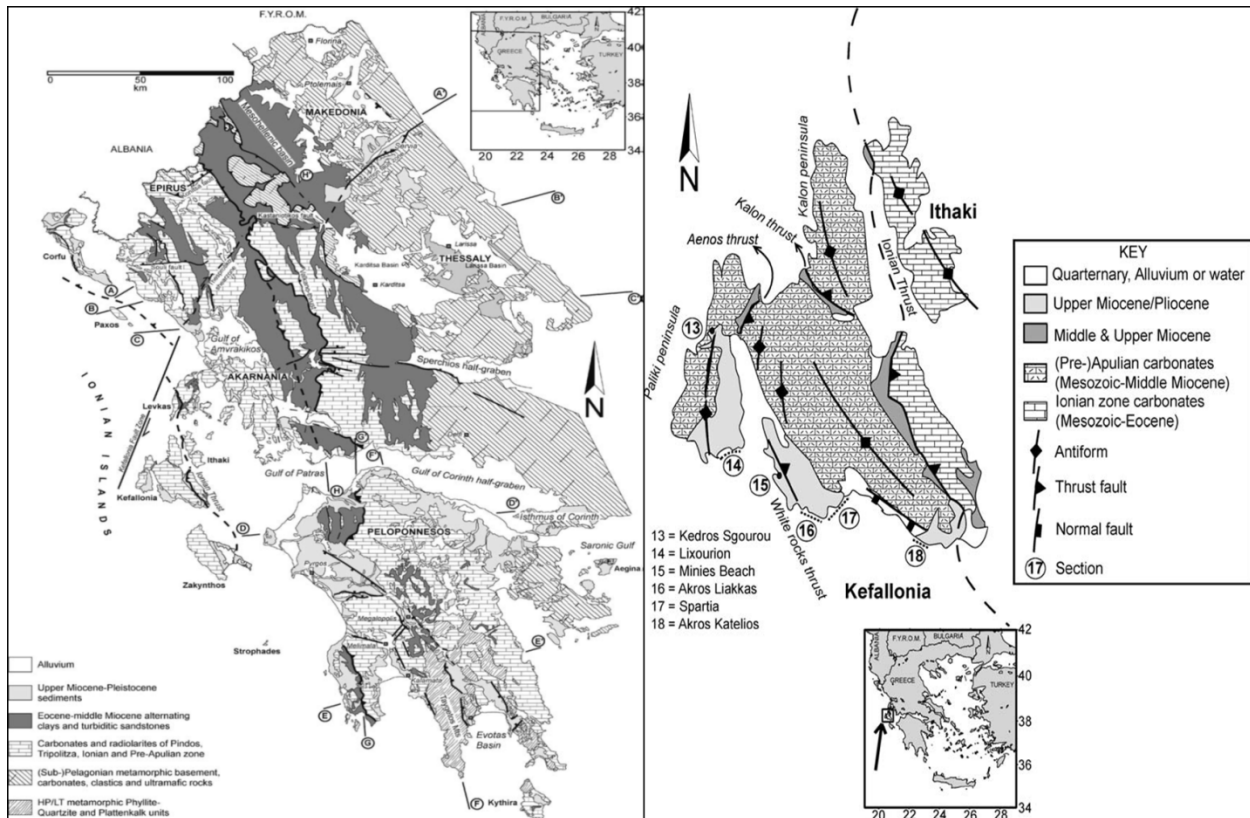


Figure 4: Geological map of Kefallonia and Western Greece (Bornovas and Rontogianni-Tsiabaou, 1983 and Underhill, 1989 modified by van Hinsbergen, 2006).

2.5 Geological setting of Kefallonia Island

In Kefallonia, the upper sections of the carbonate Paxos unit correspond to the Upper Jurassic - Lower Miocene period, as well as the clay-clastic flysch that is the continuation of the Paxos stratigraphic column (Middle Miocene - Lower Pliocene). This clastic flysch consists of marbles with intrusions of sandstones, clays, slender breccia and conglomerates and its thickness is several hundred meters. The flysch appears on Paliki peninsula, in the area of Argostoli bay and Katelli bay, with Langhian – Messinian age (BP Co., 1971).

The meta-alpine formations are placed unconformably on the alpine ones. There is a lower sequence of Lower Pliocene – Lower Pleistocene marine sediments with age Lower Pliocene – Lower Pleistocene and an upper sequence of continental deposits, which is placed unconformably on the former ones (Middle, Upper Pleistocene - Holocene) (BP Co. 1971,; Sorel 1976,; Underhill 1985, 1989; Triantaphyllou, 1996; Triantaphyllou et al., 1999; Papanikolaou and Triantaphyllou, 2013).

The Plio-Calabrian sequence is a marine sequence that extends over the formations of Paxos Unit. Its width is between 2 and 10 kilometers and its thickness is between 200 and 500 meters. This sequence consists

of horizons of conglomerates and breccia (Lower Pliocene), limestones and calcarenites, marbles, marly conglomerates in its intermediate part (Middle to Upper Pliocene) and in the upper part of the sequence (Pleistocene - Calabrian), marbles and grained calcarenites (BP Co., 1971). The Plio-Calabrian sequence it consists of Middle to Upper Pleistocene - Holocene formations. It is found mainly in the Argostoli Peninsula – Airport (Lekkas et al., 2001).

The main tectonic forms that created during the alpine deformation phase are genetically linked to the placement of the Ionian cover over the Paxos Unit (Lower Pliocene). These forms are inverted faults with direction NW-SE or SW. They are considered to be the oldest tectonic structures that defined the various paleogeographic areas during the sedimentation (Agia Efimia faults, Aenos ridge). Other forms are tectonic thrusts, anticlines, gravity faults with NW-SE and E-W directions within the Ionian Unit, axial folds and thrusts (Underhill, 1989). In the former tectonic forms of Lower Pliocene are added newer structures which are associated with the deformation of the Plio-Pleistocene episodes. These forms are called neotectonic forms (Lekkas et al., 2001).

Kefallonia Island according to the geomorphological research and mapping of the area (Karymbalis et al., 2013; Gaki-Papanastasiou et al., 2010) consists of the following geomorphological features: drainage networks, karst landforms, planation surfaces, gravitational landforms and changes in coastal geomorphology. As far as the drainage system is concerned, the water originates from the main mountain of Kefallonia, which is Aenos, and occupies the central part of the island, with direction NW-SE. The drainage system is fully developed in the eastern part of the island and the main flow of the channel is controlled by lithology, faults and upthrusts.

Kefallonia Island is karstified with the presence of dolines, poljes, sinkholes and caves. Karst landforms occur in association with the highly soluble carbonate rocks of Cretaceous age (Gaki-Papanastasiou et al., 2011). The most notable karsts are the Valsamata and Trogianata poljes. Smaller karsts are located north of the Argostoli Gulf and in the central part of the Erissos Peninsula. Karst fill sediments tend to be a mixture of terra rossa and high-energy fluvial deposits. Caves are widely distributed over the island particularly in the broader area of Sami and southeast of Argostoli.

The planation surfaces were formed by the combined action of erosion and dissolution and their development probably reflects the gradual tectonic uplift of the island (Underhill, 1989). Around Aenos Mountain several planation surfaces were located at different elevations ranging from 100-1300 meters (Karymbalis et al., 2013). The gravitational landforms were recognized in northern Kefallonia and probably triggered by a strong earthquake (normal NE – SW fault, Zola village). The nearby slope of the mountain sides played a major role in causing this landslide. This mass wasting event occurred some hundreds of years or a few thousand years ago (Gaki-Papanastasiou et al., 2011).

The western coast of the Paliki peninsula is steep comprising limestone cliffs and the eastern coast of Paliki is characterized by much lower slopes and sandy beaches. In the Paliki Peninsula, as well as along the southern coast of the main island, several uplifted geomorphological features were recognised, including marine terraces, notches, beachrocks and aeolianites. The uplifted Quaternary marine terraces are excellent morphological markers and have been used worldwide to recognize past sea-level changes.

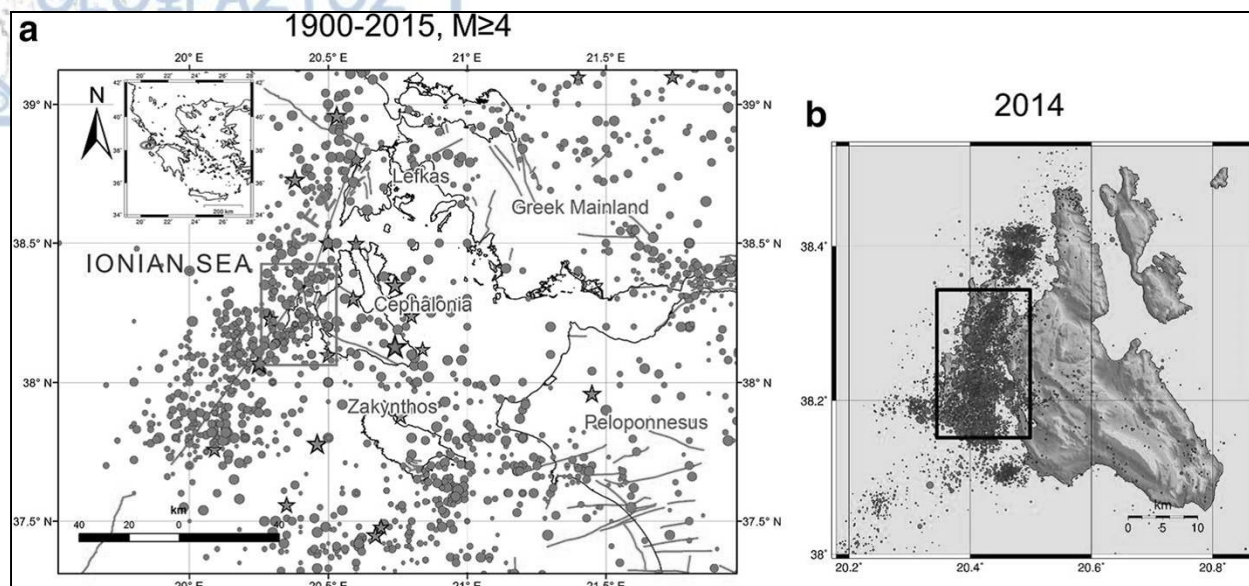


Figure 5: a. Instrumental seismicity in the broader study area. b. Spatial distribution of the 2014 sequence with the use of an optimum local velocity model. (Kassaras et al., 2017)

The area of Kefallonia, constitutes the most active unit of shallow seismicity in the Aegean and its surroundings. This area is one of the most active deforming in the Alpine – Himalayan belt, with the subduction of the eastern Mediterranean oceanic lithosphere under the Aegean along the Hellenic Arc. The microseismicity recorded in the area, provided the means of identifying secondary active structures and their geometric and kinematic properties. Although the particular structures are of smaller lengths than the ones associated with the stronger events in this region, they are capable to accommodate moderate events (Karakostas et al, 2010).

To the north – west edge of the island, the uplift seems to be bordered to the west by the Livadi Thrust, the only major fault to be active in the Upper Quaternary in the area. This thrust extends to the south, and can be identified with the Gulf of Argostoli Thrust. The discontinuity in the seismic data implies a structural discontinuity along the gulf. The eastern boundary of seismic uplift (Earthquake of 1953), correlates with the Agia Efimia Fault. The discontinuity in seismic intensities along south – west Ithaki and Kefallonia implies a discontinuity along these straits.

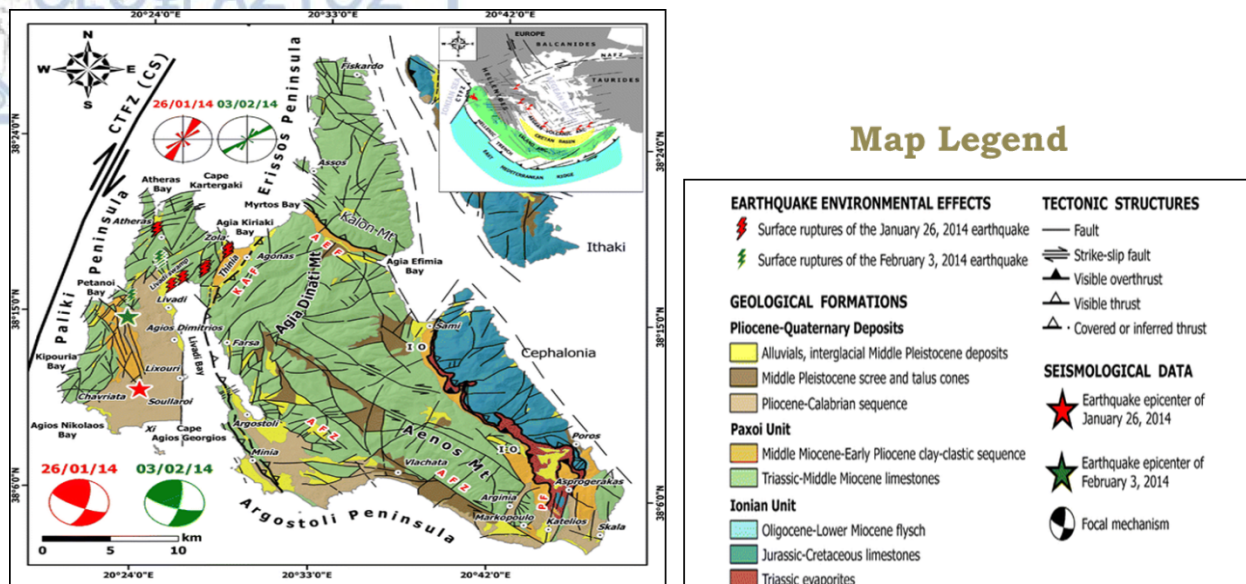


Figure 6: Geological map of Kefallonia, NW Greece (Lekkas et al., 2016).

The former geophysical research in the area of Kefallonia, concludes in frequency range between 0.7 – 17 Hz, which is clearly classified in two belts, a low (0.7–4 Hz) and a high one (5–17 Hz) (Kassaras et al., 2017). These observations clearly imply that there are two types of soils with different elastic properties. The high frequencies (Paliki Peninsula) were combined with low amplification correlate with damage in the hardest hit areas. Low frequencies are aligned in a NNE – SSW direction in the epicentral area, which is similar to the area of the activated fault, indicating that the properties of rocks along the fault unit have possibly been affected by slippage and dynamic effects (Karakostas et al., 2014). The most recent significant earthquake was in January 2014 and caused widespread damage. It pushed up the land at the top of the Gulf of Livadi by 20cm.

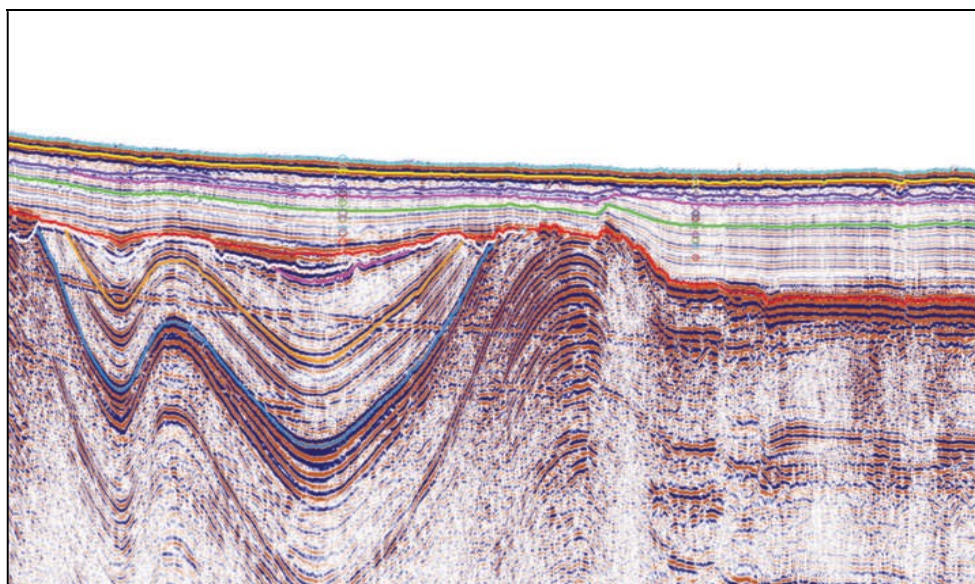


Figure 7: Geological structures of the Thinia valley and the Gulf of Livadi (Underhill, 2009).

According to geophysical surveys, which are shown above on the seismic reflection profile from the Gulf of Livadi, show a pronounced buried erosional surface (marked in red) that separates the deformed Cenozoic sediments from the Late Quaternary and Holocene transgression that flooded the channel. These data permit onshore folds and thrust faults to be traced beneath the bay. Finally, the data have shown the re-activation of the Late Cenozoic structures which have been seen beneath the bay, suggesting that during co-seismic events, tectonic strain is highly localized on the Aenos Thrust that runs along the eastern side of the Gulf of Livadi and Thinia valley, triggering the largest rockfall events (Underhill, 2009).

3. Calcareous Nannoplankton

3.1 What are Coccolithophores?

Calcareous nannoplankton is a group of modern micro-organisms, smaller than 50 microns (μm), have calcareous composition and marine phytoplankton origin. This group is included in calcareous nannofossils, with other organisms such as calcareous dinoflagellas, coccoliths, nannoliths and incertae sedis. Calcareous nannoplankton represents a major component of oceanic phytoplankton and their first records are from the Late Triassic. Their calcareous skeletons can be found in fine-grained pelagic sediments in high concentrations and the biomineralization of coccoliths is a globally significant rock-forming process.

In modern taxonomy coccolithophores/ calcareous nannoplankton belong in the phylum *Haptophyta* and division *Prymnesiophyceae*. Coccolithophores are marine unicellular, eukaryotic phytoplankton (algae) and photosynthesizing flagellate organisms, which have a filamentous appliance (haptonema), similar to flagella and consist of calcite plates (coccoliths). Coccoliths, at some stage in their life function as a protective armor that eventually falls to the ocean floor to build deep-sea ooze and fossil chalks. They are abundant in sea-floor sediments above the calcite compensation depth (CCD) and preserve the photic zone communities due to sedimentation in the faecal pellets of zooplankton or in marine snow.

3.2 The Biological Pump

The biological pump is the ocean's biological sequence of carbon cycle from the atmosphere to the ocean interior and seafloor sediments. It is the part of the oceanic carbon cycle responsible for the cycling of organic matter formed mainly by phytoplankton during photosynthesis, as well as the cycling of calcium carbonate (CaCO_3) formed into shells by certain organisms such as plankton and mollusks.

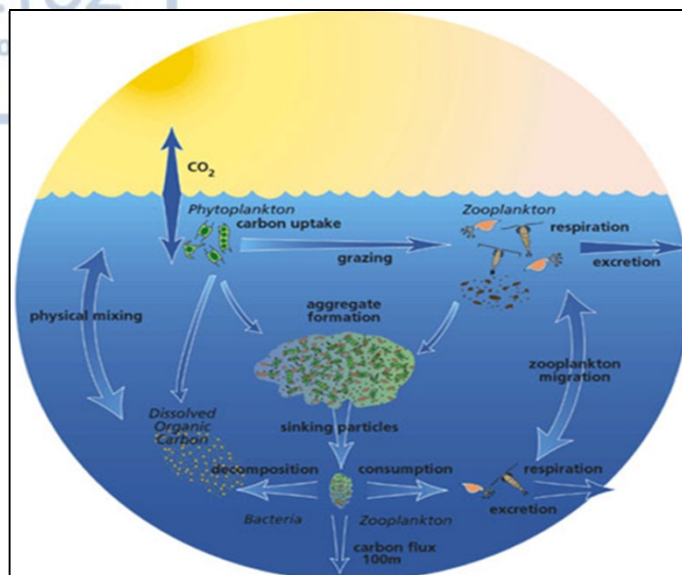
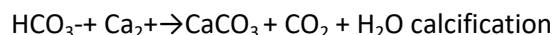
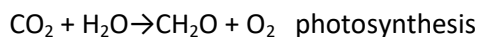


Figure 8: The biological pump.

Coccolithophores play the most important role in carbon cycle because they use carbon dioxide to produce organic matter (through photosynthesis) and they produce CO_2 by the calcification of coccoliths.



The oceans are the main carbon reservoir and the most interesting thing nowadays is the dynamic exchange of this, between the ocean and the atmosphere. Carbon when is entering the ocean is involved in the cycle of biogenic elements. It is calculated that every year, coccolithophores absorb 80% of carbon and as the main primary producers, convert the dissolved CO_2 into CaCO_3 (calcium carbonate). Coccolithophores, as organisms with high reproduction rates, are considered to be one of the main carbonate sediment production groups.

3.3 Coccolithophores Cytology and Life Cycle

Most common coccolithophores are autotrophic but they can be heterotrophs under certain environmental conditions. They are restricted to the photic zone of the water column (0 – 200 m depth). The algal cell is generally spherical and includes two golden-brown pigments, a nucleus, two flagella of equal length and a haptonema, which as we said before is a filamentous appliance, mitochondria, vacuoles and the Golgi body which is the site of coccolith secretion in many species. In some living genera there is also an alternation between a motile and a non-motile stage. The first one has a flexible skeleton with coccoliths embedded in a pliable cell membrane and in the non-motile stage; the calcification of the membrane forms a rigid shell called a coccosphere. Coccoliths are composed of calcium carbonate in the form of calcite with a low amount of magnesium and sometimes aragonite.

It is believed that haplo-diploid life cycles are widespread in haptophytes and that different phases carry different coccoliths. For coccolithophores only limited data is available from culture studies. There is also a

complicated pattern of motile and non-motile stages and development of different cell coverings. Both phases usually produce coccoliths but with different biomineralisation processes there are differences in structure.

Coccolithophores in both types of cells, diploid (2N) or haploid (N), have as main reproductive process an asexual procedure which is called mitosis. Mitosis is an asexual cell division and results in the production of two daughter cells from a single parent cell. The daughter cells are identical to one another and to the original parent cell. In a typical animal cell, mitosis can be divided into four principal stages: Prophase, Metaphase, Anaphase, Telophase and Cytokinesis. Other reproductive processes that coccolithophores prefer are meiosis and syngamy (sexual procedure). Meiosis is the first stage of sexual reproduction where daughter cells have only one version of each chromosome and eventually followed by syngamy.

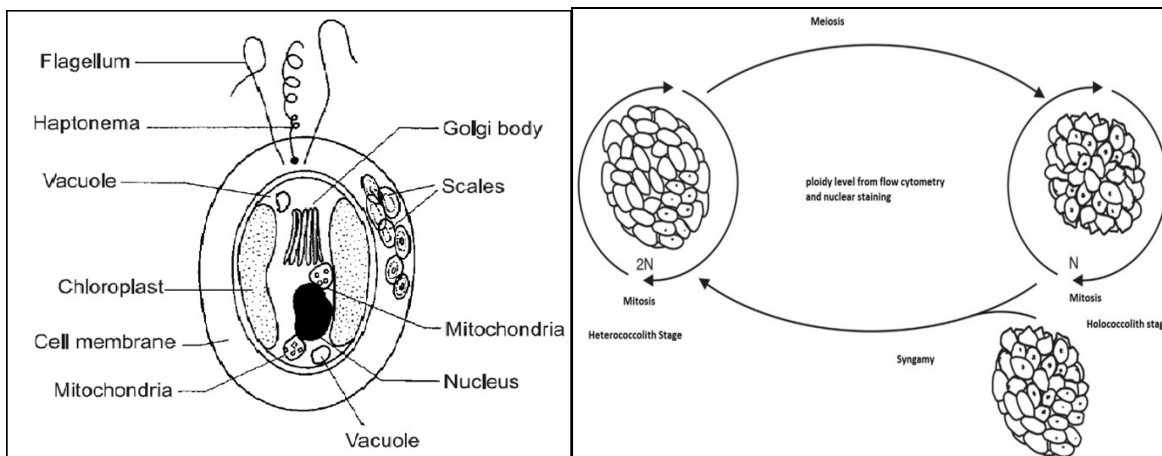
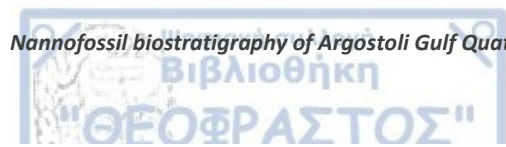


Figure 9: Schematic representation of the cell structures of coccolithophores (on the left). On the right picture: Schematic illustration of coccolithophorid life cycles.

In diploid stages may be motile or non-motile, biomineralisation occurs intercellularly and produces heterococcoliths (calcification). Coccoliths are exocytosed and arrange around the cell and form a composite exoskeleton, the coccosphere. There are three stages in coccolith growth, first is the formation of an organic baseplate, then the protococcolith ring which is a cycle of simple crystals around the margin of this baseplate (primary nucleation) and at last is the growth in three dimensions, the fully-formed coccolith. In all cases coccolith growth occurs in Golgi vesicles. Heterococcoliths are circular to elliptical discs constructed by one or more radial arrays and complex crystal units. This disc is called rim and encloses a central area which might be open, closed or with a variety of structures (e.g., central area with a bridge like *Gephyrocapsa* spp.). The rim would be a wall-like (murolith), a tube which separates two subhorizontal shields (placoliths) or a rim showing normal V/R (vertical / radial) structure, but with the proto-coccolith ring embedded within the rim (with no elevated rim – planolith).

Haploid stages are motile and the biomineralisation takes place extra-cellularly and as a result produces holococcoliths which are formed of numerous, calcite crystallites. Holococcolith formation has been less studied in comparison with heterococcoliths. From studies it is known that *Coccolithus pelagicus* produces *Crystallolithus hyalinus* holococcoliths in an alternate, motile, life-cycle stage, and *Calyptrosphaera sphaeroidea* is only known to produce holococcoliths. There are other species that have been observed to form combination coccospheres such as *Algirosphaera robusta* with holococcolith *Sphaerocalyptra quadridenta*. In the first two species above, (*C. pelagicus* – *C. hyalinus* and *Calyptrosphaera sphaeroidea*) the holococcoliths have well developed organic baseplate scales and separate body-scales. These scales can be observed forming in Golgi vesicles but the holococcoliths themselves have never been observed inside the cell. Holococcoliths have the shape of a disc or they are typically dome-shaped, with crystallites of simple form. Compared to heterococcoliths, holococcolith morphologies are more conservative, and the division between rim and central-area structures is not well



defined. The very different formation mechanisms of holococcoliths and heterococcoliths suggest that there may be only limited equivalence between them. Holococcolith crystallites are arranged in precise geometric arrays clearly showing that the location of nucleation is precisely controlled. In the same manner, individual crystallite faces are aligned, so crystal orientation must also be precisely regulated.

There is also a third group in calcareous nannoplankton, in which there are organisms with a heterogeneous morphology, including a wide range of shapes and structures, the nannoliths. Most of them show some of the features of heterococcoliths, such as rotational symmetry, complex crystal-unit shape and plate-like and disc-like shape. But they are all sufficiently different, which makes their relationship with coccolithophores uncertain. It is almost certainly a contrived grouping of nannoliths in the same category as coccoliths, but many nannoliths may prove to be modified heterococcoliths evolved from a range of ancestors (for example, *Nannotetrina*, *Discoaster*, *Florisphaera*). Others may perhaps be modified holococcoliths (such as *Ceratolithus*); still others may prove to have been formed by haptophytes with calcification mechanisms unrelated to either mode (e.g. *Braarudosphaera*, *Nannoconus*). Today, when there is a description of coccoliths / nannoliths it is always a distinction between them, but probably that doesn't mean that there is a real taxonomic difference between them.

To sum up, the process of creation, formation and development of coccoliths is called Coccolithogenesis. In the heterococcoliths, the Coccolithogenesis occurs inside the cell and then the coccoliths are extruded towards the outside of the cell. As for holococcoliths, they develop in a completely different way, in which the calcification is achieved externally of the cell, but always within the periplast.

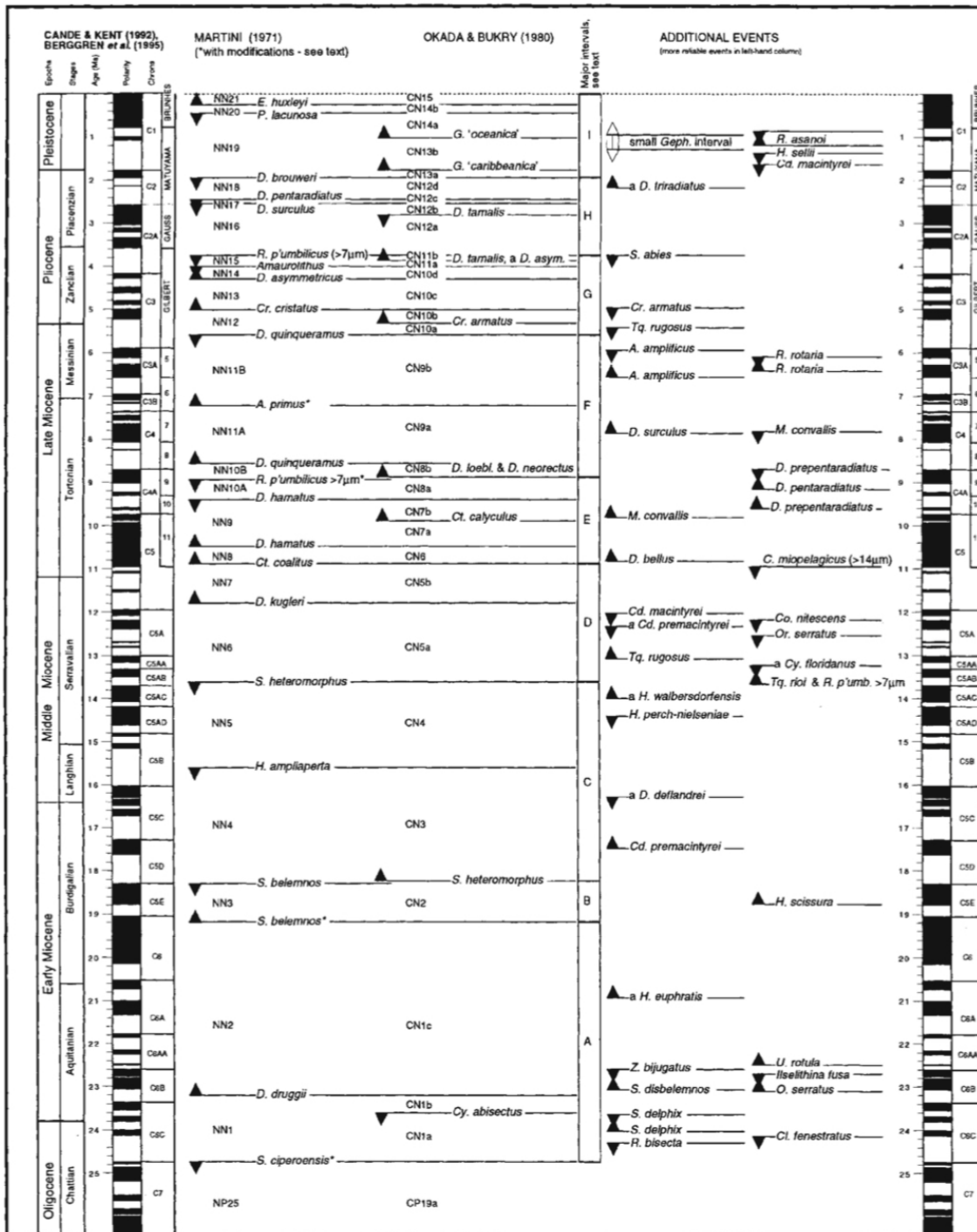
3.4 Biostratigraphy and Calcareous Nannoplankton

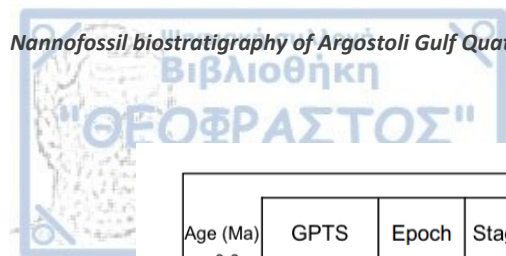
Nannofossils are exceptional biostratigraphic biomarkers since they are abundant, planktonic, rapidly evolving and largely cosmopolitan (Bown, 1998). Also, their small size and their rapid sample preparation procedure mean that they can be studied immediately after any sampling. Their biostratigraphic potential was first understood in the 1950s and was initially applied in Cenozoic studies (Bramlette and Riedel, 1954) leading to the standard zonation of Martini (1971). Their value in biostratigraphy was recognized by hydrocarbon exploration, DSDP (Deep Sea Drilling Project) and ODP (Ocean Drilling Project). Nannofossil zonations now provide one of the standard biochronological references for the Cenozoic, with biostratigraphic resolution of between one million and sixty-thousand years (Bown, 1998).

The huge volume of data on the stratigraphic distribution of nannofossils is synthesized in a number of relatively stable biostratigraphic zonation schemes covering the range of nannofossils (notably Martini, 1971; Sissingh, 1977; Okada and Bukry, 1980; Bown et al., 1988). The biozonation is based on first and last occurrences of species, in addition to abundance based events. A biostratigraphic unit, or biozone, is a body of strata that are defined on the basis of its unique content, sequential distribution, absence of fossils (Backman et al, 2012). Backman et al., (2012), compiled Miocene through Pleistocene data in order to establish a basic biostratigraphic framework for relative dating of marine sediments using calcareous nannofossils. This work was based on Martini's and Bukry's biohorizons that they used for zonal boundary definitions. Some biohorizons and zonal boundaries have proven to provide consistent results, however several of their zonal boundary defining biohorizons, however, have proven less practical and explained the need for a revised biozonation (Backman et al., 2012).

To sum up, it's important to understand that the fundamental units in biostratigraphy are the biozones. These are bodies of strata that are characterized on the basis of their contained fossils. The Base and Top of

each biozone is defined by biohorizons, which include any change in features related to the content and distribution of fossils in strata (Agnini et al., 2017).





b.

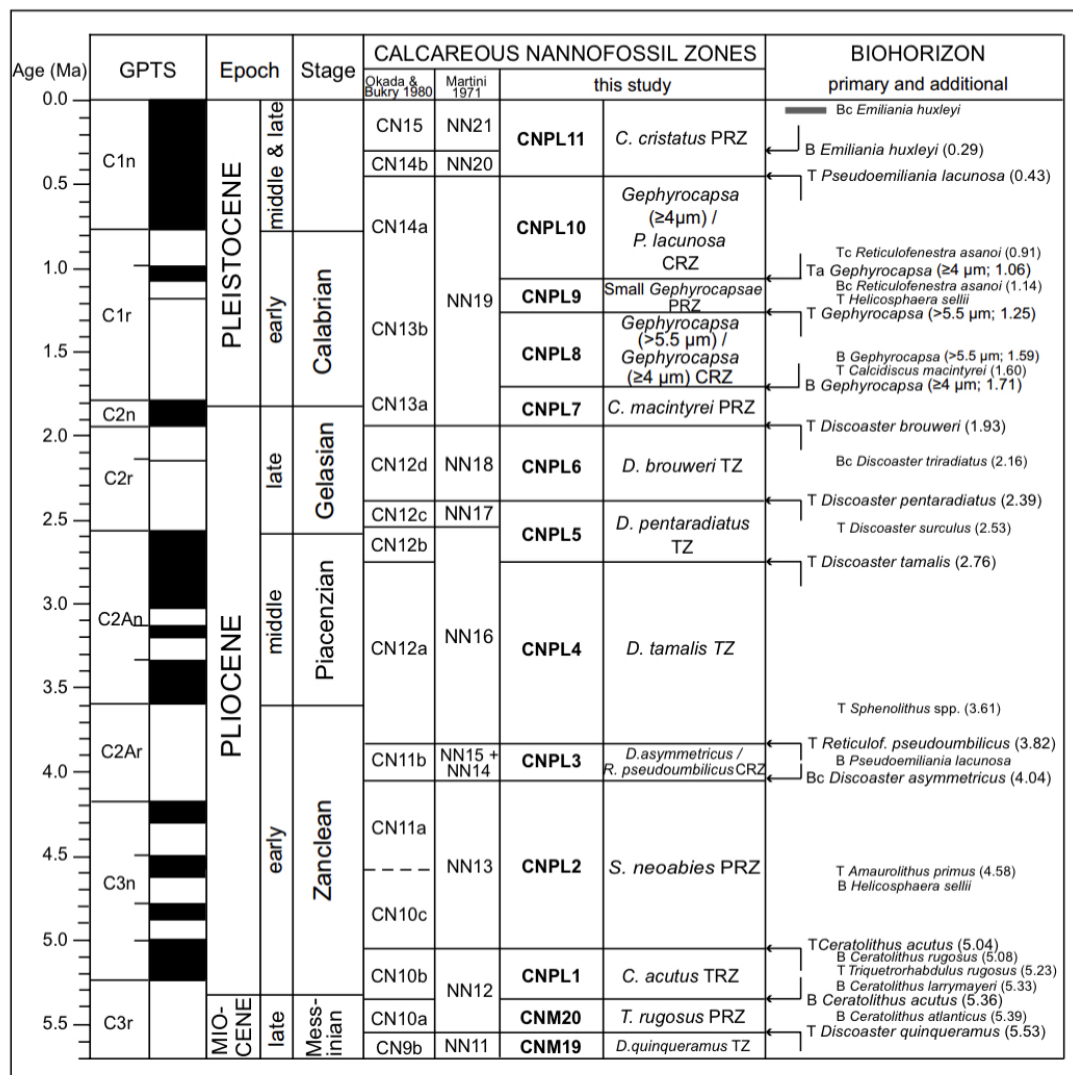


Figure 10: a. Summary of Neogene nannofossil biostratigraphic zonation schemes and bioevents. b. Pliocene and Pleistocene biozones and biohorizons (Backman et al. 2012).

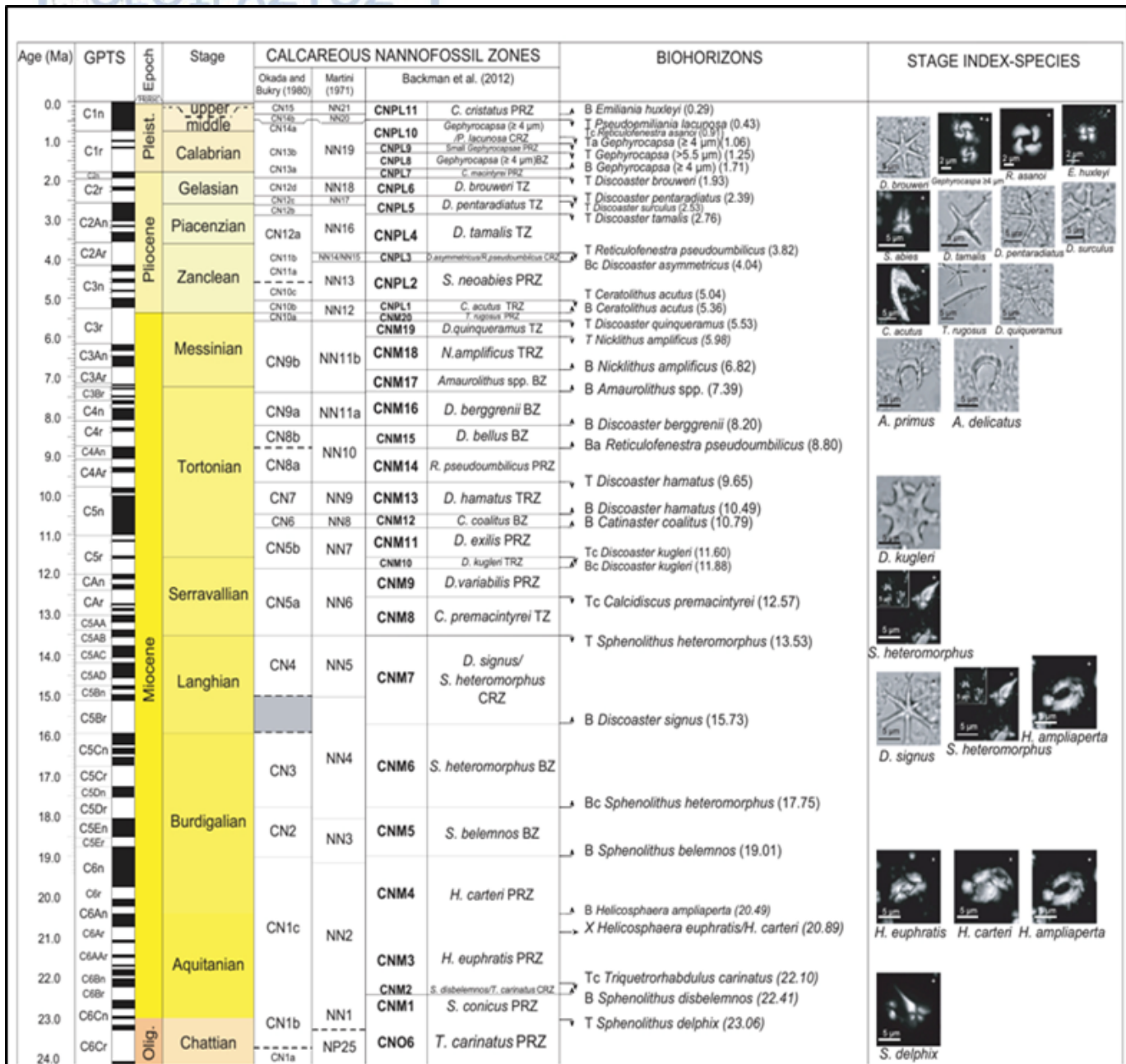


Figure 11: Neogene calcareous nannofossil biozonation (modified from Backman et al. 2012 by Agnini et al. 2017).

3.5 Calcareous nannofossil studies on Kefallonia Island

According to previous research in Lofos area (Paliki peninsula, SW Kefallonia), the biostratigraphic and paleoenvironmental data suggest the MNN19a biozone (uppermost Pliocene) due to the total absence of discoasterids, the abundance of transitional forms of *Gephyrocapsa* and the presence of *P. lacunosa*. Further biostratigraphic analysis points to biozone MNN19b, due to the presence of medium sized and transitional types of gephyrocapsids. The rest of Lofos section, including also the unconformably overlying calcarenitic beds, can be assigned to Pleistocene (Triantaphyllou et al., 1999). The first presence of *Gephyrocapsa* spp. >4μm, indicates

the boundary of biozone MNN19-MNN19b, which corresponds to the Gelasian-Calabrian boundary (Triantaphyllou, 1996; Triantaphyllou et al., 1999).

Other biostratigraphic investigations in Kefallonia Island, which were based on calcareous nannofossil, indicate to the following conclusions. In the base of the succession we have marls of Gelasian age (MNN18 biozone) followed by marls of Gelasian to Calabrian as well as Middle Pleistocene age, MNN19f. There are also, sandstone beds that form two discrete marine terraces. The older one can be found in southern Paliki Peninsula. The younger terrace can be located in Cape Kounopetra and Lyxouri area. Another example of two marine terraces can be found in the southern coast of Central Kefallonia. The base of the older terrace is of Calabrian age (MNN19c). The marls right below the sandstones of the younger terrace are of Middle Pleistocene age (MNN19f), equivalent to the younger terrace of Paliki. The biostratigraphic age assignment was based on the evaluation of calcareous nannofossil assemblages (Papanikolaou & Triantaphyllou, 2013).

4. Odysseus Unbound Foundation

Odysseus Unbound project was founded by Robert Bittlestone. Robert Bittlestone had an idea about the location of Ithaca, the homeland of Odysseus described by Homer in the Odyssey. In 2003, the British businessman, realized that a marine channel could have separated Paliki from the main part of the island in the late Mycenaean age (around the 12th century BC) and it could, subsequently, have been filled in as a result of landslips from earthquakes and other major tectonic events, turning the island into the peninsula we see today. Following exhaustive research in collaboration with leading scholars and other experts, he was able to match a series of locations on Paliki that fit with Homer's description of Odysseus' return home, including his palace and its harbor. Robert Bittlestone was also, the lead author of "Odysseus Unbound: The Search for Homer's Ithaca" and with the assistance of Professor James Diggle of Cambridge University and Professor John Underhill of the University of Edinburgh, put forth the theory that Paliki peninsula of Kefallonia is the location of Homer's Ithaca.

The Odysseus Unbound Foundation was formed in 2017. It was built upon the inspiration of the late R. Bittlestone whose innovative ideas, are showing significant promise. The Foundation is an educational charity dedicated to advancing knowledge of the ancient world. Specifically, OUF conduct and promote scientific and historical research to discover the actual locations of historical sites that have been described in ancient literature such as Homer's Odyssey.

4.1 The Enigma and the Historical Background

Homer's description of Ithaca in the Odyssey puzzled and confused scholars and scientists for centuries. The geography of the modern day Ionian island of Ithaki it doesn't fit to the description. Today's islands of Ithaki and Kefalonia lie to the west of mainland Greece, with Lefkas to the north and Zakynthos to the south. In Odyssey, Homer is describing Ithaki as an island, but in Iliad says the people who lived there are the Kephallenians.

In Odyssey, after many adventures, Odysseus found himself in Kerkyra and was saved by Nausika, the daughter of the king Alkinoos. The king of Pheaces (Scheria – Kerkyra), Alkinoos, treated Odysseus as custom and laws of hospitality commands (Filoxenia), and after a few days, asks Odysseus to finally, introduce himself.

Thus according to Odysseus's presentation of himself and his homeland, in rhapsody I (ι) and verse: 20 – 35, he explained where Ithaki was:

«εἴμ' Ὀδυσσεὺς Λαερτιάδης, ὃς πᾶσι δόλοισιν
ἀνθρώποισι μέλω, καί μευ κλέος οὐρανὸν ἵκει. 20
ναιετάω δ' Ἰθάκην εὐδείελον· ἐν δ' ὄρος αὐτῇ.
Νήριτον εἰνοσίφυλλον, ἀριπρεπές· ἀμφὶ δὲ νῆσοι
πολλαὶ ναιετάουσι μάλα σχεδὸν ἀλλήλησι,
Δουλίχιόν τε Σάμη τε καὶ ὑλήεσσα Ζάκυνθος.
αὐτὴ δὲ χθαμαλὴ πανυπερτάτῃ εἰν ἀλὶ κεῖται 25
πρὸς ζόφον, αἱ δέ τ' ἄνευθε πρὸς ἥϊω τ' ἡέλιόν τε,»

*"I am Odysseus, Laertes' son, world-famed
For stratagems: my name has reached the heavens.
Bright Ithaca is my home: it has a mountain,
Leaf-quivering Neriton, far visible.
Around are many islands, close to each other,
Doulichion and Same and wooded Zacynthos.
Ithaca itself lies low, furthest to sea
Towards dusk; the rest, apart, face dawn and sun."*

According to Homer's narration, Ithaki should be the furthest out to sea and face towards dusk (i.e. west) and the adjacent islands should face towards the dawn and sun (i.e. east). Ithaki should also be mountainous and low-lying. However, the island called Ithaki today does not have any of these features. The geographical layout is almost opposite to Homer's description, so the question that arises is how can his description of ancient Ithaki make any sense? And where are Sami and the lost island of Doulichion? Maybe, it's today's Ithaki that has often been named as Doulichion in the historical record, from Virgil through to the Venetians?

Another historical source is Strabo (63BC – 24AD), a Greek geographer, philosopher and historian. One of his most significant historical work was, Geography (Geographica), in which he writes about Kefallonia: "Where the island is narrowest it forms an isthmus so low-lying that it is often submerged from sea to sea". The only place that matches this description is the modern-day the Gulf of Livadi that separates the main part of Kefallonia from the Paliki peninsula. Today the presumed site of Strabo's Channel is known as the Thinia Valley. But at its highest point it is 180 metres above sea level.

So is there evidence for a large enough earthquake and landslide to fill the channel to such a depth?

As we described previously, in the chapters above, the Ionian Islands are located in one of the most tectonically active places in the world. It's where the African continental plate collides with the Eurasian plate. Ten kilometers to the west of Kefallonia the seabed drops from a depth of 300 meters to an incredible 3 kilometers. Every month or so the ground shakes and every few decades there is a major earthquake. For example, the catastrophic earthquake of 1953, which destroyed every building in the area and many people got killed or injured. The most recent earthquake, in January 2014, caused widespread damage and it pushed up the

land at the top of the Gulf of Livadi by 20cm. These phenomena could make anyone wonder if earthquakes are capable of changing the layout of entire islands. Can tectonics change completely the topography of a territory?

4.2 Previous Research – Geoscience 2011-2014

The objectives of this geoscientific research were to test the hypothesis that the island of Ithaca may have been as Homer described in Odyssey. Ithaca according to Homer was the furthest island of a group of four islands, was facing in the west to the open sea and also, was low-lying (Fugro marine survey team).

The main results of the geoscientific studies for the theory being tested were (Onshore Drilling Outcomes in Kefallonia – Issued 16 September 2015):

- The geology of the Thinia valley was very complex. The research has shown that seismic and geotectonic movements had a significant impact on the area. Near the northern end of the potential channel, inland of the village of Zola, it was identified some evidence of a former marine beach that lies underneath valley fill and consists of rockfall debris.
- Further research on the area has shown that the Thinia valley was intruded by marine waters more recently than the surface geology suggests. The results of this research have confirmed the existence of an ancient marine channel with Quaternary age.
- Also, it was confirmed that the existing valley fill is not simply the result of landslide and slope collapse, which makes the original hypothesis partially true and the absence of the marine channel today partially explained.
- The southern end of the valley is characterized by a large rotational, translational slump ending in an elevated thrust.
- The drilling rig on the site of Livadi Marsh area has shown an elevated channel floor and marine fossils significantly above sea level.
- An unusual trait in the Thinia valley is an elevated flat lakebed, named Lake Katachori, which was created by geotectonic movements and has subsequently dried out.
- Finally, in the Livadi Marsh were found some evidence of ancient marine sediments and beach deposits indicating the potential for an ancient harbor to have existed at the foot of Kastelli Hill.

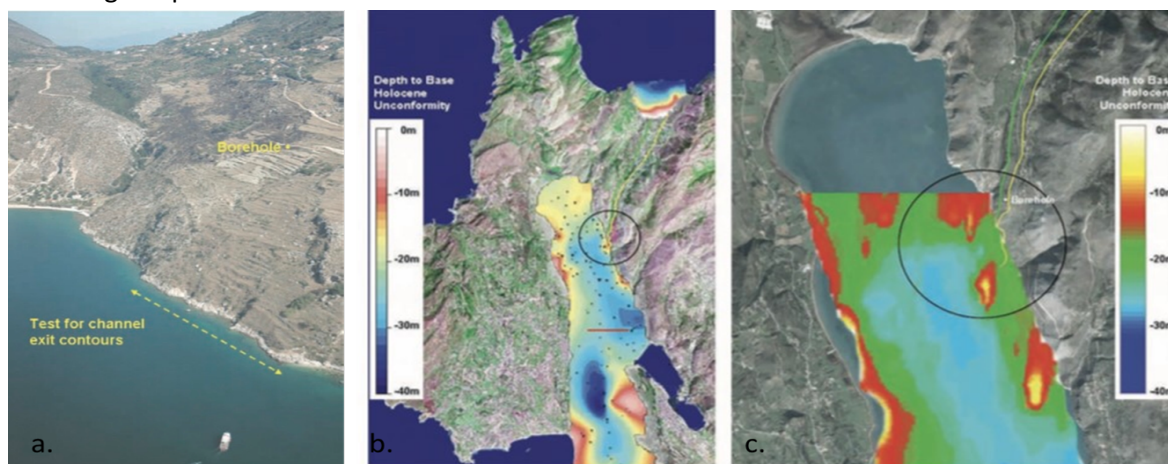


Figure 12: a. Livadi Gulf currently formed in a sub-Holocene valley and the presumed onshore line of a channel that links it to the offshore. b., c. Maps describing the depth to the Base Holocene unconformity in the Gulf of Livadi. The pictures show the previous regional surveys conducted in the area (from Underhill, 2008)



Picture 1: Upper left picture – Livadi harbor site, beside Kastelli Hill. Bottom left picture – Aerial photograph of Livadi Gulf (from Underhill, 2008). Two right pictures – The drilling rig on a platform, for the drilling project in Livadi Gulf (2017, drilling project of OUF).

To conclude the research focus is now on analyzing the biostratigraphy (with the help of Calcareous Nannoplankton) of the potential southern exit of the channel into the Gulf of Livadi. Dating (biostratigraphic age assignment of the sediments) the infill of Livadi marsh to test the theory if the site has the potential of being a harbor in Odysseus times.

5. Material and Methods

5.1 Sampling

Under the guidance of Professor in the Institute of Petroleum Engineering, Heriot-Watt University, John R. Underhill and in collaboration with the School of Mining and Metallurgical Engineering (NTUA) and the Faculty of Geology and Geoenvironment (NKUA), in 2017, an offshore drilling project took place in Livadi Gulf and four boreholes were retrieved, the first borehole (named Livadi-1) was sited close to the limestone sill that forms the south raised edge of the Gulf of Livadi, the second (Livadi-2) lies midway up the gulf on its eastern side, the third (Livadi-3) lies in the NW of the gulf nearest Livadi Marsh and finally, the fourth borehole (Livadi-4) lies in NE of the gulf and it is closest to Thinia. Afterwards, boreholes Livadi-1, Livadi-2, Livadi-4 have been carefully sampled every 10cm in-between the core depth 18m -35m.

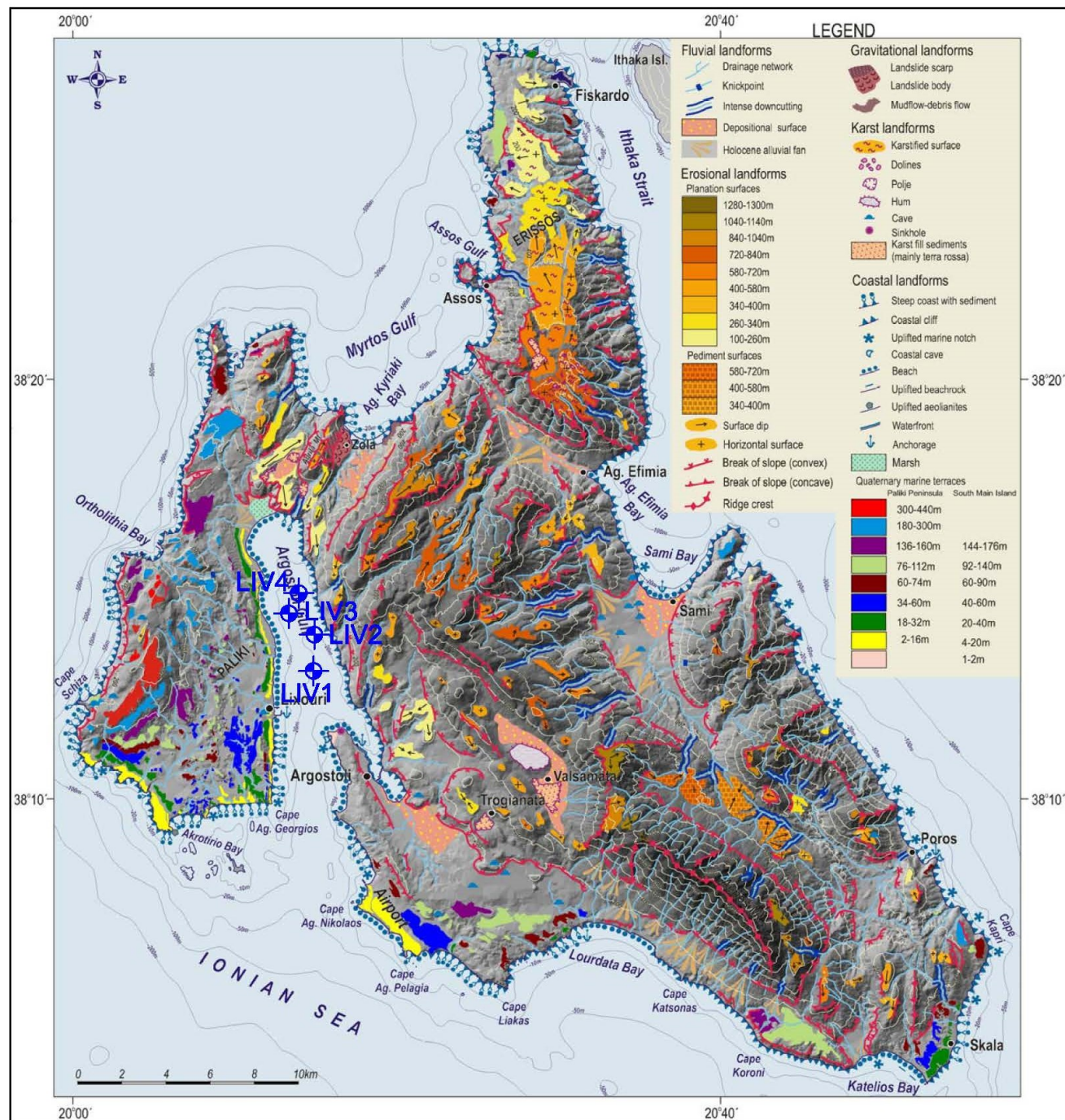


Figure 13: Geomorphological map of Kefallonia Island with the boreholes Livadi 1,2,3 and 4 (Karymbalis et al. modified)



Picture 2: Left picture – Drilling project in Livadi Gulf, right picture – Boreholes retrieved.

5.2 Sample preparation

We examined three boreholes out of four; more specifically we took our samples from the boreholes Livadi-1, 2, 4. In total 82 samples were processed and counted. In Livadi-1, 26 samples were prepared in the laboratory for micropalaeontological analysis and were analyzed under the Scanning Electron Microscope (SEM). These 26 samples were taken from cores 7, 8, 9 and 10, of borehole Livadi-1, and were sampled steadily every 10 centimeters in each core. We worked likewise with the other two boreholes, taking samples in each one core (cores 7, 8, 9 and 10) using the 10 centimeters step firmly. In Livadi-2, 22 samples and in Livadi-4, 31 samples were taken, prepared in the laboratory and analyzed under the SEM. Where, it was considered necessary we took more samples and the cores were analyzed in even higher resolution.

5.3 Laboratory Procedure

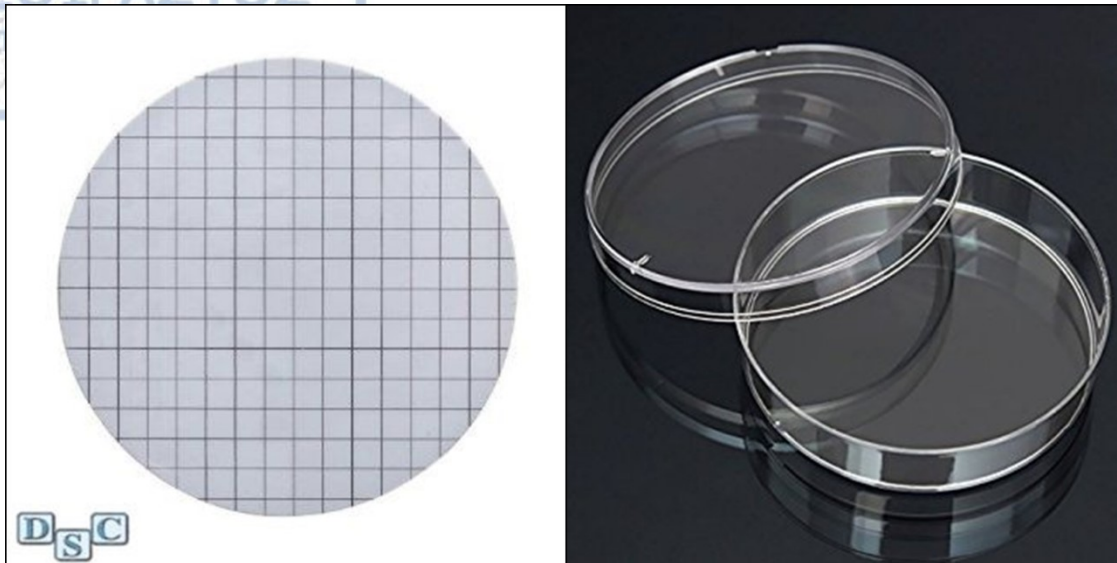


Picture 3: Laboratory of Historical Geology and Paleontology Department of NKUA.

The method followed for the sediment sample preparation of coccolithophores was by taking every sample and weighing 100 milligrams of it. Then place it in certain tubes with the sample's name on them. Afterwards we added buffered solution, which is a liquid mixture of distilled water and sodium carbonate (Na_2CO_3 , washing soda). Buffer was stirred for 45 minutes in a specific device, with the help of a magnet and then filtered. Buffer had to be alkaline with pH = 8. As it was said before, after the buffer was added in the tube with the sediment we collected from the sample, it was necessary to pass it to the ultrasound and leave it there for a minute, so there was no more material precipitating in the bottom of the test tube. The following steps were to split the liquid specimen twice into an electrical rotating liquid splitter (McLane wet Rotated Splitter) and then to filter the remaining material, through a polycarbonate membrane filter (Whatman 111206 Polycarbonate Nuclepore Track – Etched Membrane Filter, 50mm Diameter, 0.2 Micron), with the help of a diaphragm vacuum pump (ICAR MLR25L 40). The electrical wet splitter consists of a rotating table and on the top of that there are 10 small glass bottles, in which the liquid is separated into 1/10 of the original. Splitting the specimen twice means that we keep the 1/20 of the original liquid. In our work, we used and filtered the 3/20 of the processed sample and finally placed the polycarbonate filter in a petri dish and let it dry for several hours.

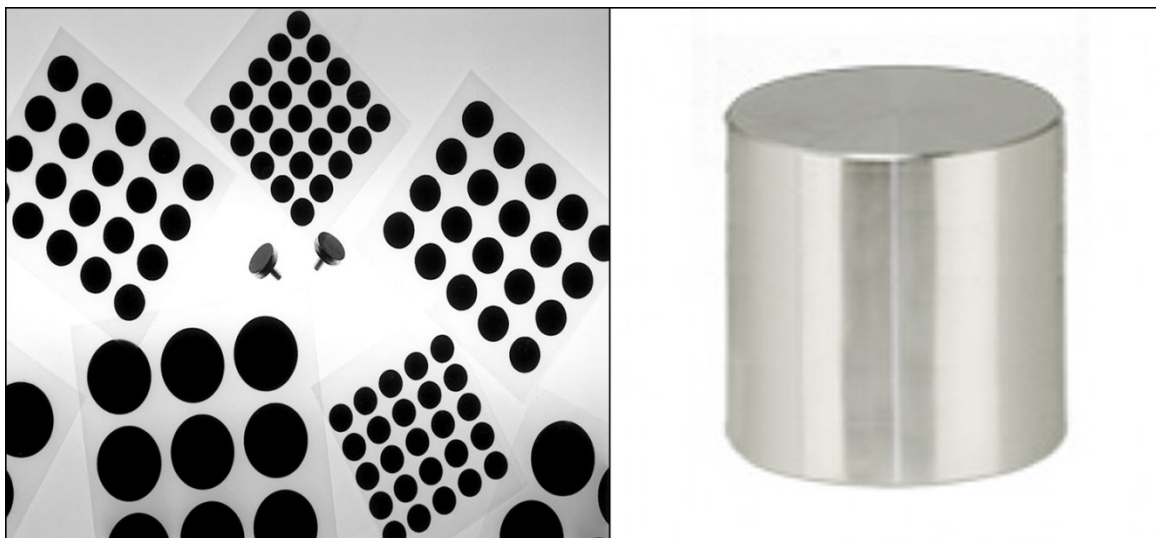


Picture 4: McLane wet Rotated Divider.



Picture 5: Whatman 111206 Polycarbonate Nucleopore Track – Etched Membrane Filter, 50mm Diameter, 0.2 Micron and on the right a petri dish.

After the first step of the laboratory process was conducted, we continued by cutting out a small surface of the dried filtered paper, which was the sample we would study in the microscope. This little piece was glued on a SEM Cylinder Specimen Mount (Stub), with the help of a carbon based, electrically conductive, double sided adhesive disc, also known as Leit tab. Afterwards, we put the stubs into the metallizer, which is a machine that sprays the specimens with gold (Au) or platinum (Pt), in order to make our samples conductive for the observation in SEM. Two cycles of plating have been conducted on our samples.



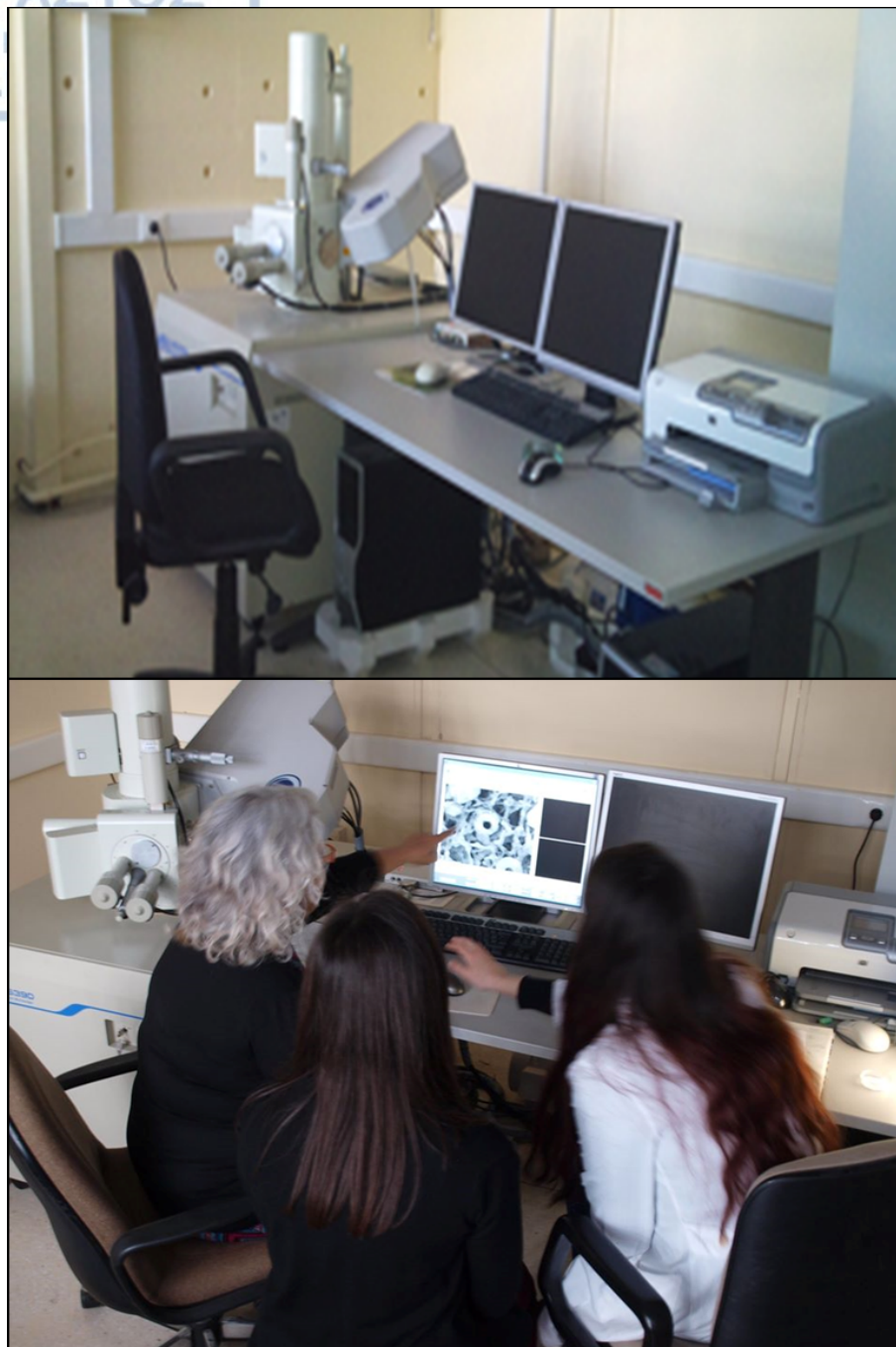
Picture 6: On the left: C carbon based, electrically conductive, double sided adhesive disc, also known as Leit tab and on the right: a SEM Cylinder Specimen Mount (Stub).

It was very important to be cautious during the whole procedure and keep our hands; tubes, petri dishes and all the sampling tools clean so there was no danger of contamination. Also, we were very careful writing down the weights of all samples and all their names on tubes, on petri dishes and on stubs.

5.4 Micropalaeontological Analysis Procedure

The micropaleontological analysis was conducted in the Scanning Electron Microscope laboratory, of the Historical Geology and Paleontology department of NKUA. We examined the samples under the SEM (JEOL – Model JSM-6390), counting 300 coccoliths, where possible, in each sample (using standard methods, Thierstein et al., 1977). The technical parts of the SEM, in order to observe our samples were Acceleration Volt 20mV, Filament in 73 – 75μA and the magnification rate x3000 (with scale 5μm). Afterwards, when we have collected the coccoliths, we conducted the statistical analysis of every sample and exported the percentages, which gave us answers about the assemblages in each sample.

For the identification of the coccolithophores we have used Nannotax3 (<http://www.mikrotax.org/Nannotax3/index.php?id=315>.), Young and Bown, 1997 and Young et al., 2003 (A guide to extant coccolithophore taxonomy). Then, the bibliography used for the biostratigraphic assignment and the biozonation was Raffi et al. (2006), Backman et al. (2012), Agnini et al. (2017). Pliocene and Pleistocene units and biohorizons were plotted in comparison with the “standard” zonations (Okada and Bukry 1980, Martini 1971) and the Geomagnetic Polarity Time Scale (GPTS; Lourens et al. 2004). These biozonations represent the biostratigraphic framework for relative dating of marine sediments using calcareous nannofossils.



Picture 7: SEM laboratory and on bottom picture, SEM in use for micropaleontological analysis.

In our research, three boreholes were examined under the SEM, in order to identify the coccoliths and the biostratigraphic age assignment. According to bibliography and the observation of our samples, we identified the Holocene (MNN21b – age less than 45ka) and the older biozone MNN19e (Pleistocene). *Emiliania huxleyi* Acme Zone (MNN21b) is defined as the interval where the frequency of *E. huxleyi* in the coccolith population exceeds 40% level (Castradori, 1993; Rio et al., 1990). Even though, according to our results *E. huxleyi*'s abundances in some samples were lower than 40% of the assemblage we did not consider this as a biostratigraphic change to older biozone MNN21a (age between 45-250 ka, FAD of *E. huxleyi*; Rio et al., 1990;

Thierstein et al., 1977), rather than as an paleoenvironmental impact on nannoplankton assemblages. For example, shallow lagoonal or even fresh water pond conditions prohibit the development of in situ assemblages (e.g. *E. huxleyi*). It is fundamental to emphasize that in our Holocene samples, there were many reworked coccoliths from older biounits (such as *Pseudoemiliana lacunosa*, *Discoaster spp.*, *Sphenolithus spp.*, large *Reticulofenestra*, *Toweius spp.*, *Calcidiscus macintyeri*, *Helicosphaera selli*, *Helicosphaera recta*, *Gephyrocapsa omega/parallela*, etc.) due to erosion from onland outcrops; which have been excluded and considered as redeposited. By excluding those coccoliths we extracted our results only with the “in situ” coccoliths (*Emiliana huxleyi* in situ).

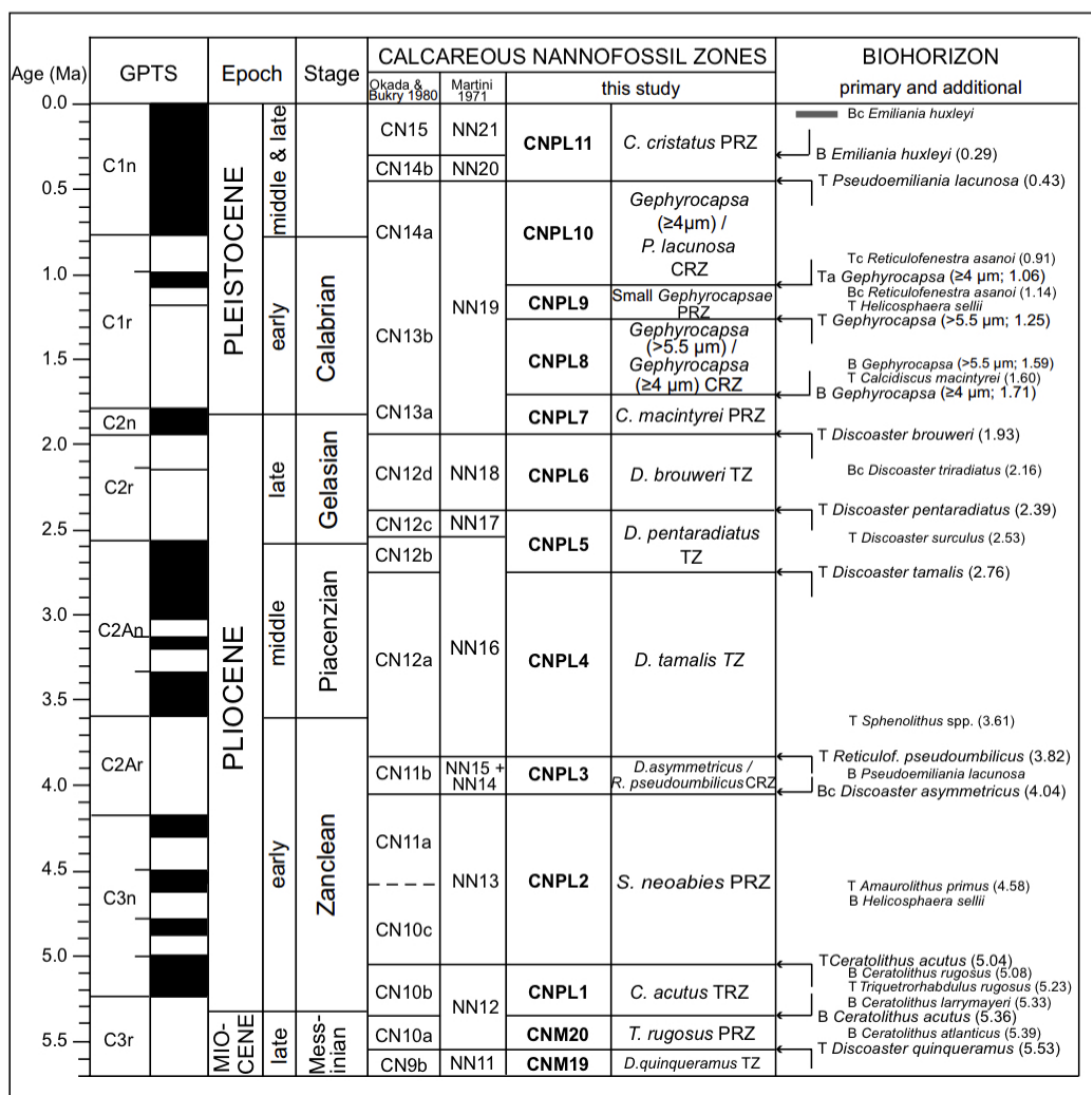


Figure 14: Pliocene and Pleistocene biounits and biohorizons (Backman et al. 2012)

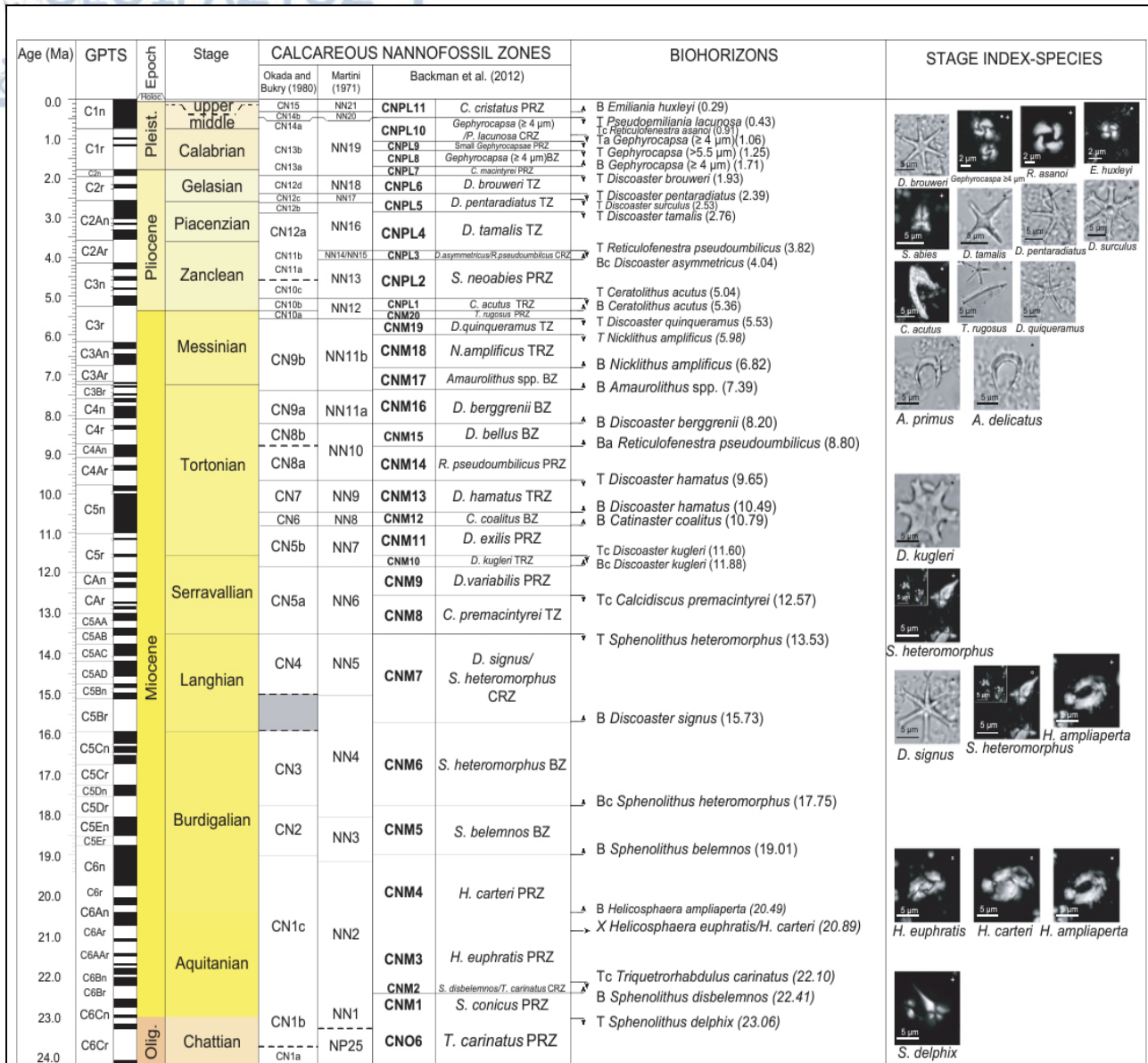
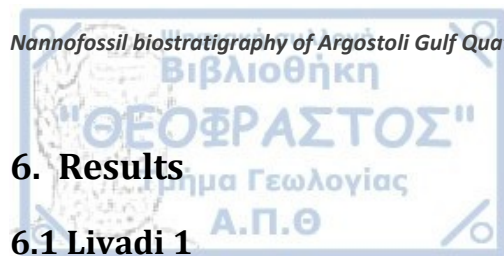


Figure 15: Neogene calcareous nannofossil biozonation (modified from Backman et al. 2012 by Agnini et al. 2017).



6. Results

6.1 Livadi 1

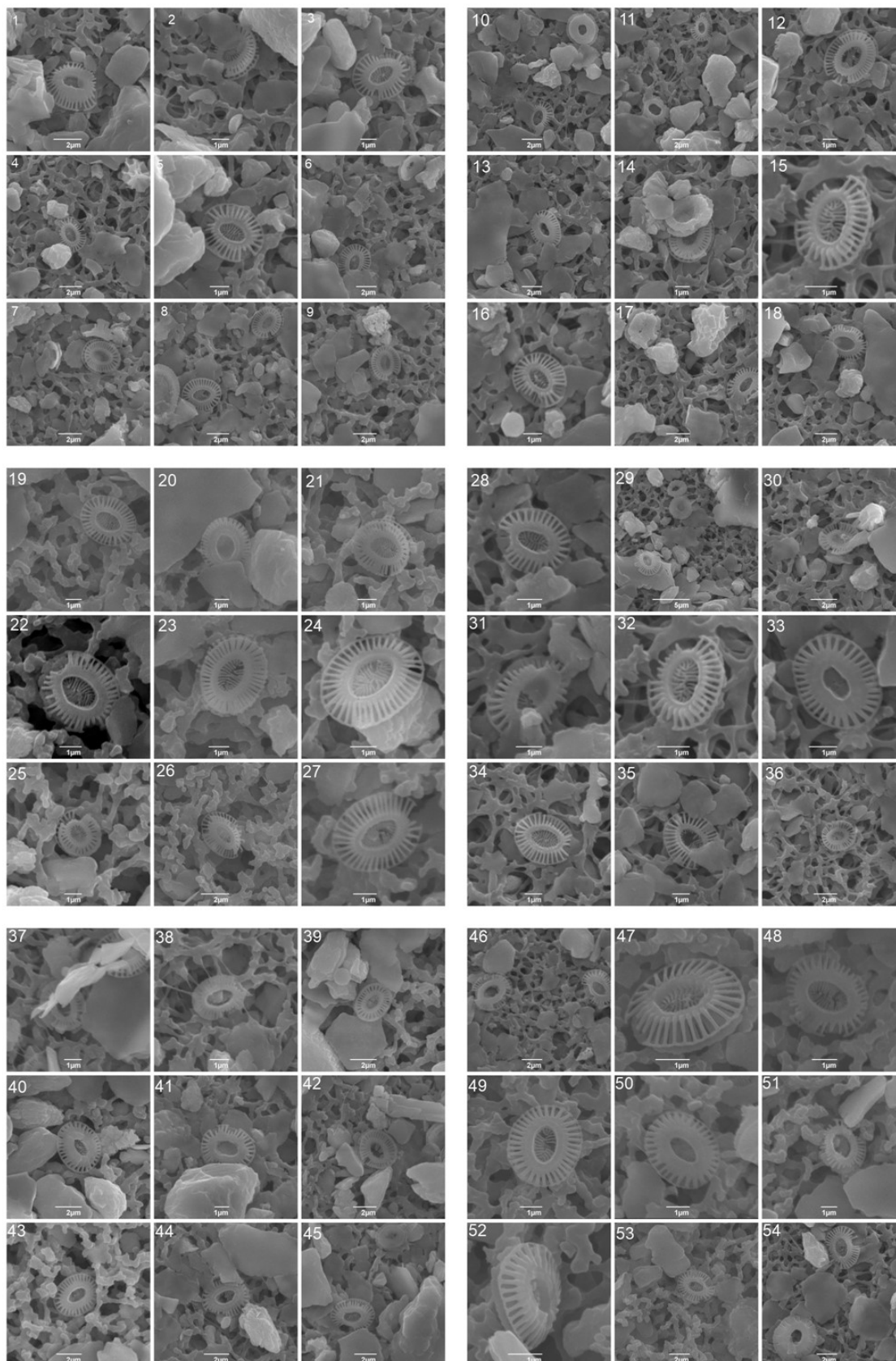
In borehole Livadi 1 core 7, nine samples have been analyzed with scanning electron microscope (SEM) for the nannofossil content in order to establish the biostratigraphic assignment. The assemblage composition of Livadi 1.7(18-20,6m depth), in average, consisted of *Emiliania huxleyi* 34,6%, *Calcidiscus leptoporus* 4%, *Rhabdosphaera* spp. 3,2%, *Helicosphaera carteri* 1,5%, *Helicosphaera wallichii* 0,1%, *Helicosphaera hyalina* 0,7%, small *Gephyrocapsa* spp. (<3μm) 14%, *Gephyrocapsa caribbeanica* 0,3%, *Coccolithus pelagicus* 0,9%, *Syracosphaera* spp. 2,5%, *Syracolithus* spp. 0,5%, *Calsiosolenia* spp. 0,1%, *Sphaerocalyptra* spp. 0,1%, *Algirosphaera* 0,1%, *Discosphaera* 0,1%, *Umbilicosphaera* spp. 2,7%. The reworked coccoliths in this core are *Calcidiscus macintyeri* 0,2%, *Reticulofenestra* spp. 49%, *Pseudoemilinia lacunosa* 11%, *Helicosphaera selli* 1%, *Gephyrocapsa omega* 0,4%, *Sphenolithus* spp. 0,5%, *Discoaster* spp. 1,2%, *Discoaster* rosette form 0,1%.

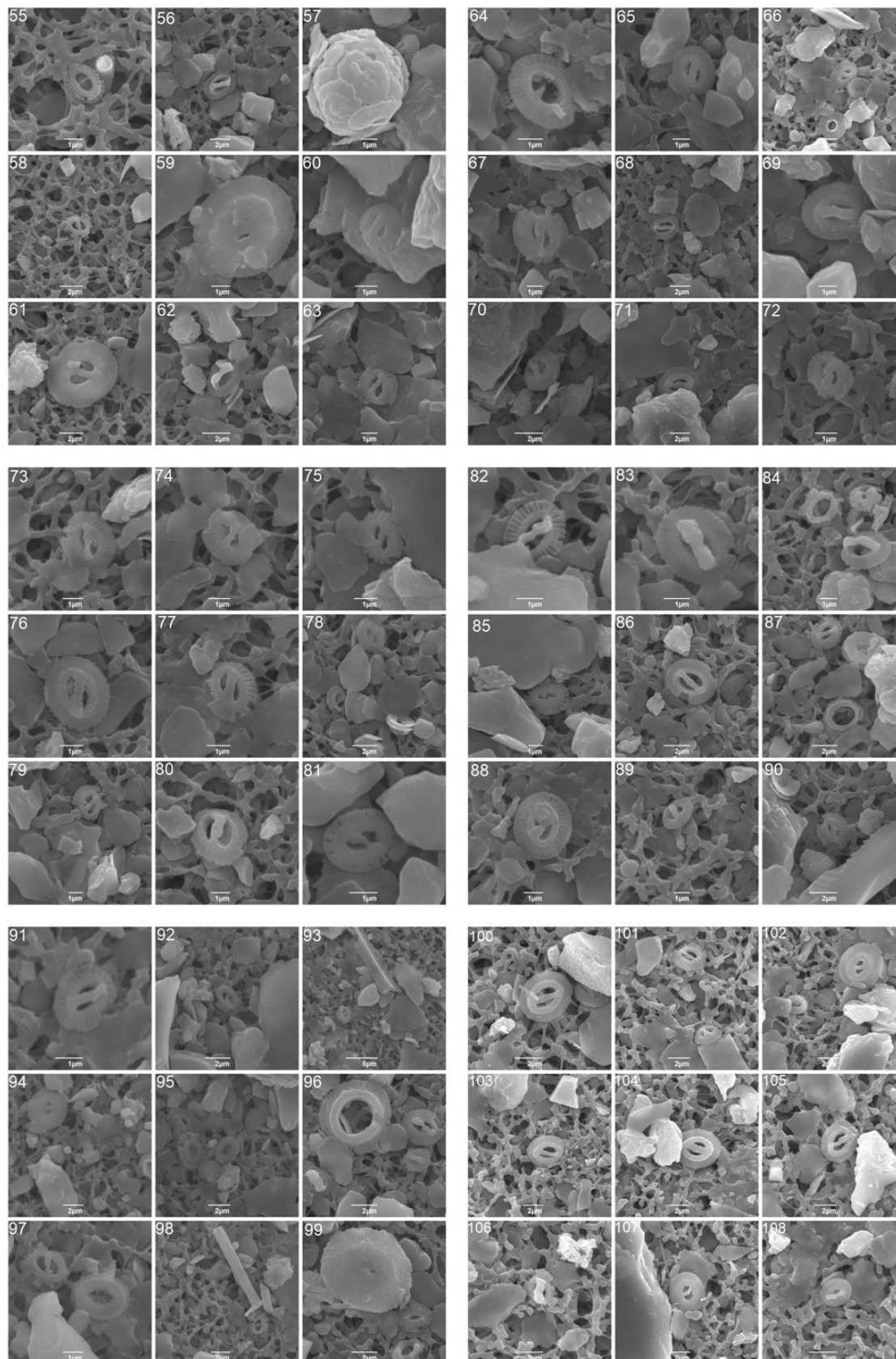
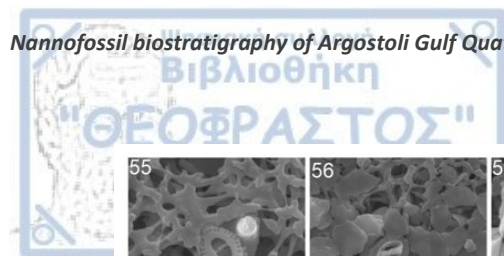
Continuing further down in borehole Livadi 1, core 8 (20,8-21,8m depth), the assemblage composition in average was, *Gephyrocapsa* spp. (<3microns) 2,8%, *Calcidiscus leptoporus* 6,3%, *Rhabdosphaera* spp. 1,7%, *Helicosphaera carteri* 0,5%, *H. wallichii* 0,2%, *H. hyalina* 0,3%, *Gephyrocapsa omega* 0,3%, *Coccolithus pelagicus* 1,6%, *Syracosphaera* spp. 0,6%, *Umbilicosphaera* spp. 2%. The rest coccoliths in this core are reworked from the Plio-Pleistocene surroundings: *Calcidiscus macintyeri* 0,5%, *Reticulofenestra* spp. 68,1%, *Pseudoemilinia lacunosa* 9,1%, *Discoaster* spp. 6,4%. *Emiliania huxleyi* was present only in sample Livadi 1.8.1, with percentage 20,6%, in the rest of core 8 *E. huxleyi* was completely absent.

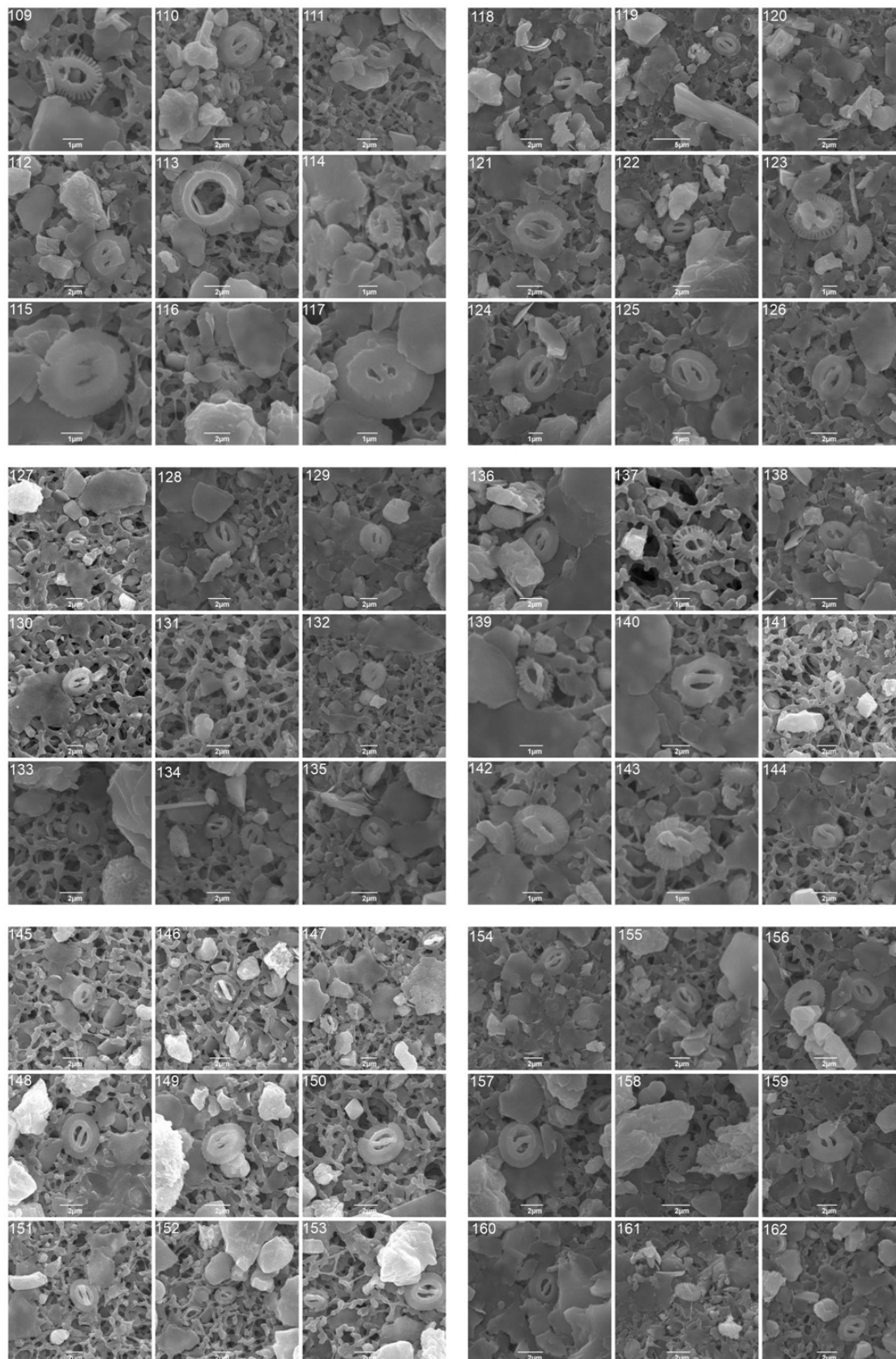
In Livadi1, core 9 (22-23,4m depth), the average assemblage composition was, *E. huxleyi* 0,00%, *C. leptoporus* 4,26%, *C. macintyeri* 0,12%, *Rhabdosphaera* 0,12%, *P. lacunosa* 4,10%, *Reticulofenestra* spp. 57,72%, small *Gephyrocapsa* (<3μm) 23,61%, *G. caribbeanica* 0,25%, *H. selli* 0,5%, *H. carteri* 0,37%, *H. hyalina* 0,13%, *Coccolithus pelagicus* 0,62%, *Syracosphaera* spp. 1%, *Syracolithus* spp. 0,5%, *Umbilicosphaera* spp. 4,60%, *Sphenolithus* spp. 0,25%, *Discoaster* spp. 1,49%, *Discoaster* rosette form 0,12%. In this core the only sample with reworked material was 1.9.5 (22m depth): small *Reticulofenestra*.

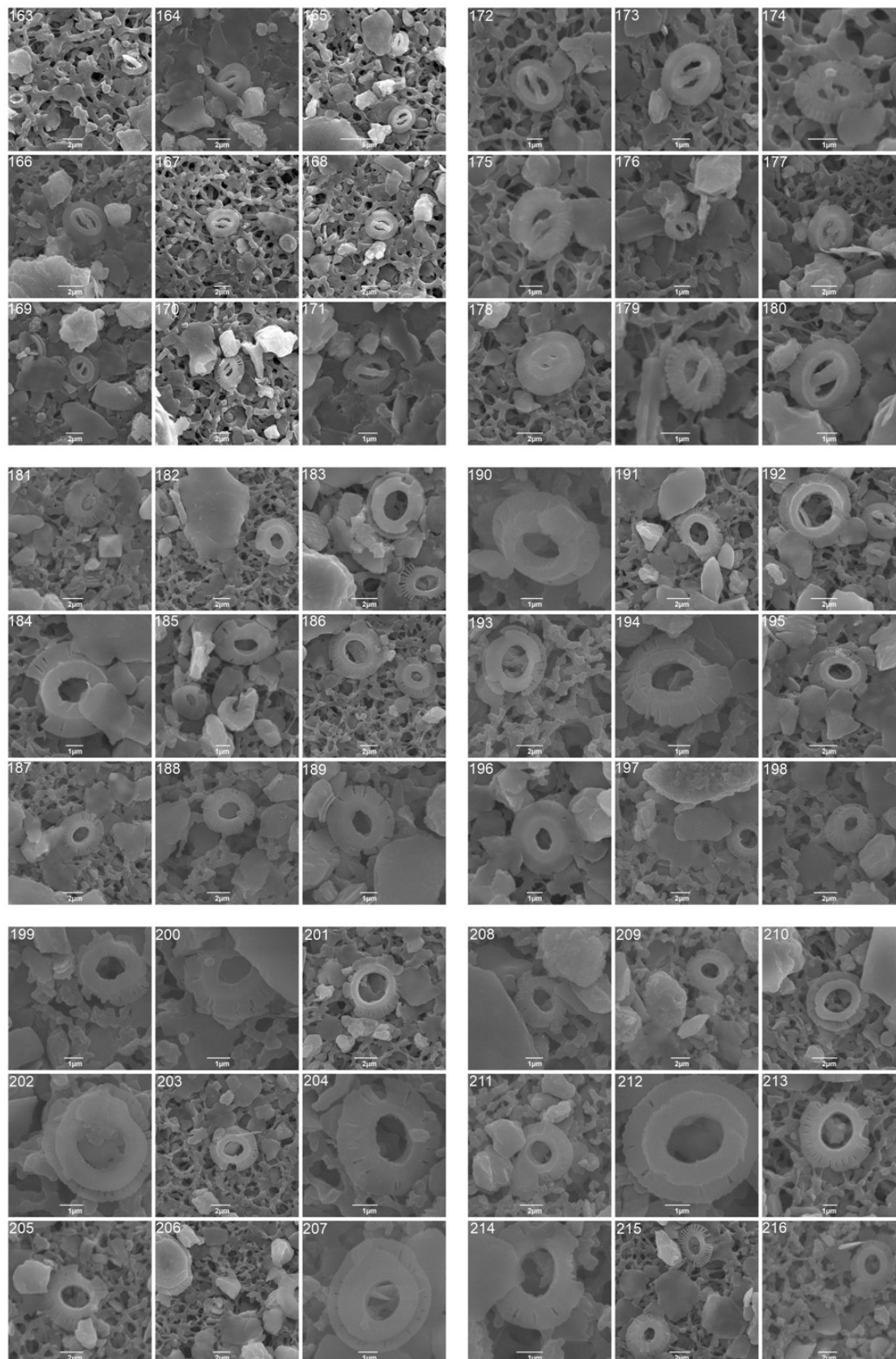
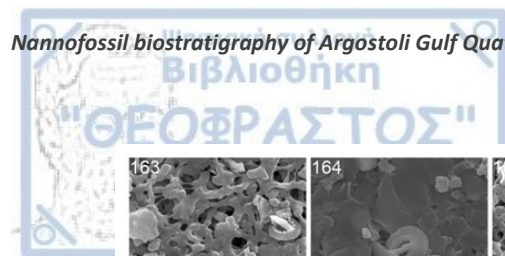
Finally, in Livadi1, core 10 (24,3-26m depth), the average assemblage composition was, *E. huxleyi* 0,00%, small *Gephyrocapsa* spp. (<3μm) 42,26%, *G. caribbeanica* 0,13%, *Umbilicosphaera* spp. 2,62%, *C. leptoporus* 1,48%, *C. macintyeri* 0,49%, *Reticulofenestra* spp. 39,4%, *Rhabdosphaera* spp. 0,88%, *P. lacunosa* 4,49%, *H. selli* 0,25%, *H. carteri* 0,44%, *H. hyalina* 0,12%, *Coccolithus pelagicus* 0,98%, *Syracosphaera* spp. 1,39%, *Discoaster* spp. 0,49%, *Syracolithus* spp. 0,43% and *Calsiosolenia* spp. 0,1%.

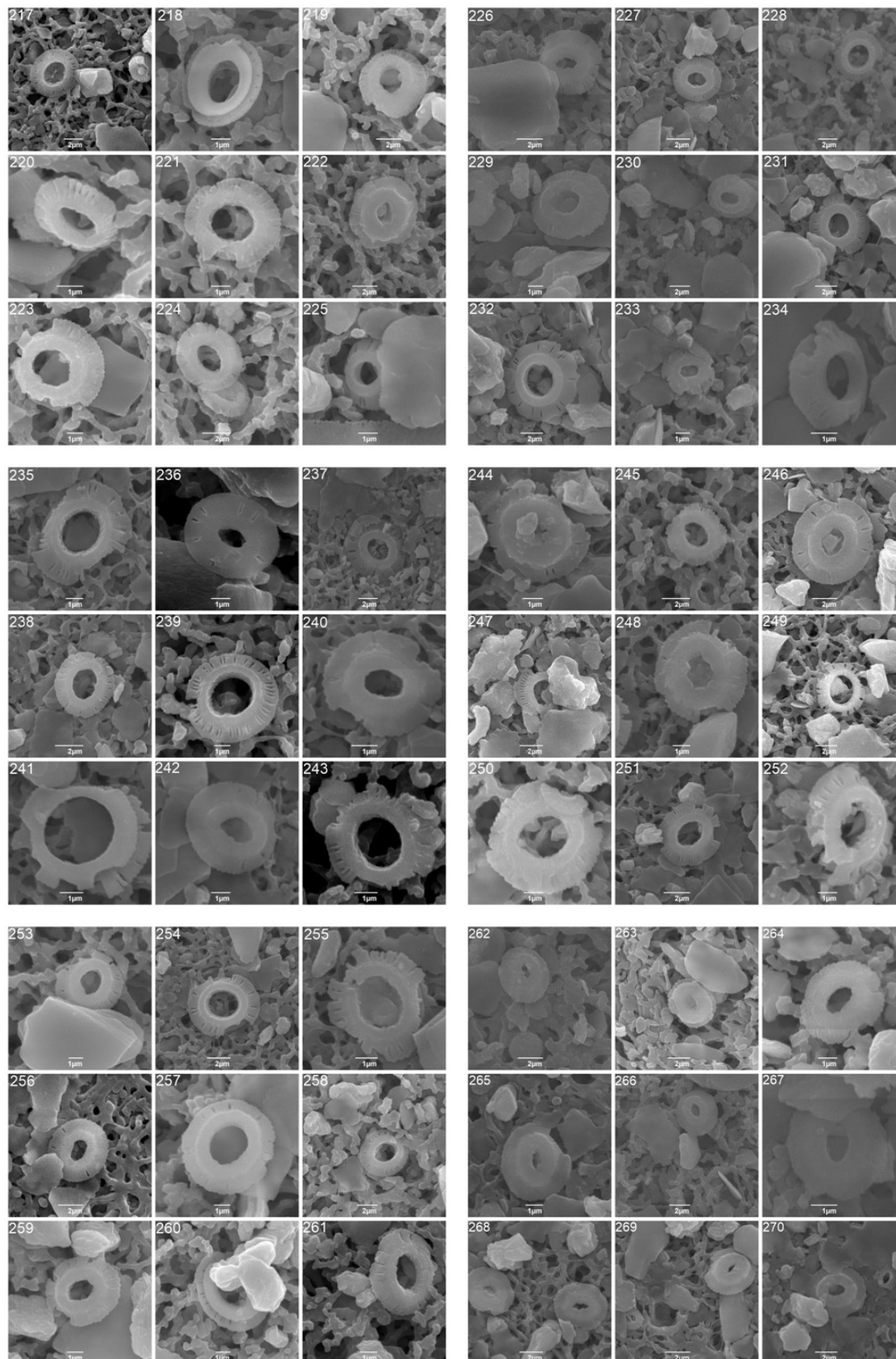
The tables and the diagrams below, show the nannofossils found in borehole Livadi1 and summarize the assemblage composition of Livadi 1 core 7, 8, 9, 10.

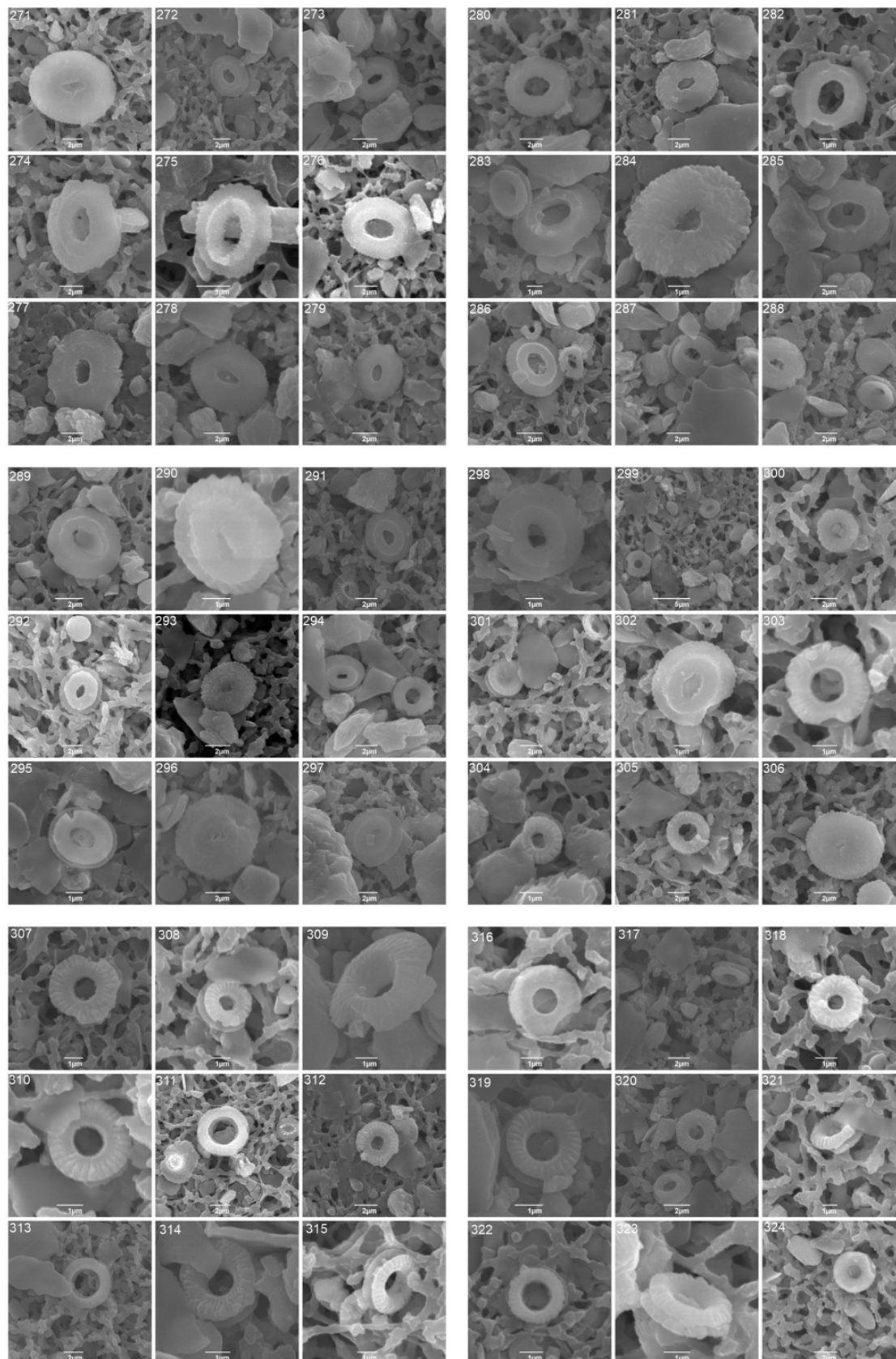
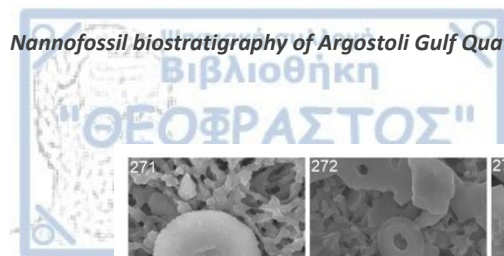


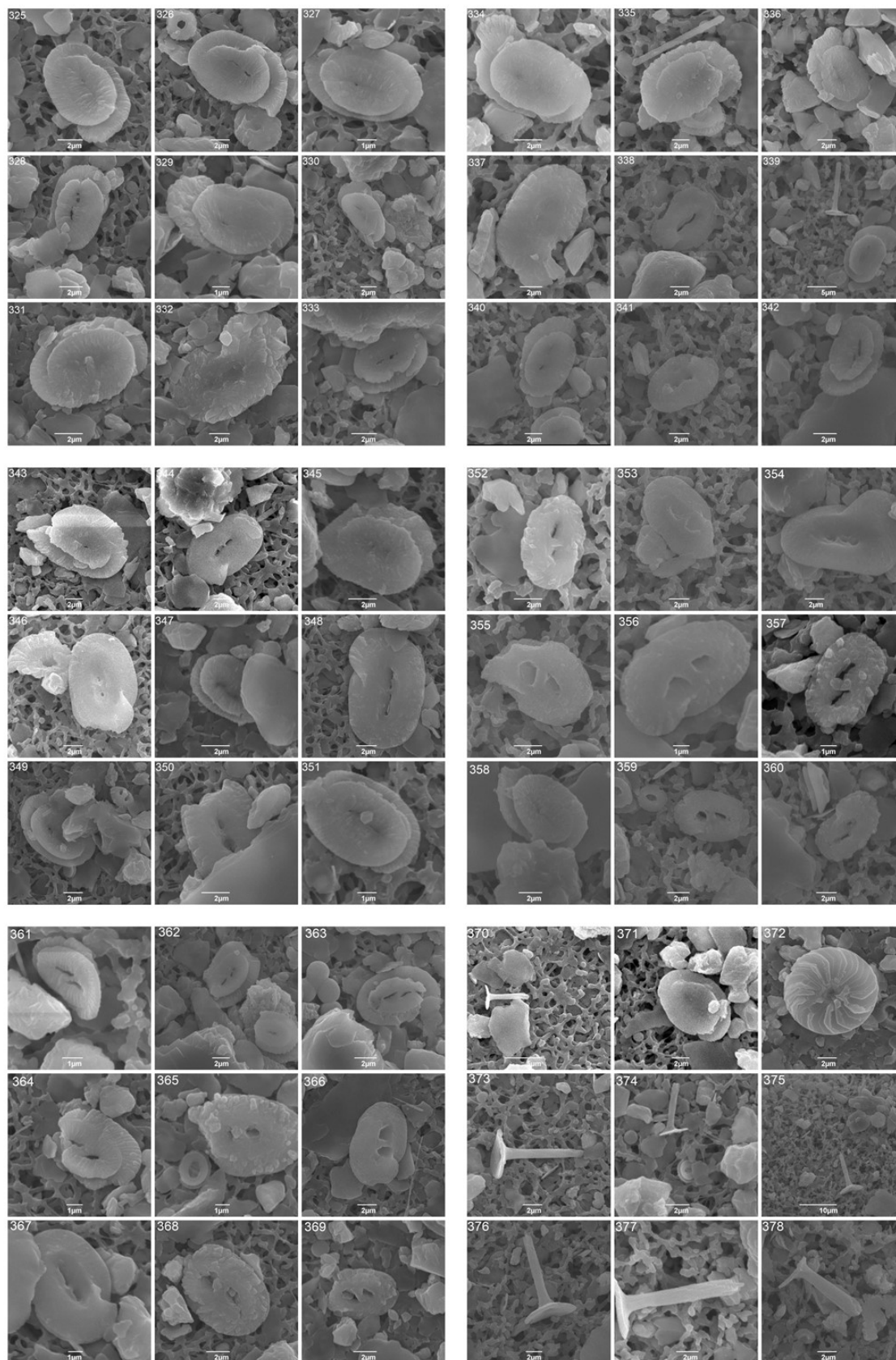


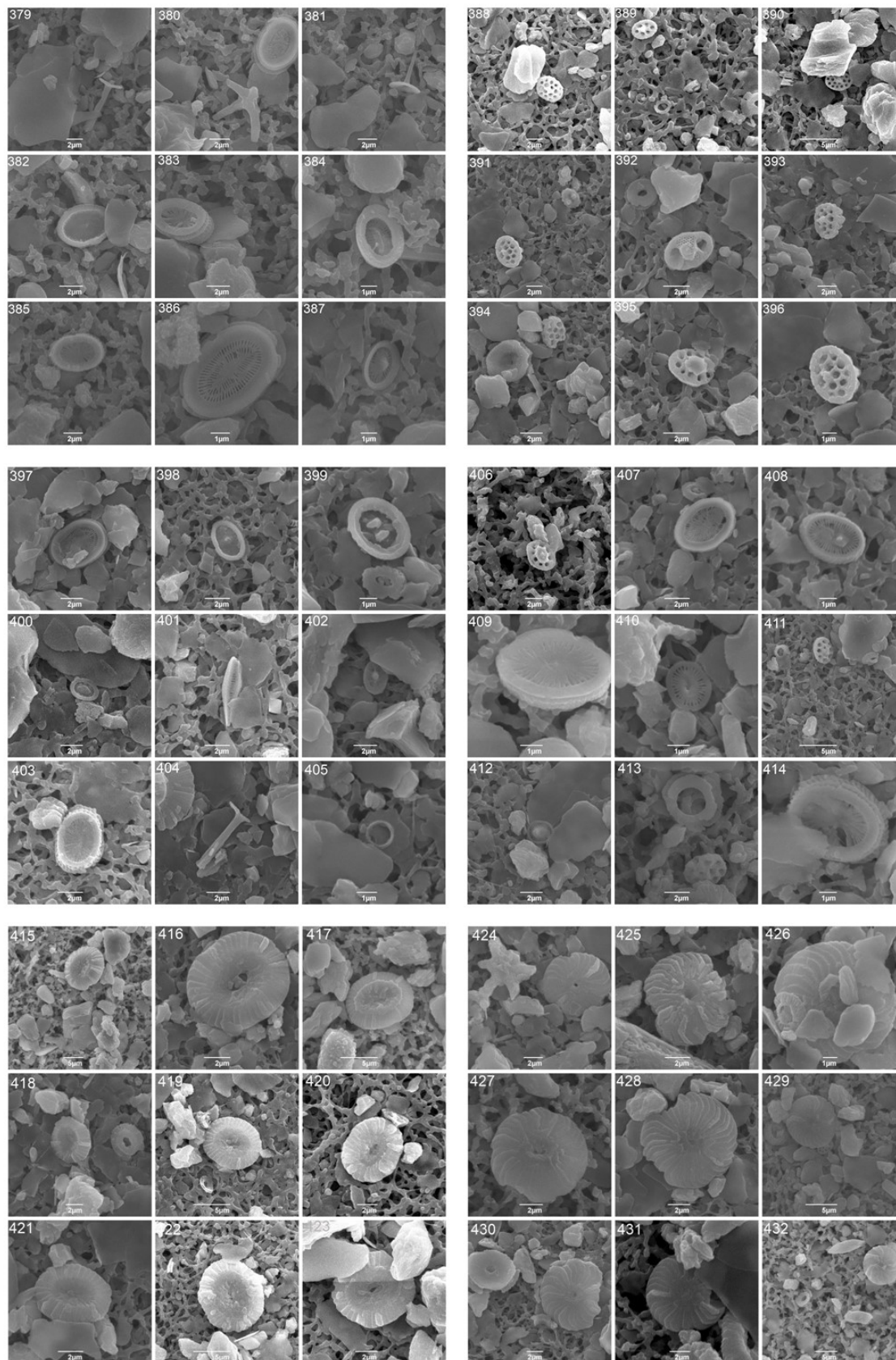
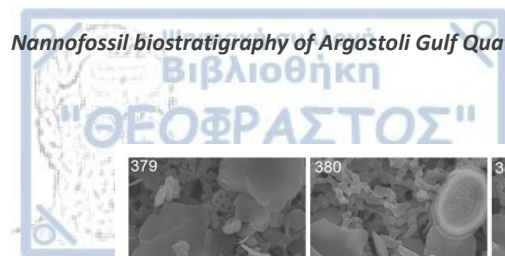












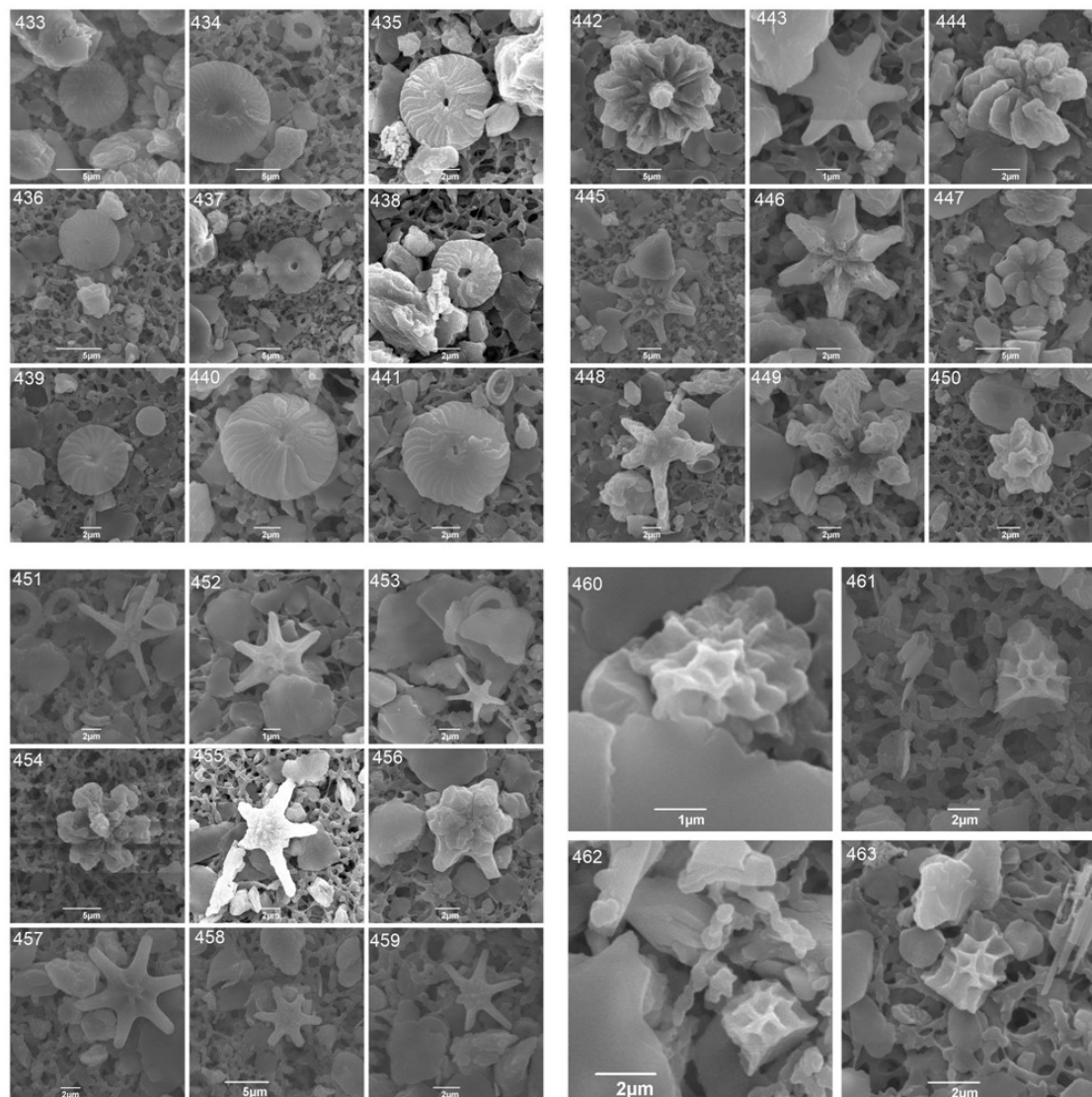
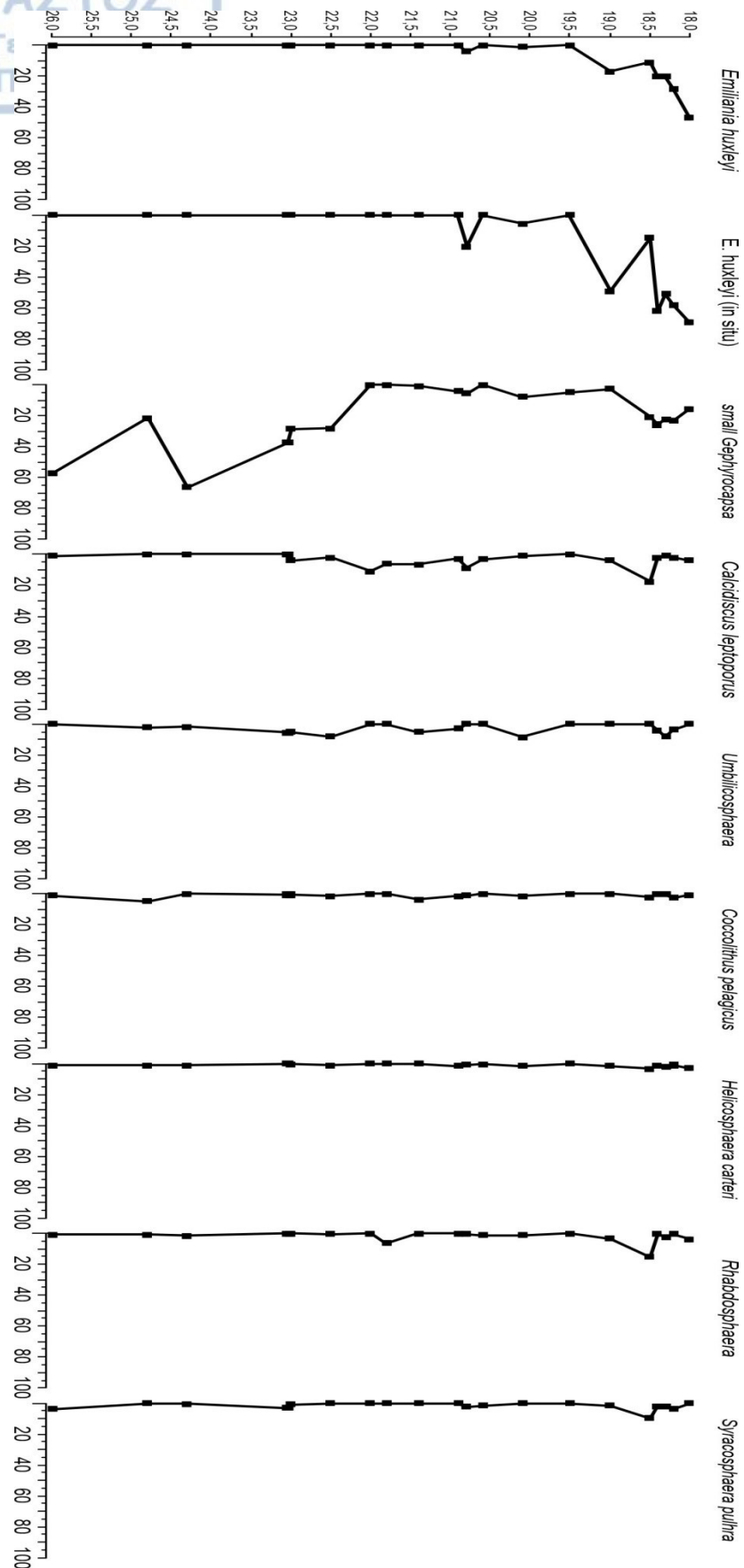
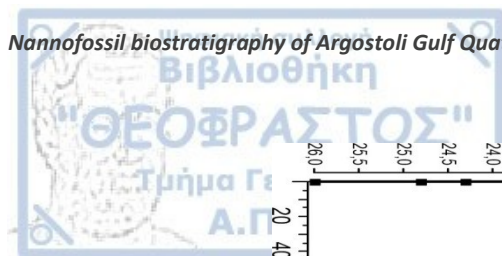


Table 1: SEM pictures from borehole Livadi-1:

1-54: *Emiliania huxleyi*, 55- 180: small *Gephyrocapsa* spp. (<3μm), 59, 112, 117, 178: *Gephyrocapsa caribbeanica*, 61: *G. omega*, 262-302: *Reticulofenestra* spp., 181-261: *Pseudoemiliania lacunosa*, 303-324: *Umbilicosphaera* spp., 325-351: *Helicosphaera carteri*, 352-369: *Helicosphaera selli*, 371: *Helicosphaera hyalina*, 370, 373-379, 404: *Rhabdosphaera* spp., 372, 425-433, 439-441: *Calcidiscus leptoporus*, 434-438: *Calcidiscus macintyeri*, 415-423: *Coccolithus pelagicus*, 380-387, 397-400, 407-409, 414: *Syracosphaera* spp., 392, 402: *Corisphaera*, 410, 412: *Cyrtosphaera*, 388-391, 393-396, 411, 413: *Syracolithus* spp., 442, 444, 447: *Discoaster* rosette form, 443, 445, 446, 448-459: *Discoaster* spp., 460-463: *Sphenolithus* spp.



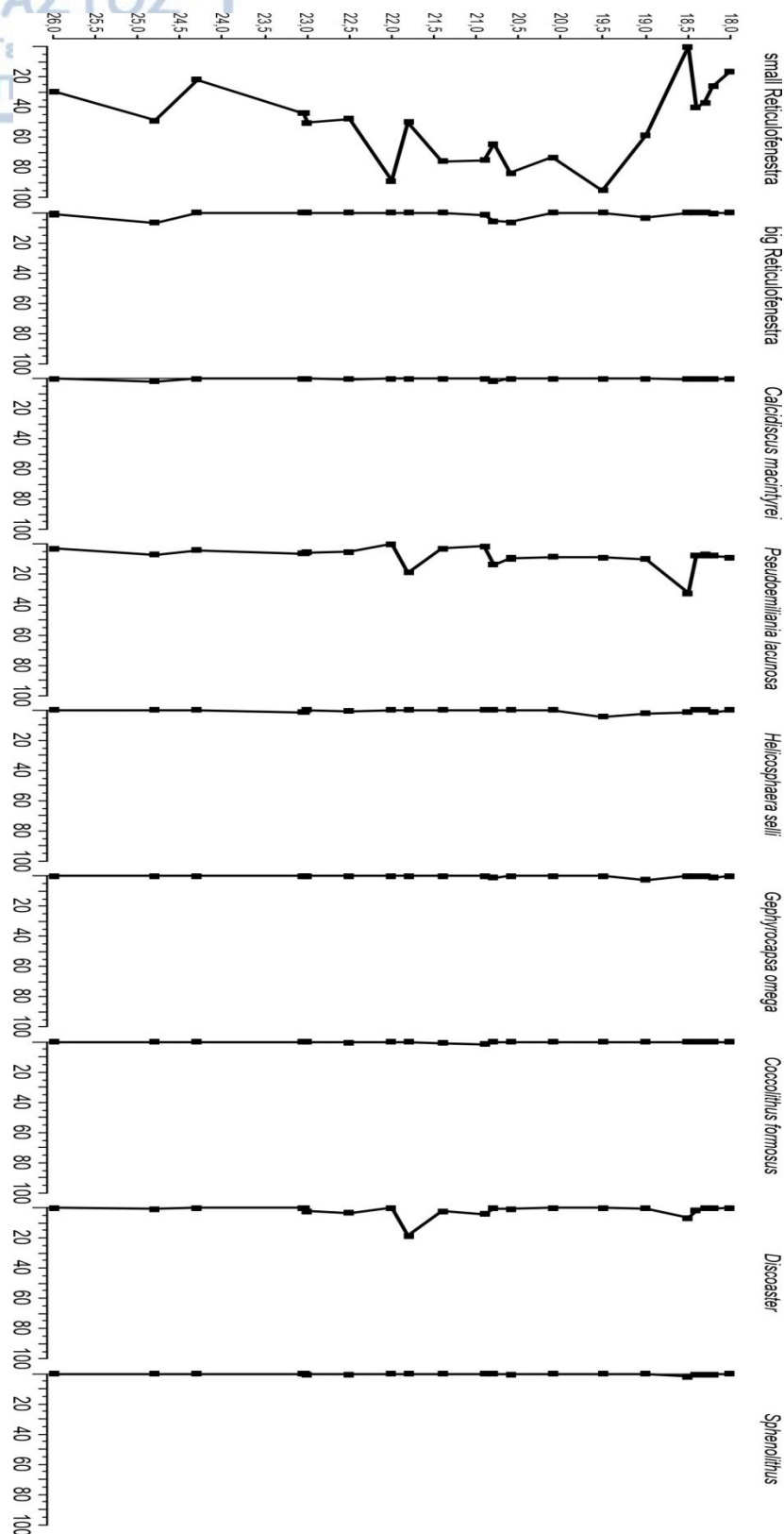
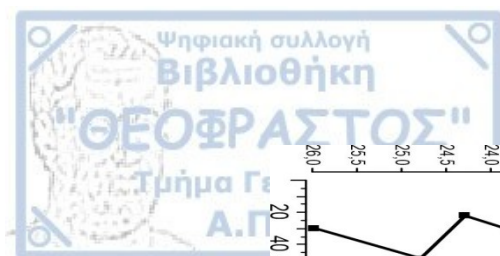


Figure 16: Diagrams of calcareous nannoplankton assemblages vs. core depth in borehole Livadi -1. First diagram shows the coccoliths in situ and the second the reworked coccoliths.

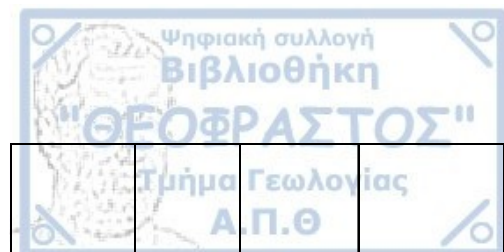
Sampling			Biostratigraphy				
			Calcareous Nannoplakton				
			Scanning Electron Microscope (SEM)				
Sample Code	Sample interval (cm)	Depth (m)	Light Microscope	In situ	Plio-Pleistocene Reworked	Notes	Results
1.4.	6.79-6.80	6.79-6.80	E. huxleyi (abundant) - Plio-Pleistocene reworking	-	-	-	MNN21b
1.7.1	0-2	18	Plio-Pleistocene reworking	<i>Emiliana huxleyi</i> , <i>Rhabdosphaera</i> spp., <i>Helicosphaera carteri</i> , <i>Coccolithus pelagicus</i> , <i>Calcidiscus leptoporus</i>	small <i>Reticulofenestra</i> (<i>minuta</i> , <i>minutula</i>), <i>Pseudoemiliana lacunosa</i> , small <i>Gephyrocapsa</i>	<i>E. huxleyi</i> (69,77%) - abundant and Plio-Pleistocene reworked from surroundings due to erosion	MNN21b
1.7.3	10-12	18,2		<i>Emiliana huxleyi</i> , <i>Calcidiscus leptoporus</i> , <i>Rhabdosphaera</i> , <i>Helicosphaera carteri</i> , <i>Coccolithus pelagicus</i> , <i>Syracosphaera pulhra</i> , <i>Algirosphaera</i> , <i>Umbilicosphaera</i> , <i>Syracolithus</i> , <i>Calciosolenia</i> , <i>Dictyococcides</i> , <i>Sphaerocalyptra</i>	<i>Calcidiscus macintyreii</i> , small <i>Reticulofenestra</i> (<i>minuta</i> , <i>minutula</i>), big <i>Reticulofenestra</i> , <i>Pseudoemiliana lacunosa</i> , <i>Helicosphaera selli</i> , small <i>Gephyrocapsa</i> , <i>Gephyrocapsa</i> (<i>omega</i> - <i>parallela</i>), <i>Gephyrocapsa caribbeanica</i> , <i>Sphenolithus</i> , <i>Discaster</i> spp, <i>Discoaster</i> rosette form	<i>E. huxleyi</i> (58,06%) - abundant and Plio-Pleistocene reworked from surroundings due to erosion	MNN21b
1.7.4	20-22	18,3		<i>Emiliana huxleyi</i> , <i>Calcidiscus leptoporus</i> , <i>Rhabdosphaera</i> , <i>Helicosphaera carteri</i> , <i>Helicosphaera hyalina</i> , <i>Coccolithus pelagicus</i> , <i>Syracosphaera pulhra</i> , <i>Umbilicosphaera</i> , <i>Syracolithus</i> , <i>Discosphaera</i>	<i>Calcidiscus macintyreii</i> , small <i>Reticulofenestra</i> (<i>minuta</i> , <i>minutula</i>), <i>Pseudoemiliana lacunosa</i> , small <i>Gephyrocapsa</i> , <i>Gephyrocapsa caribbeanica</i> , <i>Sphenolithus</i>	<i>E. huxleyi</i> (51,19%) - abundant and Plio-Pleistocene reworked from surroundings due to erosion	MNN21b

1.7.5	30-32	18,4		<i>Emiliana huxleyi</i> , <i>Calcidiscus leptoporus</i> , <i>Rhabdosphaera</i> , <i>Helicosphaera carteri</i> , <i>Helicosphaera hyalina</i> , <i>Coccolithus pelagicus</i> , <i>Syracosphaera pulhra</i> , <i>Umbilicosphaera</i>	<i>Calcidiscus macintyreii</i> , small <i>Reticulofenestra (minuta, minutula)</i> , big <i>Reticulofenestra</i> , <i>Pseudoemiliana lacunosa</i> , small <i>Gephyrocapsa</i> , <i>Gephyrocapsa omega (parallela)</i> , <i>Gephyrocapsa caribbeanica</i> , <i>Sphenolithus</i> , <i>Discoaster</i> spp., <i>Discoaster rosette</i> form	<i>E. huxleyi</i> (62,34%) - abundant and Plio-Pleistocene reworked from surroundings due to erosion	MNN21b
1.7.6	40-42	18,5	Plio - Pleistocene reworking	<i>Emiliana huxleyi</i> , <i>Calcidiscus leptoporus</i> , <i>Rhabdosphaera</i> , <i>Helicosphaera carteri</i> , <i>Helicosphaera wallichii</i> , <i>Helicosphaera hyalina</i> , <i>Coccolithus pelagicus</i> , <i>Syracosphaera pulhra</i> , <i>Algirosphaera</i>	<i>Calcidiscus macintyreii</i> , <i>Pseudoemiliana lacunosa</i> , small <i>Gephyrocapsa</i> , <i>Sphenolithus</i> , <i>Discoaster</i> spp.	<i>E. huxleyi</i> (14,71%) - abundant and Plio-Pleistocene reworked from surroundings due to erosion	MNN21b
1.7.11	100-102	19	Plio-Pleistocene reworking	<i>Emiliana huxleyi</i> , <i>Calcidiscus leptoporus</i> , <i>Rhabdosphaera</i> , <i>Helicosphaera carteri</i> , <i>Helicosphaera hyalina</i> , <i>Syracosphaera pulhra</i>	small <i>Reticulofenestra (minuta, minutula)</i> , big <i>Reticulofenestra</i> , <i>Pseudoemiliana lacunosa</i> , <i>Helicosphaera selli</i> , small <i>Gephyrocapsa</i> , <i>Gephyrocapsa omega (parallela)</i> , <i>Discoaster</i> spp., <i>Toweius</i> or <i>Prinsius</i>	<i>E. huxleyi</i> (49,18%) - abundant and Plio-Pleistocene reworked from surroundings due to erosion	MNN21b
1.7.15	150-152	19,5	Plio-Pleistocene reworking	no sign of in situ coccoliths-due to environmental conditions (lagoon interval)- very few coccoliths mostly reworked	small <i>Reticulofenestra (minuta, minutula)</i> , <i>Pseudoemiliana lacunosa</i> , <i>Helicosphaera selli</i> , small <i>Gephyrocapsa</i>	<i>E. huxleyi</i> (0.00%) - Shallow marine with fresh water input	MNN21b

1.7.21	210-212	20,1	Plio-Pleistocene reworking	<i>Emiliania huxleyi</i> , <i>Calcidiscus leptoporus</i> , <i>Rhabdosphaera carteri</i> , <i>Helicosphaera hyalina</i> , <i>Coccolithus pelagicus</i> , <i>Umbilicosphaera</i>	small <i>Reticulofenestra</i> (<i>minuta</i> , <i>minutula</i>), <i>Pseudoemiliana lacunosa</i> , small <i>Gephyrocapsa</i>	<i>E. huxleyi</i> (5,71%) - lagoonal conditions	MNN21b - Lagoon
1.7.26	260-262	20,6	Plio-Pleistocene reworking	<i>Calcidiscus leptoporus</i> , <i>Rhabdosphaera carteri</i> , <i>Helicosphaera wallichii</i> , <i>Helicosphaera hyalina</i> , <i>Syracosphaera</i> spp.	small <i>Reticulofenestra</i> (<i>minuta</i> , <i>minutula</i>), big <i>Reticulofenestra</i> , <i>Pseudoemiliana lacunosa</i> , <i>Sphenolithus</i> , <i>Discoaster</i> spp.	<i>E. huxleyi</i> (0.00%) - lagoon	MNN21b - Lagoon
1.8.1	0-2	20,62	Plio-Pleistocene reworking	<i>Emiliania huxleyi</i> , <i>Calcidiscus leptoporus</i> , <i>Rhabdosphaera carteri</i> , <i>Helicosphaera wallichii</i> , <i>Helicosphaera hyalina</i> , <i>Coccolithus pelagicus</i> , <i>Syracosphaera</i> spp., <i>Algirosphaera</i>	small <i>Reticulofenestra</i> (<i>minuta</i> , <i>minutula</i>), big <i>Reticulofenestra</i> , <i>Pseudoemiliana lacunosa</i> , small <i>Gephyrocapsa</i> , <i>Gephyrocapsa omega</i> (<i>parallela</i>), <i>Calcidiscus macintyeri</i> , <i>Discoaster</i> spp.	<i>E. huxleyi</i> (20,59%) - Shallow marine with freshwater input	MNN21b - Lagoon
1.8.6	50-52	21,12		<i>Calcidiscus leptoporus</i> , <i>Helicosphaera carteri</i> , <i>Coccolithus pelagicus</i> , <i>Umbilicosphaera</i> , <i>Calsiolenia</i> -very few coccoliths and no sign of <i>E.huxleyi</i> due to lagoonal conditions	small <i>Reticulofenestra</i> (<i>minuta</i> , <i>minutula</i>), big <i>Reticulofenestra</i> , <i>Pseudoemiliana lacunosa</i> , small <i>Gephyrocapsa</i> , <i>Coccolithus formosus</i> , <i>Discoaster</i> spp.	<i>E. huxleyi</i> (0.00%) - open lagoon	MNN21b - Lagoon
1.8.11	100-102	21,62		<i>Calcidiscus leptoporus</i> , <i>Coccolithus pelagicus</i> , <i>Umbilicosphaera</i> , <i>Calsiolenia</i> -very few coccoliths and no sign of <i>E.huxleyi</i> due to lagoonal conditions	small <i>Reticulofenestra</i> (<i>minuta</i> , <i>minutula</i>), <i>Pseudoemiliana lacunosa</i> , small <i>Gephyrocapsa</i> , <i>Coccolithus formosus</i> , <i>Discoaster</i> spp.	<i>E. huxleyi</i> (0.00%) - open lagoon	MNN21b - Lagoon

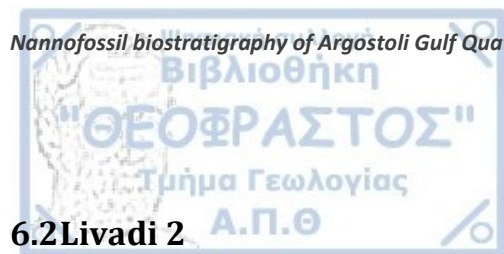
1.8.15	140-142	22		<i>Calcidiscus leptoporus</i> , <i>Rhabdosphaera</i> - very few coccoliths and no sign of <i>E. huxleyi</i> due to lagoonal conditions	small <i>Reticulofenestra</i> (<i>minuta</i> , <i>minutula</i>), <i>Pseudoemiliana lacunosa</i> , <i>Discoaster</i> spp.	<i>E. huxleyi</i> (0.00%) - open lagoon	MNN21b - Lagoon
1.9.5	50-52	22,5		<i>Calcidiscus leptoporus</i> - very few (almost none) coccoliths - <i>E. huxleyi</i> absent - due to lagoonal conditions	small <i>Reticulofenestra</i> (<i>minuta</i> , <i>minutula</i>)	<i>E. huxleyi</i> (0.00%) - open lagoon	MNN21b - Lagoon
1.9.10	100-102	23		small <i>Gephyrocapsa</i> , small <i>Reticulofenestra</i> (<i>minuta</i> , <i>minutula</i>), big <i>Reticulofenestra</i> , <i>Calcidiscus leptoporus</i> , <i>C. macintyeri</i> , <i>Rhabdosphaera</i> , <i>Helicosphaera selli</i> , <i>H. carteri</i> , <i>Umbilicosphaera</i> , <i>Syracolithus</i> , <i>Coccolithus pelagicus</i> , <i>C. formosus</i> , <i>Sphenolithus</i> , <i>Discoaster</i> spp., <i>Pseudoemiliana lacunosa</i>	no reworked- biozonal transition	small <i>Gephyrocapsa</i> < 3μm (28,36%), small <i>Reticulofenestra</i> spp. (49.76%) <i>Pseudoemiliana lacunosa</i> (5%), <i>E. huxleyi</i> (0.00%) - biozonal transition	MNN19e
19.19-19.20	19.19-19.20	23,9		small <i>Gephyrocapsa</i> , <i>Gephyrocapsa caribbeanica</i> , small <i>Reticulofenestra</i> (<i>minuta</i> , <i>minutula</i>), <i>Calcidiscus leptoporus</i> , <i>Helicosphaera carteri</i> , <i>Umbilicosphaera</i> , <i>Syracosphaera</i> , <i>Syracolithus</i> , <i>Coccolithus pelagicus</i> , <i>Sphenolithus</i> , <i>Discoaster</i> spp., <i>Discoaster rosette</i> form, <i>Pseudoemiliana lacunosa</i>	no reworked- biozonal transition	small <i>Gephyrocapsa</i> ≤3μm (28,57%) <i>Reticulofenestra</i> spp. (50.25%) <i>Pseudoemiliana lacunosa</i> (5%) <i>E. huxleyi</i> (0.00%)	MNN19e

1.9.14	164-166	24	small <i>Gephyrocapsa</i> , small <i>Reticulofenestra</i> (<i>minuta</i> , <i>minutula</i>), <i>Helicosphaera selli</i> , <i>H. hyalina</i> , <i>Umbilicosphaera</i> , <i>Syracosphaera</i> , <i>Syracolithus</i> , <i>Coccolithus pelagicus</i> , <i>Pseudoemiliana lacunosa</i>	no reworked-Pleistocene biozone	<i>Small Gephyrocapsa</i> $\leq 3\mu\text{m}$ (38%) <i>Reticulofenestra</i> spp. (44%) <i>Pseudoemiliana lacunosa</i> (6%)	MNN19e
1.10.6	50-52	24,15	small <i>Gephyrocapsa</i> , <i>Gephyrocapsa caribbeanica</i> , small <i>Reticulofenestra</i> (<i>minuta</i> , <i>minutula</i>), <i>Helicosphaera carteri</i> , <i>Helicosphaera</i> sp., <i>Umbilicosphaera</i> , <i>Rhabdosphaera</i> , <i>Syracosphaera</i> , <i>Coccolithus</i> sp., <i>Calsiosolenia</i> , <i>Pseudoemiliana lacunosa</i> , <i>Ericsonia</i> sp.	no reworked-Pleistocene biozone	small <i>Gephyrocapsa</i> $\leq 3\mu\text{m}$ (31,40%), <i>Reticulofenestra</i> spp. (41,86%), <i>Pseudoemiliana lacunosa</i> (6,98%)	MNN19e
1.10.11	100-102	24,63	small <i>Gephyrocapsa</i> , small <i>Reticulofenestra</i> (<i>minuta</i> , <i>minutula</i>), big <i>Reticulofemestra</i> , <i>Helicosphaera carteri</i> , <i>Helicosphaera hyalina</i> , <i>Umbilicosphaera</i> , <i>Rhabdosphaera</i> , <i>Syracolithus</i> , <i>Calcidiscus macintyeri</i> , <i>Coccolithus pelagicus</i> , <i>Pseudoemiliana lacunosa</i> , <i>Ericsonia</i> sp., <i>Discoaster</i> sp.	no reworked-Pleistocene biozone	small <i>Gephyrocapsa</i> $\leq 3\mu\text{m}$ (22%) <i>Reticulofenestra</i> spp. (50%) <i>Pseudoemiliana lacunosa</i> (5%)	MNN19e



1.10.23	220-222	25,85	small <i>Gephyrocapsa</i> , small <i>Reticulofenestra</i> (<i>minuta</i> , <i>minutula</i>), big <i>Reticulofemestra</i> , <i>Helicosphaera</i> <i>carteri</i> , <i>Rhabdosphaera</i> , <i>Syracosphaera</i> , <i>Syracolithus</i> , <i>Calcidiscus</i> <i>leptoporus</i> , <i>Coccolithus</i> <i>pelagicus</i> , <i>Pseudoemiliana</i> <i>lacunosa</i>	no reworked- Pleistocene biozone	small <i>Gephyrocapsa</i> $\leq 3\mu\text{m}$ (56,3%), <i>Reticulofenestra</i> spp. (29,1%), <i>Pseudoemiliana</i> <i>lacunosa</i> (3%)	MNN19e
---------	---------	-------	-----------------------------------------------------------------------------------------------------------------------------------------------------------------------------------------------------------------------------------------------------------------------------------------------------------------------------------------------------------------------------------------------------	-------------------------------------	--------------------------------------------------------------------------------------------------------------------------------------------------------	--------

Table 2: Table of borehole Livadi 1. Samples, depth, sample interval in every core. Calcareous nannoplankton that collected and identified in every sample, the biozonal indicators in each one and the biostratigraphic age.



6.2 Livadi 2

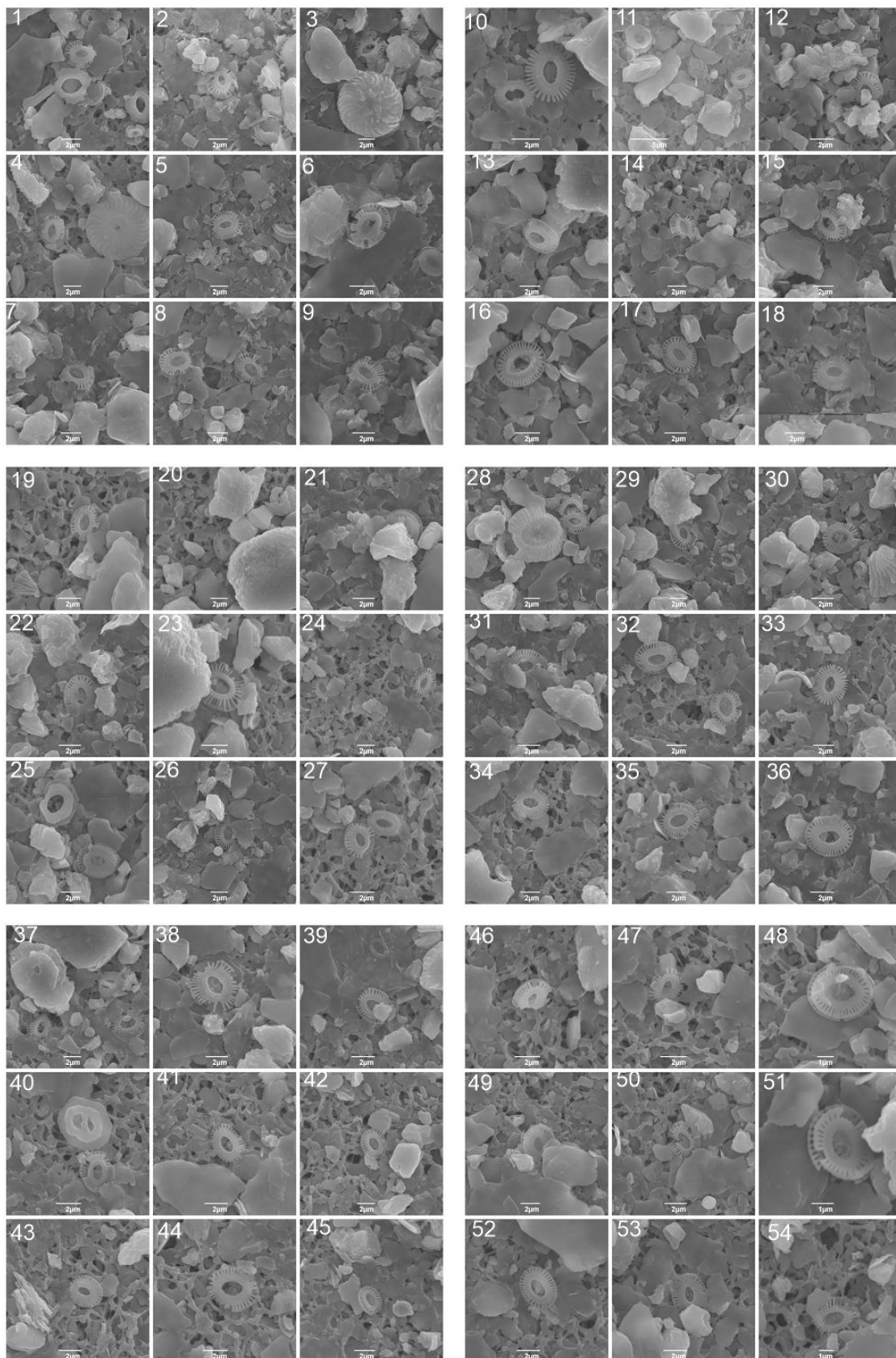
In borehole Livadi 2 core 7 (18-20,3m depth), nine samples have been analyzed with scanning electron microscope (SEM) for the nannofossil content in order to establish the biostratigraphic assignment. The assemblage composition of Livadi 2.7 (18-20,3m depth), in average, consisted of *Emiliania huxleyi* 55,35%, *Calcidiscus leptoporus* 1,63%, *Rhabdosphaera* spp. 1,72%, *Helicosphaera carteri* 0,54%, *Helicosphaera hyalina* 0,18%, small *Gephyrocapsa* spp. (<3μm) 20,06%, *Gephyrocapsa caribbeanica* 0,18%, *Coccolithus pelagicus* 0,27%, *Syracosphaera* spp. 3,41%, *Syracolithus* spp. 1,80%, *Umbilicosphaera* spp. 5,22%. The reworked coccoliths in this core were: *Calcidiscus macintyeri* 0,64%, *Reticulofenestra* spp. 42,49%, *Pseudoemilinia lacunosa* 6,9%, *Helicosphaera selli* 1%, *Gephyrocapsa omega* 1,05%, *Sphenolithus* spp. 0,33%, *Discoaster* spp. 0,74%.

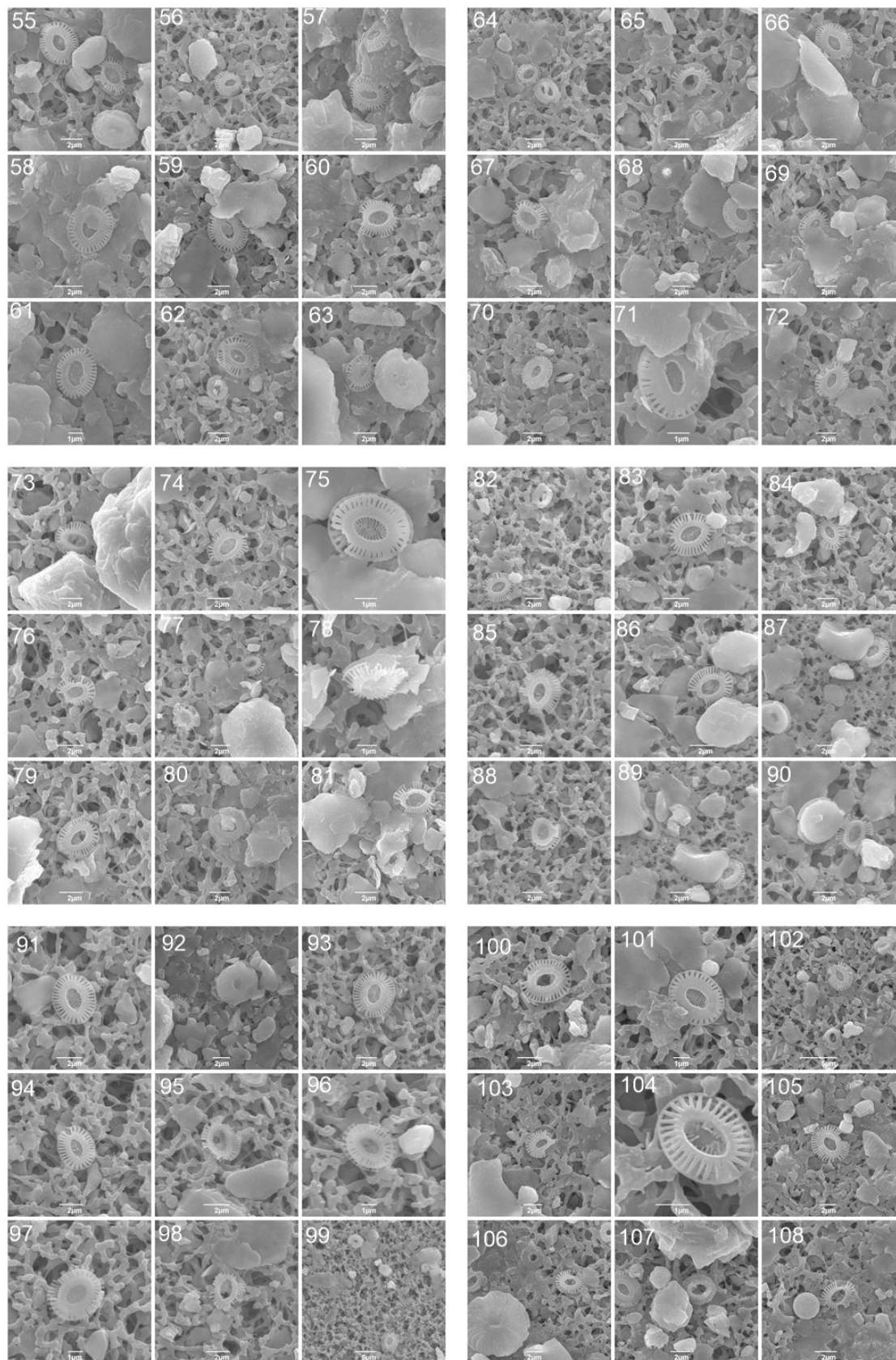
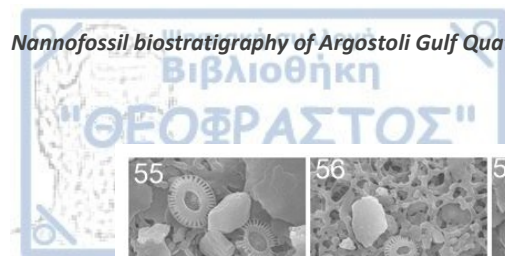
Continuing downwards in borehole Livadi 2, core 8 (20,4-23,5m depth), the assemblage composition in average was, *E. huxleyi* 43,35%, *Gephyrocapsa* spp. (<3microns) 26,53%, *C. leptoporus* 2,21%, *Rhabdosphaera* spp. 2,25%, *H. carteri* 0,83%, *H. wallichii* 0,39%, *H. hyalina* 0,83%, *G. caribbeanica* 0,94%, *C. pelagicus* 0,57%, *Syracosphaera* spp. 2,93%, *Syracolithus* spp. 2,07%, *Calsiosolenia* 0,26%, *Umbilicosphaera* spp. 4,43%, *Discosphaera* spp. 0,3%, *Umbellosphaera* spp. 0,53%. The reworked coccoliths in this core were: *C. macintyeri* 0,29%, *Reticulofenestra* spp. 38,13%, *P. lacunosa* 5,84%, *H. sellii* 0,21%, *H. recta* 0,08%, *G. omega* 0,43%, *Discoaster* spp. 1,61%, *D. surculus* 0,07%, *D. brouwerii* 0,07%, *Sphenolithus* spp. 0,26%.

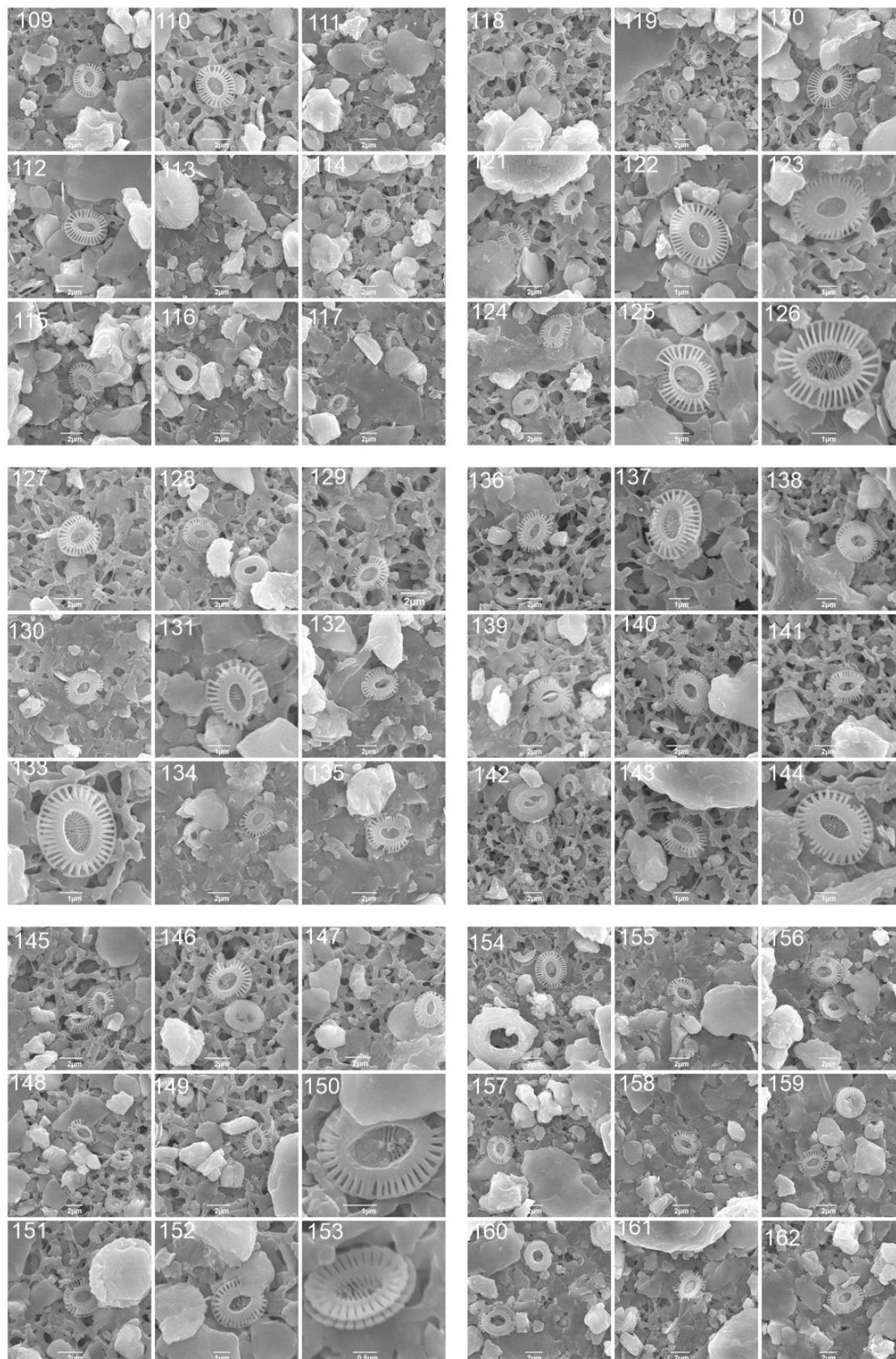
In Livadi2, core 9 (23,6-25m depth), the average assemblage composition was, *E. huxleyi* 37%, *C. leptoporus* 2,2%, *Rhabdosphaera* 2,1%, small *Gephyrocapsa* (<3μm) 26,4%, *G. caribbeanica* 0,6%, *H. carteri* 0,9%, *H. hyalina* 0,2%, *H. wallichii* 0,1%, *C. pelagicus* 0,3%, *Syracosphaera* spp. 3,5%, *Syracolithus* spp. 1%, *Calsiosolenia* spp. 0,1%, *Discosphaera* spp. 0,4%, *Umbilicosphaera* spp. 9,2%. The reworked coccoliths in this core were: *C. macintyeri* 0,6%, *P. lacunosa* 7,6%, *Reticulofenestra* spp. 37,6%, *G. omega* 0,2%, *H. recta* 0,1%, *Discoaster* spp. 0,6%, *Discoaster* rosette form 0,1%, *Tribrachiatum* 0,1%.

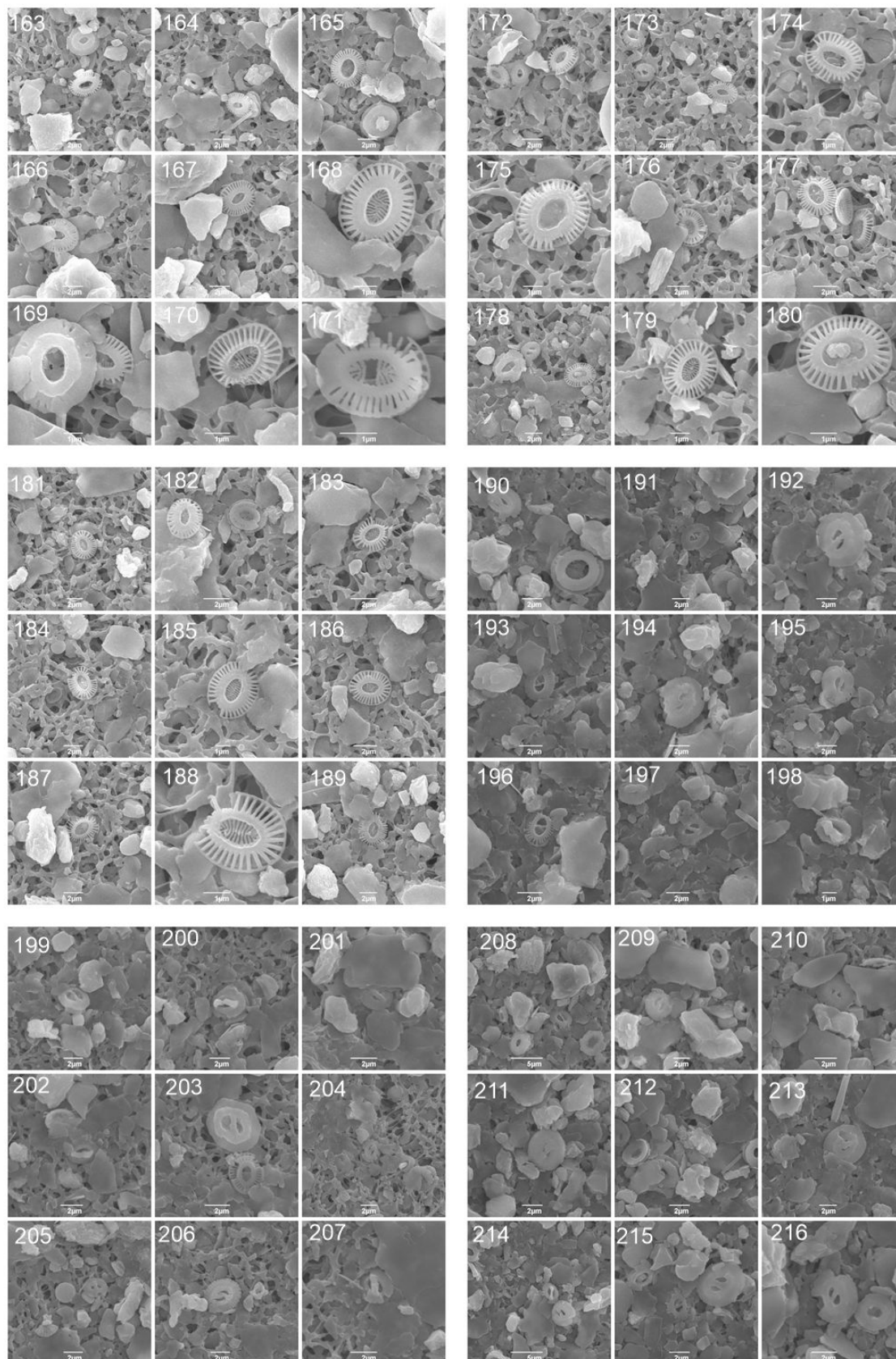
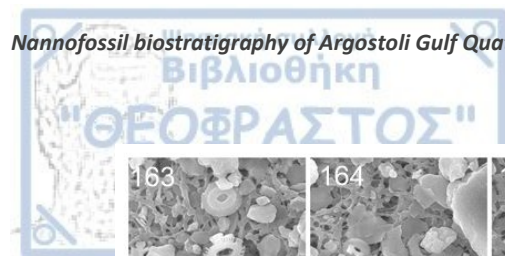
Finally, in Livadi2, core 10 (25,5-26,6m depth), the average assemblage composition was, *E. huxleyi* in sample 2.10.1 was 8,64% and in the rest of core 10 was completely absent, small *Gephyrocapsa* spp. (<3μm) 8,71%, *Umbilicosphaera* spp. %, *C. leptoporus* 2,82%, *Rhabdosphaera* spp. 0,77%, %, *H. carteri* 1,47%, *H. hyalina* 1,07%, *H. wallichii* 0,3%, *H. pavimentum* 0,12%, *C. pelagicus* 0,62%, *Syracosphaera* spp. 2,05%, *Umbilicosphaera* spp. 11,6%, *Syracolithus* spp. 0,44% and *Umbellosphaera* spp. 0,12%. The reworked coccoliths in this core were: *G. omega* 0,12%, *C. macintyeri* 0,5%, *Reticulofenestra* spp. 52,05%, *P. lacunosa* 4,92%, *H. sellii* 0,62%, *H. recta* 0,5%, *Discoaster* spp. 2,62%, *D. brouweri* 0,1%, *D. triradiatus* 0,1%, *Sphenolithus* spp. 0,4%.

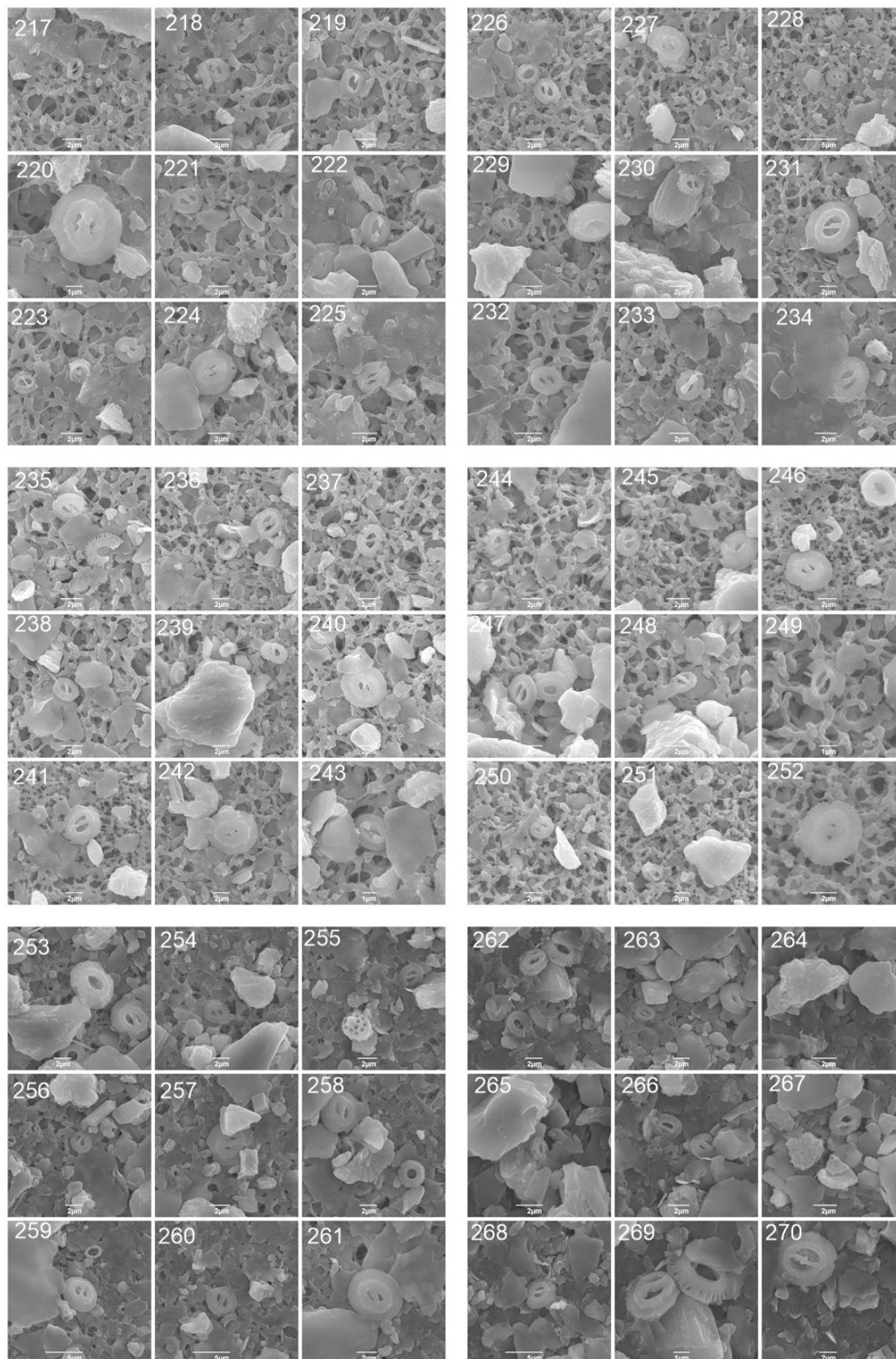
The tables and the diagrams below, show the nannofossils found in borehole Livadi 2 and summarize the assemblage composition of Livadi 2 core 7, 8, 9, 10.

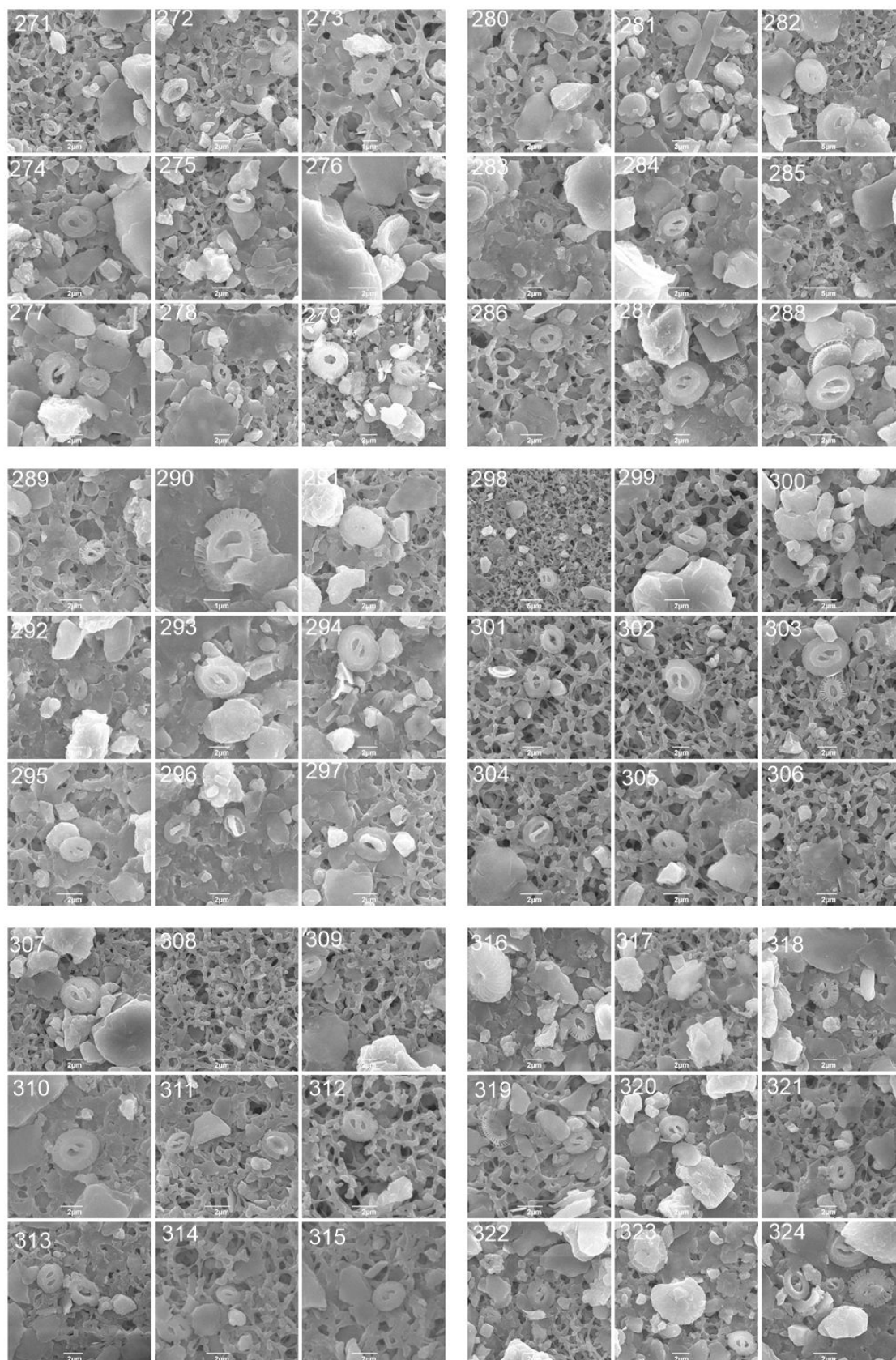
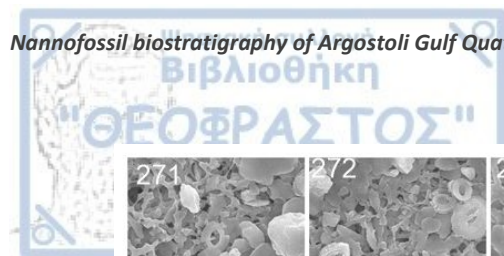


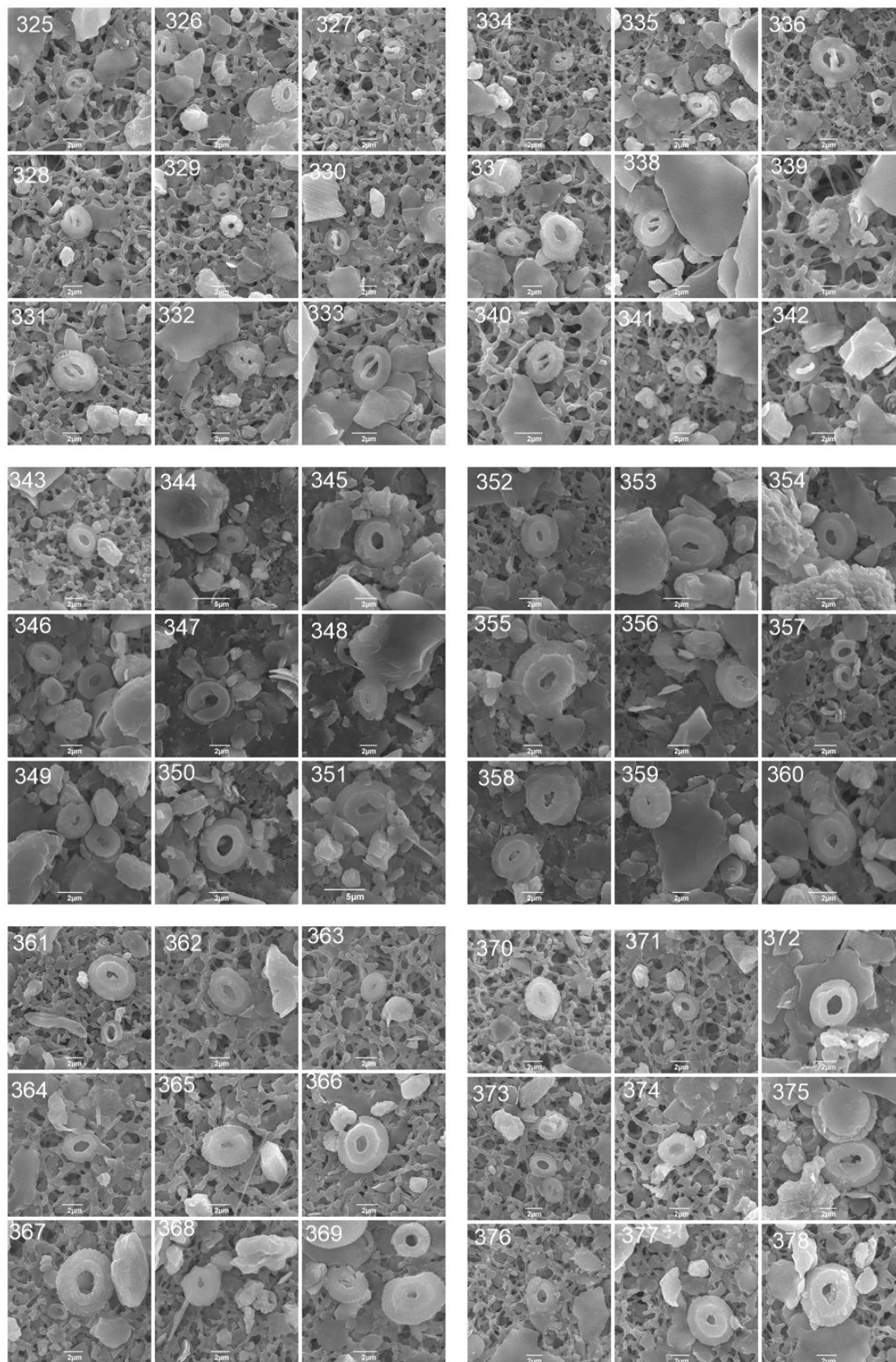


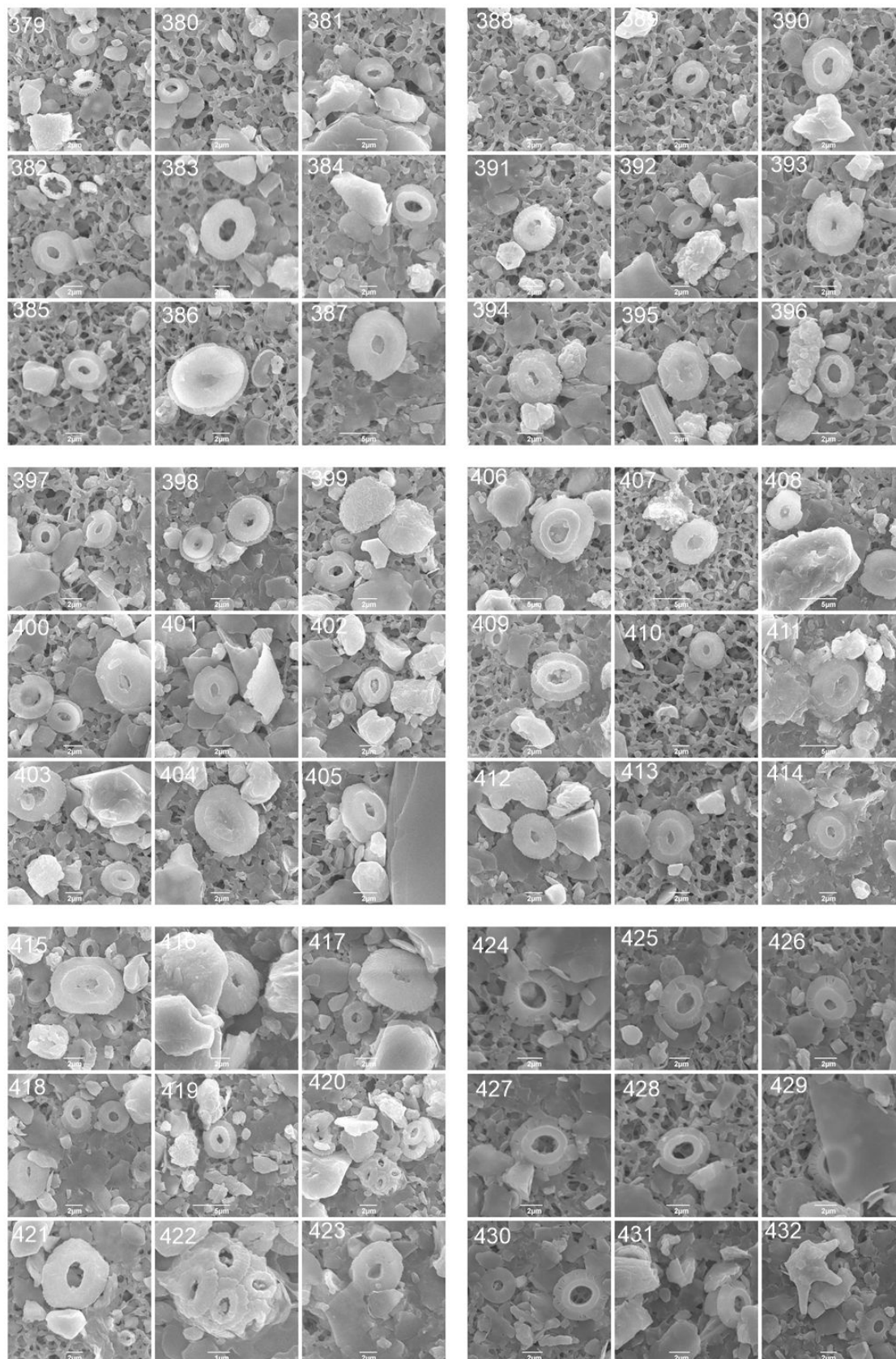
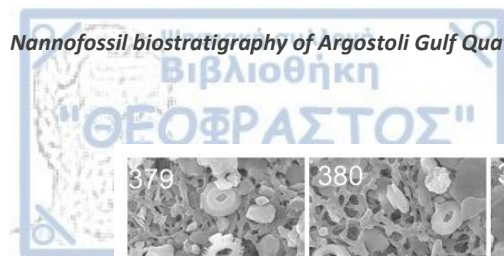


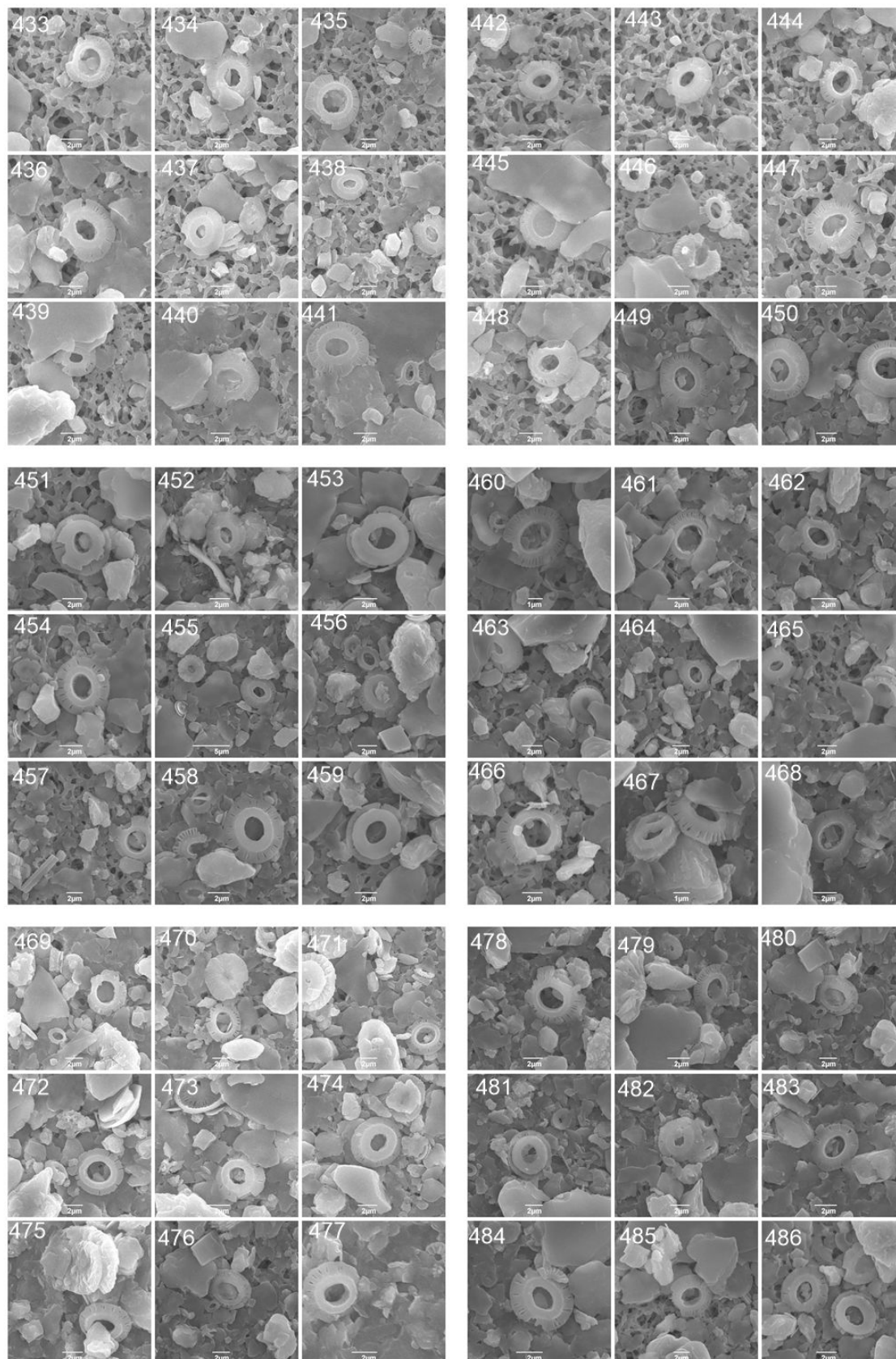


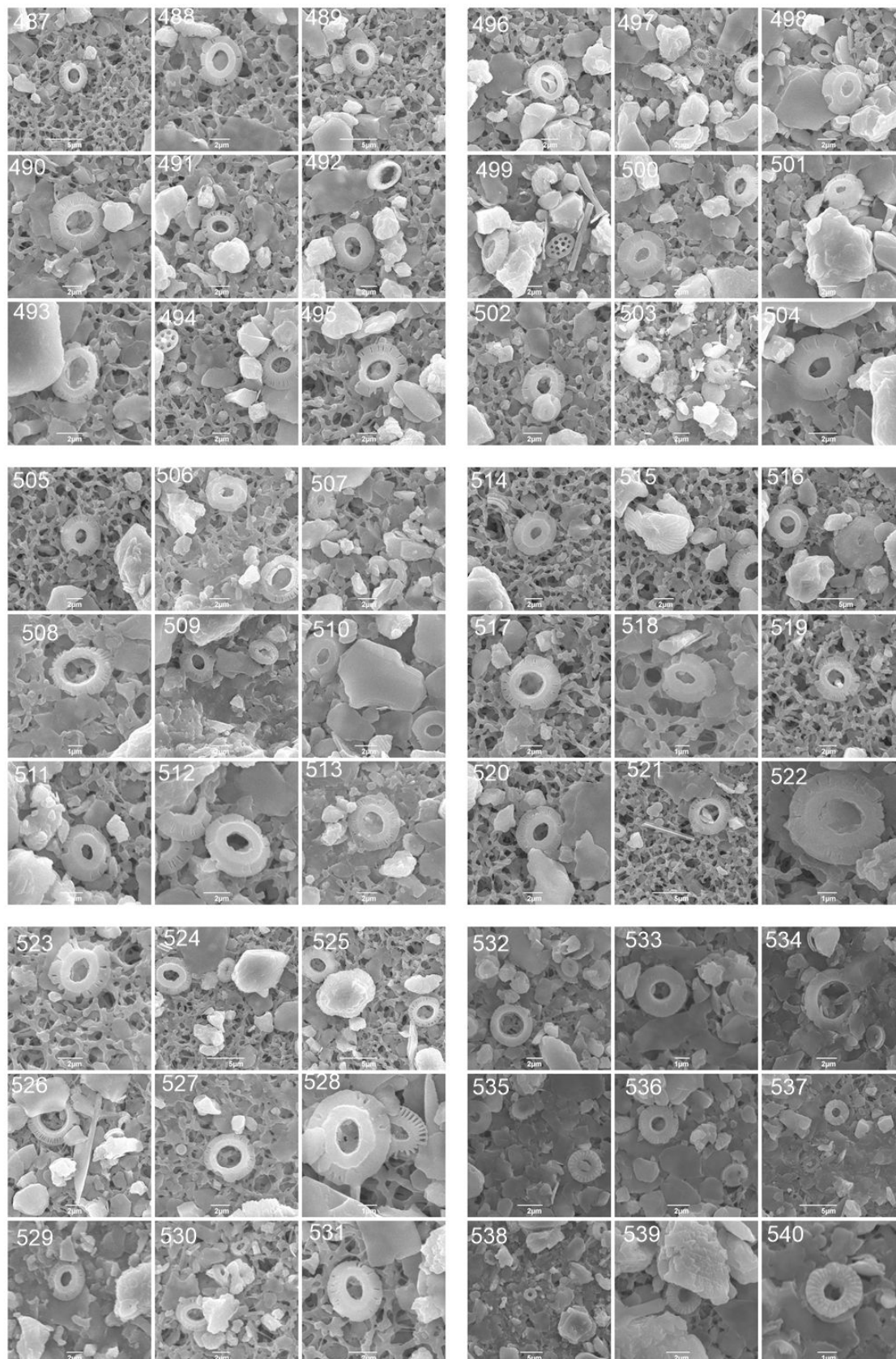
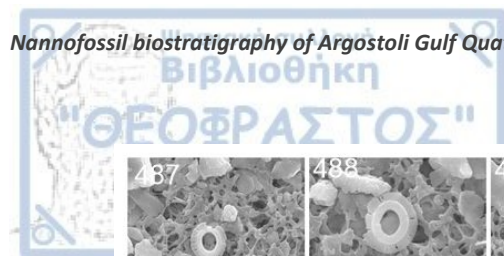


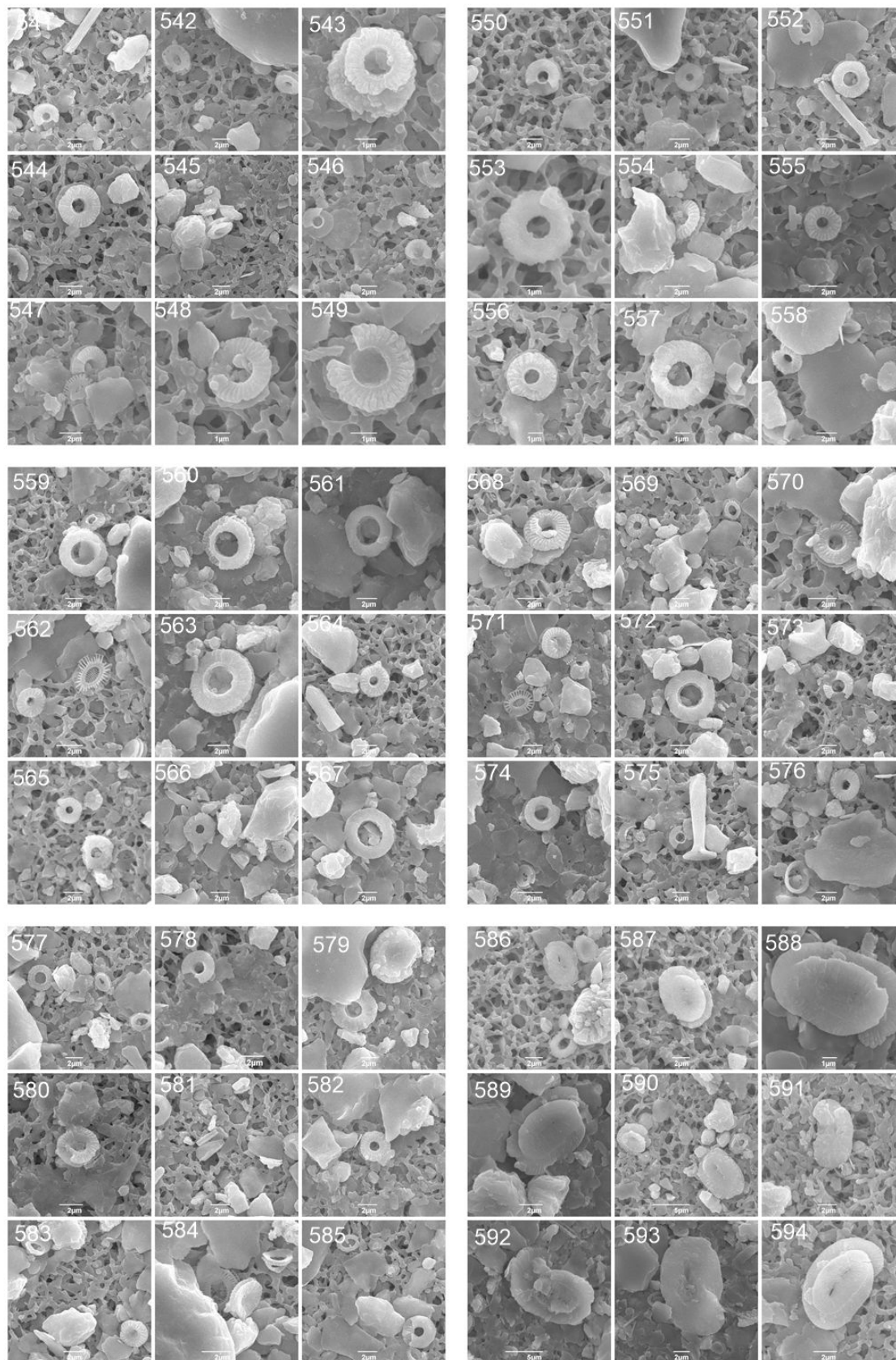


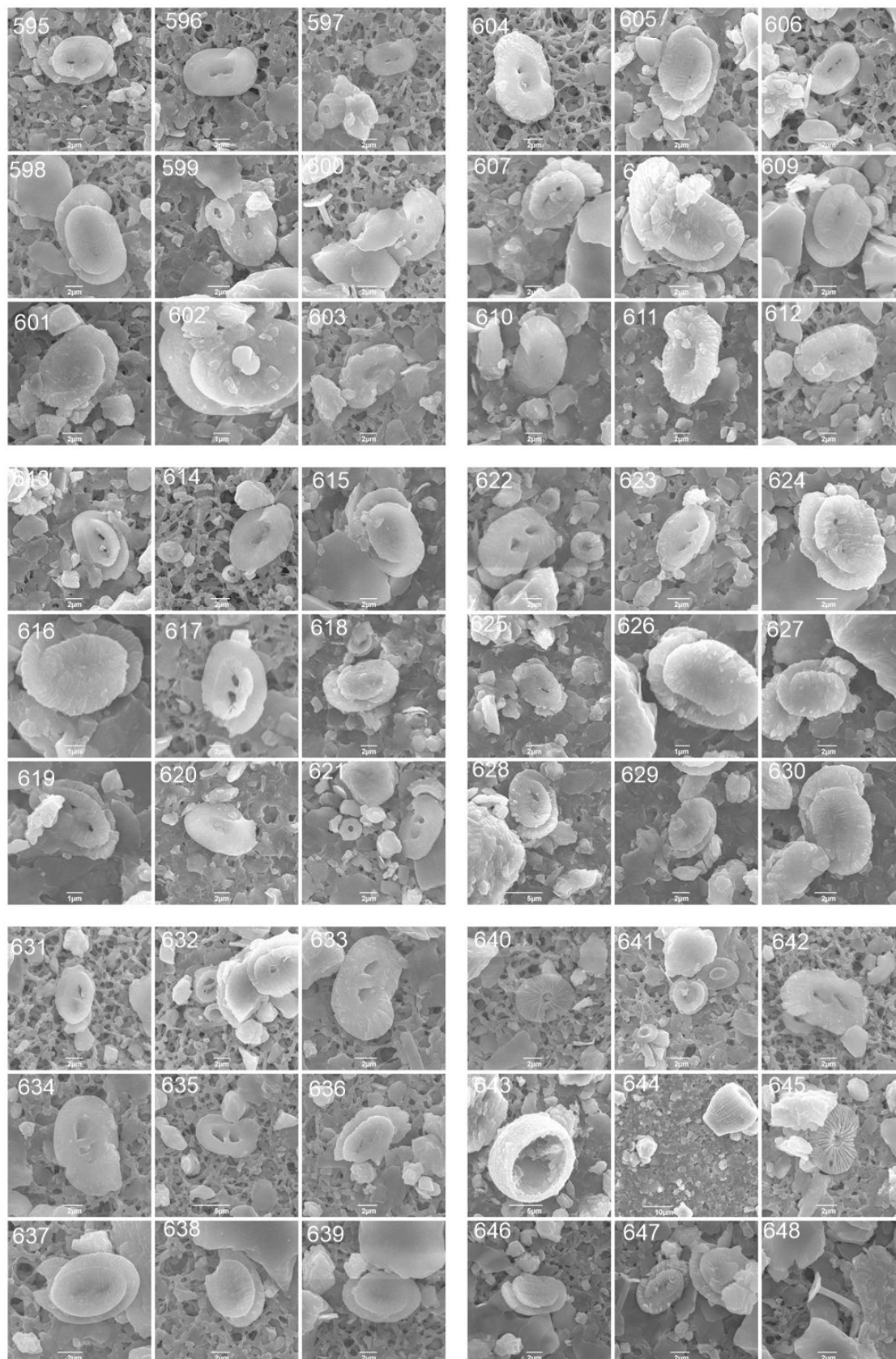
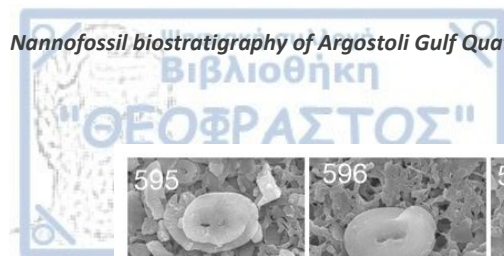


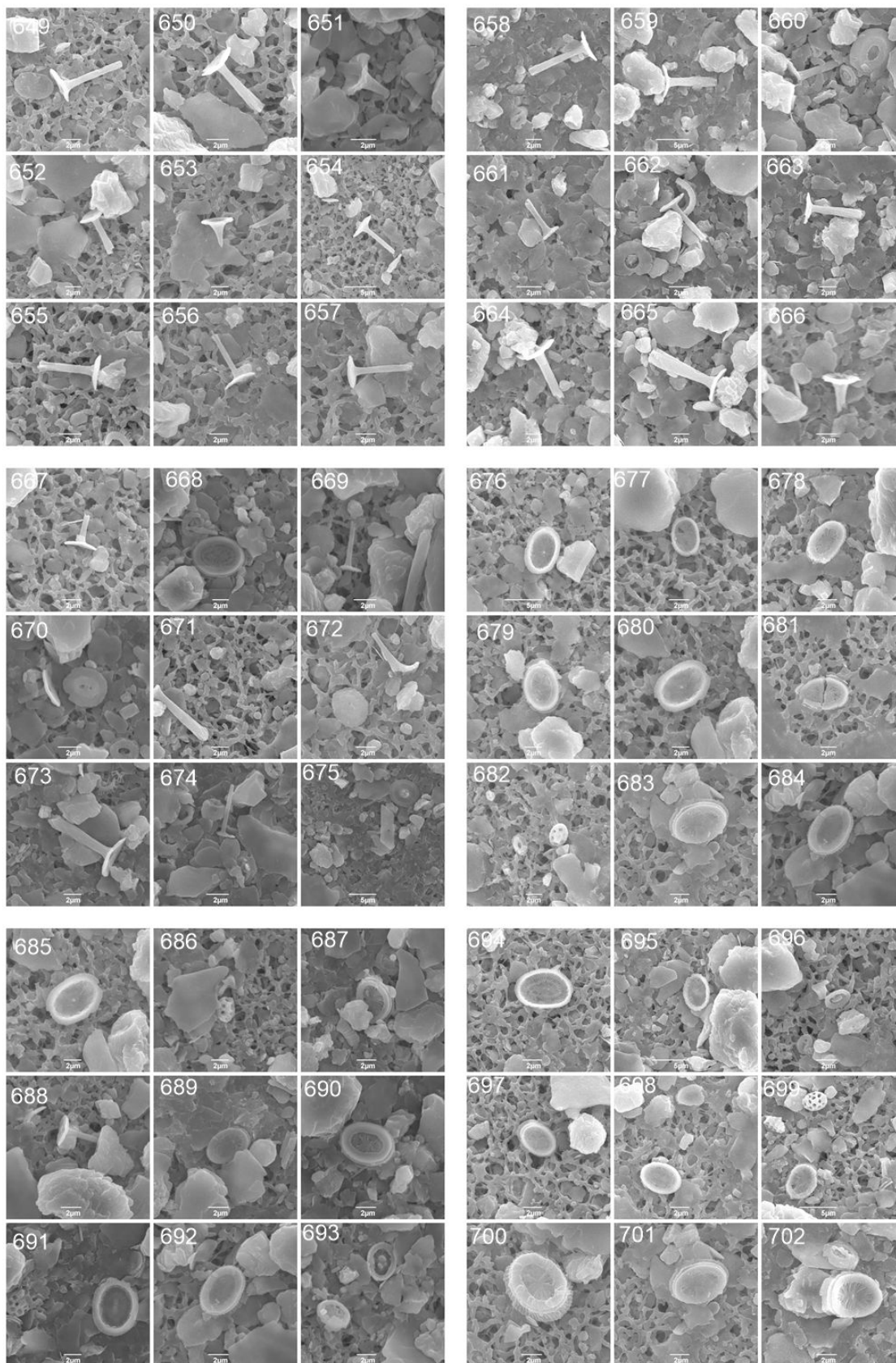


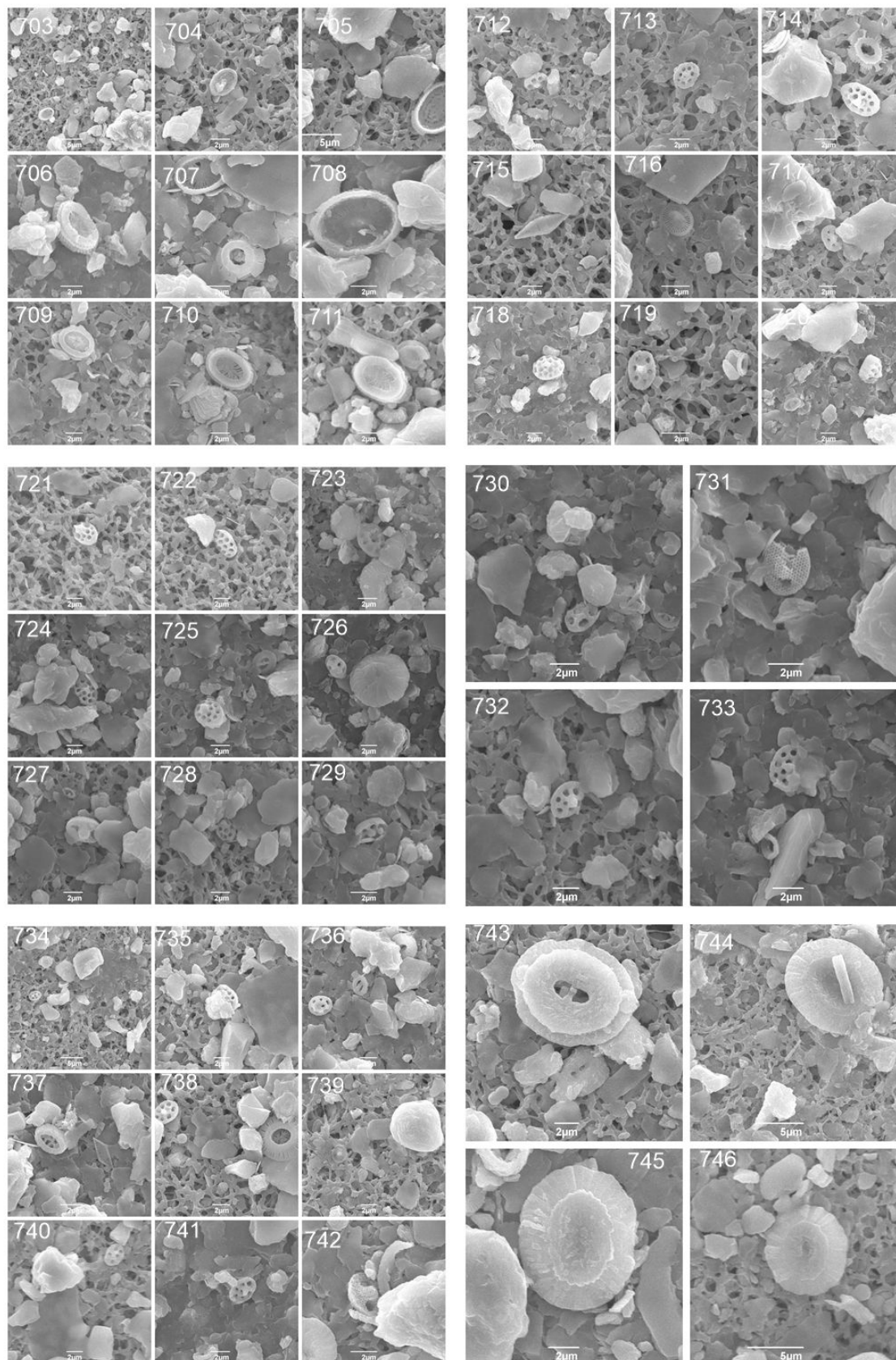
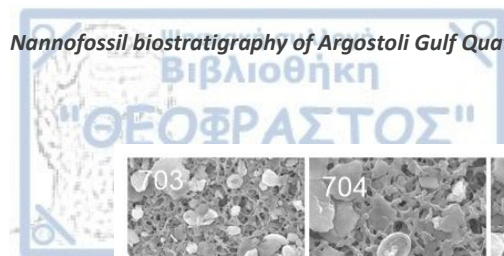


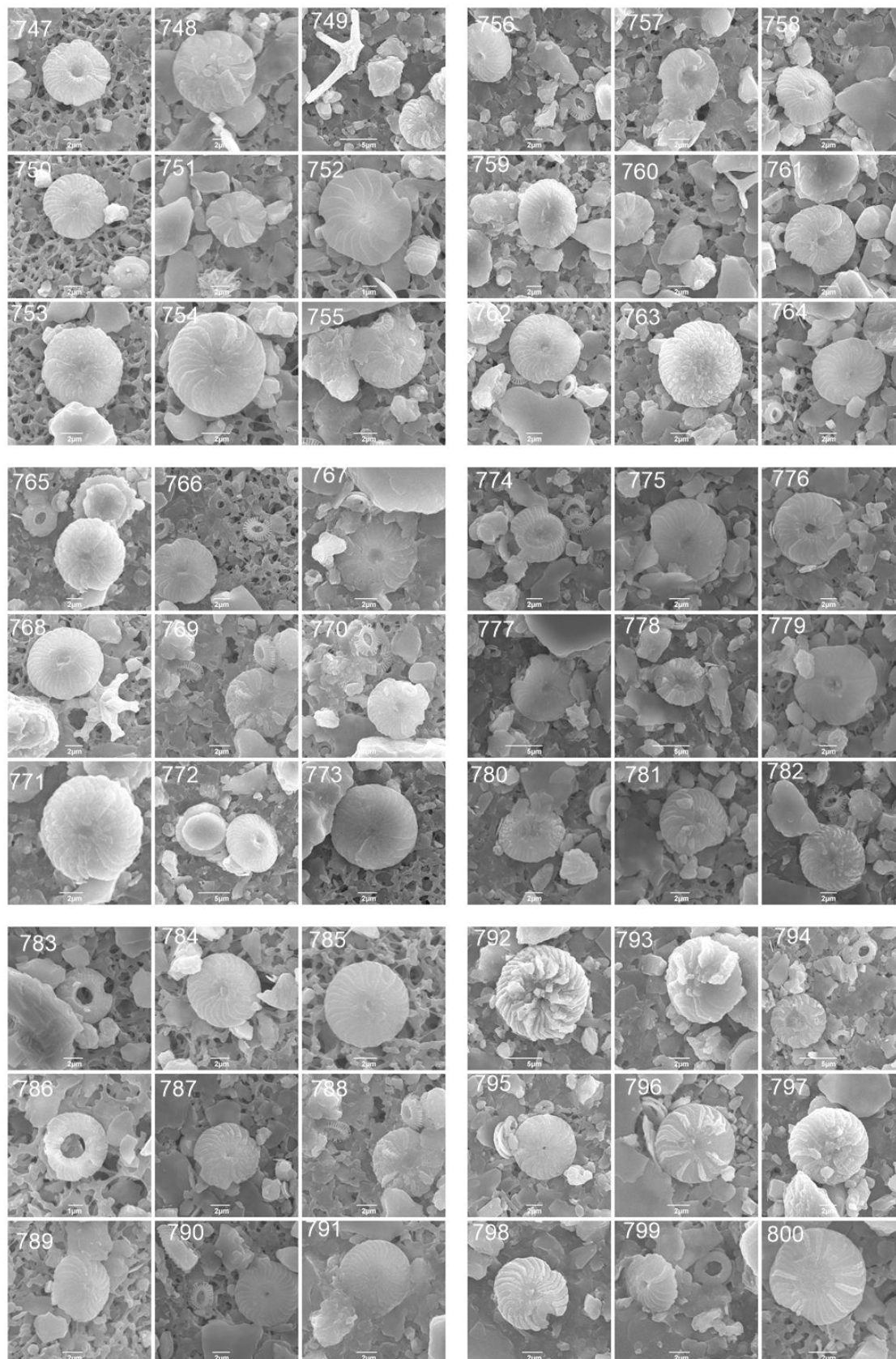


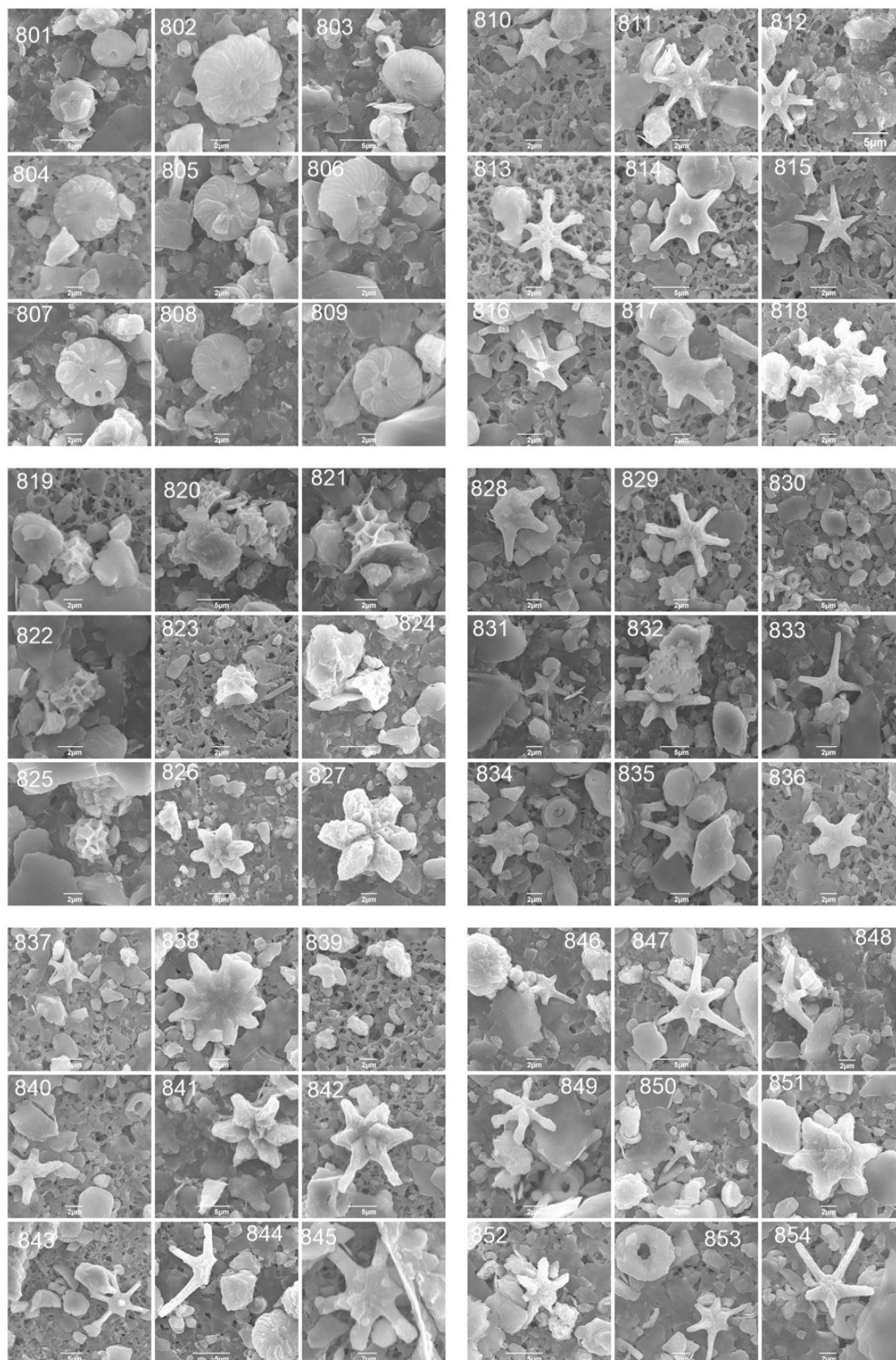
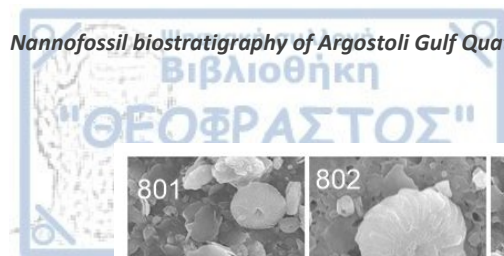












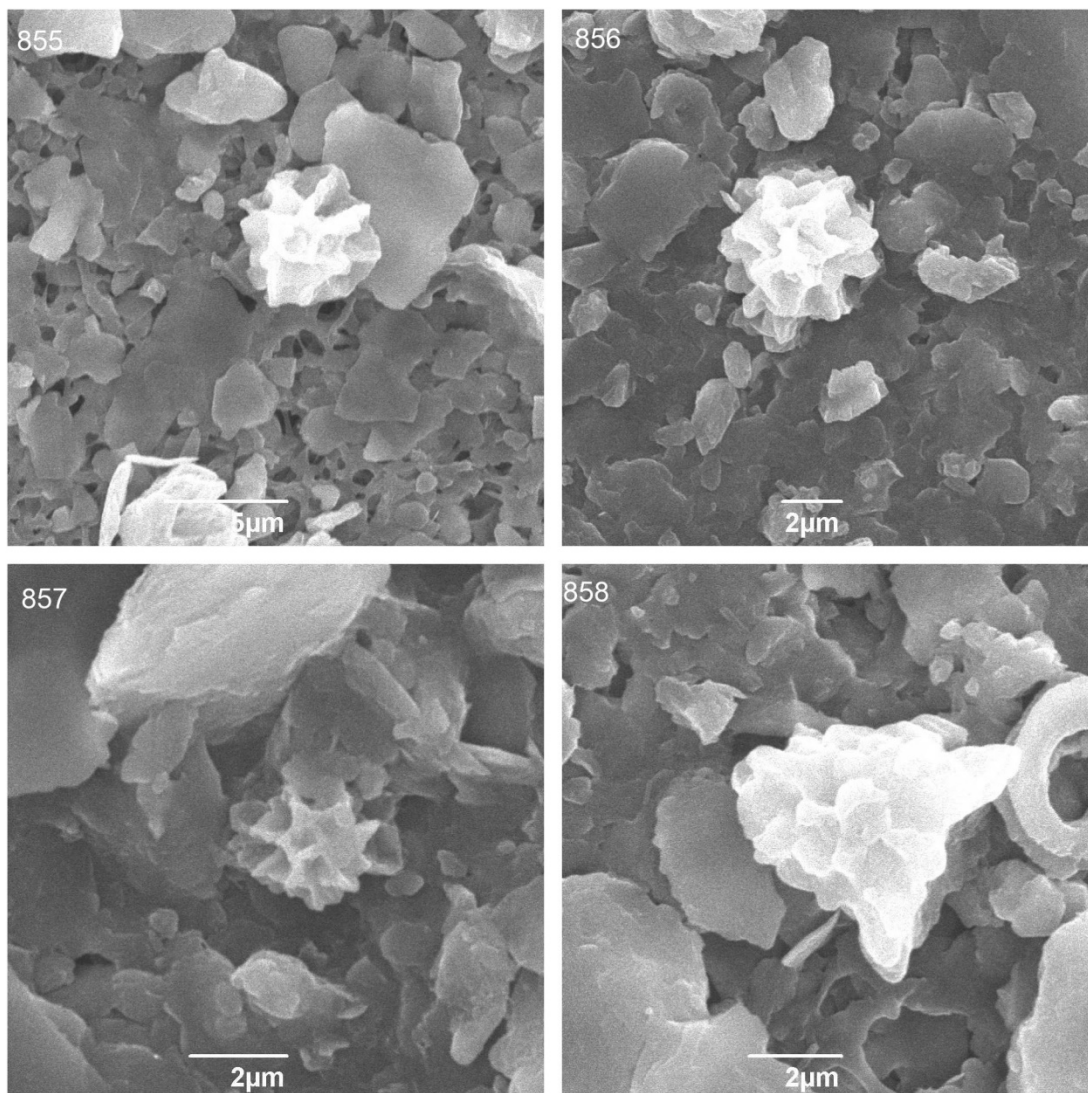
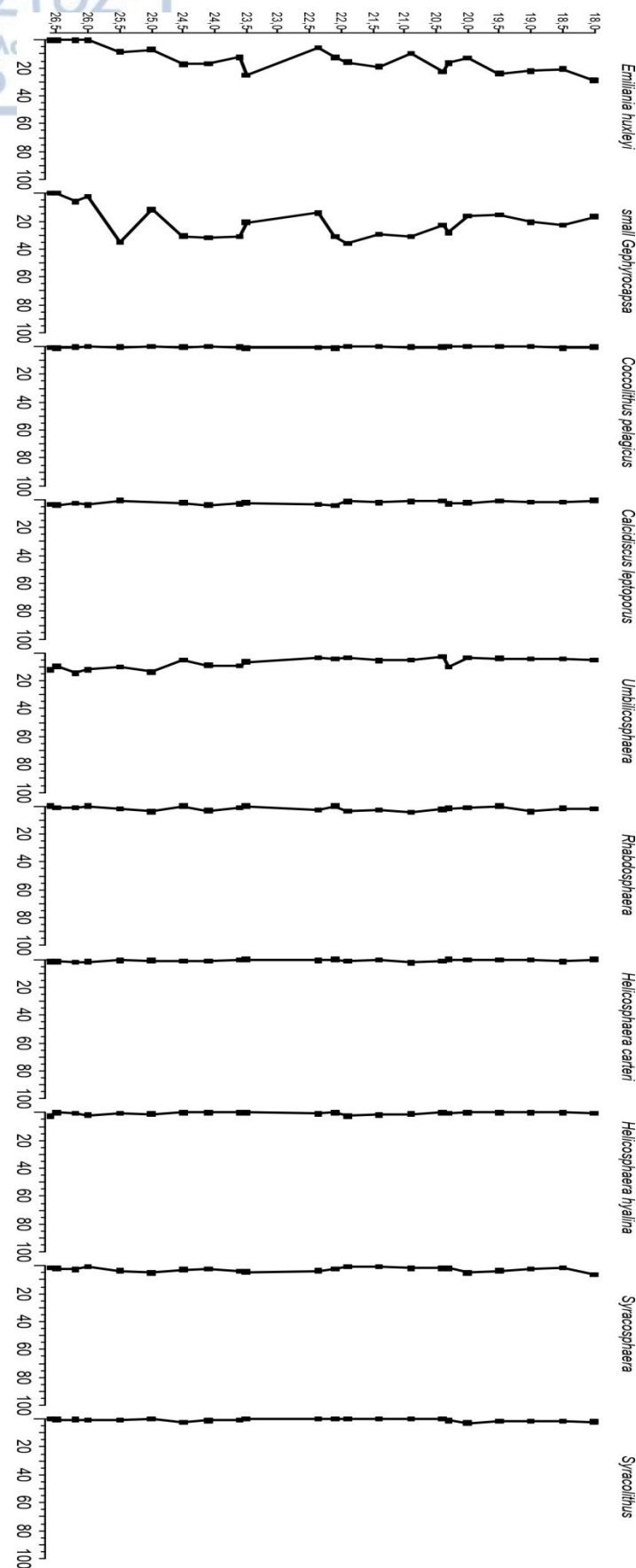
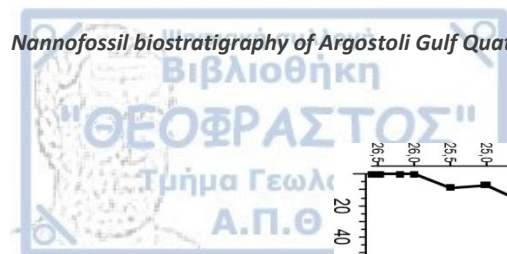


Table 3: SEM pictures from borehole Livadi 2:

1-189: *Emiliana huxleyi*, 190-342: small *Gephyrocapsa* (<3μm), 343-423: *Reticulofenestra* spp. (422: *Reticulofenestra* Coccosphere), 424-531: *Pseudoemiliana lacunosa*, 532-585: *Umbilicosphaera* spp., 586-612: *Helicosphaera carteri*, 613, 628, 637, 642: *H. wallichii*, 614-616, 620, 626, 627, 630, 638, 639, 646, 647: *H. hyalina*, 621-623, 625, 631, 633-636: *H. sellii*, 617, 629, 632: *H. recta*, 619, 624: *H. ethologa*, 645, 675: *Umbellosphaera* spp., 643, 644: *Scyphosphaera* spp., 649-674, 688: *Rhabdosphaera* spp., 676-711: *Syracosphaera* spp., 712-742: *Syracolithus*, 743-746: *Coccolithus pelagicus*, 747-785, 787-780, 804, 805: *Calcidiscus leptoporus*, 786, 801-803, 806-809: *C. macintyeri*, 810-818, 826-854: *Discoaster* spp., 819-825, 855-858: *Sphenolithus* spp. (820, 821, 823, 858: *S. abies*).



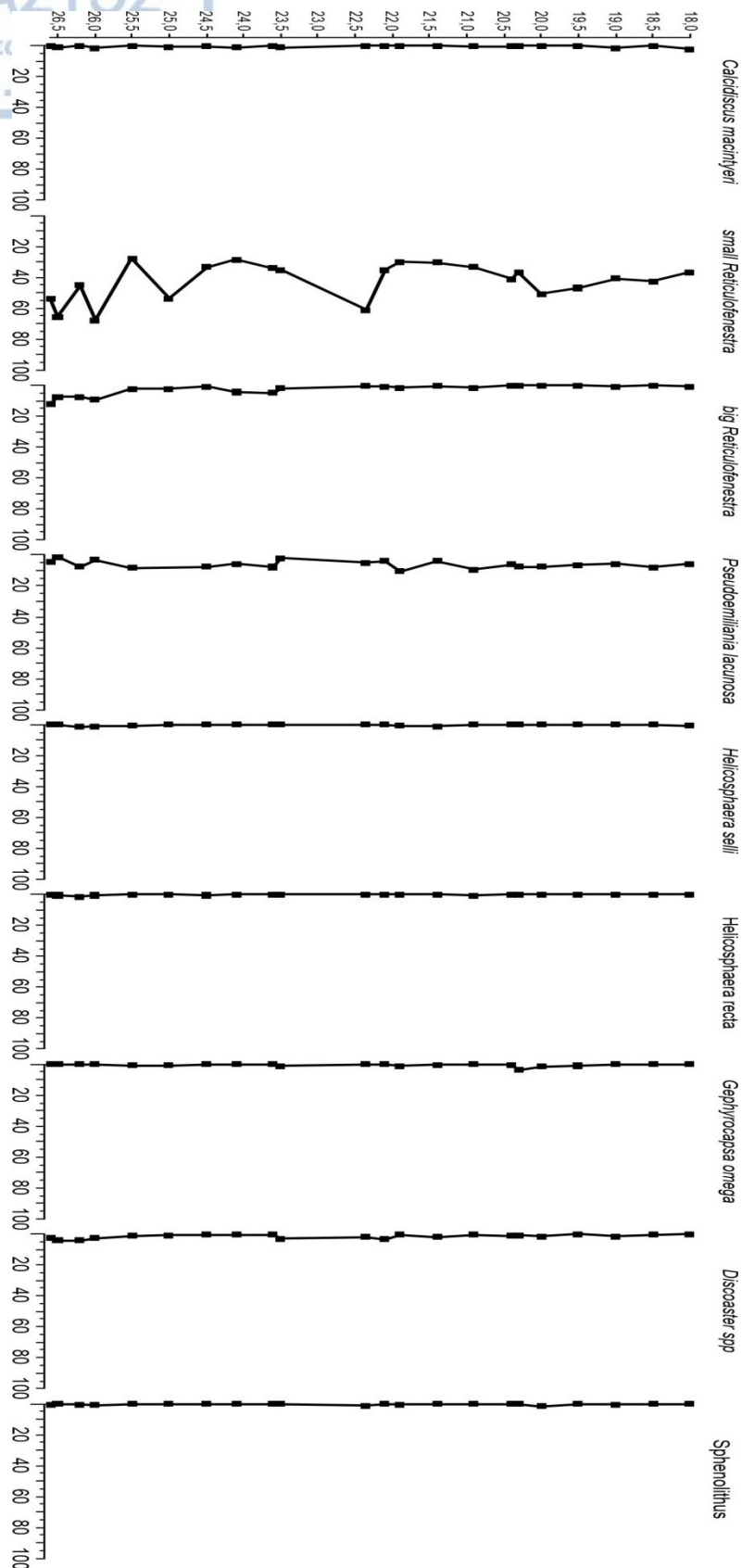


Figure 17: Diagrams of calcareous nannoplankton assemblages vs. core depth in borehole Livadi 2 (> 3%). First diagram: coccoliths in situ and second diagram: reworked coccoliths.

<u>Sampling</u>			<u>Biostratigraphy</u>			
			<u>Calcareous Nannoplakton</u>			
			<u>Scanning Electron Microscope (SEM)</u>			
<u>Sample Code</u>	<u>Sample interval (cm)</u>	<u>Depth (m)</u>	<u>In situ</u>	<u>Plio-Pleistocene Reworked</u>	<u>Notes</u>	<u>Results</u>
2.7.1	0-2	18	<i>Emiliana huxleyi</i> , <i>Calcidiscus leptoporus</i> , <i>Rhabdosphaera</i> , <i>Helicosphaera hyalina</i> , <i>Coccolithus pelagicus</i> , <i>Syracosphaera</i> , <i>Syracolithus</i> , <i>Calsiosolenia</i> , <i>Umbilicosphaera</i>	small <i>Reticulofenestra (minuta,minutula)</i> , big <i>Reticulofenestra</i> , small <i>Gephyrocapsa</i> , <i>G. caribbeanica</i> , <i>Calcidiscus macintyeri</i> , <i>Helicosphaera selli</i> , <i>H. recta</i> , <i>Coccolithus formosus</i>	<i>E. huxleyi</i> (62,5%) abundant and Plio-Pleistocene reworked from surroundings due to erosion	MNN21b
2.7.6	50-52	18,5	<i>Emiliana huxleyi</i> , <i>Calcidiscus leptoporus</i> , <i>Rhabdosphaera</i> , <i>Helicosphaera carteri</i> , <i>Coccolithus pelagicus</i> , <i>Syracosphaera</i> , <i>Syracolithus</i> , <i>Umbilicosphaera</i>	small <i>Reticulofenestra (minuta,minutula)</i> , small <i>Gephyrocapsa</i> , <i>Pseudoemiliana lacunosa</i> , <i>Discoaster</i> sp.	<i>E. huxleyi</i> (60,94 %) abundant and Plio-Pleistocene reworked from surroundings due to erosion	MNN21b
2.7.11	100-102	19	<i>Emiliana huxleyi</i> , <i>Calcidiscus leptoporus</i> , <i>Rhabdosphaera</i> , <i>Helicosphaera carteri</i> , <i>Syracosphaera</i> , <i>Syracolithus</i> , <i>Umbilicosphaera</i>	small <i>Reticulofenestra (minuta,minutula)</i> , big <i>Reticulofenestra</i> , small <i>Gephyrocapsa</i> , <i>G. caribbeanica</i> , <i>Calcidiscus macintyeri</i> , <i>Pseudoemiliana lacunosa</i> , <i>Sphenolithus</i> , <i>Discoaster</i> sp.	<i>E. huxleyi</i> (57,75%) abundant and Plio-Pleistocene reworked from surroundings due to erosion	MNN21b

2.7.16	150-152	19,5	<i>Emiliana huxleyi</i> , <i>Calcidiscus leptoporus</i> , <i>Helicosphaera carteri</i> , <i>Syracosphaera</i> , <i>Syracolithus</i> , <i>Umbilicosphaera</i>	small <i>Reticulofenestra (minuta,minutula)</i> , small <i>Gephyrocapsa</i> , <i>G. omega (parallela)</i> , <i>G. caribbeanica</i> , <i>Pseudoemiliana lacunosa</i>	<i>E. huxleyi</i> (64,38%) abundant and Plio-Pleistocene reworked from surroundings due to erosion	MNN21b
2.7.21	200-202	20	<i>Emiliana huxleyi</i> , <i>Calcidiscus leptoporus</i> , <i>Rhabdosphaera</i> , <i>Helicosphaera carteri</i> , <i>Syracosphaera</i> , <i>Syracolithus</i> , <i>Umbilicosphaera</i>	small <i>Reticulofenestra (minuta,minutula)</i> , small <i>Gephyrocapsa</i> , <i>G. omega</i> , <i>P. lacunosa</i> , <i>Sphenolithus</i> , <i>Discoaster</i> sp.	<i>E. huxleyi</i> (39,66%) abundant and Plio-Pleistocene reworked from surroundings due to erosion	MNN21b
2.7.25	232-235	20,3	<i>Emiliana huxleyi</i> , <i>Calcidiscus leptoporus</i> , <i>Rhabdosphaera</i> , <i>H. hyalina</i> , <i>Syracosphaera</i> , <i>Syracolithus</i> , <i>Umbilicosphaera</i>	small <i>Reticulofenestra (minuta,minutula)</i> , small <i>Gephyrocapsa</i> , <i>G. omega</i> , <i>P. lacunosa</i> , <i>Discoaster</i> sp.	<i>E. huxleyi</i> (46,88%) abundant and Plio-Pleistocene reworked from surroundings due to erosion	MNN21b
2.8.1	0-2	20,4	<i>Emiliana huxleyi</i> , <i>Calcidiscus leptoporus</i> , <i>Rhabdosphaera</i> , <i>Helicosphaera carteri</i> , <i>H. wallichii</i> , <i>Coccolithus pelagicus</i> , <i>Syracosphaera</i> , <i>Umbilicosphaera</i>	small <i>Reticulofenestra (minuta,minutula)</i> , <i>P. lacunosa</i> , small <i>Gephyrocapsa</i> , <i>G. caribbeanica</i> , <i>G. omega</i> , <i>C. formosus</i> , <i>C. macintyeri</i> , <i>D. surculus</i> , <i>Discoaster</i> sp.	<i>E. huxleyi</i> (63,64%) abundant and Plio-Pleistocene reworked from surroundings due to erosion	MNN21b

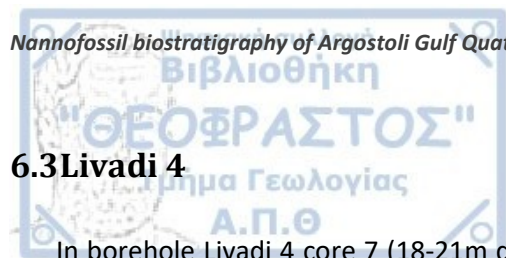
2.8.6	50-52	20,9	<i>E. huxleyi</i> , <i>C. leptoporus</i> , <i>Rhabdosphaera</i> , <i>H. carteri</i> , <i>H. hyalina</i> , <i>C. pelagicus</i> , <i>Syracosphaera</i> , <i>Umbilicosphaera</i> , <i>Umbellosphaera</i>	<i>C. macintyeri</i> , small <i>Reticulofenestra</i> , big <i>Reticulofenestra</i> , <i>H. recta</i> , small <i>Gephyrocapsa</i> , <i>G. caribbeanica</i> , <i>C. formosus</i> , <i>Discoaster</i> sp., <i>Ericsonia</i>	<i>E. huxleyi</i> (27,42%) abundant and Plio-Pleistocene reworked from surroundings due to erosion	MNN21b
2.8.11	100-102	21,4	<i>E. huxleyi</i> , <i>C. leptoporus</i> , <i>Rhabdosphaera</i> , <i>H. carteri</i> , <i>H. hyalina</i> , <i>H. wallichii</i> , <i>Syracosphaera</i> , <i>Calsiosolenia</i> , <i>Umbilicosphaera</i>	small <i>Reticulofenestra</i> (<i>minuta</i> , <i>minutula</i>), big <i>Reticulofenestra</i> , <i>P. lacunosa</i> , <i>H. selli</i> , small <i>Gephyrocapsa</i> , <i>G. omega</i> , <i>G. caribbeanica</i> , <i>C. formosus</i> , <i>Discoaster</i> sp., <i>Discoaster</i> rosette form, <i>Ericsonia</i>	<i>E. huxleyi</i> (48%) abundant and Plio-Pleistocene reworked from surroundings due to erosion	MNN21b
2.8.16	150-152	21,9	<i>E. huxleyi</i> , <i>C. leptoporus</i> , <i>Rhabdosphaera</i> , <i>H. carteri</i> , <i>H. hyalina</i> , <i>H. wallichii</i> , <i>Syracosphaera</i> , <i>Calsiosolenia</i> , <i>Umbilicosphaera</i>	small <i>Reticulofenestra</i> (<i>minuta</i> , <i>minutula</i>), big <i>Reticulofenestra</i> , <i>P. lacunosa</i> , <i>H. selli</i> , small <i>Gephyrocapsa</i> , <i>G. omega</i> , <i>G. caribbeanica</i> , <i>C. formosus</i> , <i>Sphenolithus</i> , <i>D. brouweri</i> , <i>Discaster</i> sp.	<i>E. huxleyi</i> (46,55%) abundant and Plio-Pleistocene reworked from surroundings due to erosion	MNN21b
2.8.21	200-202	22,1	<i>E. huxleyi</i> , <i>C. leptoporus</i> , <i>C. formosus</i> , <i>Syracosphaera</i> , <i>Umbilicosphaera</i> , <i>Discosphaera</i> , <i>Umbellosphaera</i>	small <i>Reticulofenestra</i> (<i>minuta</i> , <i>minutula</i>), big <i>Reticulofenestra</i> , <i>P. lacunosa</i> , small <i>Gephyrocapsa</i> , <i>G. caribbeanica</i> , <i>C. formosus</i> , <i>Discoaster</i> sp.	<i>E. huxleyi</i> (37,50%) abundant and Plio-Pleistocene reworked from surroundings due to erosion	MNN21b

2.8.26	260-262	22,36	<i>E. huxleyi</i> , <i>C. leptoporus</i> , <i>Rhabdosphaera</i> , <i>H. carteri</i> , <i>H. hyalina</i> , <i>C. pelagicus</i> , <i>Syracosphaera</i> , <i>Calsiosolenia</i> , <i>Umbilicosphaera</i>	small <i>Reticulofenestra</i> (<i>minuta</i> , <i>minutula</i>), big <i>Reticulofenestra</i> , <i>P. lacunosa</i> , small <i>Gephyrocapsa</i> , <i>C. formosus</i> , <i>Sphenolithus</i> , <i>Discoaster</i> sp.	<i>E. huxleyi</i> (22,86%) abundant and Plio-Pleistocene reworked from surroundings due to erosion	MNN21b
2.8.31	310-312	23,5	<i>E. huxleyi</i> , <i>C. leptoporus</i> , <i>C. pelagicus</i> , <i>Syracosphaera</i> , <i>Umbilicosphaera</i>	small <i>Reticulofenestra</i> (<i>minuta</i> , <i>minutula</i>), big <i>Reticulofenestra</i> , <i>C. macintyeri</i> , <i>P. lacunosa</i> , small <i>Gephyrocapsa</i> , <i>G. omega</i> , <i>G. caribbeanica</i> , <i>C. formosus</i> , <i>Discoaster</i> sp.	<i>E. huxleyi</i> (57,50%) abundant and Plio-Pleistocene reworked from surroundings due to erosion	MNN21b
2.9.1	0-2	23,6	<i>E. huxleyi</i> , <i>C. leptoporus</i> , <i>Rhabdosphaera</i> , <i>H. carteri</i> , <i>C. pelagicus</i> , <i>Syracosphaera</i> , <i>Syracolithus</i> , <i>Umbilicosphaera</i> , <i>Discosphaera</i>	small <i>Reticulofenestra</i> (<i>minuta</i> , <i>minutula</i>), big <i>Reticulofenestra</i> , <i>P. lacunosa</i> , small <i>Gephyrocapsa</i> , <i>G. caribbeanica</i> , <i>C. formosus</i> , <i>Discoaster</i> sp., <i>Discoaster</i> rosette form, <i>Cruciplacolith</i> , <i>Tribrachiatus</i>	<i>E. huxleyi</i> (36,1%) abundant and Plio-Pleistocene reworked from surroundings due to erosion	MNN21b
2.9.6	50-52	24,1	<i>E. huxleyi</i> , <i>C. leptoporus</i> , <i>Rhabdosphaera</i> , <i>H. carteri</i> , <i>H. wallichii</i> , <i>Syracosphaera</i> , <i>Syracolithus</i> , <i>Calsiosolenia</i> , <i>Umbilicosphaera</i> , <i>Discosphaera</i>	small <i>Reticulofenestra</i> (<i>minuta</i> , <i>minutula</i>), big <i>Reticulofenestra</i> , <i>C. macintyeri</i> , <i>P. lacunosa</i> , small <i>Gephyrocapsa</i> , <i>Discoaster</i> sp.	<i>E. huxleyi</i> (43,7%) abundant and Plio-Pleistocene reworked from surroundings due to erosion	MNN21b

2.9.11	100-102	24,5	<i>E. huxleyi</i> , <i>C. leptoporus</i> , <i>H. carteri</i> , <i>Syracosphaera</i> , <i>Syracolithus</i> , <i>Calsiosolenia</i> , <i>Umbilicosphaera</i>	small <i>Reticulofenestra</i> (<i>minuta</i> , <i>minutula</i>), big <i>Reticulofenestra</i> , <i>C. macintyeri</i> , <i>P. lacunosa</i> <i>H. recta</i> , small <i>Gephyrocapsa</i> , <i>G. caribbeanica</i> , <i>Discoaster</i> sp., <i>Ericsonia</i>	<i>E. huxleyi</i> (48,4%) abundant and Plio-Pleistocene reworked from surroundings due to erosion	MNN21b
2.9.16	150-152	25	<i>E. huxleyi</i> , <i>Rhabdosphaera</i> , <i>H. carteri</i> , <i>H. hyalina</i> , <i>Syracosphaera</i> , <i>Umbilicosphaera</i>	small <i>Reticulofenestra</i> (<i>minuta</i> , <i>minutula</i>), big <i>Reticulofenestra</i> , small <i>Gephyrocapsa</i> , <i>G. omega</i> , <i>Discoaster</i> sp.	<i>E. huxleyi</i> (20%) abundant and Plio-Pleistocene reworked from surroundings due to erosion	MNN21b
2.10.1	0-2	25,5	<i>E. huxleyi</i> , <i>C. leptoporus</i> , <i>Rhabdosphaera</i> , <i>H. carteri</i> , <i>H. hyalina</i> , <i>H. pavementum</i> , <i>C. pelagicus</i> , <i>Syracosphaera</i> , <i>Syracolithus</i> , <i>Umbilicosphaera</i>	small <i>Reticulofenestra</i> (<i>minuta</i> , <i>minutula</i>), big <i>Reticulofenestra</i> , <i>P. lacunosa</i> , <i>H. selli</i> , small <i>Gephyrocapsa</i> , <i>G. omega</i> , <i>Discoaster</i> sp.	<i>E. huxleyi</i> (23,3%) abundant and Plio-Pleistocene reworked from surroundings due to erosion	MNN21b
2.10.6	50-52	26	<i>C. leptoporus</i> , <i>H. carteri</i> , <i>H. hyalina</i> , <i>Syracosphaera</i> , <i>Syracolithus</i> , <i>Umbilicosphaera</i> , <i>Umbellosphaera</i>	small <i>Reticulofenestra</i> (<i>minuta</i> , <i>minutula</i>), big <i>Reticulofenestra</i> , <i>H. selli</i> , <i>H. recta</i> , small <i>Gephyrocapsa</i> , <i>C. formosus</i> , <i>C. tropicus</i> , <i>Sphenolithus</i> , <i>D. brouweri</i> , <i>D. triradiatus</i> , <i>Discoaster</i> sp.	<i>E. huxleyi</i> (0,00%), small <i>Gephyrocapsa</i> $\leq 3\mu\text{m}$ (2,38%), <i>Reticulofenestra</i> spp. (67,86%), <i>Pseudoemiliana lacunosa</i> (3%)	MNN21b - Lagoon
2.10.8	100-102	26,2	<i>C. leptoporus</i> , <i>Rhabdosphaera</i> , <i>H. carteri</i> , <i>H. wallichii</i> , <i>C. pelagicus</i> , <i>Syracosphaera</i> , <i>Syracolithus</i> , <i>Umbilicosphaera</i>	small <i>Reticulofenestra</i> (<i>minuta</i> , <i>minutula</i>), big <i>Reticulofenestra</i> , <i>P. lacunosa</i> , small <i>Gephyrocapsa</i> , <i>H. recta</i> , <i>Discoaster</i> sp.	<i>E. huxleyi</i> (0,00%), small <i>Gephyrocapsa</i> $\leq 3\mu\text{m}$ (5,97%), <i>Reticulofenestra</i> spp. (45,27%), <i>Pseudoemiliana lacunosa</i> (7,46%)	MNN21b - Lagoon

2.10.11	150-152	26,5	<i>C. leptoporus</i> , <i>Rhabdosphaera</i> , <i>H. carteri</i> , <i>H. wallichii</i> , <i>C. pelagicus</i> , <i>Syracosphaera</i> , <i>Syracolithus</i> , <i>Umbilisphaera</i>	small <i>Reticulofenestra</i> (<i>minuta</i> , <i>minutula</i>), big <i>Reticulofenestra</i> , <i>C. macintyeri</i> , <i>P. lacunosa</i> , <i>H. recta</i> , <i>Discoaster</i> sp.	<i>E. huxleyi</i> (0,00%), <i>Reticulofenestra</i> spp. (65,67%), <i>P. lacunosa</i> (1,49%) - Lagoon very restricted (stressed) environment with even fresh water	MNN21b - Lagoon
2.10.12	108-110	26,6	<i>C. leptoporus</i> , <i>H. carteri</i> , <i>H. hyalina</i> , <i>H. wallichii</i> , <i>C. pelagicus</i> , <i>Syracosphaera</i> , <i>Umbilicosphaera</i>	small <i>Reticulofenestra</i> (<i>minuta</i> , <i>minutula</i>), big <i>Reticulofenestra</i> , <i>P. lacunosa</i> , <i>C. formosus</i> , <i>Sphenolithus</i> , <i>Discoaster</i> sp., <i>Discoaster rossette</i> <i>form</i>	<i>E. huxleyi</i> (0,00%), <i>Reticulofenestra</i> spp. (53,69%), <i>P. lacunosa</i> (4,43%) - Lagoon very restricted (stressed) environment with even fresh water	MNN21b - Lagoon

Table 4: Table of borehole Livadi 2. Samples, depth, sample interval in every core. Calcareous nannoplankton that collected and identified in every sample, the biozonal indicators in each one and the biostratigraphic age.



6.3 Livadi 4

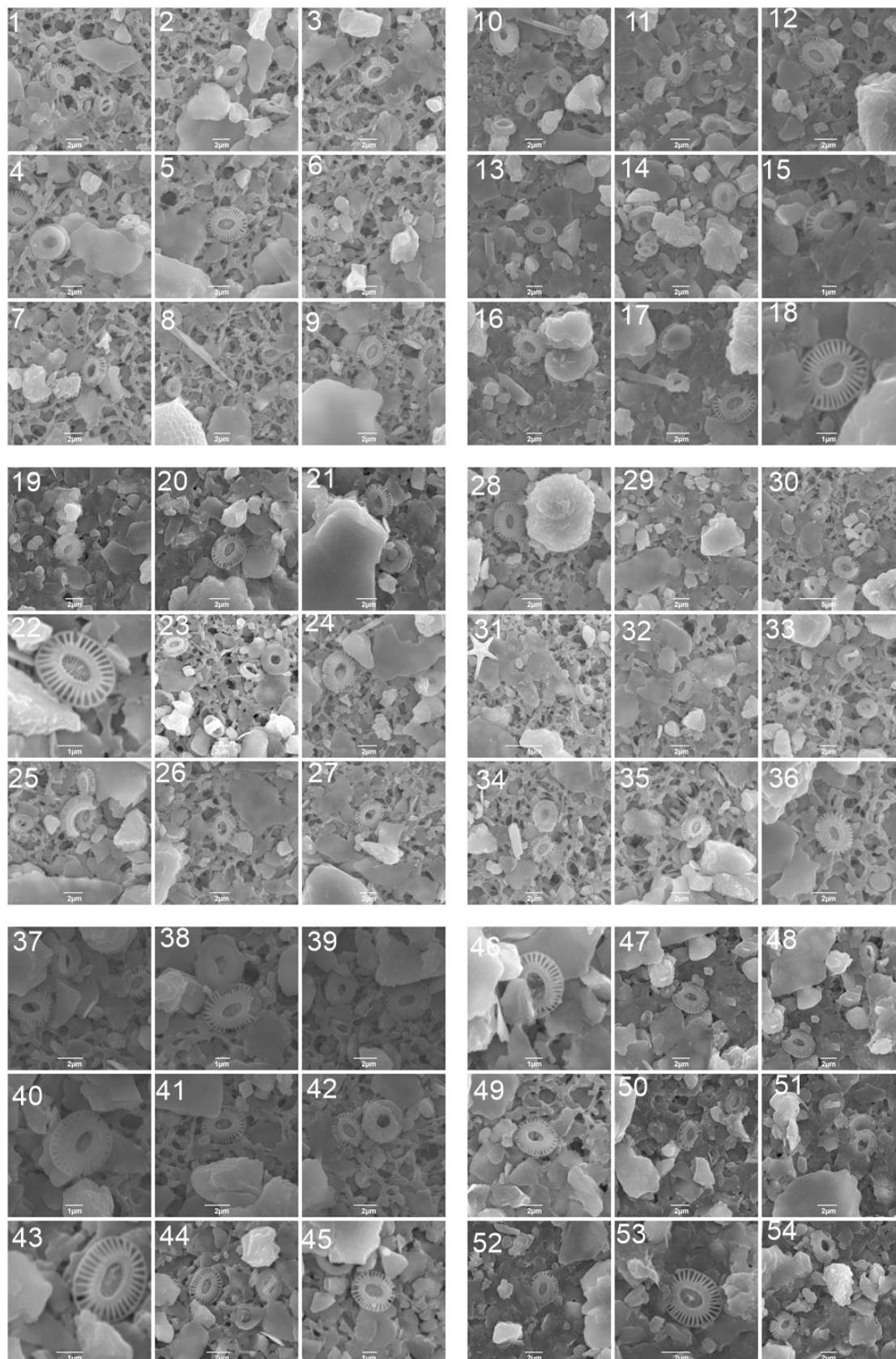
In borehole Livadi 4 core 7 (18-21m depth), nine samples have been analyzed with SEM for the nannofossil content in order to establish the biostratigraphic assignment. The assemblage composition of Livadi 4.7, in average, consisted of *E. huxleyi* 33,35%, *C. leptoporus* 2,21%, *Rhabdosphaera* spp. 1,15%, *H. carteri* 1,17%, *H. hyalina* 0,59%, *H. wallichii* 0,29%, small *Gephyrocapsa* spp. (<3μm) 19,88%, *G. caribbeanica* 0,62%, *C. pelagicus* 0,5%, *Syracosphaera* spp. 2,70%, *Syracolithus* spp. 1,96%, *Umbilicosphaera* spp. 5,11%, *Calsiosolenia* spp. 0,1%, *Corisphaera* spp. 0,14%, *Coronosphaera* spp. 0,21%, *Umbellosphaera* spp. 0,22%, *Scyphosphaera* spp. 0,15%. The reworked coccoliths in this core were: *C. macintyeri* 0,21%, *Reticulofenestra* spp. 44,58%, *P. lacunosa* 5,58%, *H. selli* 0,66%, *H. recta* 0,1%, *G. omega* 0,21%, *Sphenolithus* spp. 0,36%, *Discoaster* spp. 0,99%, *Discoaster* rosette form 0,07%,

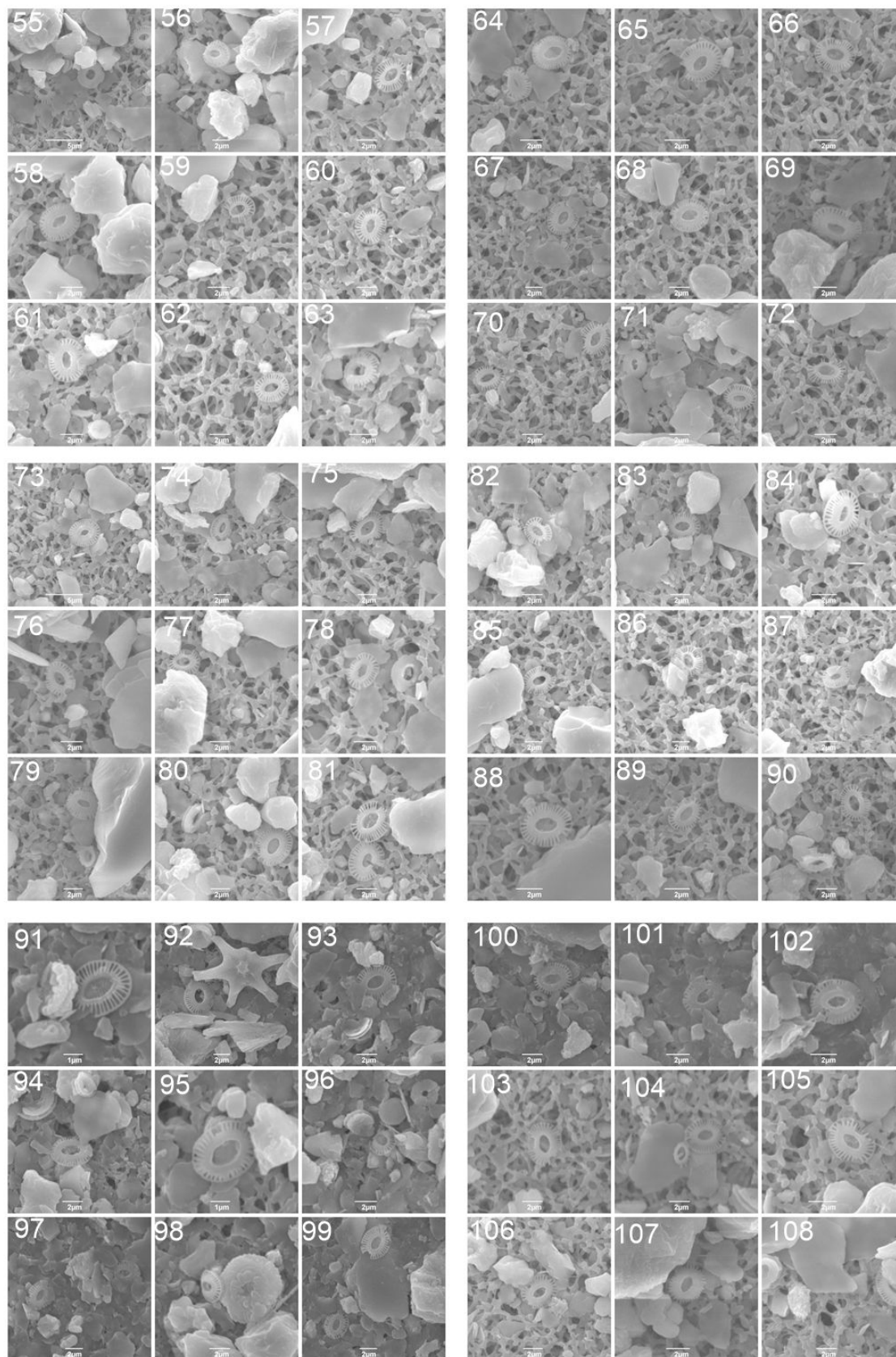
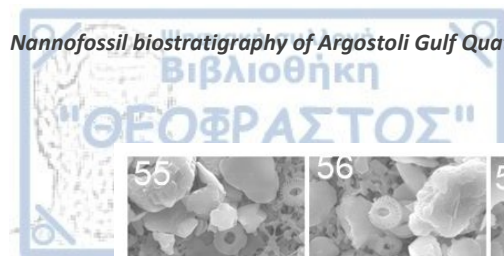
Continuing downwards in borehole Livadi 4, core 8 (21,5-26,4m depth), the assemblage composition in average was, *E. huxleyi* 30,01%, *Gephyrocapsa* spp. (<3microns) 20,80%, *C. leptoporus* 1,51%, *Rhabdosphaera* spp 1,59%, *H. carteri* 1,03%, *H. wallichii* 0,21%, *H. hyalina* 0,27%, *H. elongata* 0,04%, *G. caribbeanica* 0,72%, *C. pelagicus* 0,68%, *Syracosphaera* spp. 2,22%, *Syracolithus* spp. 1,06%, *Calsiosolenia* 0,39%, *Umbilicosphaera* spp. 6,27%, *Algirosphaera* spp. 0,04%, *Discosphaera* spp. 0,01%, *Umbellosphaera* spp. 0,05%, *Corisphaera* spp. 0,09%, *Coronosphaera* spp. 0,04%, *Umbellosphaera* spp. 0,21%, *Coronocylus* spp. 0,17%, *Cyrtosphaera* spp. 0,15%. The reworked coccoliths in this core were: *C. macintyeri* 0,37%, *Reticulofenestra* spp. 45,15%, *P. lacunosa* 5,95%, *H. sellii* 0,28%, *G. omega* 0,4%, *Discoaster* spp. 0,54%, *Discoaster* rosette form 0,04%, *Sphenolithus* spp. 0,2%

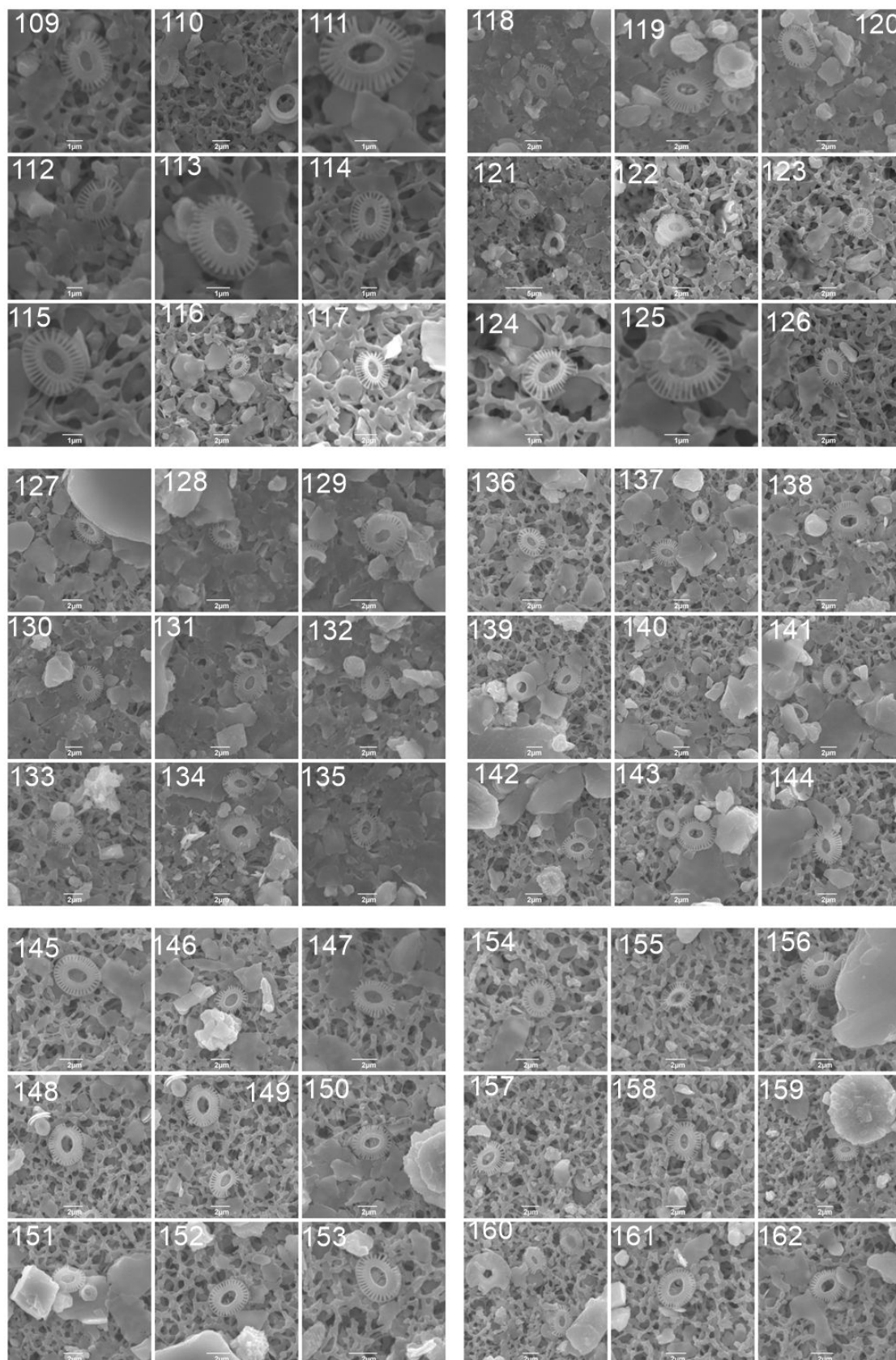
In Livadi 4, core 9 (26,9-29,5m depth), the average assemblage composition was, *E. huxleyi* 18,39%, *C. leptoporus* 1,30%, *Rhabdosphaera* 0,52%, small *Gephyrocapsa* (<3μm) 25,05%, *G. caribbeanica* 0,93%, *H. carteri* 1,38%, *H. hyalina* 0,26%, *H. wallichii* 0,44%, *H. elongata* 0,09%, *C. pelagicus* 0,18%, *Umbilicosphaera* spp. 9,91%, *Syracosphaera* spp. 2,63%, *Syracolithus* spp. 1,35%, *Calsiosolenia* spp. 0,26%, *Umbellosphaera* spp. 0,34% The reworked coccoliths in this core were: *C. macintyeri* 0,63%, *P. lacunosa* 5,37%, *Reticulofenestra* spp. 43,12%, *G. omega* 0,08%, *H. sellii* 0,42%, *Discoaster* spp. 0,51%, *Discoaster* rosette form 0,25%, *Sphenolithus* spp. 0,26%.

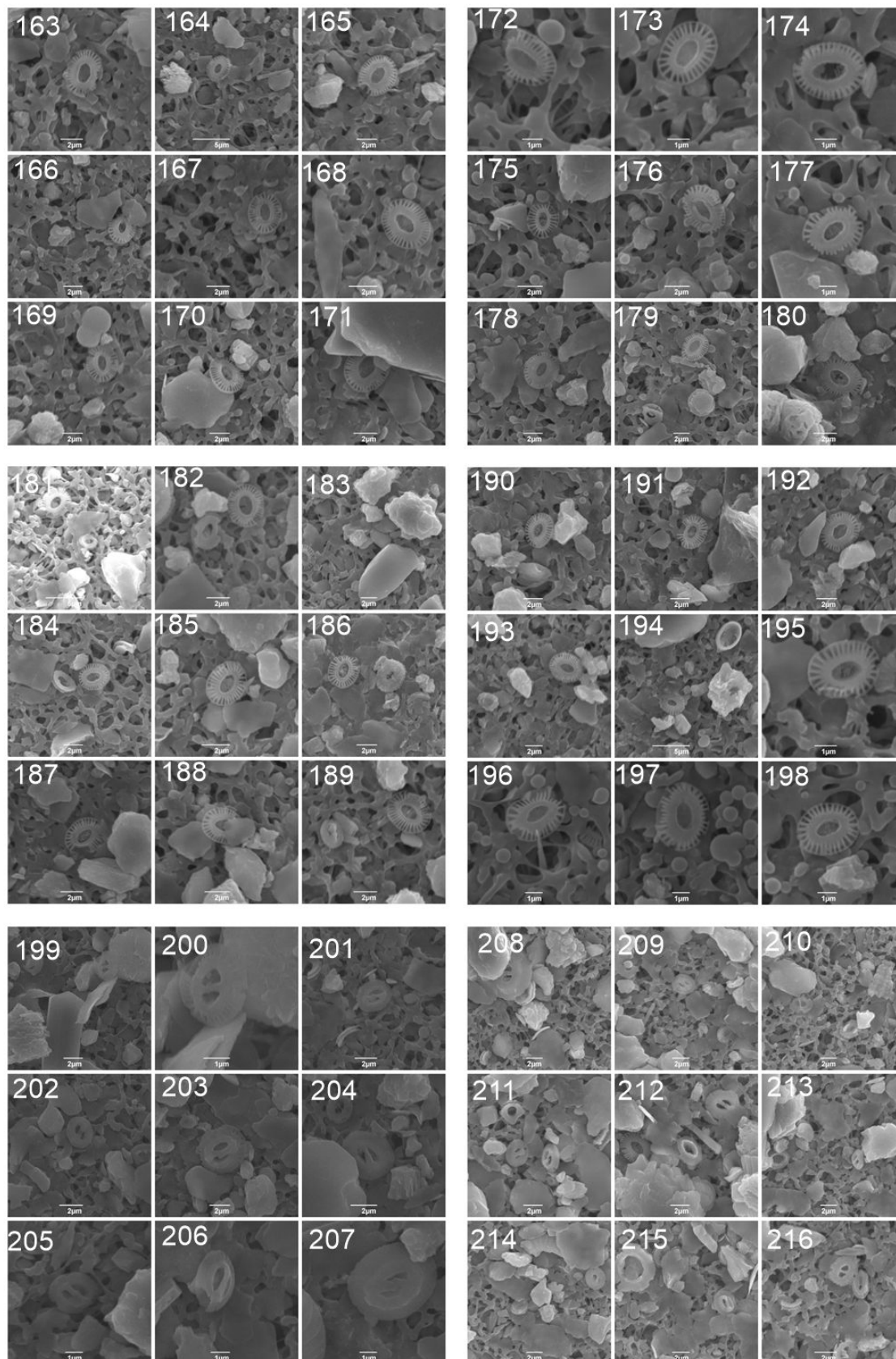
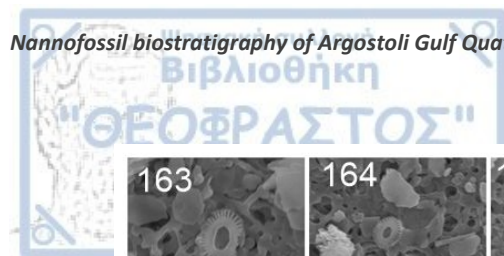
Finally, in Livadi 4, core 10 (30-32,5m depth), the average assemblage composition was: *E. huxleyi* was completely absent except samples 4.10.1 and 4.10.6 (with average percentage 23,64%), small *Gephyrocapsa* spp. (<3μm) 9,95%, *G. caribbeanica* 0,12%, *Umbilicosphaera* spp. %, *C. leptoporus* 3,21%, *Reticulofenestra* spp. 46,64%, *Rhabdosphaera* spp. 0,41%, *P. lacunosa* 7,35%, *H. sellii* 0,06%, *H. carteri* 0,45%, *H. hyalina* 0,48%, *H. wallichii* 0,06%, *C. pelagicus* 0,71%, *Syracosphaera* spp. 1,28%, *Umbilicosphaera* spp. 26,42%, *Discoaster* spp. 8,28%, *Syracolithus* spp. 0,66%, *Scyphosphaera* spp. 0,06%, *Sphenolithus* spp. 0,25 %. In sample 4.10.21 there was no sign of coccolithophores.

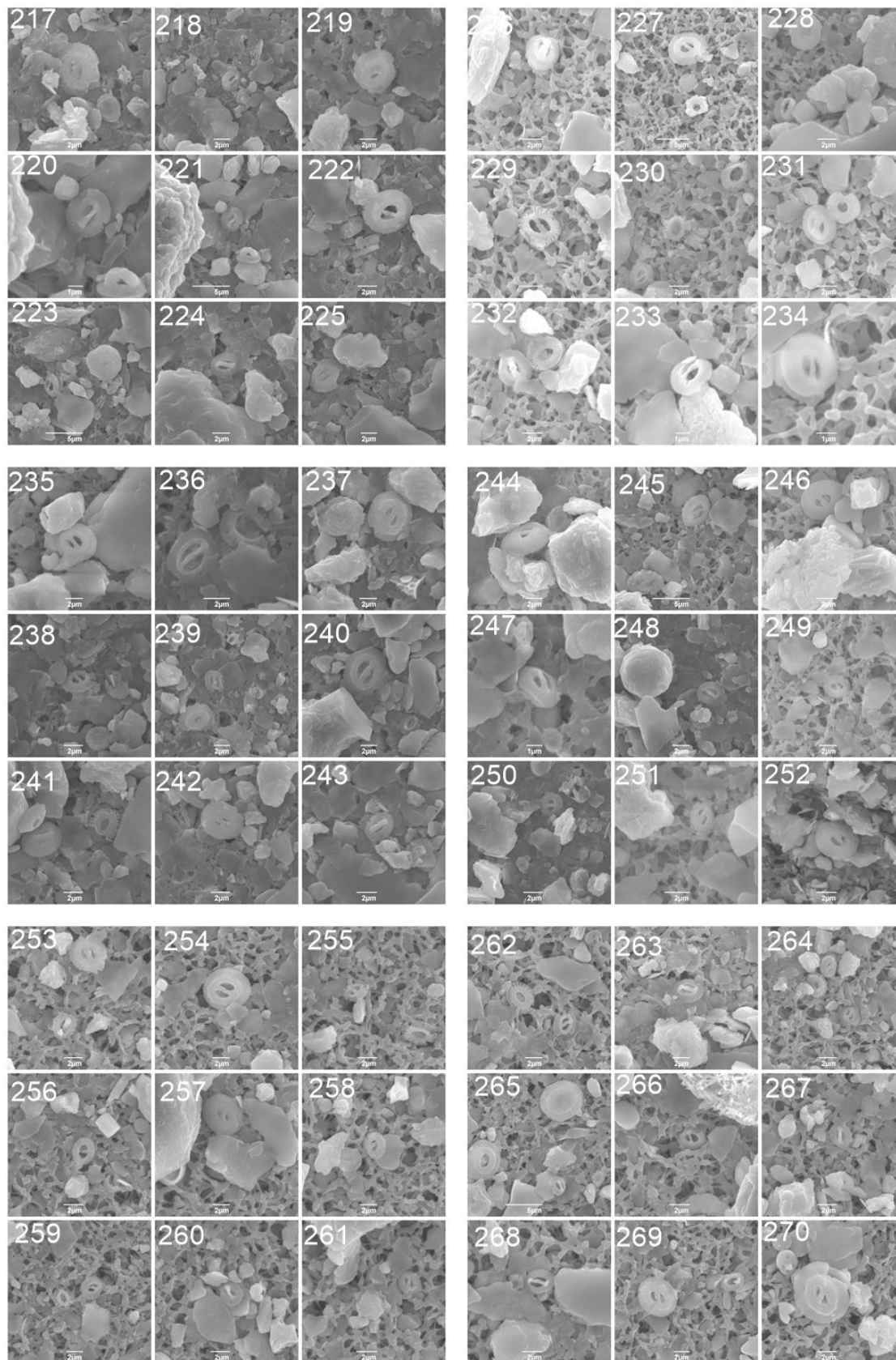
The tables and the diagrams below, show the nannofossils found in borehole Livadi 4 and summarize the assemblage composition of Livadi 4 in cores 7, 8, 9, 10.

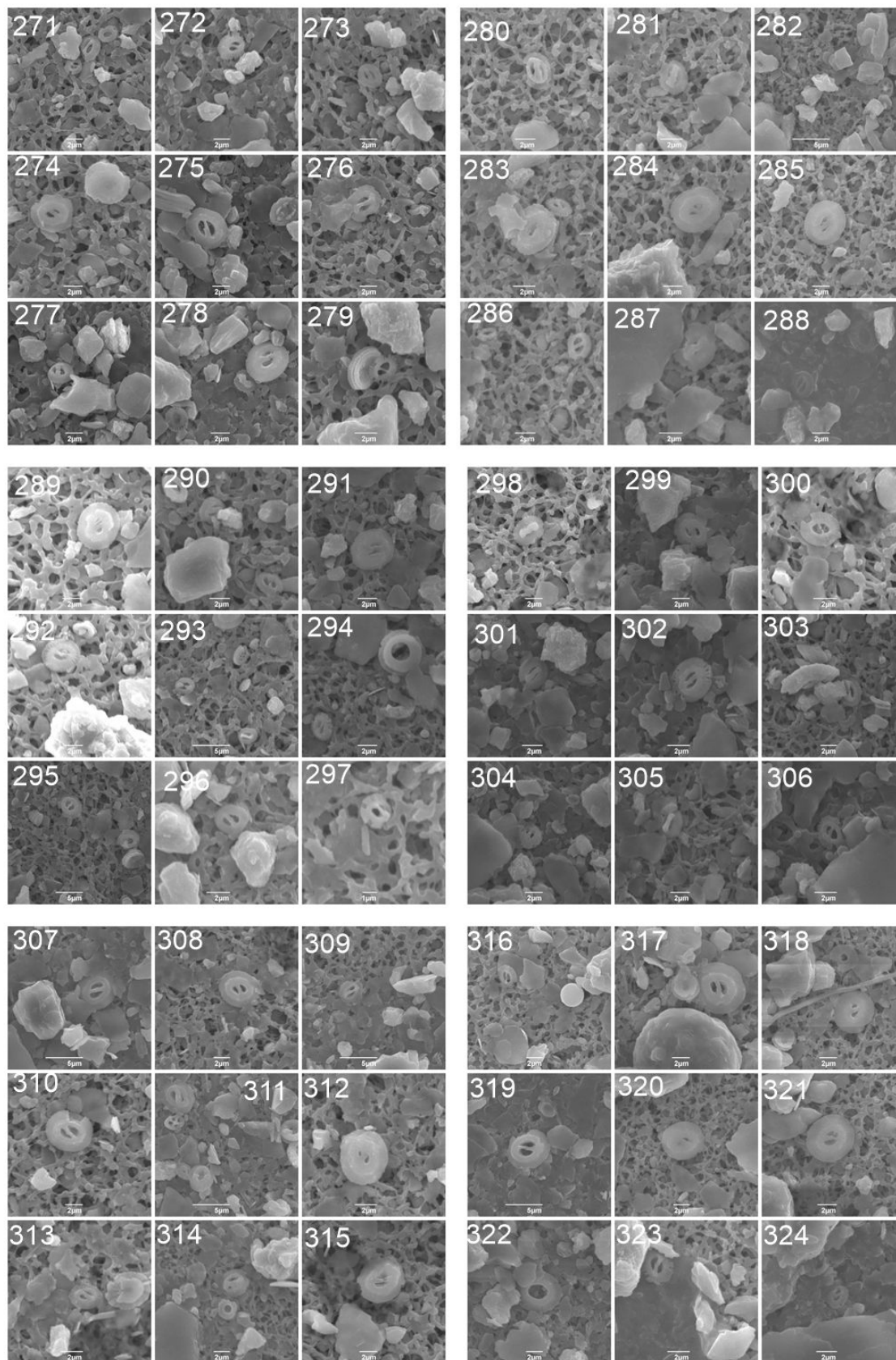
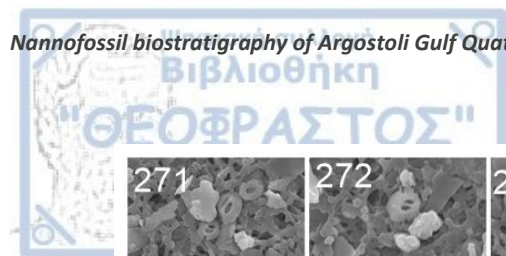


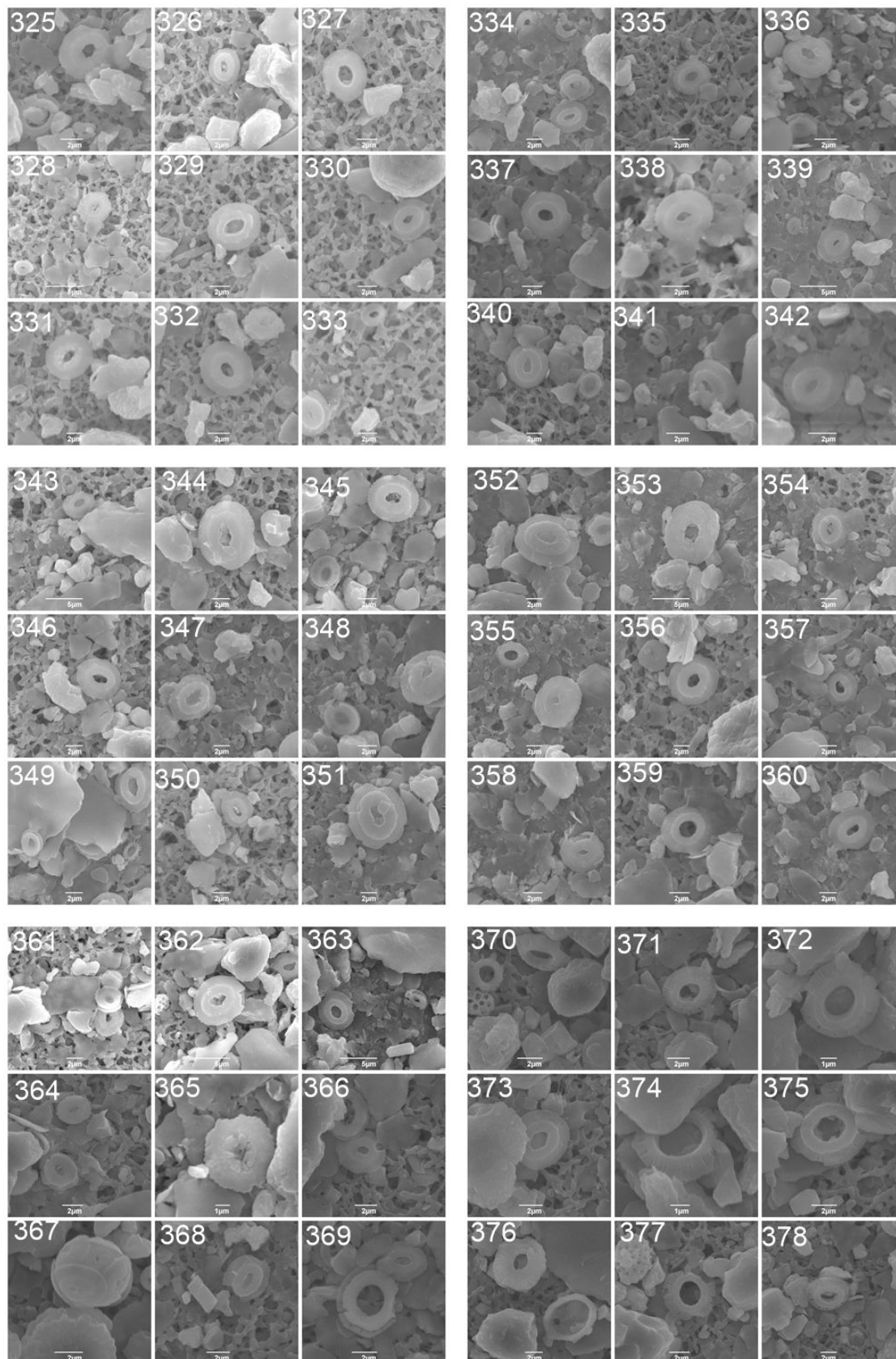


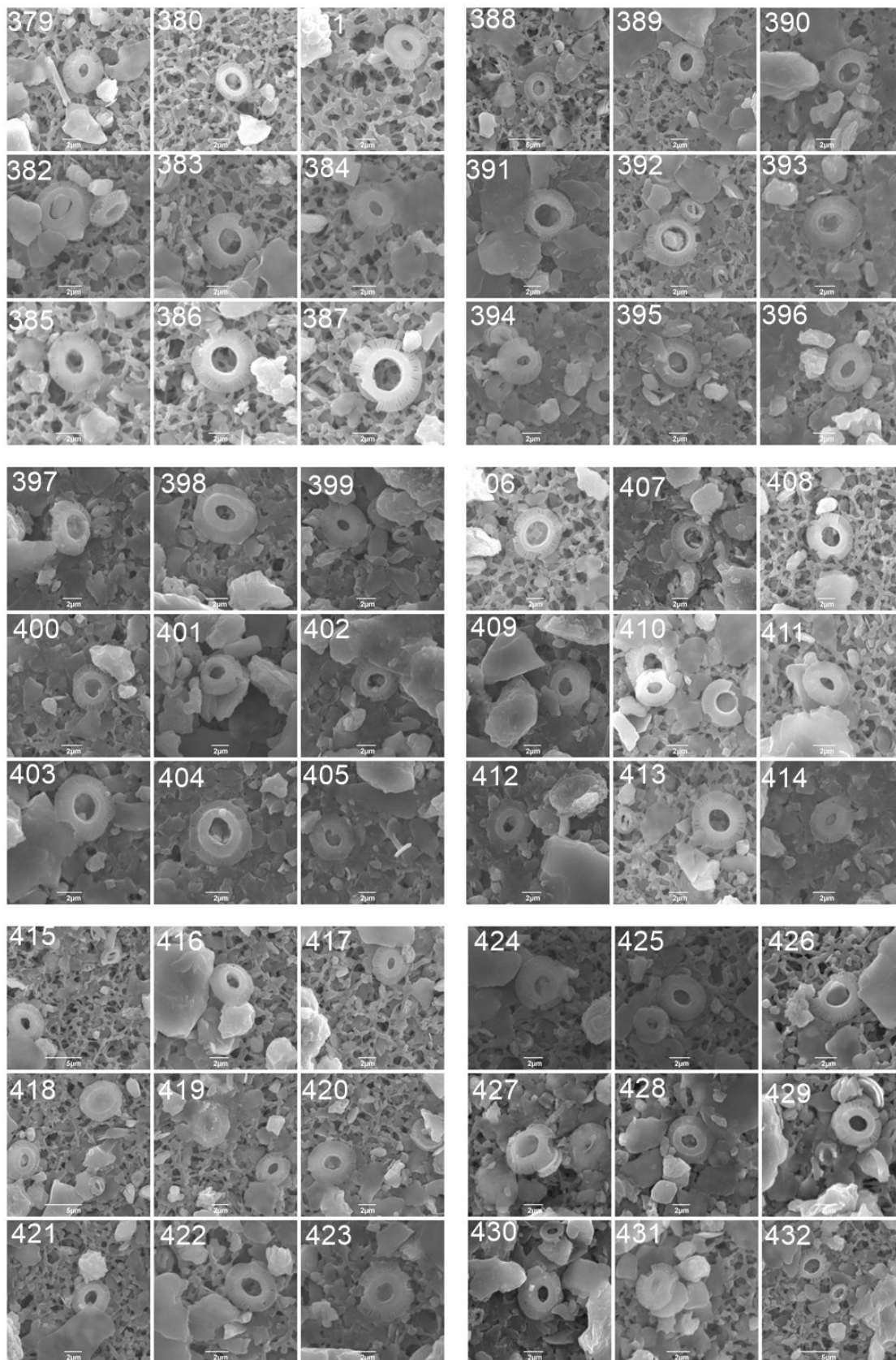
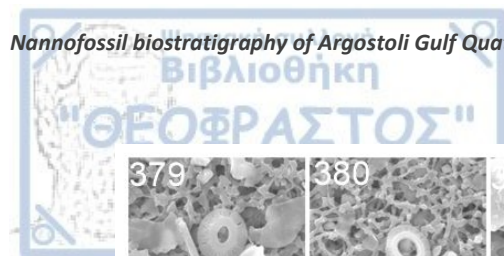


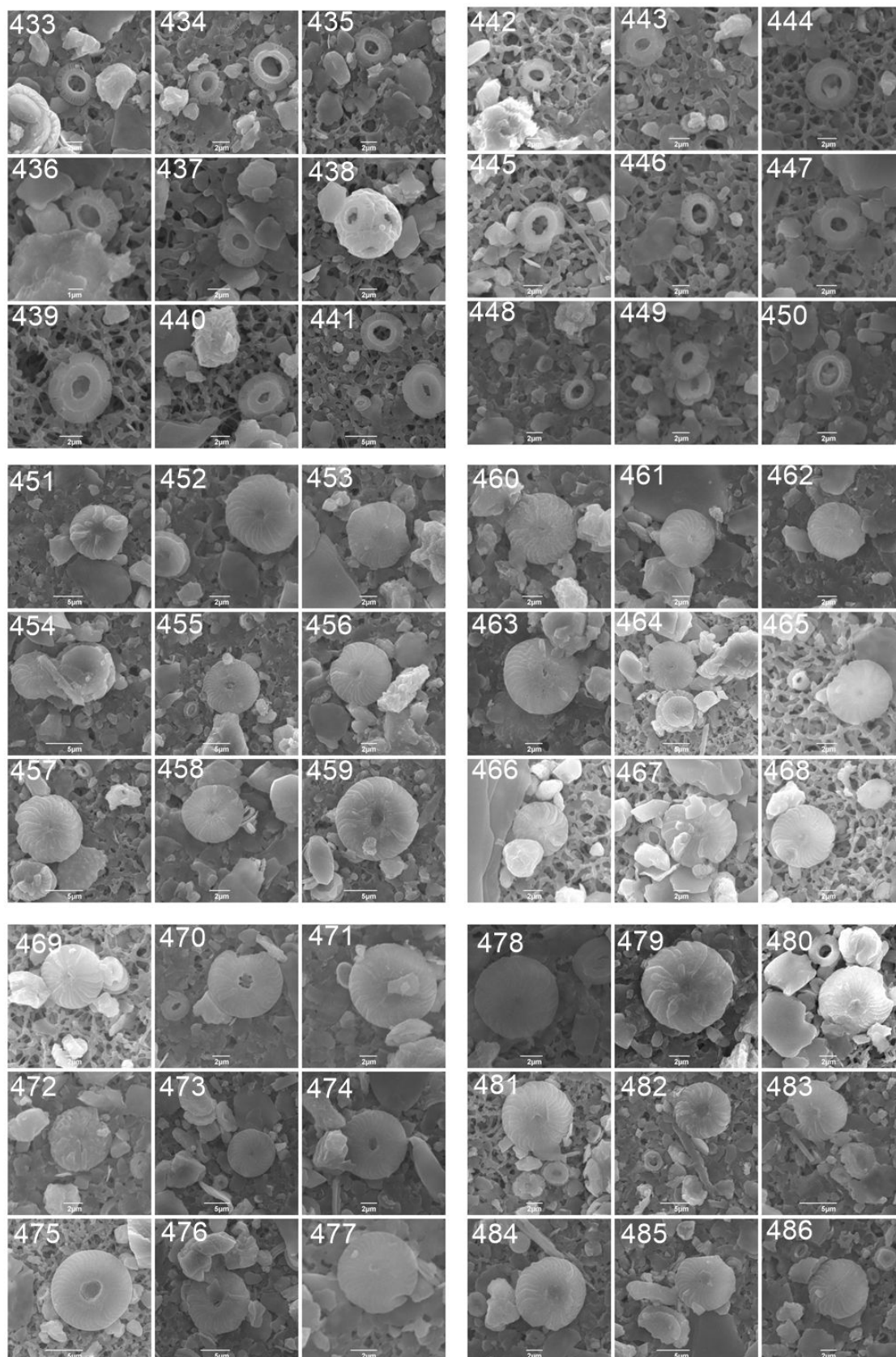


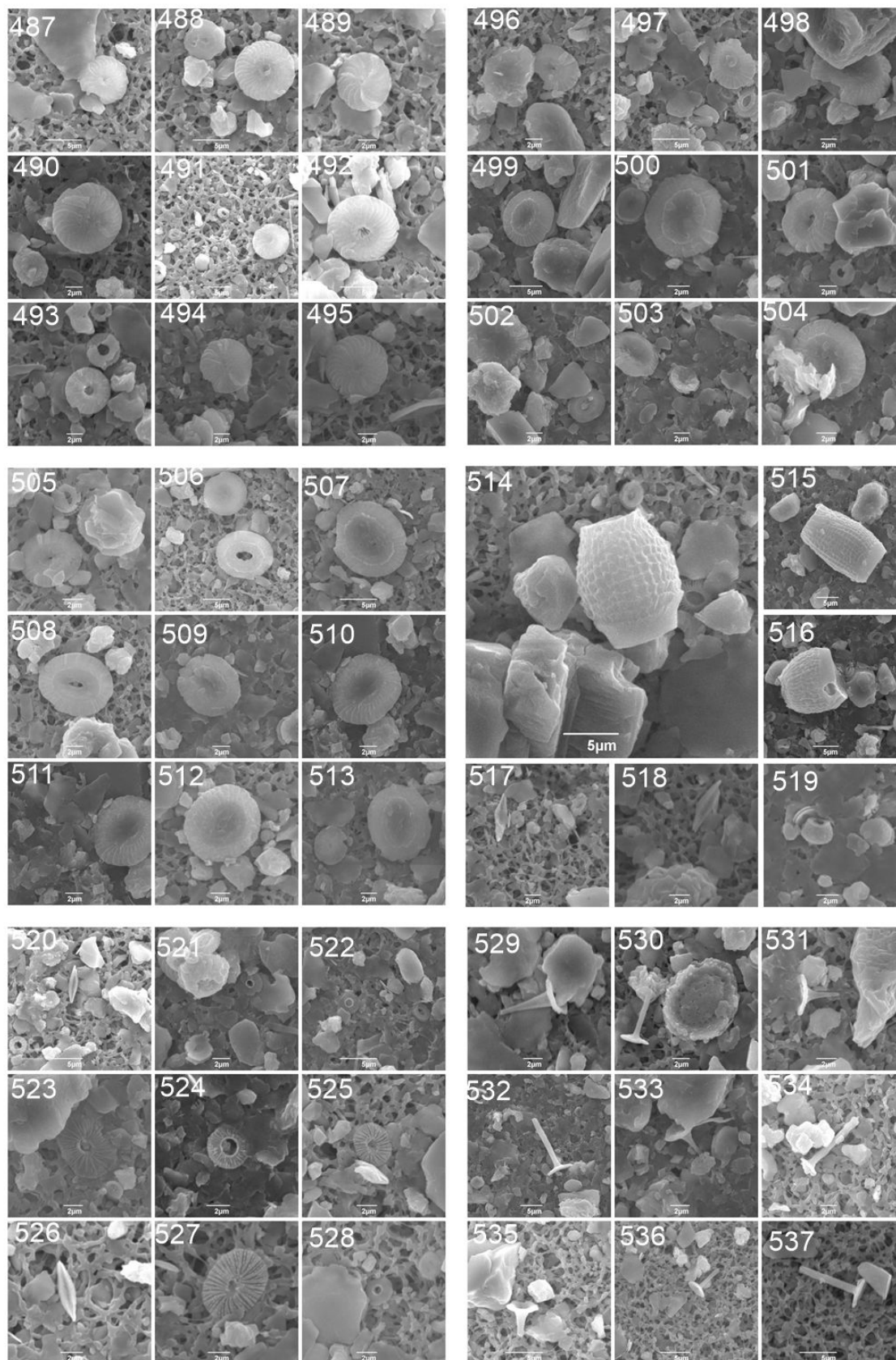
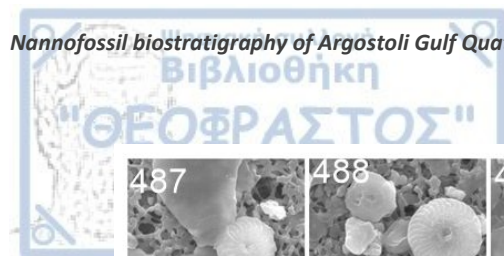


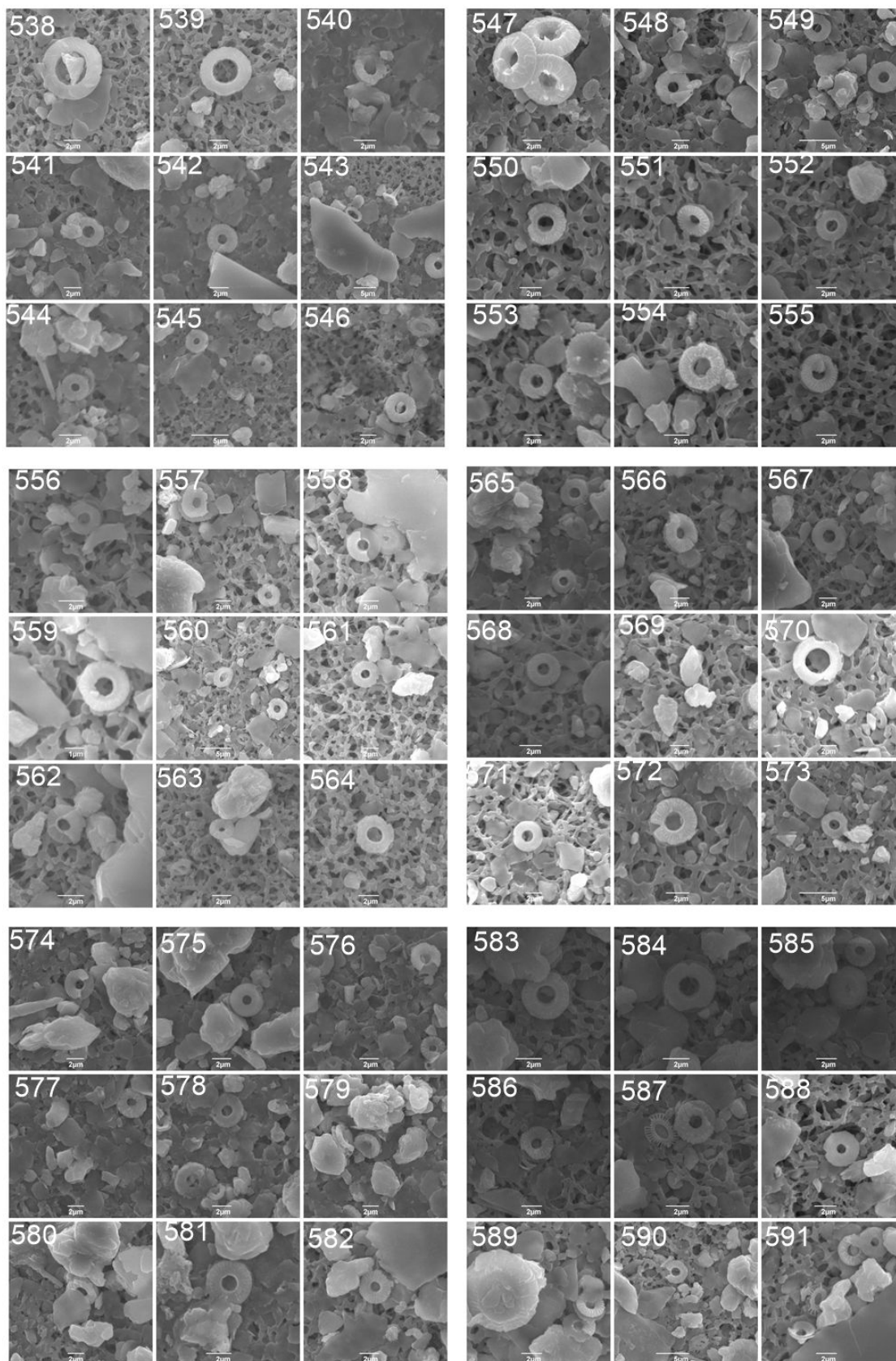


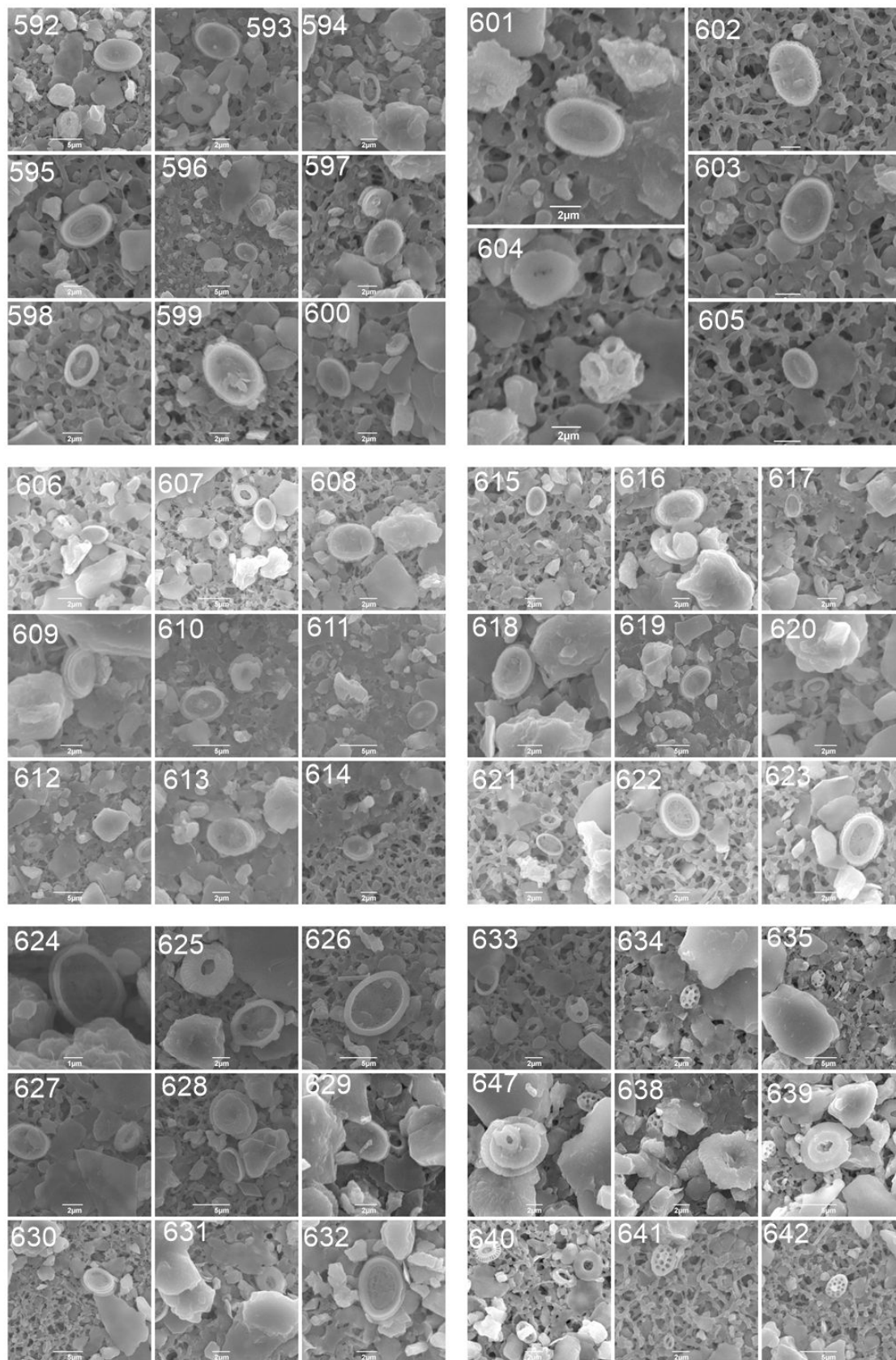
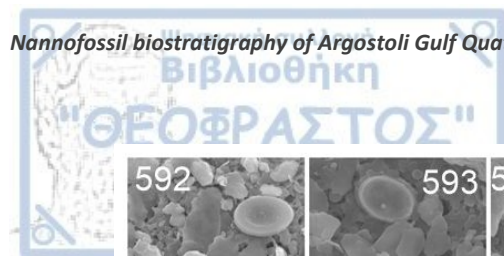


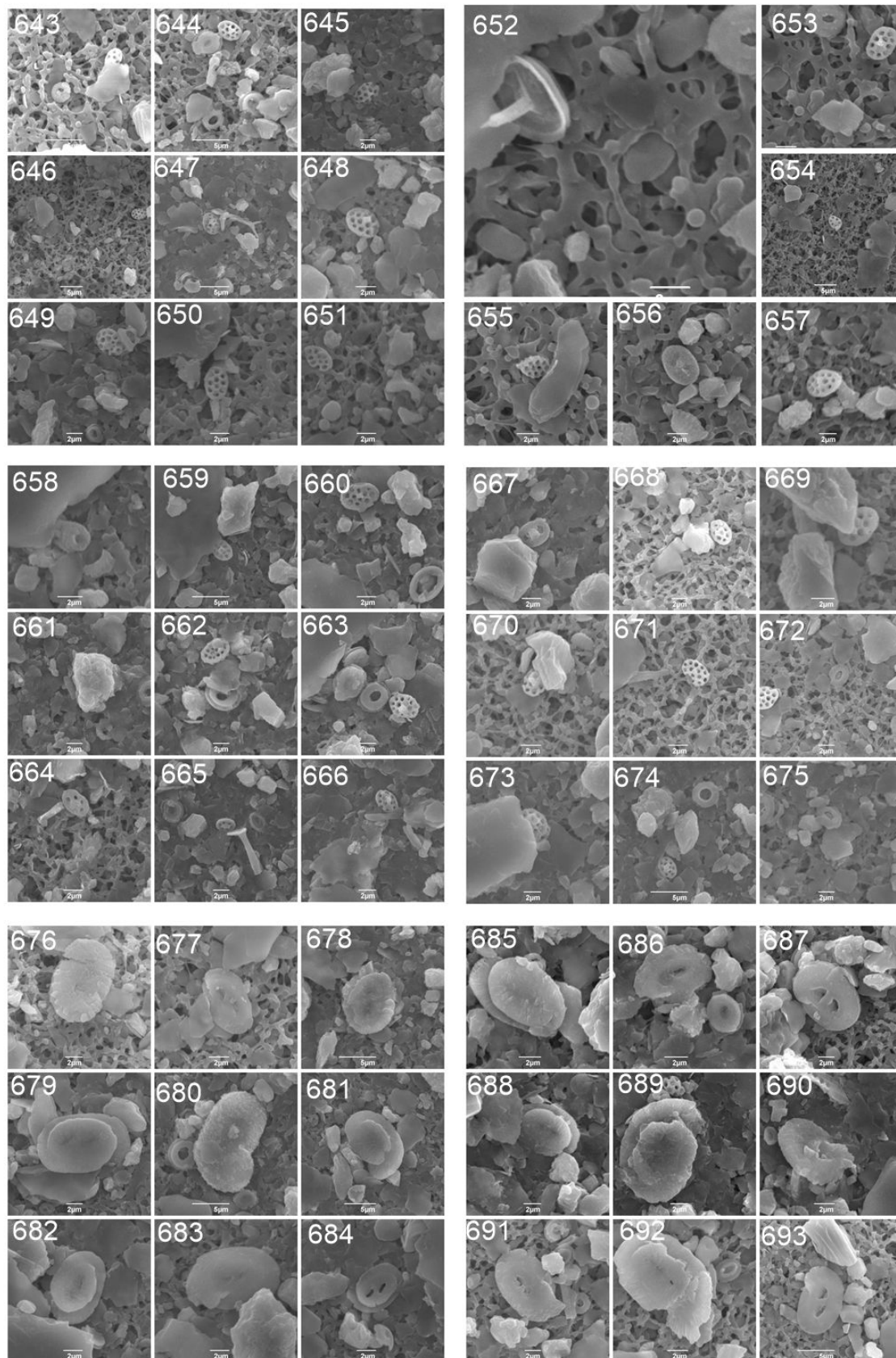


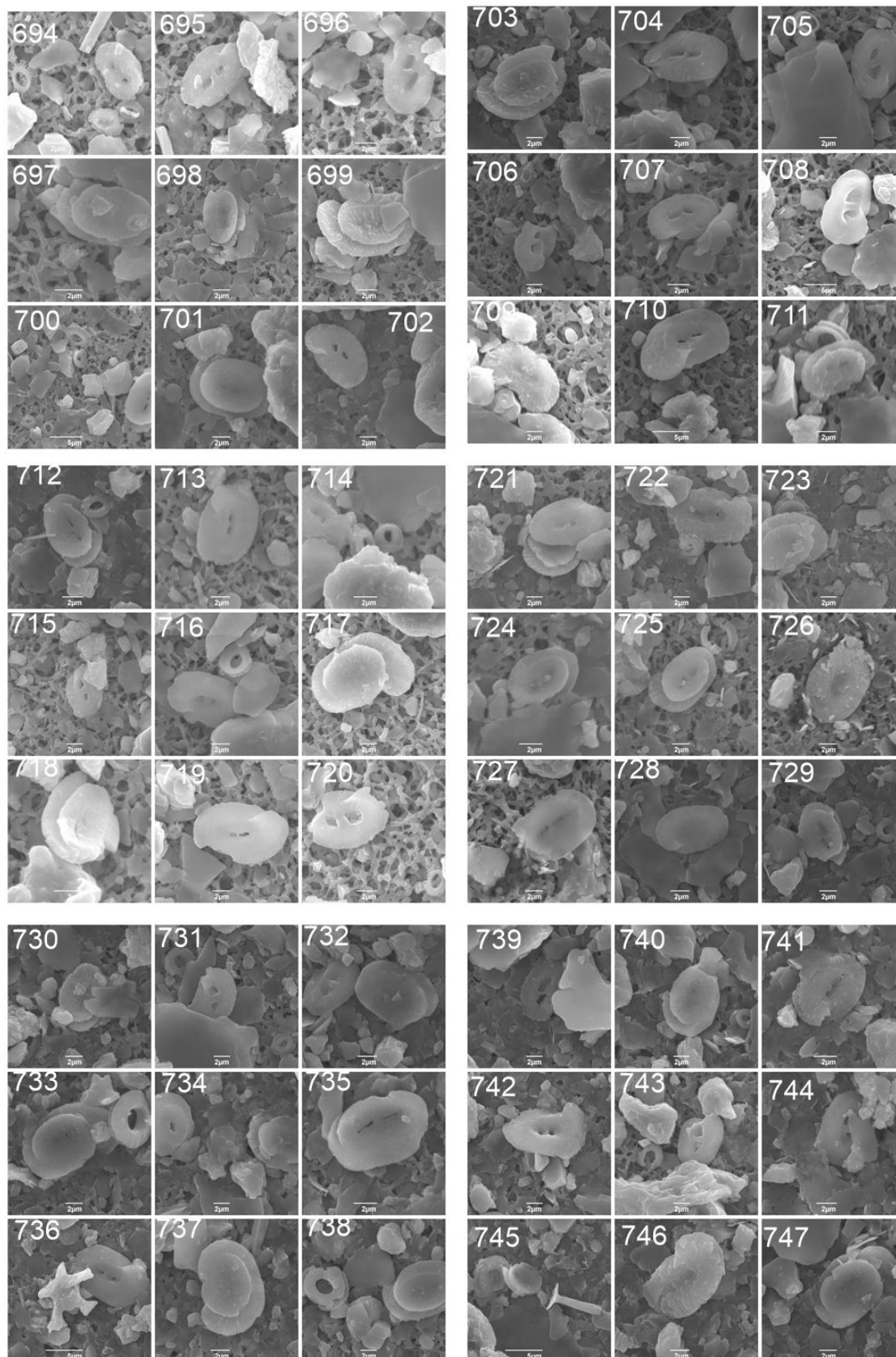
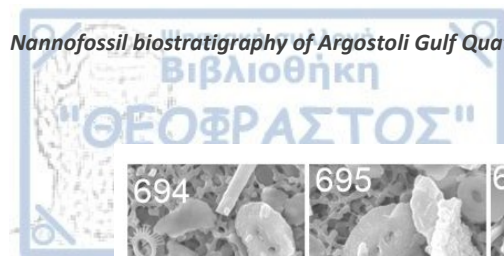












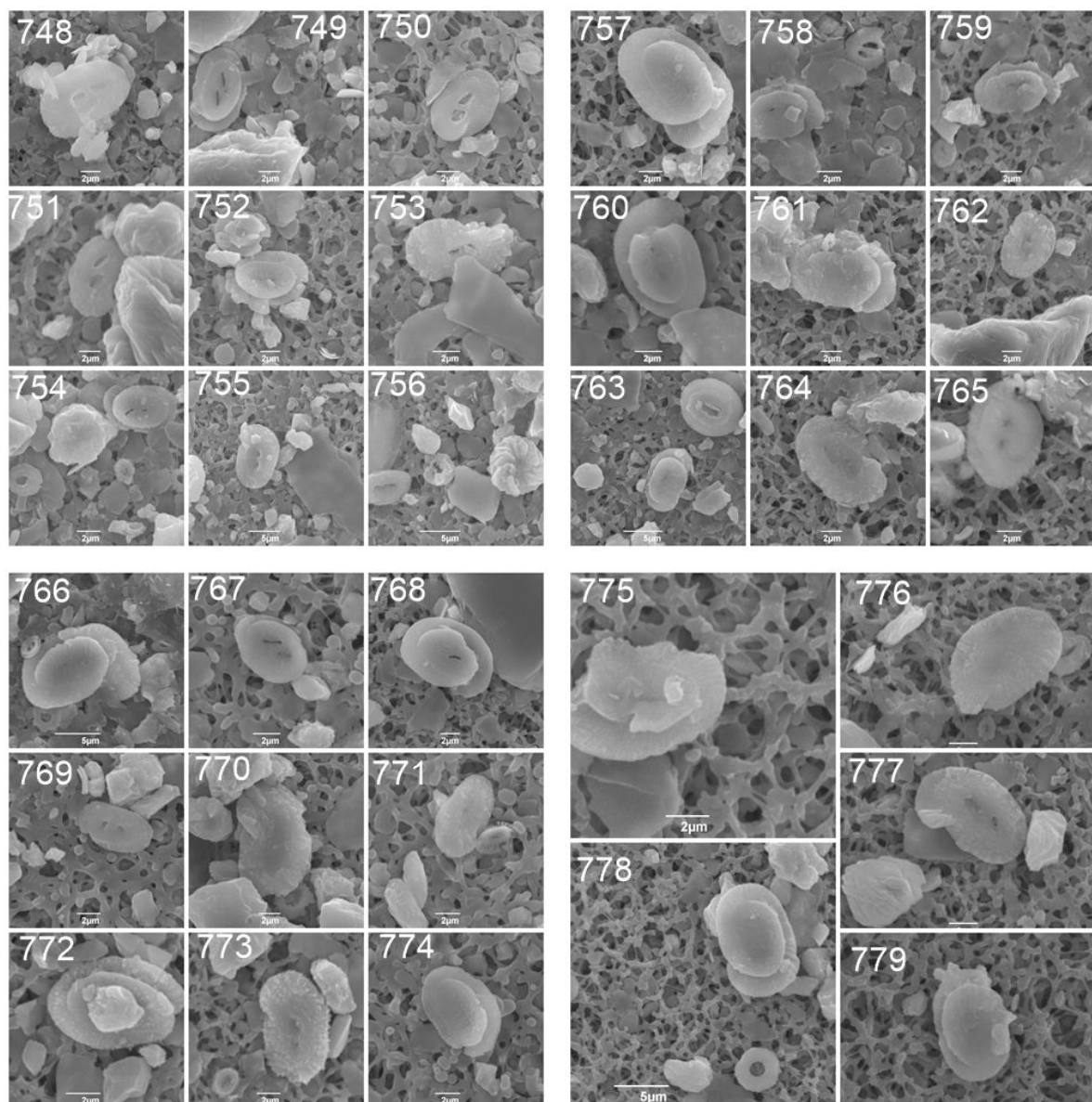
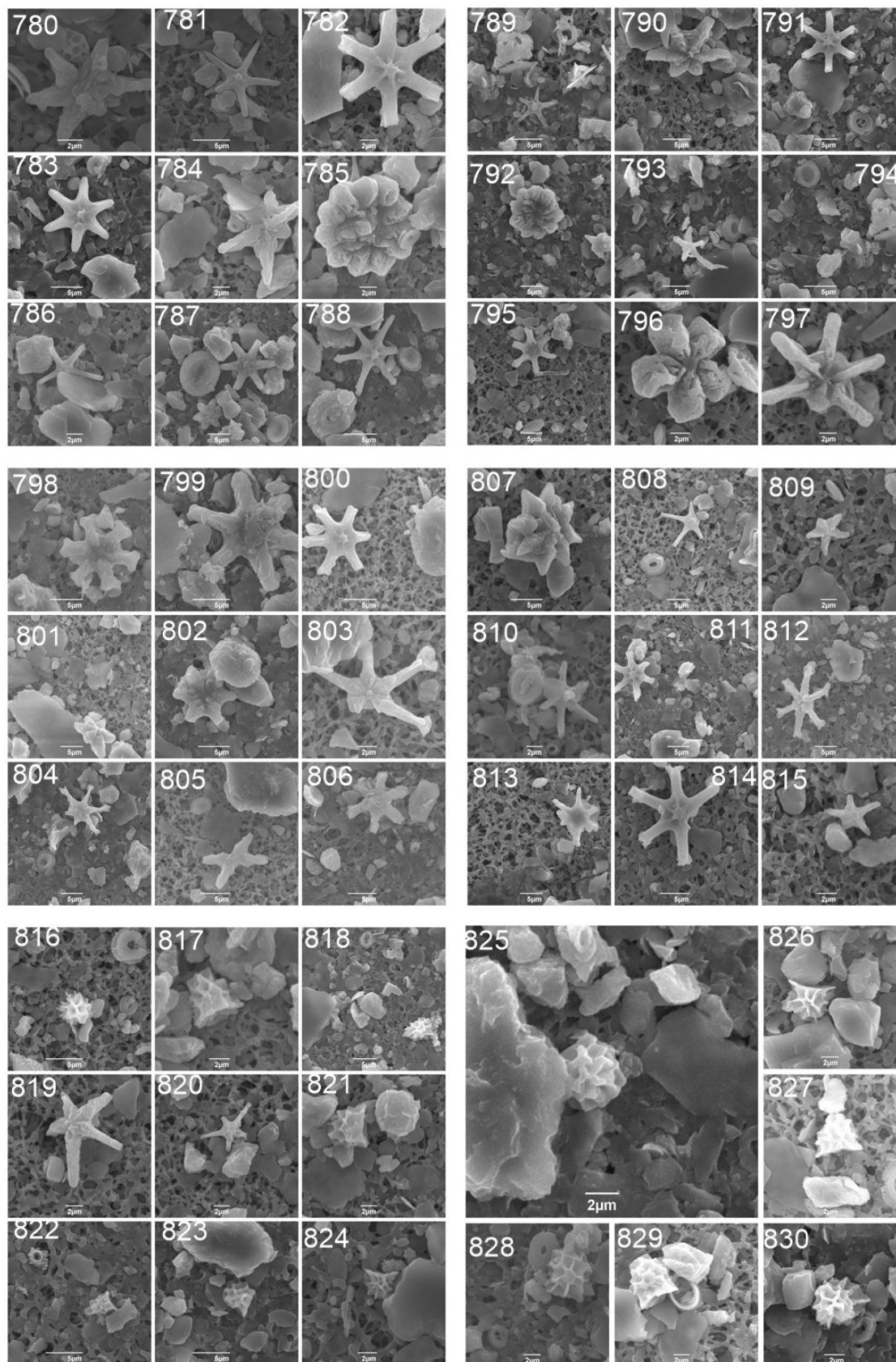
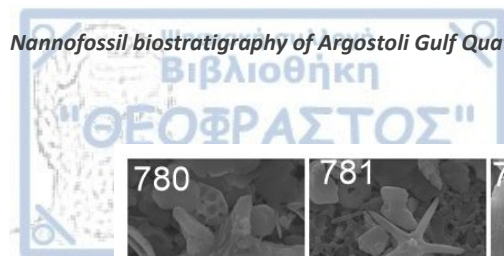
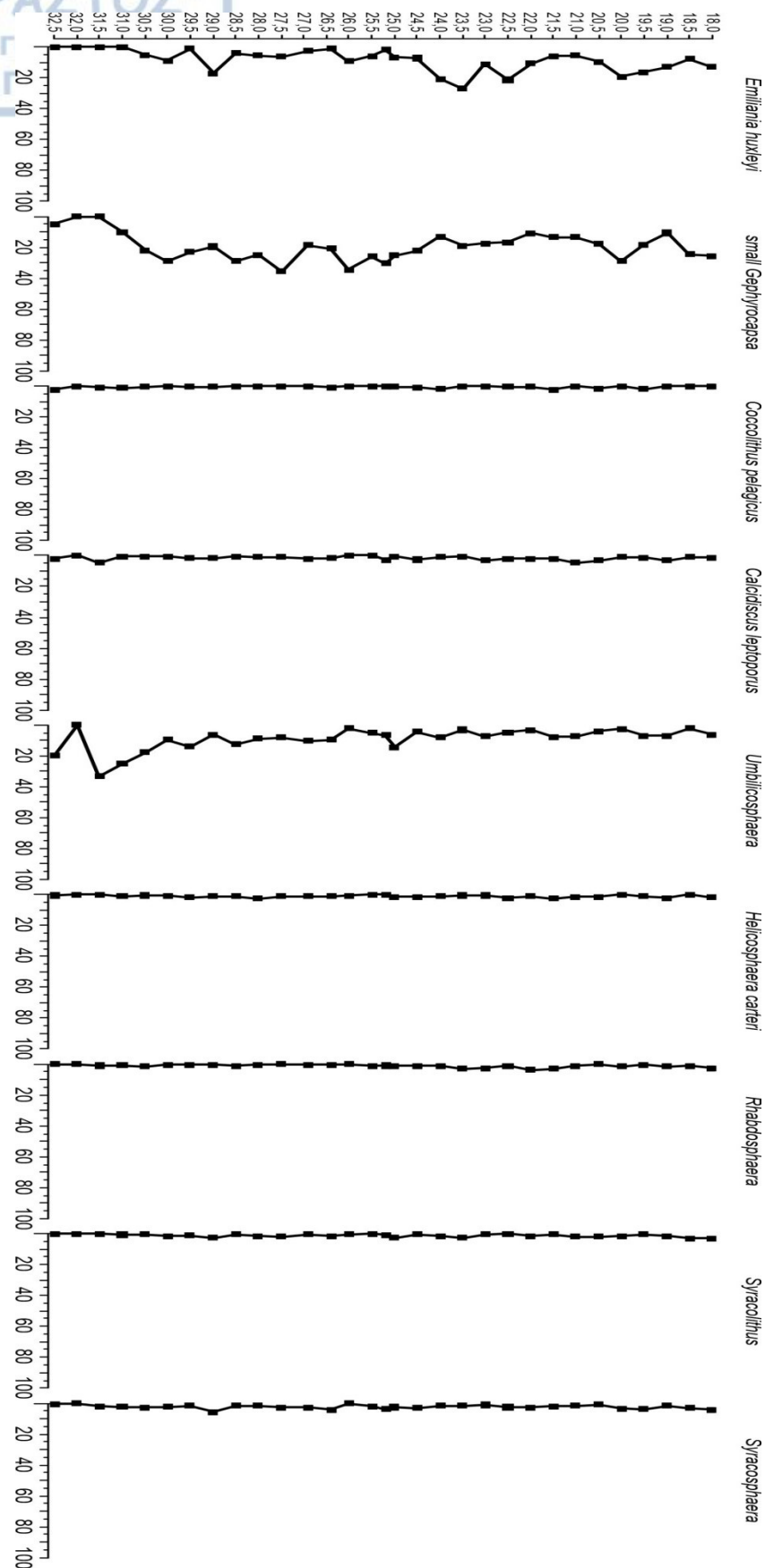


Table 5: SEM pictures from borehole Livadi 4:

1-98: *Emiliania huxleyi*, 199-324: small *Gephyrocapsa* spp. (<3μm), 254 & 317: *G. omega*, 207, 270, 284 and 312: *G. caribbeanica*, 325-369: *Reticulofenestra* spp., 370-450: *Pseudoemiliania lacunosa* (438: *P. lacunosa* coccosphere), 451-458, 460-469, 471-473, 477-492, 494 and 495: *Calcidiscus leptoporus*, 459, 470, 474-476 and 493: *C. macintyeri*, 496-513: *Coccolithus pelagicus*, 514-516: *Scyphosphaera* spp., 517-520, 526: *Calsiosolenia* spp., 521-525, 527 & 528: *Umbellosphaera*, 529-537 & 652, *Rhabdosphaera*, 538-591: *Umbilicosphaera* spp., 592-632: *Syracosphaera* (604: *Syracosphaera* coccosphere), 594: *Coronosphaera* sp., 640 & 658: *Corisphaera* sp., 633-675: *Syracolithus* spp., 676, 680-683, 688-692, 695, 699, 700, 701, 704, 707, 709-714, 719, 721-22, 727, 735-36, 741-42, 747-48, 752-53, 755-763, 7699, 771, 773-74, 777: *Helicosphaera carteri*, 677, 684, 686-87, 693, 702, 705-06, 708, 720, 732, 739, 743-44, 750 & 754: *H. sellii*, 679, 712, 724, 729, 749, 751, 764, 767-68: *H. wallichii*, 697-699, 703, 717, 723, 726, 728, 730, 733-34, 737-38, 740, 746, 766, 770, 776-78-79: *H. hyalina*, 678, 718, 745, 772 & 775: *H. recta*, 765: *H. elongata*, table continues on the next page: 780-815, 819 & 820: *Discoaster* spp., 812-818 & 812-830: *Sphenolithus* spp..





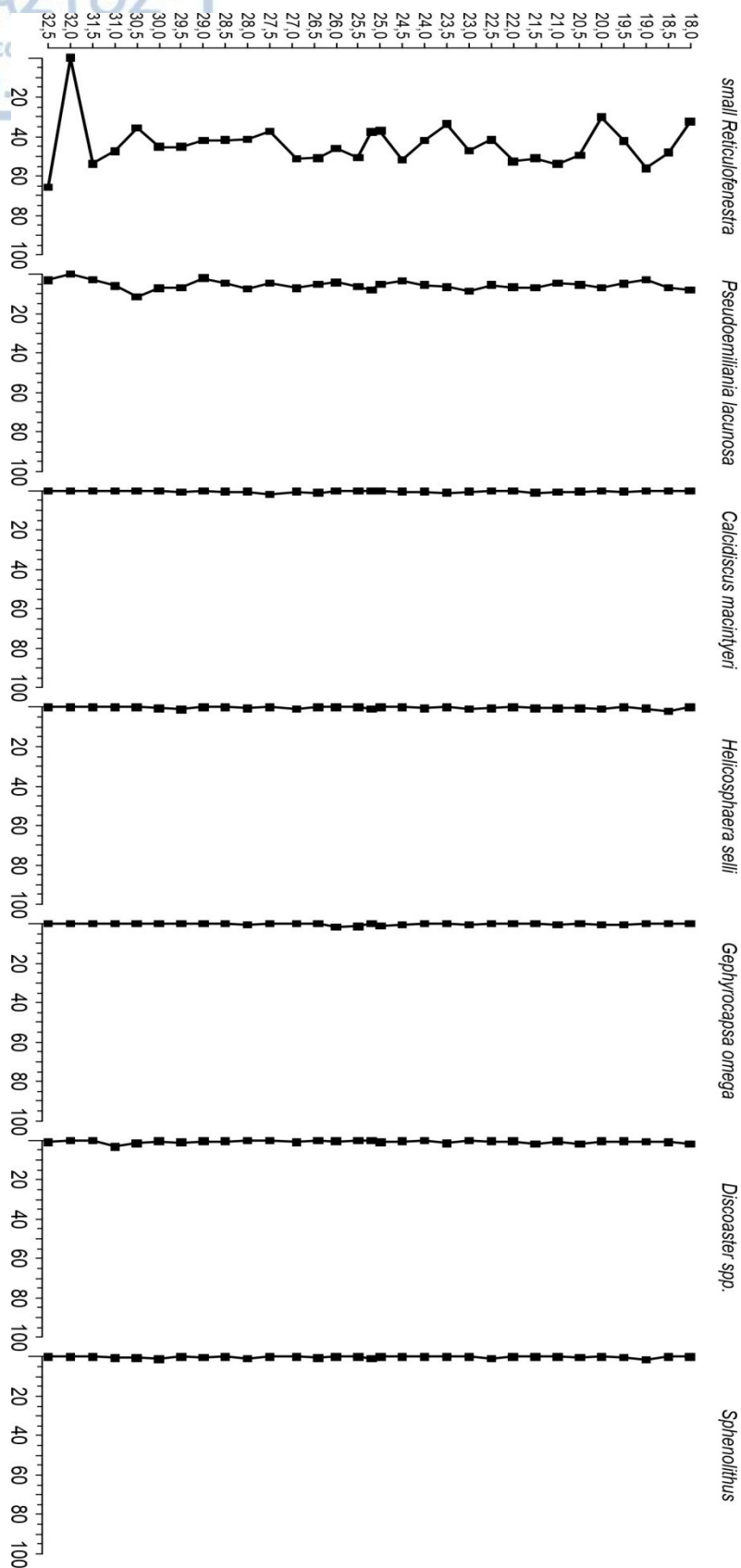
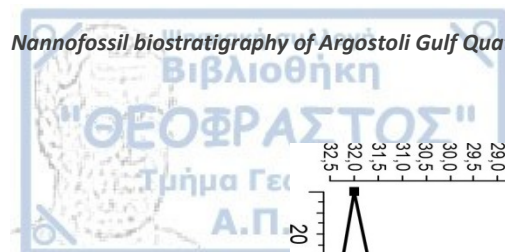


Figure 18: Diagrams of calcareous nannoplankton assemblages vs. core depth in borehole Livadi 4. First diagram: coccoliths in situ and second diagram: reworked coccoliths.

Sampling			Biostratigraphy			
			Calcareous Nannoplakton			
			Scanning Electron Microscope (SEM)			
Sample Code	Sample interval (cm)	Depth (m)	In situ	Plio-Pleistocene Reworked	Notes	Results
4.7.1	0-2	18	<i>Emiliania huxleyi</i> , <i>Calcidiscus leptoporus</i> , <i>Rhabdosphaera</i> , <i>Helicosphaera carteri</i> , <i>H. hyalina</i> , <i>Syracosphaera</i> , <i>Syracolithus</i> , <i>Umbilicosphaera</i> , <i>Calsiosolenia</i>	small <i>Reticulofenestra</i> (minuta, minutula), <i>Pseudoemiliania lacunosa</i> , <i>Discoaster</i> sp.	<i>E. huxleyi</i> (30,88%) abundant Plio-Pleistocene reworked from surroundings due to erosion	MNN21b
4.7.6	50-52	18,5	<i>Emiliania huxleyi</i> , <i>Calcidiscus leptoporus</i> , <i>Rhabdosphaera</i> , <i>Syracosphaera</i> , <i>Syracolithus</i> , <i>Helicosphaera hyalina</i> , <i>Umbilicosphaera</i>	small <i>Reticulofenestra</i> spp., small <i>Gephyrocapsa</i> spp., <i>P. lacunosa</i> , <i>Helicosphaera selli</i> , <i>Discoaster</i> sp.	<i>E. huxleyi</i> (28,57%), abundant Plio-Pleistocene reworked from surroundings due to erosion	MNN21b
4.7.11	100-102	19	<i>E. huxleyi</i> , <i>C. leptoporus</i> , <i>Rhabdosphaera</i> , <i>H. carteri</i> , <i>Syracosphaera</i> , <i>Syracolithus</i> , <i>Umbilicosphaera</i>	<i>Reticulofenestra</i> spp., <i>P. lacunosa</i> , small <i>Gephyrocapsa</i> , <i>G. caribbeanica</i> , <i>Sphenolithus</i> spp., <i>Discoaster</i> spp.	<i>E. huxleyi</i> (38,64%), abundant Plio-Pleistocene reworked from surroundings due to erosion	MNN21b

4.7.16	150-152	19,5	<i>E. huxleyi</i> , <i>C. leptoporus</i> , <i>H. carteri</i> , <i>H. hyalina</i> , <i>C. pelagicus</i> , <i>Syracosphaera</i> , <i>Syracolithus</i> , <i>Umbilicosphaera</i> , <i>Corisphaera</i> , <i>Coronosphaera</i>	small <i>Reticulofenestra</i> (<i>minuta</i> , <i>minutula</i>), small <i>Gephyrocapsa</i> , <i>Gephyrocapsa omega</i> , <i>G. caribbeanica</i> , <i>P. lacunosa</i> , <i>Sphenolithus</i> , <i>Discoaster</i> sp., <i>Discoaster</i> rosette form	<i>E. huxleyi</i> (40,74%) abundant Plio-Pleistocene reworked from surroundings due to erosion	MNN21b
4.7.21	200-202	20	<i>E. huxleyi</i> , <i>C. leptoporus</i> , <i>Rhabdosphaera</i> , <i>H. hyalina</i> , <i>Syracosphaera</i> , <i>Syracolithus</i> , <i>Umbilicosphaera</i> , <i>Umbellosphaera</i> , <i>Scyphosphaera</i>	<i>Reticulofenestra</i> spp., <i>P. lacunosa</i> , <i>H. selli</i> , small <i>Gephyrocapsa</i> , <i>G. caribbeanica</i> , <i>G. omega</i> , <i>Discoaster</i> sp.	<i>E. huxleyi</i> (47,50%) abundant and Plio-Pleistocene reworked from surroundings due to erosion	MNN21b
4.7.26	250-252	20,5	<i>E. huxleyi</i> , <i>C. leptoporus</i> , <i>Umbilicosphaera</i> , <i>H. carteri</i> , <i>H. hyalina</i> , <i>H. wallichii</i> , <i>C. pelagicus</i> , <i>Syracosphaera</i> , <i>Syracolithus</i>	<i>Reticulofenestra</i> sp., small <i>Gephyrocapsa</i> , <i>G. caribbeanica</i> , <i>P. lacunosa</i> , <i>C. macintyeri</i> , <i>H. selli</i> , <i>H. recta</i> , <i>Sphenolithus</i> , <i>Discoaster</i> sp.	<i>E. huxleyi</i> (29,7%) abundant Plio-Pleistocene reworked from surroundings due to erosion	MNN21b
4.7.31	300-302	21,5	<i>E. huxleyi</i> , <i>C. leptoporus</i> , <i>Umbilicosphaera</i> , <i>Corisphaera</i> , <i>Rhabdosphaera</i> , <i>Coronosphaera</i> , <i>Umbellosphaera</i> , <i>Helicosphaera carteri</i> , <i>H. hyalina</i> , <i>H. pavimentum</i> , <i>Scyphosphaera</i> , <i>Syracosphaera</i> , <i>Syracolithus</i>	small <i>Gephyrocapsa</i> , <i>G. omega</i> , <i>Reticulofenestra minuta</i> - <i>minutula</i> , <i>Reticulofenestra</i> sp., <i>C. macintyeri</i> , <i>H. selli</i> , <i>Discoaster</i> sp, <i>P. lacunosa</i>	<i>E. huxleyi</i> (17,46%) abundant Plio-Pleistocene reworked from surroundings due to erosion	MNN21b

4.8.1	0-2	21,7	<i>E. huxleyi</i> , <i>C. leptoporus</i> , <i>Umbilicosphaera</i> , <i>Rhabdosphaera</i> , <i>Coronosphaera</i> , <i>Helicosphaera carteri</i> , <i>H. hyalina</i> , <i>H. wallichii</i> , <i>H. pavimentum</i> , <i>C. pelagicus</i> , <i>Syracosphaera</i> , <i>Syracolithus</i>	<i>Reticulofenestra minuta - minutula</i> , <i>Reticulofenestra</i> sp., small <i>Gephyrocapsa</i> , <i>P. lacunosa</i> , <i>H. selli</i> , <i>C. macintyeri</i> , <i>Discoaster</i> sp.	<i>E. huxleyi</i> (17,14%) - Plio-Pleistocene reworked from surroundings due to erosion	MNN21b
4.8.6	50-52	22,2	<i>E. huxleyi</i> , <i>C. leptoporus</i> , <i>Umbilicosphaera</i> , <i>Corisphaera</i> , <i>Rhabdosphaera</i> , <i>Umbellosphaera</i> , <i>H. carteri</i> , <i>H. wallichii</i> , <i>H. hyalina</i> , <i>Coronocyclus</i> , <i>Syracolithus</i> , <i>Syracosphaera</i> , <i>C. pelagicus</i>	<i>Reticulofenestra minuta - minutula</i> , <i>Reticulofenestra</i> sp., small <i>Gephyrocapsa</i> , <i>P. lacunosa</i> , <i>Discoaster</i> sp.	<i>E. huxleyi</i> (29,58%) - Plio-Pleistocene reworked from surroundings due to erosion	MNN21b
4.8.11	100-102	22,7	<i>E. Huxleyi</i> , <i>C. leptoporus</i> , <i>Umbilicopshaera</i> , <i>Corisphaera</i> , <i>Rhabdosphaera</i> , <i>H. carteri</i> , <i>C. pelagicus</i> , <i>Syracosphaera</i>	small <i>Gephyrocapsa</i> , <i>Reticulofenestra minuta - minutula</i> , <i>Reticulogenestra</i> sp., <i>H. selli</i> , <i>H. elongata</i> , <i>P. lacunosa</i> , <i>Discoaster</i> sp., <i>Sphenolithus</i>	<i>E. huxleyi</i> (51,22%) - abundant -Plio-Pleistocene reworked from surroundings due to erosion	MNN21b
4.8.16	150-152	23,2	<i>E. huxleyi</i> , <i>C. leptoporus</i> , <i>Umbilicosphaera</i> , <i>Rhabdosphaera</i> , <i>H. carteri</i> , <i>H. wallichii</i> , <i>Syracosphaera</i> , <i>Syracolithus</i>	<i>Reticulofenestra minuta - minutula</i> , <i>Reticulofenestra</i> sp., <i>P. lacunosa</i> , small <i>Gephyrocapsa</i> , <i>G. omega</i> , <i>C. macintyeri</i> , <i>H. selli</i>	<i>E. huxleyi</i> (31,88%), Plio-Pleistocene reworked from surroundings due to erosion	MNN21b

4.8.21	200-202	23,7	<i>E. huxleyi</i> , <i>C. leptoporus</i> , <i>Umbilicosphaera</i> , <i>Calsiosolenia</i> , <i>Rhabdosphaera</i> , <i>H. carteri</i> , <i>H. hyalina</i> , <i>Syracosphaera</i> , <i>Syracolithus</i>	<i>Reticulofenestra minuta</i> - <i>minutula</i> , small <i>Gephyrocapsa</i> , <i>G. caribbeanica</i> , <i>P. lacunosa</i> , <i>C. macintyeri</i> , <i>Discoaster</i> sp.	<i>E. huxleyi</i> (57%) abundant	MNN21b
4.8.26	250-252	24,2	<i>E. huxleyi</i> , <i>C. leptoporus</i> , <i>Umbilicosphaera</i> , <i>Calsiosolenia</i> , <i>Rhabdosphaera</i> , <i>H. carteri</i> , <i>Syracosphaera</i> , <i>Syracolithus</i> , <i>C. pelagicus</i>	<i>Reticulofenestra minuta</i> - <i>minutula</i> , <i>P. lacunosa</i> , <i>C. macintyeri</i> , <i>H. selli</i> , small <i>Gephyrocapsa</i> , <i>G. caribbeanica</i>	<i>E. huxleyi</i> (46,07%) - abundant	MNN21b
4.8.31	300-302	24,7	<i>E. huxleyi</i> , <i>C. leptoporus</i> , <i>Umbilicosphaera</i> , <i>Rhabdosphaera</i> , <i>Umbellosphaera</i> , <i>H. carteri</i> , <i>H. hyalina</i> , <i>Syracosphaera</i> , <i>Syracolithus</i> , <i>C. pelagicus</i>	<i>Reticulofenestra minuta</i> - <i>minutula</i> , <i>Reticulofenestra</i> spp., small <i>Gephyrocapsa</i> , <i>G. omega</i> , <i>P. lacunosa</i> , <i>Discoaster</i> sp., <i>Discoaster rosette form</i>	<i>E. huxleyi</i> (28%) - Plio-Pleistocene reworked from surroundings due to erosion	MNN21b
4.8.36	350-352	25,2	<i>E. huxleyi</i> , <i>C. leptoporus</i> , <i>Umbilicosphaera</i> , <i>Rhabdosphaera</i> , <i>Umbellosphaera</i> , <i>H. carteri</i> , <i>H. wallichii</i> , <i>Syracosphaera</i> , <i>Syracolithus</i> , <i>C. pelagicus</i> , <i>Coronocyclus</i> , <i>Algirosphaera</i>	<i>Reticulofenestra minuta</i> - <i>minutula</i> , <i>Reticulofenestra</i> spp., small <i>Gephyrocapsa</i> , <i>G. omega</i> , <i>G. caribbeanica</i> , <i>P. lacunosa</i> , <i>Discoaster</i> sp.	<i>E. huxleyi</i> (17,6%) - Plio-Pleistocene reworked from surroundings due to erosion	MNN21b

4.8.38	370-372	25,5	<i>E. huxleyi</i> , <i>C. leptoporus</i> , <i>Umbilicosphaera</i> , <i>Rhabdosphaera</i> , <i>Umbellosphaera</i> , <i>Calsiosolenia</i> , <i>Cytosphaera</i> , <i>Syracosphaera</i> , <i>Syracolithus</i>	<i>Reticulofenestra minuta</i> - <i>minutula</i> , small <i>Gephyrocapsa</i> , <i>G. caribbeanica</i> , <i>H. selli</i> , <i>P. lacunosa</i> , <i>Sphenolithus</i>	<i>E. huxleyi</i> (5,71%) - shallow marine	MNN21b
4.8.41	400-402	25,7	<i>E. huxleyi</i> , <i>Umbilicosphaera</i> , <i>Rhabdosphaera</i> , <i>Calsiosolenia</i> , <i>Syracosphaera</i> , <i>H. hyalina</i>	<i>Reticulofenestra minuta</i> - <i>minutula</i> , <i>Reticulofenestra</i> spp., small <i>Gephyrocapsa</i> , <i>G. omega</i> , <i>G. caribbeanica</i> , <i>H. selli</i> , <i>P. lacunosa</i> , <i>Sphenolithus</i>	<i>E. huxleyi</i> (25%)	MNN21b
4.8.46	450-452	26,2	<i>E. huxleyi</i> , <i>Umbilicosphaera</i> , <i>Umbellosphaera</i> , <i>H. carteri</i> , <i>Syracolithus</i>	<i>Reticulofenestra minuta</i> - <i>minutula</i> , <i>Reticulofenestra</i> spp., small <i>Gephyrocapsa</i> , <i>G. omega</i> , <i>G. caribbeanica</i> , <i>H. selli</i> , <i>P. lacunosa</i> , <i>Discoaster</i> sp.	<i>E. huxleyi</i> (47,22%) abundant	MNN21b
4.8.50	490-492	26,6	<i>E. huxleyi</i> , <i>C. leptoporus</i> , <i>Umbilicosphaera</i> , <i>H. carteri</i> , <i>H. wallichii</i> , <i>Syracosphaera</i> , <i>Syracolithus</i> , <i>C. pelagicus</i> , <i>Rhabdosphaera</i>	<i>Reticulofenestra minuta</i> - <i>minutula</i> , <i>Reticulofenestra</i> spp., small <i>Gephyrocapsa</i> , <i>P. lacunosa</i> , <i>Sphenolithus</i> , <i>C. macintyeri</i>	<i>E. huxleyi</i> (3,70%) - shallow marine	MNN21b

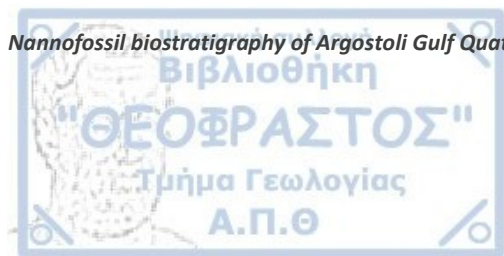
4.9.1	0-2	26,7	<i>E. huxleyi</i> , <i>C. leptoporus</i> , <i>Umbilicosphaera</i> , <i>H. carteri</i> , <i>Syracosphaera</i> , <i>Syracolithus</i> , <i>Calsiosolenia</i> , <i>Rhabdosphaera</i>	<i>Reticulofenestra minuta</i> - <i>minutula</i> , <i>Reticulofenestra</i> spp., small <i>Gephyrocapsa</i> , <i>G. caribbeanica</i> , <i>H. selli</i> , <i>P. lacunosa</i> , <i>Discoaster</i> sp., <i>C. macintyeri</i>	<i>E. huxleyi</i> (8,77%) - shallow marine	MNN21b
4.9.6	50-52	27,2	<i>E. huxleyi</i> , <i>C. leptoporus</i> , <i>Umbilicosphaera</i> , <i>H. carteri</i> , <i>Syracosphaera</i> , <i>Syracolithus</i>	<i>Reticulofenestra minuta</i> - <i>minutula</i> , small <i>Gephyrocapsa</i> , <i>G. caribbeanica</i> , <i>P. lacunosa</i> , <i>C. macintyeri</i>	<i>E. huxleyi</i> (23,33%) - shallow marine environment	MNN21b
4.9.11	100-102	27,7	<i>E. huxleyi</i> , <i>C. leptoporus</i> , <i>Umbilicosphaera</i> , <i>H. carteri</i> , <i>H. hyalina</i> , <i>H. wallichii</i> , <i>Umbellosphaera</i> , <i>Rhabdosphaera</i> , <i>Syracosphaera</i> , <i>Syracolithus</i>	<i>Reticulofenestra minuta</i> - <i>minutula</i> , <i>Reticulofenestra</i> spp., small <i>Gephyrocapsa</i> , <i>G. caribbeanica</i> , <i>G. omega</i> , <i>P. lacunosa</i> , <i>H. selli</i> , <i>C. macintyeri</i> , <i>Sphenolithus</i> , <i>Discoaster rossette form</i>	<i>E. huxleyi</i> (16,67%) - shallow marine	MNN21b
4.9.16	150-152	28,2	<i>E. huxleyi</i> , <i>C. leptoporus</i> , <i>Umbilicosphaera</i> , <i>Calsiosolenia</i> , <i>H. carteri</i> , <i>H. hyalina</i> , <i>H. wallichii</i> , <i>Rhabdosphaera</i> , <i>Syracosphaera</i> , <i>Syracolithus</i>	<i>Reticulofenestra minuta</i> - <i>minutula</i> , <i>Reticulofenestra</i> spp., small <i>Gephyrocapsa</i> , <i>G. caribbeanica</i> , <i>P. lacunosa</i> , <i>H. selli</i> , <i>C. macintyeri</i> , <i>Discoaster</i> sp.	<i>E. huxleyi</i> (14,04%) - shallow marine	MNN21b

4.9.21	200-202	28,7	<i>E. huxleyi</i> , <i>C. leptoporus</i> , <i>Umbilicosphaera</i> , <i>H. carteri</i> , <i>C. pelagicus</i> , <i>Rhabdosphaera</i> , <i>Syracosphaera</i> , <i>Syracolithus</i>	<i>Reticulofenestra minuta</i> - <i>minutula</i> , <i>Reticulofenestra spp.</i> , small <i>Gephyrocapsa</i> , <i>G. caribbeanica</i> , <i>P. lacunosa</i> , <i>H. selli</i> , <i>C. macintyeri</i> , <i>Discoaster sp.</i> , <i>Discoaster rosette form</i> , <i>Sphenolithus</i>	<i>E. huxleyi</i> (44%) abundant	MNN21b
4.9.26	250-252	29,2	<i>E. huxleyi</i> , <i>C. leptoporus</i> , <i>Umbilicosphaera</i> , <i>H. carteri</i> , <i>H. hyalina</i> , <i>H. wallichii</i> , <i>C. pelagicus</i> , <i>Rhabdosphaera</i> , <i>Syracosphaera</i> , <i>Syracolithus</i>	<i>Reticulofenestra minuta</i> - <i>minutula</i> , <i>Reticulofenestra spp.</i> , small <i>Gephyrocapsa</i> , <i>G. caribbeanica</i> , <i>P. lacunosa</i> , <i>H. selli</i> , <i>H. elongata</i> , <i>C. macintyeri</i> , <i>Discoaster sp.</i>	<i>E. huxleyi</i> (3,51%) - shallow marine environment	MNN21b
4.10.1	0-2	29,3	<i>E. huxleyi</i> , <i>C. leptoporus</i> , <i>Umbilicosphaera</i> , <i>H. carteri</i> , <i>H. hyalina</i> , <i>H. wallichii</i> , <i>Rhabdosphaera</i> , <i>Syracosphaera</i> , <i>Syracolithus</i>	<i>Reticulofenestra minuta</i> - <i>minutula</i> , <i>Reticulofenestra spp.</i> , small <i>Gephyrocapsa</i> , <i>G. caribbeanica</i> , <i>P. lacunosa</i> , <i>H. selli</i> , <i>C. macintyeri</i> , <i>Discoaster sp.</i> , <i>Sphenolithus</i>	<i>E. huxleyi</i> (34,78%) - shallow marine	MNN21b

4.10.6	50-52	29,8	<i>E. huxleyi</i> , <i>C. leptoporus</i> , <i>Umbilicosphaera</i> , <i>H. carteri</i> , <i>Rhabdosphaera</i> , <i>Syracosphaera</i> , <i>Syracolithus</i> , <i>C. pelagicus</i> , <i>Scyphosphaera</i>	<i>Reticulofenestra minuta</i> - <i>minutula</i> , <i>Reticulofenestra</i> spp., small <i>Gephyrocapsa</i> , <i>G. caribbeanica</i> , <i>P. lacunosa</i> , <i>C. macintyeri</i> , <i>Discoaster</i> sp., <i>Sphenolithus</i>	<i>E. huxleyi</i> (12,5%) - shallow marine	MNN21b
4.10.11	100-102	30,3	<i>C. leptoporus</i> , <i>Umbilicosphaera</i> , <i>H. carteri</i> , <i>H. hyalina</i> , <i>Rhabdosphaera</i> , <i>Syracosphaera</i> , <i>Syracolithus</i> , <i>C. pelagicus</i> , <i>Coronocyclous</i>	<i>Reticulofenestra minuta</i> - <i>minutula</i> , <i>Reticulofenestra</i> spp., small <i>Gephyrocapsa</i> , <i>P. lacunosa</i> , <i>Discoaster</i> sp., <i>Sphenolithus</i>	<i>E. huxleyi</i> (0,00%) due to environment conditions - very shallow marine environment	MNN21b
4.10.16	150-152	30,8	<i>C. leptoporus</i> , <i>Umbilicosphaera</i> , <i>H. hyalina</i> , <i>Rhabdosphaera</i> , <i>Syracosphaera</i> , <i>C. pelagicus</i>	<i>Reticulofenestra minuta</i> - <i>minutula</i> , <i>Reticulofenestra</i> spp.	<i>E. huxleyi</i> (0,00%) due to environment conditions - very shallow marine environment	MNN21b
4.10.21	200-202	31,3	NO SIGN OF COCCOLITHOPHORES			MNN21b - restricted lagoon
4.10.22	210-212	31,4	<i>Calcidiscus leptoporus</i> , <i>Umbilicosphaera</i>	<i>P. lacunosa</i> , small <i>Gephyrocapsa</i> , <i>Reticulofenestra minuta</i> - <i>minutula</i>	VERY FEW COCCOLITHOPHORES	MNN21b - very shallow lagoon
4.10.23	220-222	31,5	<i>Umbilicosphaera</i> spp.	<i>Discoaster</i> sp.	VERY FEW COCCOLITHOPHORES	MNN21b - lagoon

4.10.24	230-232	31,6	<i>C. leptoporus</i> , <i>Umbilicosphaera</i> , <i>Syracosphaera</i> , <i>Syracolithus</i> , <i>Reticulofenestra minuta</i> - <i>minutula</i> , <i>Reticulofenestra</i> spp., <i>C. formosus</i> , <i>P. lacunosa</i> , <i>Discoaster</i> spp., <i>Discoaster rossette form</i> , small <i>Gephyrocapsa</i>	no reworked - biozonal transition	small <i>Gephyrocapsa</i> $\leq 3\mu\text{m}$ (3,7%), <i>Reticulofenestra</i> spp. (63%), <i>Pseudoemiliana lacunosa</i> (4,84%), <i>E. huxleyi</i> (0,00%)	MNN19f - Pleistocene
4.10.25	240-242	31,7	<i>C. leptoporus</i> , <i>Umbilicosphaera</i> , <i>H. carteri</i> , <i>H. hyalina</i> , <i>Cytosphaera</i> , <i>Syracolithus</i> , <i>C. pelagicus</i> , <i>Reticulofenestra minuta</i> - <i>minutula</i> , <i>Reticulofenestra</i> spp., <i>C. formosus</i> , <i>P. lacunosa</i> , small <i>Gephyrocapsa</i>	no reworked- Pleistocene biozone	small <i>Gephyrocapsa</i> $\leq 3\mu\text{m}$ (1,23%), <i>Reticulofenestra</i> spp. (65,43%), <i>P. lacunosa</i> (6,1%)	MNN19f - Pleistocene
4.10.26	250-252	31,8	<i>C. leptoporus</i> , <i>Umbilicosphaera</i> , <i>H. carteri</i> , <i>H. hyalina</i> , <i>Syracosphaera</i> , <i>C. pelagicus</i> , <i>Reticulofenestra minuta</i> - <i>minutula</i> , <i>Reticulofenestra</i> spp., <i>P. lacunosa</i> , small <i>Gephyrocapsa</i> , <i>Discoaster</i> sp.	no reworked- Pleistocene biozone	small <i>Gephyrocapsa</i> $\leq 3\mu\text{m}$ (5,1%), <i>Reticulofenestra</i> spp. (65,7%), <i>P. lacunosa</i> (2,9%)	MNN19f - Pleistocene

Table 6: Borehole Livadi 4. Samples, depth, sample interval in every core. Calcareous nannoplankton that collected and identified in every sample, the biozonal indicators in each one and the biostratigraphic age.



7. Discussion

7.1 Reworked Coccoliths within Holocene

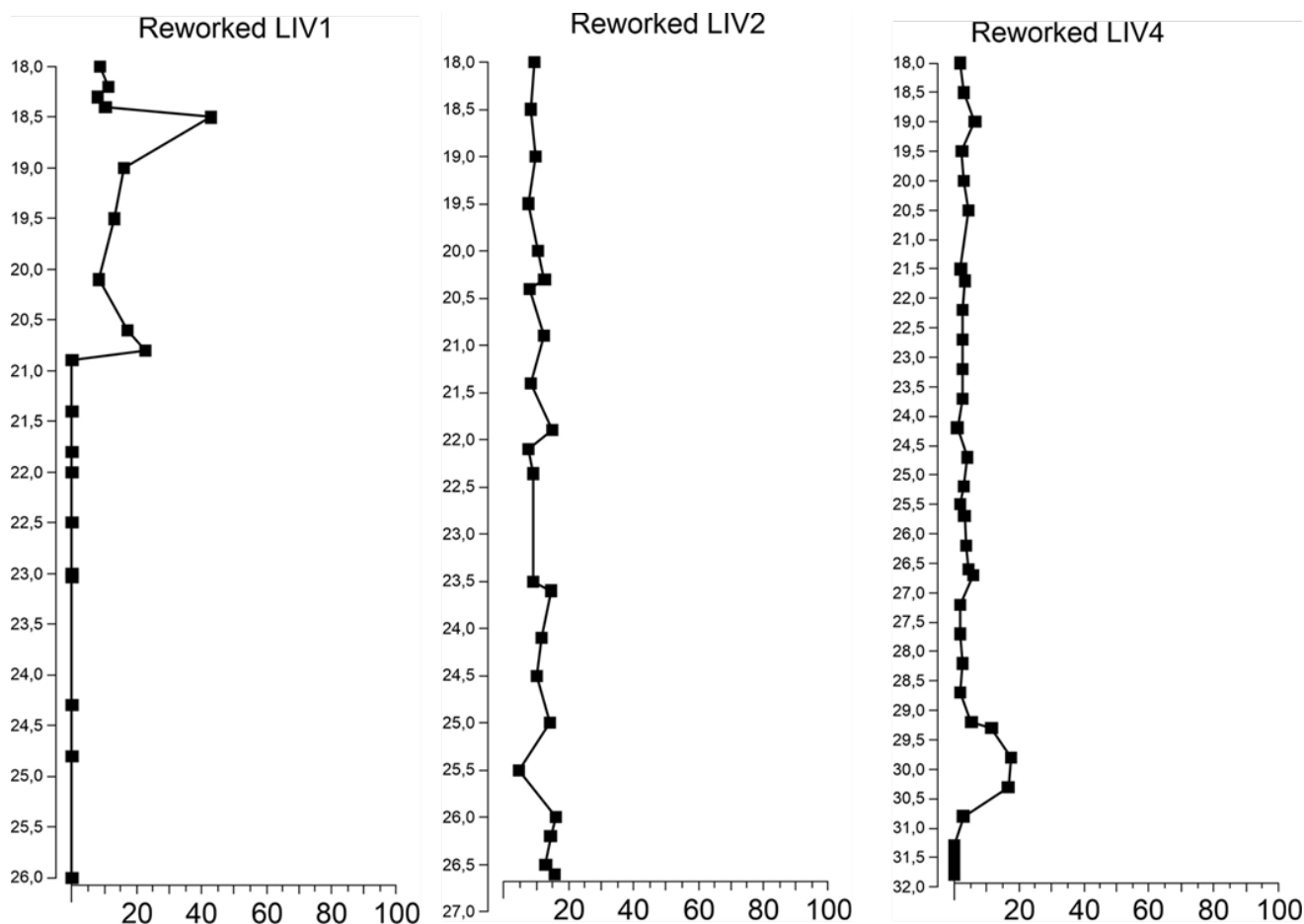


Figure 19: Reworked coccoliths in boreholes Livadi 1, 2 and 4.

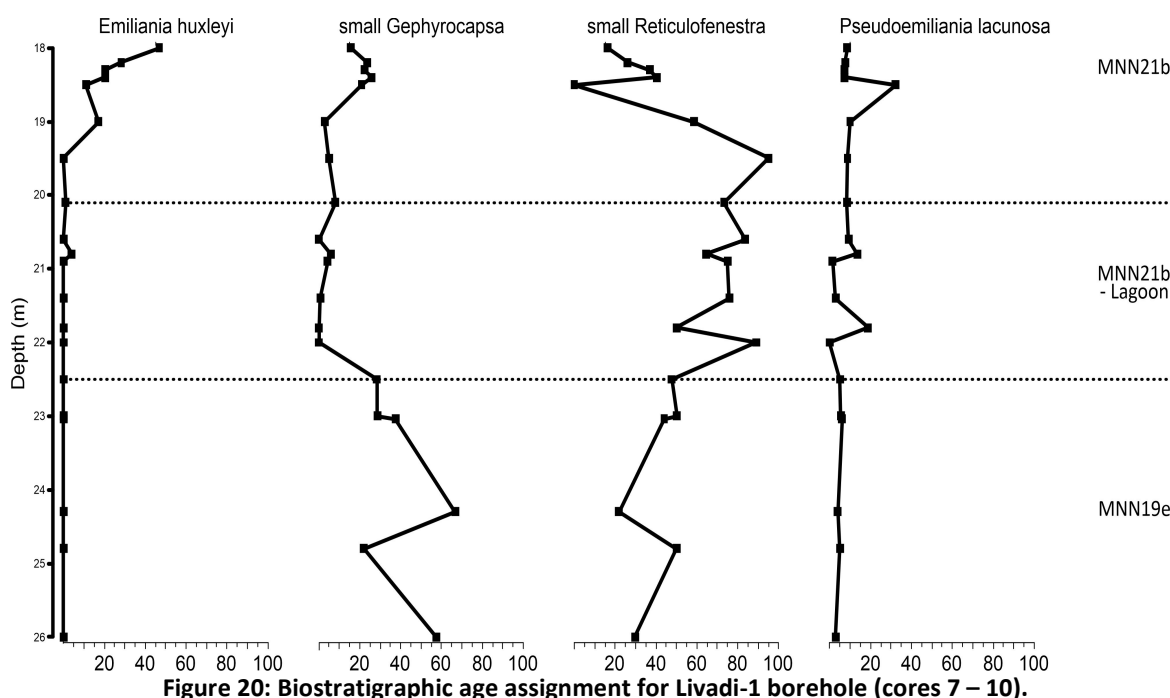
The main problem we came across in all boreholes Livadi 1, Livadi 2 and Livadi 4 was the reworked coccoliths within the Holocene samples. The nannofossil assemblages in these samples (*Pseudoemiliania lacunosa*, *Reticulofenestra* sp., *Calcidiscus macintyeri*, *Toweius* sp., *Helicosphaera sellii*, *Gephyrocapsa omega*, *Discoaster* sp., *Sphenolithus* sp. etc.) are considered as redeposited from the Pliocene - Pleistocene surrounding outcrops (Triantaphyllou, 1996; Triantaphyllou et al., 1998; Papanikolaou & Triantaphyllou, 2013).

More specific according to previous research in the area (Triantaphyllou, 1993, 1996), *Discoaster variabilis* and *Sphenolithus* sp., were from the Pliocene surroundings (Miocene/Pliocene boundary, MNN12). More over the rest of *Discoaster* sp. representatives were from the middle and late Pliocene (*D. brouwerii* - MNN18, late Pliocene). The coccoliths *C. macintyeri*, *H. sellii* were from the early Pleistocene (MNN19, Triantaphyllou, 1993, 1996). More specific *C. macintyeri* and *H. sellii* characterize the biozones MNN19b and MNN19c and *P. lacunosa* the biozone MNN19f - middle Pleistocene (Rio et al., 1990). This problematic situation would not give us the

real abundances of *Emiliana huxleyi* in the assemblages, which made us skeptical. So we recalculated *E. huxleyi*'s percentages, by excluding all the redeposited (reworked) coccoliths. The most reworked material was found in the boreholes that were closest to the land (Livadi 2 and 4). The redeposited coccoliths were from the Plio/Pleistocene surroundings due to erosion (Triantaphyllou, 1993, 1996; Triantaphyllou et al., 1998; Papanikolaou & Triantaphyllou, 2013). It is therefore reasonable that the boreholes nearest to the shore would have received more reworked material rather than Livadi 1 which is placed in the middle of Livadi Gulf.

7.2 Biostratigraphy

7.2.1 Biostratigraphic Analysis of Livadi 1



Twenty-six (26) samples have been analyzed under Scanning Electron Microscope (SEM) for the nannofossil content in order to establish biostratigraphic assignment in Livadi-1 borehole. *Emiliana huxleyi* abundances in sample 1.7.1 are more than 40% suggesting the biostratigraphic assignment in MNN21b (age less than 45ka) (Castradori, 1993; Rio et al., 1990). The calculations of the abundances of *E. huxleyi* were based on excluding several species considered as redeposited (see chapter 7.1, about reworked coccoliths). Nannofossil biozone MNN21b is verified in samples 1.7.1 (18m depth), whereas *E. huxleyi* had been documented less than 40% from 1.7.3 (18,2m depth) up to 1.7.4 (18,3m depth) and 1.7.5 (18,4m depth) up to sample 1.8.1 (20,8m depth). Even though, *E. huxleyi* abundances are reduced to approximately to 20% (samples 1.7.3 to 1.7.21 - 18,2-20,1m depth respectively) and are 0% in samples 1.7.26 (20,6m depth) up to 1.9.5 (22m depth), we do not consider this as a biostratigraphic change to older biozone MNN21a (age between 45-250 ka), rather than as an paleoenvironmental impact on nannoplankton assemblages (see paleoenvironmental analysis of LIV1 in the following chapter 7.2.1). For example, shallow lagoonal conditions (even fresh water pond) prohibit the development of in situ assemblages (i.e. *E. huxleyi*). The rest of nannofossil assemblages in these samples (*Pseudoemiliana lacunosa*, *Reticulofenestra* etc.) are considered as redeposited from the Plio-Pleistocene

surrounding outcrops (Triantaphyllou, 1996; Triantaphyllou et al., 1998; Papanikolaou & Triantaphyllou, 2013). *P. lacunosa* (extinct, disappeared in Pleistocene) is actually always redeposited in all Livadi 1 samples. Therefore samples in between Livadi 1.7.26 – 1.9.5 (20,6-22m depth), are biostratigraphically interpreted as assigned again in biozone MNN21b.

The analysis continued downwards borehole Livadi 1 and core 9 (22,5-23,04m depth); the samples analyzed were 1.9.10 (22,5m), sample 19.19–19.20m (23m depth) and 1.9.14 (23,04m). This analysis displayed an obvious change in the assemblage, with abundant small *Gephyrocapsa* spp. (smaller than 3μm), that implies the Pleistocene basement (biozone MNN19e, Backman et al. 2012). In core Livadi 1-10 (24,3-26m depth), have also been verified the absence of *E. huxleyi* (0.00%) and the abundance of small *Gephyrocapsa* spp. > approx. 48%. Therefore Livadi 1-10 is confirmed as assigned to biozone MNN19e (Pleistocene).

7.2.2 Biostratigraphic Analysis of Livadi 2

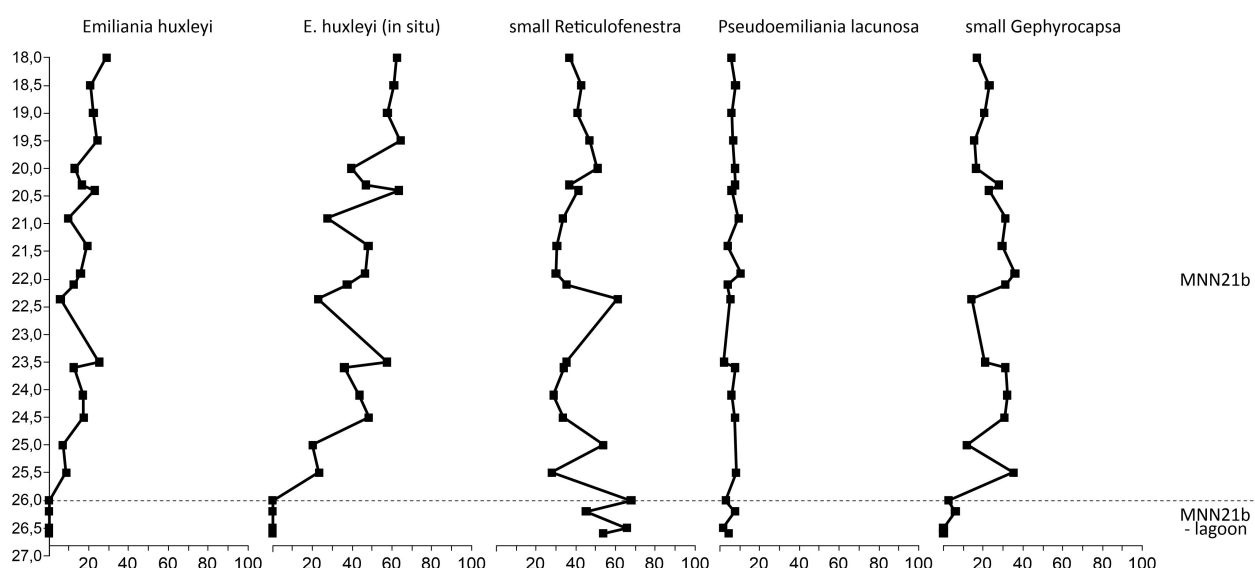


Figure 21: Biostratigraphic age assignment for Livadi 2 borehole (cores 7 – 10).

Twenty-two (22) samples have been analyzed under the Scanning Electron Microscope (SEM) for the nannofossil content in order to establish the biostratigraphic assignment in Livadi 2 borehole. *E. huxleyi* abundances in depth 18m (sample LIV2.7.1) up to 20,3m (sample 2.7.25) are more than 40% suggesting the biostratigraphic assignment in MNN21b. The calculations of the abundances of *E. huxleyi* were based on excluding several species considered as redeposited (see chapter 7.1, about reworked coccoliths). A similar approach has been applied for the following samples in between 20,4-23,5m depth (samples LIV2.8.1 – 2.8.31) and core 9 (23,6-25m depth) of the borehole, suggesting again biozone MNN21b.

The analysis continued downwards the borehole Livadi 2, in core 10 (25,5-26,6m depth). In this core, *E. huxleyi*'s abundances are reduced to approximately 20% and finally are 0% in 20,9-21,4m depth (samples 2.10.6 up to 2.10.11). We did not consider this as a biostratigraphic change to older biozone MNN21a, rather than a paleoenvironmental impact on nannoplankton assemblages (see paleoenvironmental analysis of LIV2 in the following chapter 7.2.2), which prohibit the development of in situ assemblages (lagoonal conditions). The rest of nannofossil assemblages in these samples, as it said before, are considered as redeposited from the Pleistocene surroundings due to erosion. Consequently, Livadi 2 core 10 (25,5-26,6m depth), is considered

biostratigraphically interpreted as assigned again in biozone MNN21b. In this borehole no sign of Pleistocene has been recorded.

7.2.3 Biostratigraphic Analysis of Livadi 4

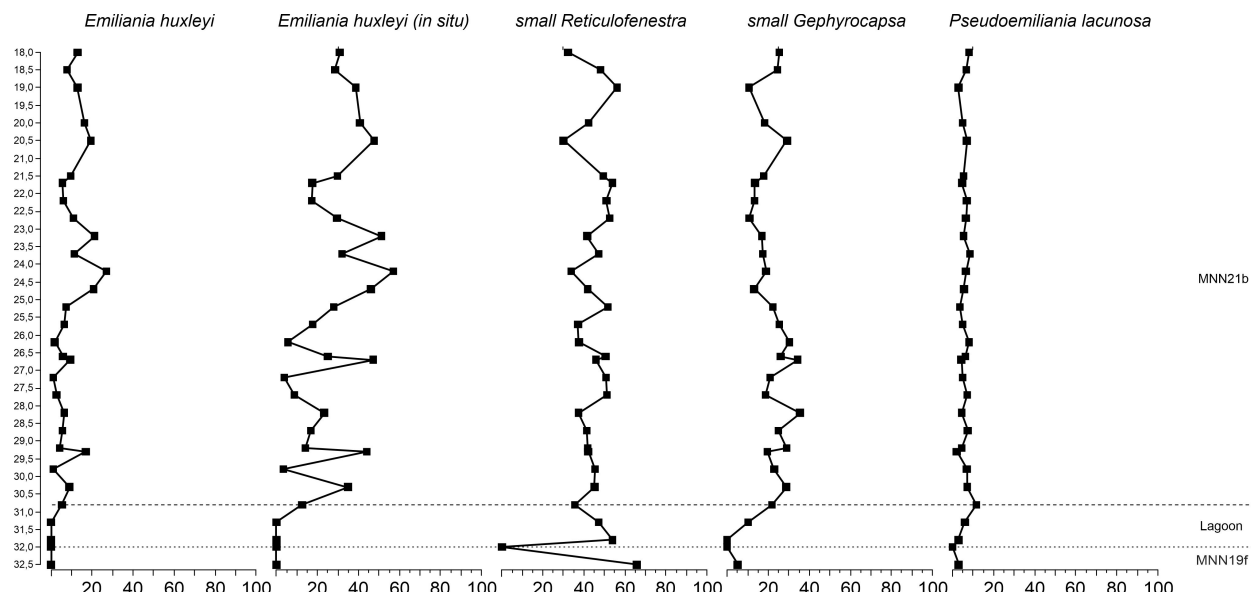


Figure 22: Biostratigraphic age assignment for Livadi 4 borehole (cores 7 – 10).

Thirty-five (35) samples have been analyzed under the Scanning Electron Microscope (SEM) for the nannofossil content in order to verify the biostratigraphic assignment of LIV4 borehole. Samples LIV4.7.1, 4.7.6, 4.7.11 (18m, 18.5m, 19m depth, respectively) displayed *E. huxleyi* ranging in between 29 – 39%, assigned in MNN21b. The calculations of the abundances of *E. huxleyi* were based on excluding several species considered as redeposited (see chapter 7.1, about reworked coccoliths). Marine with algal vegetation conditions appear in 18-19m depth (samples 4.7.1 and 4.7.6) and marine to shallow marine with algal vegetation conditions appear in 18.5m (sample 4.7.11).

E. huxleyi abundances in 19.5-25.2m depth (samples 4.7.16 up to 4.8.36) suggest the biostratigraphic assignment in MNN21b. Then *E. huxleyi* abundances are reduced to less than 9% in 25.7-26.7m depth (samples 4.8.41 – 4.9.1). That is considered as a paleoenvironmental change, shallow marine conditions with algal vegetation. The rest of nannofossil assemblages in these samples (*P. lacunosa*, *Reticulofenestra* etc.) are considered as redeposited from the Pleistocene surroundings due to erosion; *P. lacunosa* (extinct, disappeared in Pleistocene) is actually always redeposited in all LIV4 samples.

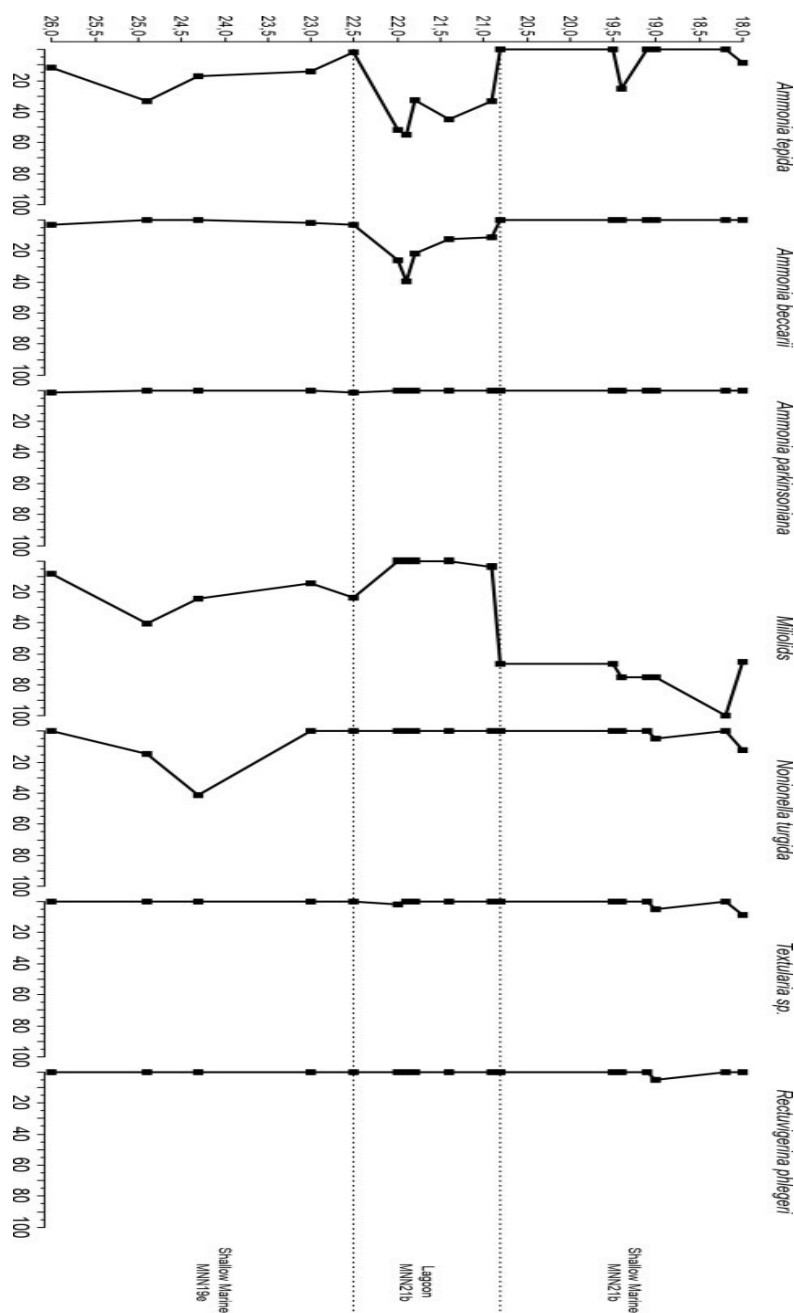
E. huxleyi is present in all samples 4.8.38 and 4.9.6 up to 4.9.26 (25.5m and 27.2-29.2m respectively), suggesting the biostratigraphic assignment still in MNN21b. *E. huxleyi* abundances are low and ranging between 3% - 23%, in all the examined samples. The only exception is sample 4.9.26 (29.2m depth), where *E. huxleyi*'s abundance is 44%. The prevailing reduced abundances of *E. huxleyi* are supported by the restricted paleoenvironmental conditions.

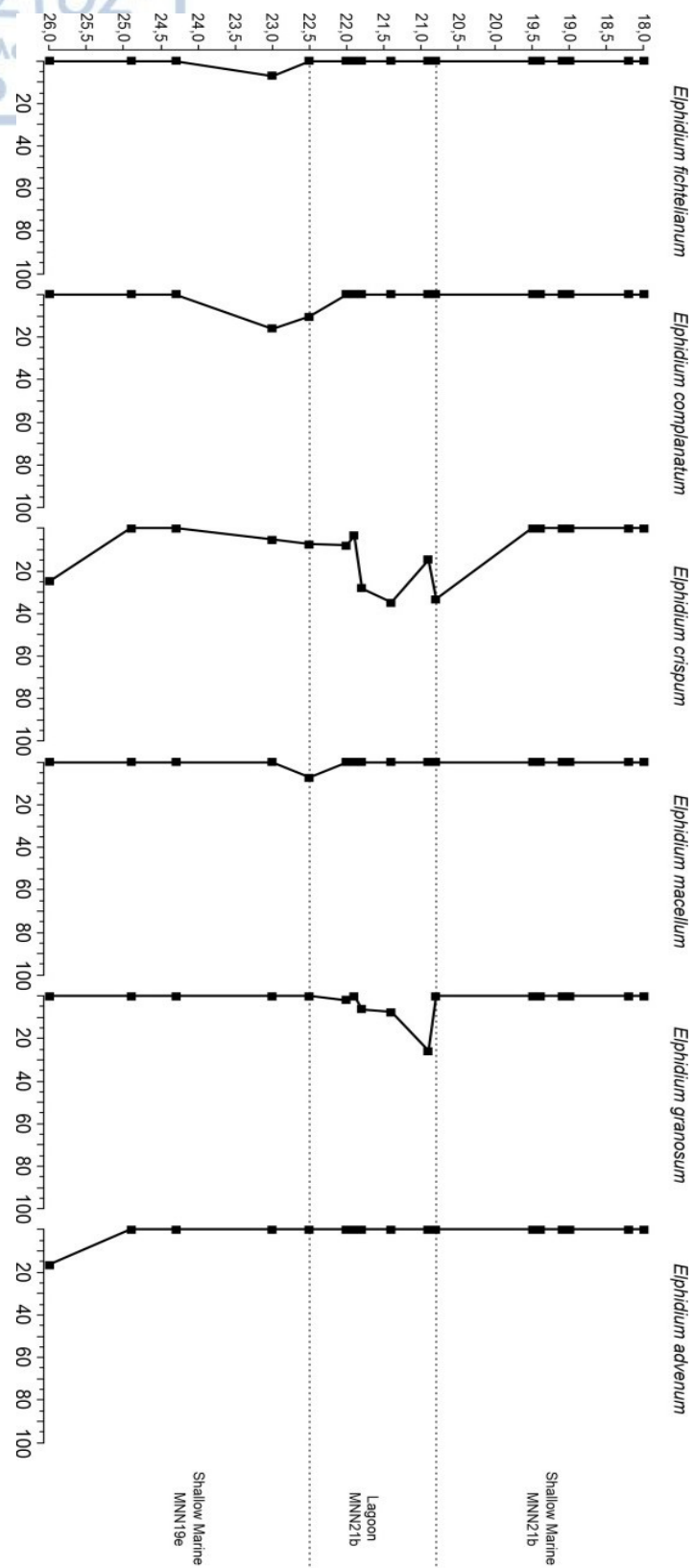
E. huxleyi is present in 30m and 30.5m depth (samples 4.10.1 and 4.10.6 with abundances 35% and 12.5% respectively), suggesting the biostratigraphic assignment again in MNN21b. Then *E. huxleyi* abundances become 0% in 30.3-30.8m depth (samples 4.10.11, 4.10.16). In sample 4.10.21 (31.3m depth) there is no sign of

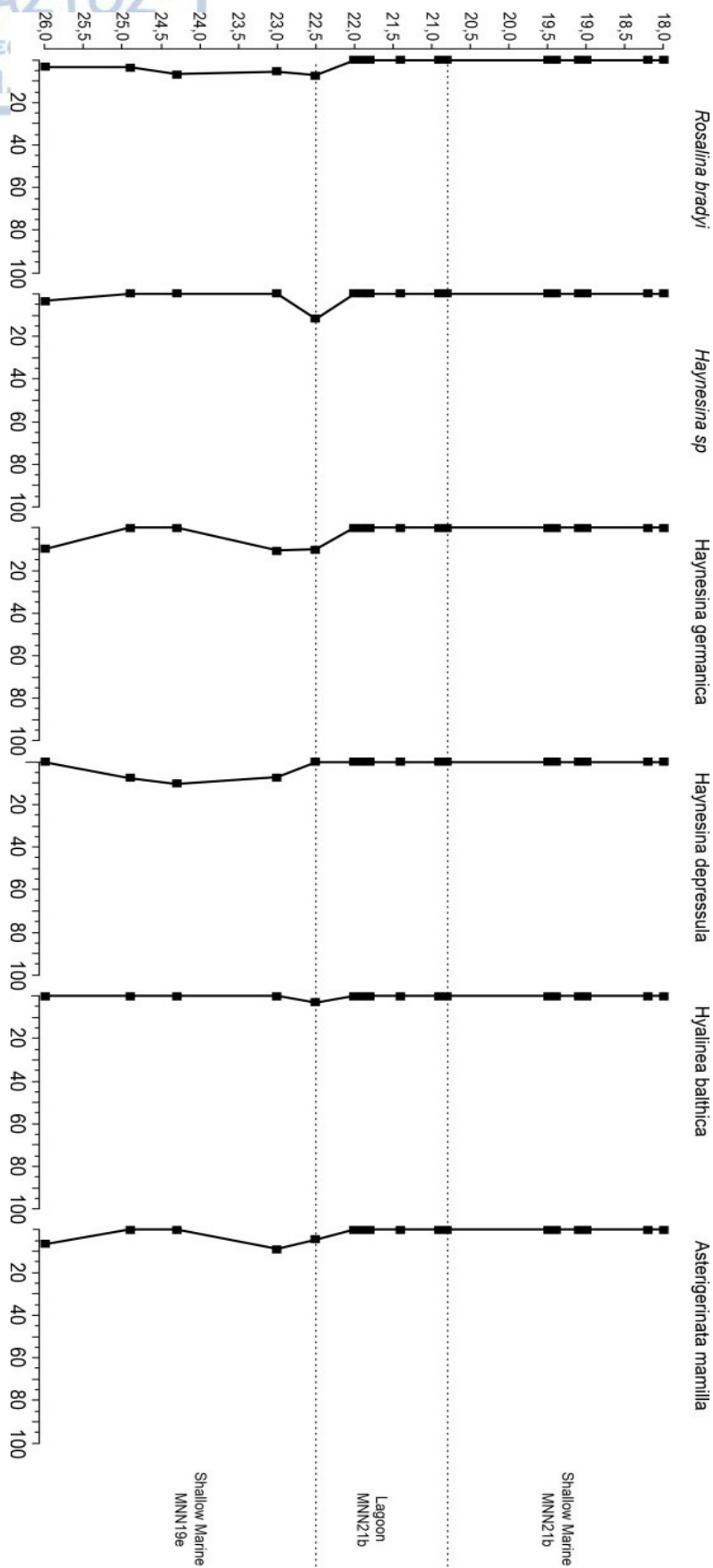
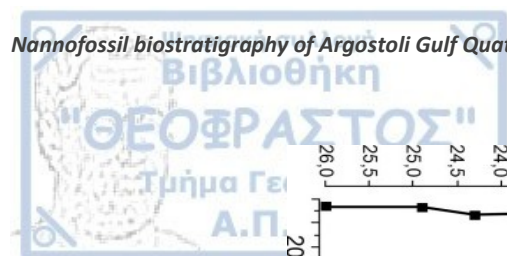
coccolithophores at all. We consider this as a paleoenvironmental change that had an impact on nannoplankton assemblages (shallow lagoonal conditions). In 31,4- 31,5m (sample 4.10.22 and 4.10.23), there are only a few coccoliths (16 and 3), suggesting that the lagoon continues up to these samples. *E. huxleyi* is absent in all these samples. Samples 4.10.24, 4.10.25 and 4.10.26 (31,6 up to 31,8m depth) displayed again abundant nannofossil content, but *E. huxleyi* was totally absent. The rest of the assemblage points to Pleistocene age (MNN19f).

7.3 Paleoenvironment

7.3.1 Paleoenvironmental Analysis of Livadi 1







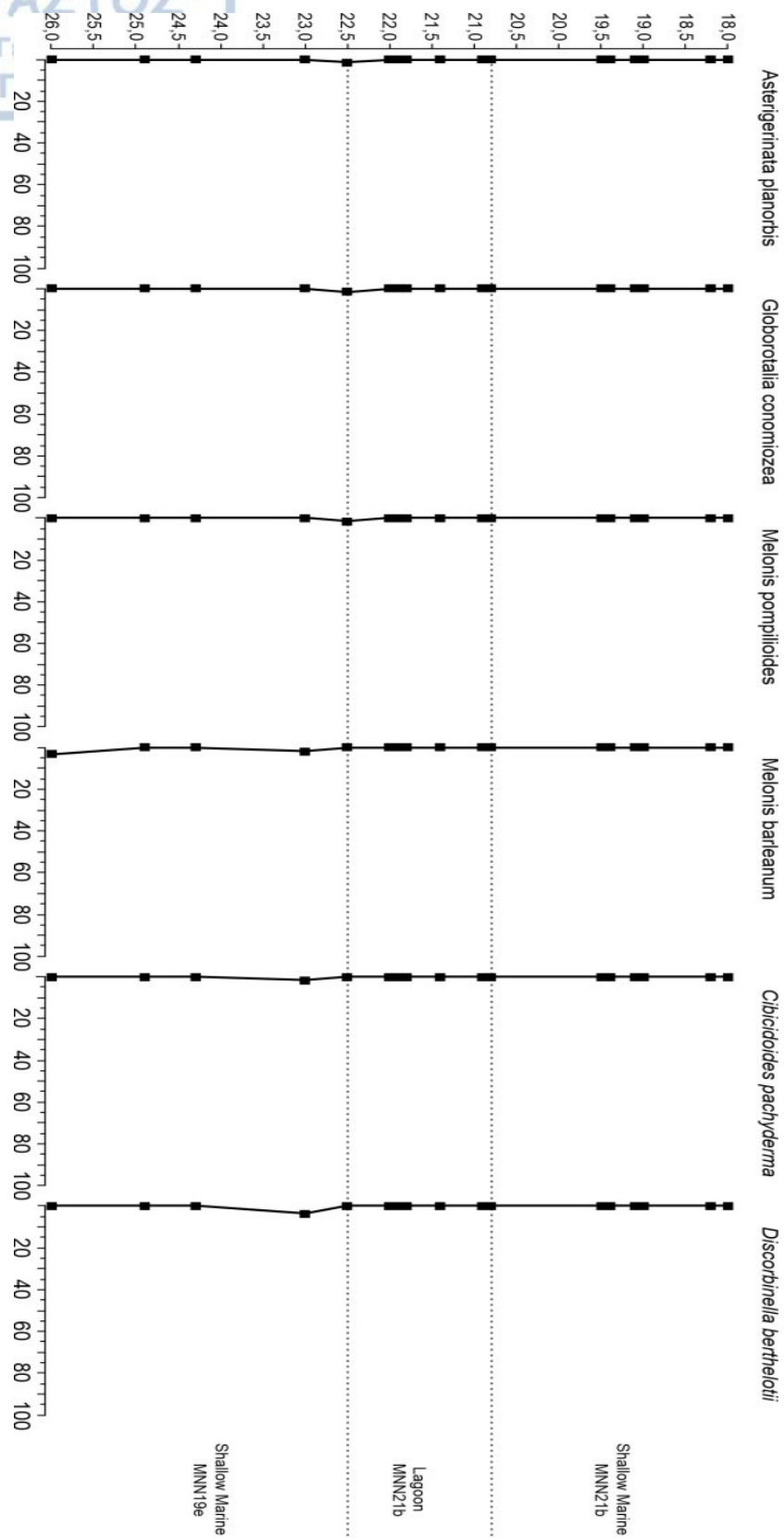
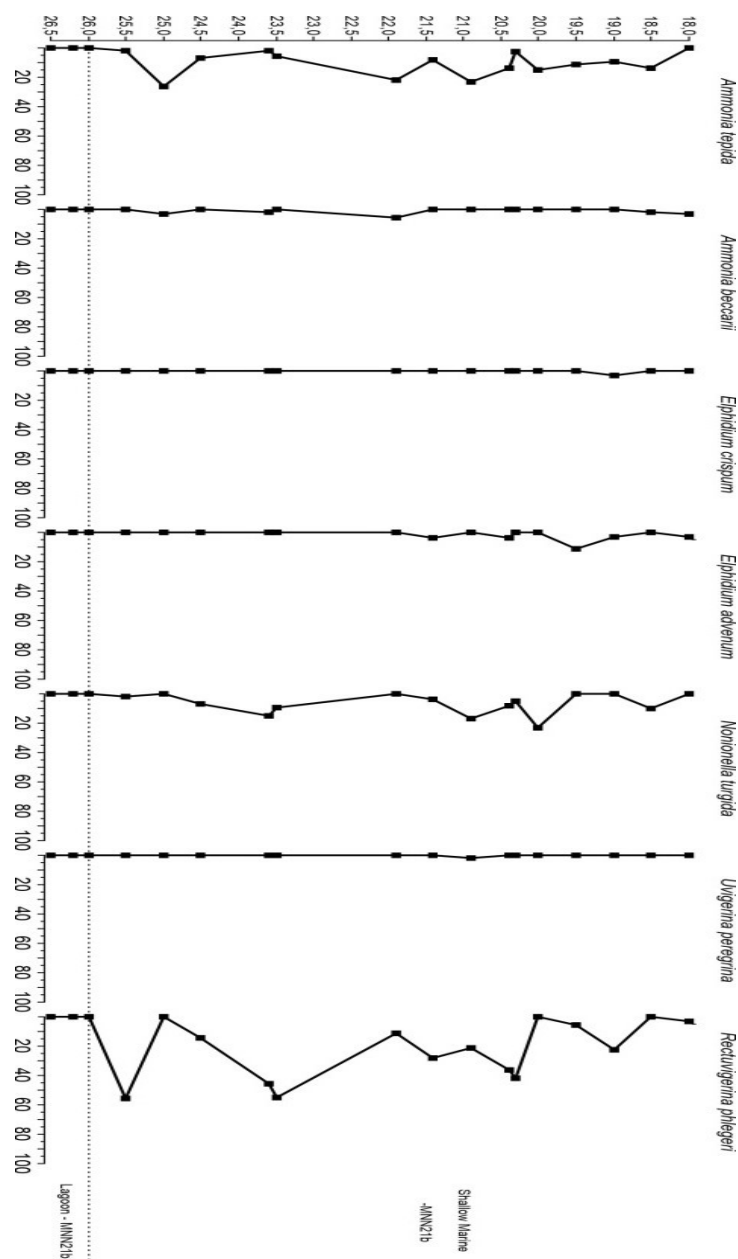


Figure 23: Paleoenvironmental Interpretation of Livadi-1 borehole.

Data from foraminifera and ostracods have shown that in Livadi 1, core 7 the environmental conditions were shallow marine to lagoonal. The foraminifera pointing to that conclusion were *Ammonia tepida*, *Rectuvigerina phlegeri*, *Elphidium crispum*, *E. granosum*, *Nonionella turgida* etc. (see Figure 22, above) and the ostracods were *Cyprideis* spp., *Tyrrhenocythere amnicola*, *Candona* spp. These ostracods suggest brackish water (very low salinity). In Livadi 1 core 8, the dominant foraminifera were *A. tepida*, *A. beccarii*, *E. crispum*, *E. granosum* and the ostracod that points to brackish water was *Cyprideis* spp., these data indicate to an open lagoon. Finally, in Livadi 1 cores 9 and 10, the paleoenvironmental conditions according to foraminifera and ostracods assemblages, were shallow marine to open marine.

7.3.2 Paleoenvironmental Analysis of Livadi 2



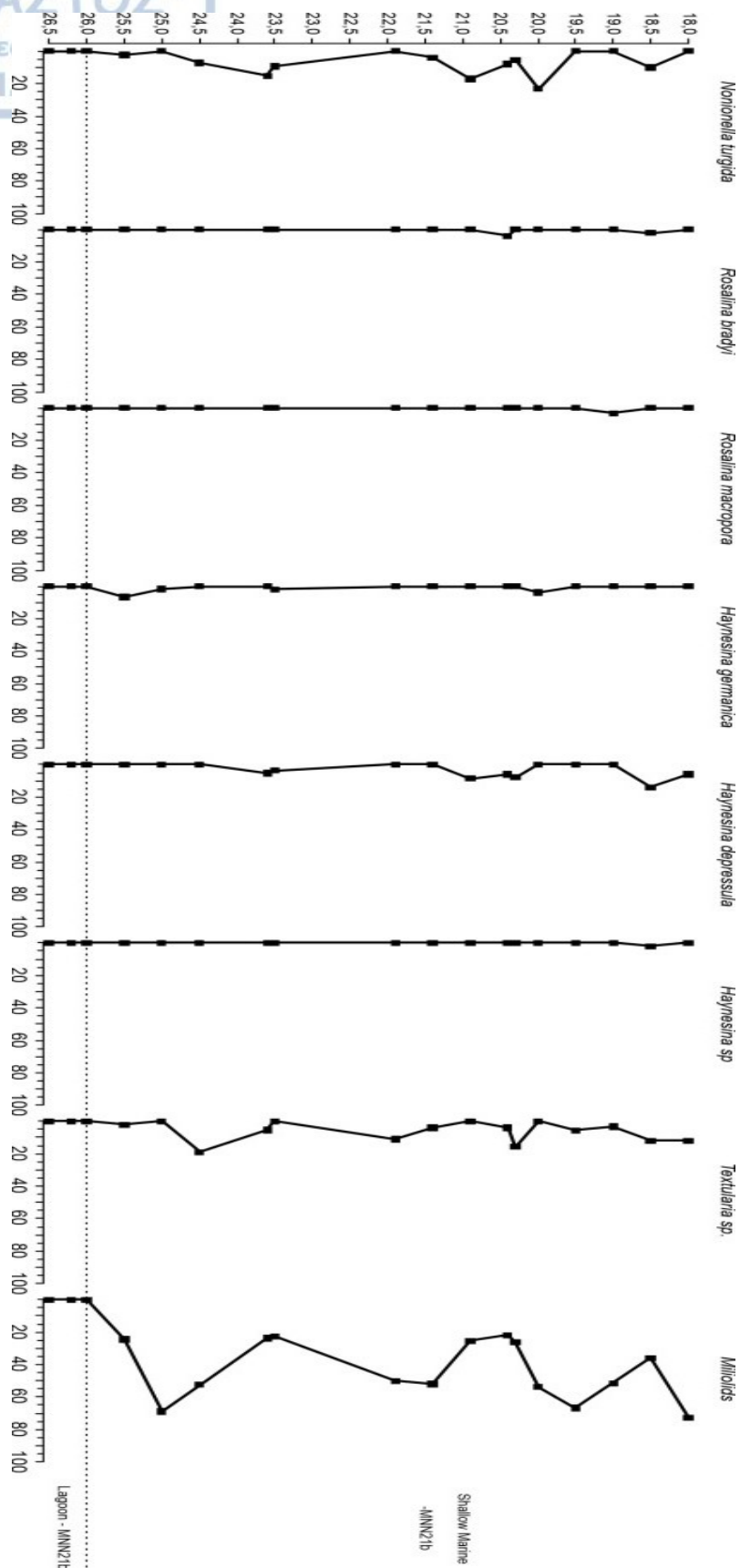
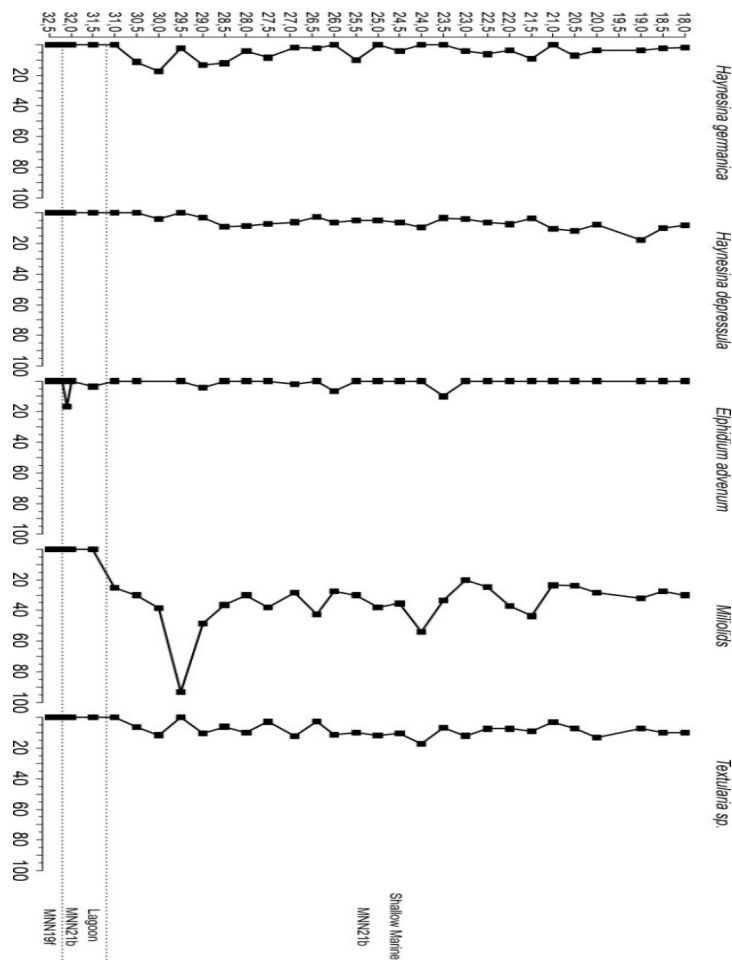


Figure 24: Paleoenvironmental Interpretation of Livadi-2 borehole.

In Livadi 2 core 7, the data from forams and ostracods indicate to shallow marine to marine environment with algal vegetation (samples 2.7.1 - 2.7.26). The foraminifera in Livadi 2.7, were *A. tepida*, *A. beccarii*, *N. turgida*, *Quinqueloculina* sp., *Triloculina* sp., *Miliolinella*, *T. agglutinans*, *R. bradyi*, *Haynesina* sp., *H. depressula*. The ostracods in Livadi 2.7, that indicate to marine environment were *Xestoleberis communis*, *Leptocythere* spp., *Loxoconcha ovulate*, *Cytheridea* sp.. In core Livadi 2-8, the high percentages of the foraminifera *N. turgida* and *R. phlegeri* and ostracods *Xestoleberis* sp., indicate to shallow marine – marine with algal vegetation and terrestrial organic matter input conditions. Shallow marine environment with terrestrial organic matter input conditions, continued to appear downwards the Livadi 2.8, in samples 2.8.31 up to 2.9.16, which was indicated by high percentages of *N. turgida* and *R. phlegeri*. The ostracods confirming the shallow marine environment were *Paradoxostoma* spp., *Cytheridea*, *Pterygocythere* spp. Finally, in Livadi 2 core 10, shallow marine conditions appear in sample 2.10.1 and then lagoonal conditions even fresh water environment (samples 2.10.11-2.10.12) have been recognized in samples 2.10.6 up to 2.10.12 (end of core 10). No sign of Pleistocene had been recorded in Livadi 2.

7.3.3 Paleoenvironmental Analysis of Livadi 4



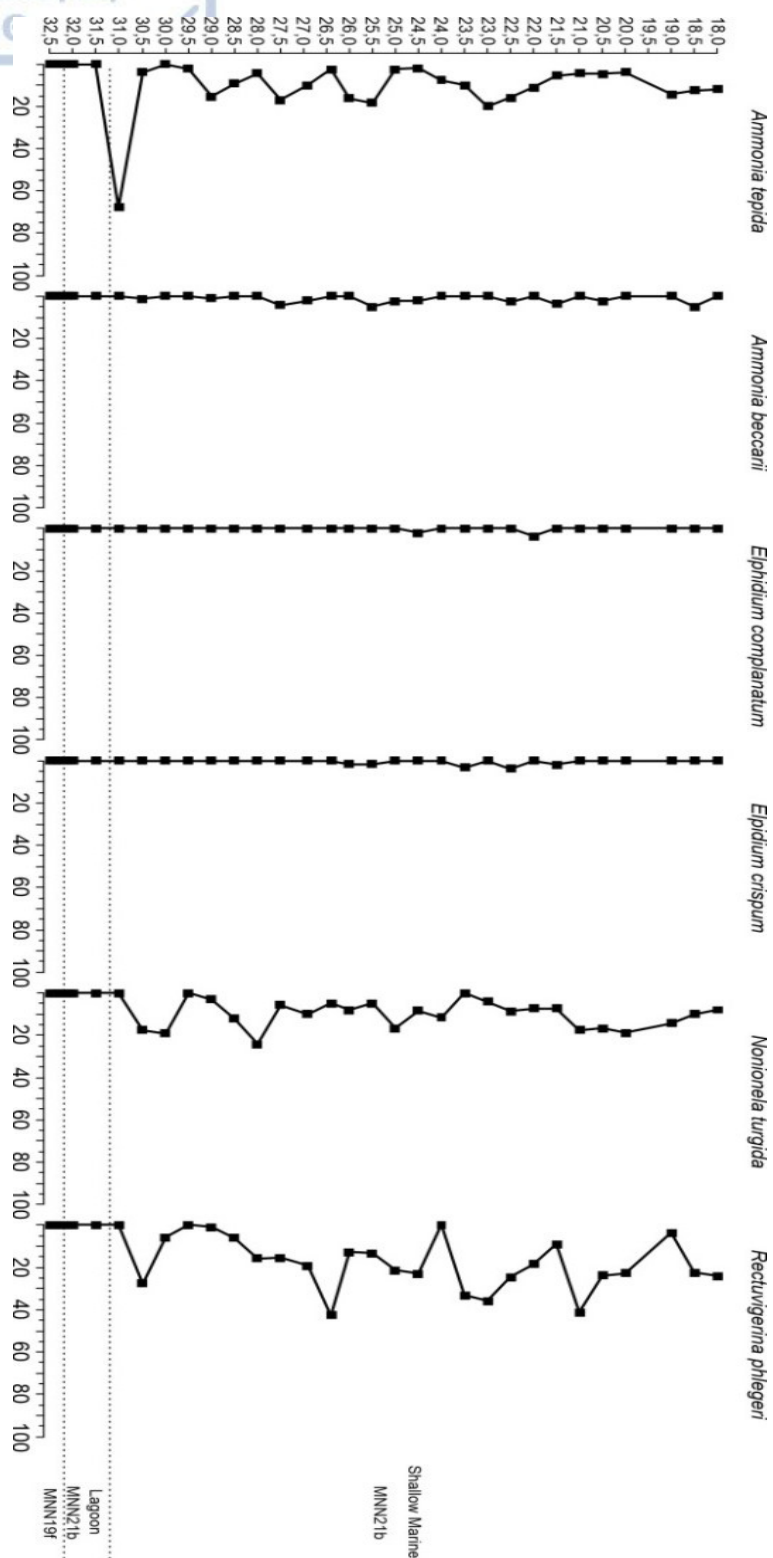


Figure 25: Paleoenvironmental Interpretation of Livadi-4 borehole.

Marine with algal vegetation conditions appear in samples 4.7.1 up to 4.7.11 and marine to shallow marine with algal vegetation conditions appear in the rest of Livadi 4 core 7. All samples in Livadi 4.8, (4.8.1 up to 4.8.50) are characterized by a shallow marine environment with algal vegetation; yet no sign for a typical lagoonal environment. Open Lagoon conditions appear in sample 4.10.16 due to presence of *Cyprideis* spp. and *Aurila* spp. and possible lagoonal – fresh water conditions in sample 4.10.21 due to lack of ostracoda. Sample 4.10.16 is characterized by a mixed environment (ostracod content indicates open lagoon) due to the presence of Plio -Pleistocene reworked foraminiferal specimens, both benthic and planktonic. In sample 4.10.22 an important amount of coal was present. Sample 4.10.23 had no foraminiferal or ostracod content, with only traces of algae which indicates to a very shallow lagoonal environment like sample 4.10.21. Samples 4.10.24 up to 4.10.26 are representing Pleistocene deposits due to the occurrence of deep-water benthic foraminifera such as *Uvigerina mediterranea*, *Cibicides* spp., *Bulimina marginata* etc., and also large numbers of planktonic foraminifera that indicate deep marine paleoenvironment (Figure 23, for paleoenvironmental changes in borehole Livadi 4).

7.4 Paleoenvironmental Correlation between the studied boreholes

The biostratigraphy and data from simultaneous research on the paleoenvironment have shown that the boundary between the lagoon and the marine Holocene sediments (MNN21b) is transitional and represents a marine transgression, marine ravinement and is characterized by reworking material.

The graph below shows the 4 boreholes Livadi 1,2,3,4 and their calculated depths from the sea level. The graph also, shows the sea level and the sea bottom and the direction of the 4 boreholes (N-S). Livadi-3 was not sampled for micropaleontological analysis. The other boreholes were analyzed under the SEM in order to identify the nannofossil content and under the Stereo Microscope for the foraminifera content. The micropaleontological analysis in Livadi-1 started at 41 meters depth, according to biostratigraphy based on calcareous nannoplankton and the paleoenvironmental analysis, the lagoon was found in the Holocene (MNN21b), at 43,1m depth and the Pleistocene basement (MNN19e) at 45,5m depth. In Livadi-2 the examination of the borehole began at 37,6 meters depth and the lagoon was found at 45,6m depth. In this borehole no sign of Pleistocene has been recorded. The analysis in Livadi-4 began at 37,5m depth and the lagoonal conditions were found at 49,8m depth. The Pleistocene basement (MNN19f) was found at 51,1m depth.

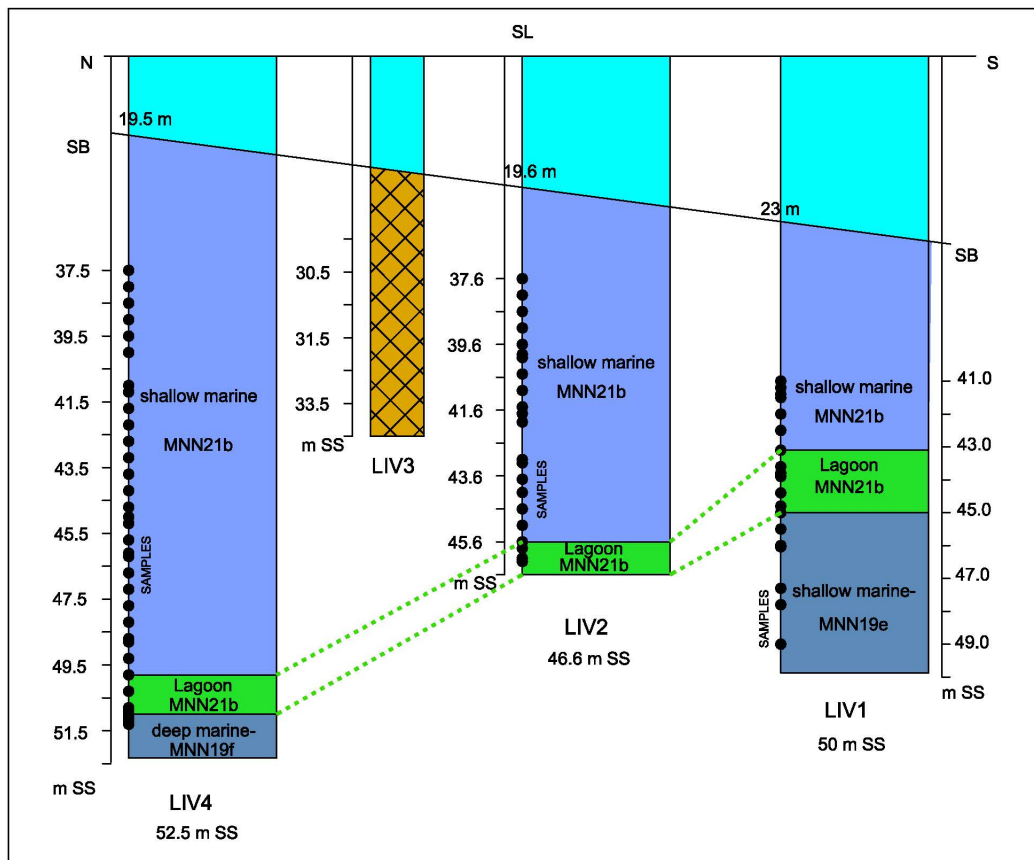


Figure 26: Correlation graph of the four boreholes Livadi 1, 2, 3 and 4.

Finally, additional research needs to be done in the area in order to get a more complete picture of the past. Next steps that could be suggested for further investigations are the need to quantify the marine transgression timing by sampling and radiocarbon analysis, something that the present work pin points the depths to focus on. In all boreholes the most appropriate pin points for radiocarbon analysis are by taking a few samples within the marine environment and the most important samples should be taken before and after the lagoon. Furthermore, another idea for future studies could be an onshore drilling in order to identify and date the cataclysmic event that appears to have closed the marine channel.

8. Conclusions

After taking into consideration the data we have gathered, and the results from the experimental procedures and the micropaleontological analysis, we came to the following conclusions.

In all the cores we examined (Livadi 1, 2, 4); it was found an unconformity within the Holocene that reflects an environmental change. In particular, this environmental change is a closed or an open lagoon at a time, depending on the location of each core (closer to land or deeper in the Gulf of Livadi). Over time, this lagoon filled with water and shaped the area into the Gulf we see today. With this discovery of the unconformity, within the Holocene sediments (MNN21b), it is realized that the study area was very shallow in the past, so shallow in some of the examined places that the Coccolithophores were completely absent, due to paleoenvironmental conditions.

According to previous research, the marine seismic data in the area have shown the presence of a channel outlet carved into the basal sediments of Ormos Agias Kiriakis and the Gulf of Livadi, where the marine channel would have run through to connect the northern and southern parts of the Ionian Sea (Underhill, 2009). This unconformity and the shallow lagoon that was discovered, are confirming the filled-channel hypothesis that might have isolated the Paliki peninsula from the rest of Kefallonia.

Bibliography

- Agnini C., Monechi S. & Raffi, I. , 2017. Calcareous nannofossil biostratigraphy: historical background and application in Cenozoic chronostratigraphy. *Lethaia*, Volume 50, p. 447–463.
- Armstrong H. A., Brasier M. D.,, 2005. Microfossils (2nd Ed). *Blackwell, Oxford*.
- Aubouin, J. & Decourt, J., 1962. Zone Preapulienne, zone Ionienne et zone du Gavrovo en Peloponnese occidental. *Bull. Soc. Geol. France*, Volume 4, pp. 785-794.
- Aubouin, J., 1959. Contribution à l'étude géologique de la Grèce Septentrionale. Les confins de l'Épire et de la Thessalie. *Ann. Geol. d. Pay Helen*, Volume 10, pp. 1-525.
- Backman Jan, Raffi Isabella, Rio Domenico, Fornaciari Eliana, Pälike Heiko, 2012. Biozonation and biochronology of Miocene through Pleistocene calcareous nannofossils from low and middle latitudes. *Newsletters on Stratigraphy*, 45(3), p. 221–244.
- Bauman et al., 1998. Comparison of different preparation techniques for Quantative Nannofossil studies. *Journal of Nannoplakton Research*, 20(2), pp. 75-80.
- Bown P.R, 1998. *Black book-Calcareous nannofossil biostratigraphy*. British Micropalaeontological Society Publications Series: Springer; Softcover reprint of the original 1st ed. 1998 edition.
- Bown Paul R., 1998. *Calcareous Nannofossil Biostratigraphy*. London, UK: KLUWER ACADEMIC PUBLISHERS.
- Briole P., Elias P., Parcharidis I., Bignami C., Benekos G., Samsonov S., Kyriakopoulos C., Stramondo S., Chamot-Rooke N., Drakatos M.L., Drakatos G., 2015. The seismic sequence of January–February 2014 at Cephalonia Island (Greece): constraints from SAR interferometry and GPS. *Geophys. J. Int.*, Volume 203, p. 1528–1540.
- Brooks M., Clews J. E. and Melis N. S., Underhill J. R., 1988. Structural development of Neogene basins in western Greece. *Basin Research*, Volume 1, pp. 129-138.
- Castradori D., 1993. Calcareous Nannofossils and the origin of Eastern Mediterranean Sapropels. *Paleoceanography*, 8(4), pp. 459-471.
- Cepek P., Hay W.W., 1969. Calcareous Nannoplankton and Biostratigraphic Subdivision of Upper Cretaceous. *AAPG Bulletin*.
- De La Rocha CL, 2006. The Biological Pump. In: Treatise on Geochemistry. *Pergamon Press*, Volume 6, pp. 83-111.
- De Vargas C., Aubry M.P., Probert I., J. Young, 2007. Origin and Evolution of Coccolithophores: From Coastal Hunters to Oceanic Farmers. In: s.l.:s.n.
- Dermitzakis M., 1977. Stratigraphy and sedimentary history of the Miocene of Zakynthos (Ionian Islands, Greece). *Ann. Geol. Pays Hell.*, Volume 29, pp. 47-186.

Dimiza M.D., Maliverno E., Trantaphyllou M.V., Dermitzakis M.D. , Corselli C., 2008. *Coccolithophores of the eastern Mediterranean Sea*. s.l.:ION.

Gaki - Papanastassiou, Karymbalis, Maroukian, & Tsanakas, 2010. GEOMORPHIC EVOLUTION OF WESTERN (PALIKI) KEPHALONIA ISLAND (GREECE) DURING THE QUATERNARY. *Bulletin of the Geological Society of Greece*, Volume 43, pp. 418-427.

Gartner S., 1977. Calcareous Nannofossil Biostratigraphy and revised zonation of the Pleistocene. *Marine Micropaleontology*, Volume 2 , p. 1—25.

Gartner Stefan and Emiliani Cesare, 1976. Nannofossil Biostratigraphy and Climatic Stages of Pleistocene Brunhes Epoch. *The American Association of Petroleum Geologists. All rights reserved*, pp. 1562-1564.

Geisen et al., 2004. Species level Variation in coccolithophores.

Giraudeau Jacques and Beaufort Luc, 2007. Coccolithophores: From Extant Populations to Fossil Assemblages. In: s.l.:UMR5805 EPOC contribution no. 1603, p. Chapter 10.

Gluyas, J. & Swarbrick, R., 2004. Petroleum Geoscience. *Blackwell Publishing*, pp. 80-82.

Guerreiro C., Cachão M., Drago T., 2005. Calcareous nannoplankton as a tracer of the marine influence on the NW coast of Portugal over the last 14 000 years. *J. Nannoplankton Res*, 27(2), pp. 159-172.

Haq Bilal U., 1998. Calcareous Nannoplakton.

Hibberd D. J., 1976 . The ultrastructure and taxonomy of the Chrysophyceae and Prymnesiophyceae (Haptophyceae): a survey with some new observations on the ultrastructure of the Chrysophyceae. *Botanical Journal of the Linnean Society*, Volume 72, pp. 55-80.

Jordan Richard W., Cros Lluisa and Young Jeremy R, 2004. A Revised Classification Scheme for Living Haptophytes. *The Micropaleontology Project Inc.*, 50(1: Advances in the biology, ecology and taphonomy of extant calcareous nannoplankton), pp. 55-79.

Karakitsios V. and Rigakis N., 2007. Evolution and petroleum potential of Western Greece. *Journal of Petroleum Geology*, 30(3), pp. 197-218.

Karakostas, Papadimitriou, Karamanos, & Kementzetzidou, 2010. MICROSEISMICITY AND SEISMOTECTONIC PROPERTIES OF THE LEFKADA – KEFALONIA SEISMIC ZONE. *Bulletin of the Geological Society of Greece*, Volume 43, pp. 2053-2063.

Karymbalis Efthimios, Papanastassiou Dimitrios, Gaki-Papanastassiou Kalliopi, Tsanakas Konstantinos & Maroukian Hampik , 2013. Geomorphological study of Cephalonia Island, Ionian Sea, Western Greece. *Journal of Maps*, Volume 9:1, pp. 121-134.

Kassaras I., Papadimitriou P., Kapetanidis V., Voulgaris N., 2017. Seismic site characterization at the western Cephalonia Island in the aftermath of the 2014 earthquake series. *Geo-Engineering*, Volume 8:7.

Marino et al., 2003. Quantitative Pleistocene Calcareous Nannofossil Biostratigraphy of LEG 86, SITE 577 (Shatsky Rise, NW Pacific Ocean). *Journal of Nannoplakton Research*, 25(1), p. 25037.

Mutterlose Jörg, Bornemann André, Herrle Jens O., March 2005. Mesozoic calcareous nannofossils — state of the art. *Paläontologische Zeitschrift*, Volume 79(Issue 1), pp. pp 113-133.

Papanikolaou D., Ebner F., 1997. Tectono-stratigraphic maps and terrane descriptions. *Ann. Geol. Pays Hell.*, Volume 37, pp. 195-197.

Papanikolaou D., 1997. The tectonostratigraphic terranes of the Hellenides.. *Ann. Geol. Pays Hell.*, Volume 37, pp. 495-514.

Papanikolaou D, 2010. MAJOR PALEOGEOGRAPHIC, TECTONIC AND GEODYNAMIC CHANGES FROM THE LAST STAGE OF THE HELLENIDES TO THE ACTUAL HELLENIC ARC AND TRENCH SYSTEM. *Bulletin of the Geological Society of Greece*, Volume XLIII, p. 1 – 72.

Papanikolaou Dimitrios, Triantaphyllou Maria, 9-14 October 2013. *Growth folding and uplift of Lower and Middle Pleistocene marine terraces in Kefalonia: implications to active tectonics*. Aachen, Germany, 4th International INQUA Meeting on Paleoseismology, Active Tectonics and Archeoseismology (PATA).

Papanikolaou Dimitrios, 2013. Tectonostratigraphic models of the Alpine terranes and subduction history of the Hellenides. *Tectonophysics*.

Papanikolaou M., Papanikolaou D. , Triantaphyllou M. , 2010. POST- ALPINE LATE PLIOCENE – MIDDLE PLEISTOCENE UPLIFTED MARINE SEQUENCES IN ZAKYNTHOS ISLAND. *Bulletin of the Geological Society of Greece*, Volume 43, pp. 475-485.

Raffi, I., Backman, J., Fornaciari, E., Palike, H., Rio, D., Lourens, L., Hilgen, F., 2006. A review of calcareous nannofossil astrobiochronology encompassing the past 25 million years. *Quat. Sci. Rev.*, 25(23), pp. 3113-3137.

Rio D., Raffi I., Villa G., 1990 . Pliocene-Pleistocene Calcareous Nannofossil Distribution Patterns in the Western Mediterranean. *Proceedings of the Ocean Drilling Program, Scientific Results*, Volume 107 , pp. 513-533.

Rost Bjorn and Riebesell Ulf, 2004. Coccolithophores and the biological pump: responses to environmental changes.

Roth H. Peter, 1989. Ocean circulation and Calcareous Nannoplakton evolution during the Jurassic and Cretaceous. *Palaeogeography, Palaeoclimatology, Palaeoecology*, Volume 74, p. 111 126 111.

Sheward Rosie M. et al., 2017. Physiology regulates the relationship between coccosphere geometry and growth phase in coccolithophores. *Biogeosciences*.

Sigman DM, Haug GH, 2006. The biological pump in the past. ; In: *Treatise on Geochemistry. Pergamon Press*, Volume vol. 6, pp. pp. 491-528.

Slipper I. J, 2005. *Micropalaeontological Techniques. Elsevier Ltd. All Rights Reserved.*

Stiros S. C., Pirazzoli P. A., Laborel J., Laborel-Deguen F., 1994. The 1953 earthquake in Cephalonia (Western Hellenic Arc): coastal uplift and halotectonic faulting. *Geophys. J. Int.*, Volume 117, pp. 834-849.

Thierstein Hans R., 1976. Mesozoic Calcareous Nannoplakton Biostratigraphy Sediments of Marine. *Marine Micropaleontology*, Volume 1, pp. 325 - 362.

Triantaphyllou M.V., Drinia H., Dermitzakis M.D., 1999. Biostratigraphical and paleoenvironmental determination of a marine Plio/Pleistocene outcrop in Cefallinia Island (Greece). *In: Géologie Méditerranéenne*, Volume 26, numéro 1-2, pp. 3-18.

Triantaphyllou, M., Drinia, H., Dermitzakis, M.D., 1997. The Plio-Pleistocene boundary in the Gerakas section, Zakynthos (Ionian Islands). *N. Jb. Geol. Palaont. Mh, Stuttgart*, Volume H.1, p. 12–30.

Underhill John R. , 2009 . Relocating Odysseus' homeland. *nature geoscience*, Volume 2 .

Underhill, J.R., 1988. Triassic evaporites and Plio-Quaternary diapirism in western Greece. *Journal Geological Society of London*, Volume 145, p. 269–282.

Underhill, J.R., 1989. Late Cenozoic deformation of the Hellenide foreland, western Greece. *Geological Society of America Bulletin*, Volume 101, pp. 613-634.

van Hinsbergen D. J. J., van der Meer D. G., Zachariasse W. J., Meulen Kamp J. E., 2006. Deformation of western Greece during Neogene clockwise rotation and collision with Apulia. *Int J Earth Sci (Geol Rundsch)*, Volume 95, p. 463–490.

Young et al., 2005. Taxonomy Guide. *JRN* , Issue Special issue.

Young et Bown, 1997. Proposals for a revised classification system for calcareous nannoplankton.. *JRN*.

Young Jeremy R. and Bown Paul R., 2014. Some Emendments to Calcareous Nannoplankton Taxonomy. *J. Nannoplankton Res*, 33 (1), pp. 39-46.

ΛΕΚΚΑΣ, Ε., ΔΑΝΑΜΟΣ, Γ., & ΜΑΥΡΙΚΑΣ, Γ, 2001. Geological Structure and Evolution of Kefallonia and Ithaki islands. *Bulletin of the Geological Society of Greece*, 34(1), pp. 11-17.